THESE DE DOCTORAT DE
L'UNIVERSITE PIERRE ET MARIE CURIE

Spécialité

Tectonique et Géodynamique

Présentée par

M. César Witt

Pour obtenir le grade de

DOCTEUR de l'UNIVERSITÉ PIERRE ET MARIE CURIE

CONSTRAINTS ON THE TECTONIC EVOLUTION OF THE NORTH ANDEAN BLOCK TRAILING TAIL: EVOLUTION OF THE GULF OF GUAYAQUIL-TUMBES BASIN AND THE INTERMONTANE BASINS OF THE CENTRAL ECUADORIAN ANDES

Soutenue à Villefranche sur mer le 26 janvier 2007 devant le jury composé de:

M. J. Bourgois	Directeur de Recherche, CNRS-IRD	Directeur de Thèse
M. F. Michaud	Maître de Conférence, Paris VI	co-Directeur de Thèse
M. E. Jaillard	Directeur de Recherche, IRD	Rapporteur
M. T. Sempéré	Chargé de Recherche, IRD	Rapporteur
M. J. Boulègue	Professeur, Paris VI	Examinateur
M. J. Angelier	Professeur, Paris VI	Examinateur
M. P. Charvis	Directeur de Recherche, IRD	Examinateur
M. W. Winkler	Professeur ETH, Zurich	Invité

ABSTRACT

The tectonic escape of an upper-plate sliver is considered to be influenced by the relationship between subducting and overriding plates in terms of obliquity, interplate coupling and overriding plate strength. Trailing edges of tectonic escape system define major subsiding zones related to a trench-parallel extensional regime. The Gulf of Guayaquil-Tumbes basin (GGTB) is located at the southernmost limit of the North Andean block (NAB), which drifts to the north at ~1cm/yr. The extensional regime along the GGTB results from the northward drifting of the NAB along a major dextral transcurrent system that extends between Ecuador, Colombia and probably further north to Venezuela. The Puná-Santa Clara fault system (PSCFS) has been generally defined as the NAB frontier at the GGTB area. However, the location of the structures controlling GGTB evolution, as well as the periods of basin opening, has been a matter of discussion. Further east, along the continental zone, Andean intermountain basin formation has been also considered as NAB drifting-induced.

Industrial multichannel seismic and well data acquired by Petroecuador and Perupetro, Ecuadorian and Peruvian Petroleum Companies, respectively, document the existence of two major zones showing two different tectonic regimes. It includes the continental margin and the shelf areas. The inner Domito fault system, the Banco Peru fault and the Talara detachment define the limit between these two tectonic domains. An ~E-W directed extensive strain characterizes the continental margin during the past 10-15 Myr. We assume that this extensional tectonic regime is related to tectonic erosion working at depth along the upper-lower plate boundary.

The GGTB evolved along the shelf area through two main tectonic steps. The first one, during the Mio-Pliocene, is characterized by low subsidence-low sedimentation rates; the second one, during the Pleistocene, is characterized by an abrupt increase of subsidence leading to maximum deposition of ~3500 m of sediments at site. Three major detachment faults, the Posorja, Jambelí and Tumbes detachment systems controlled the subsidence of GGTB depocenters including the Esperanza, Jambelí and Tumbes basins. These basins resulted from the N-S directed extensional strain linked to NAB drifting and recorded the major subsidence phase of the southern Ecuadorian and northern Peruvian forearcs for at least the past 10 Myr. The PSCFS commonly associated to the southernmost tip of the NAB frontier acts as a transfer zone since the Lower Pleistocene time. It accommodated the opposite verging directions between the southward dipping Posorja and the northward dipping Jambelí detachments. The PSCFS shows no landward prolongation to the north and no seaward prolongation to the south toward the trench, it ends at sites where no transfer motion is required. The PSCFS is not the prolongation of the NAB frontier at the GGTB area as commonly accepted. The main period of NAB drifting is defined from the high rates of subsidence and related sedimentation beginning at 1.8-1.6 Ma. Taking into account the strong dependence of the subsidence in the GGTB area with respect to the northward drifting of the NAB, we assume that the Pliocene–early Pleistocene boundary is associated with a major change in the northward migration rate of the NAB, produced by the increase of the interplate coupling probably caused by the Carnegie ridge subduction. The total lengthening of a complete N-S transect between the Posorja and Tumbes detachments ranges between 13.5 and 20 km. This lengthening is coherent with the documented NAB drifting rate combined with an early Pleistocene age for GGTB main opening pulse.

The northward drifting of the NAB results in subsidence along the shelf area, while the continental margin is relatively unaffected by this process. Seismic evidence suggests that the interplate coupling beneath the continental margin is low. We suggest that tectonic escape systems are highly sensitive to local interplate coupling variations and that these variations are important to define the zones where subsidence results from escape tectonics. The modelling of convergence partitioning in terms of convergence obliquity, constant interplate coupling and constant overriding plate strength at the scale of the whole system seems to be insufficient when analysing the trailing edge of the tectonic escape system. We also propose that major lengthening along the GGTB weakens the crust resulting in strong decrease of earthquake recurrence.

The central and southern Andes have undergone major extensional periods leading to intermountain basin formation during at least the last 15 Ma. Transtensional and pure extensional regimes result in discrete intermountain basin formation along major pre-existing Andean trending structures, from north to south these basins include the Cañar, Azogues and Santa Isabel basins. All basins show a deformed zone to the east and an undeformed zone to the west. However, along the Cañar and Azogues basins, active subsidence during ~15-9 Ma finish with a compressive step at 8.5-9 Ma, while at the Santa Isabel basin the compressive step seems considerably older and extensional processes has been active at 15-9 Ma and during present times. Our first approximation to a regional model on Andean intermountain evolution, point out that the Santa Isabel basin represents the southern ‘extensional free face’ of an undeformed detached block that moves to the north and promotes pervasive subsidence to the south and dyacronous compressive deformation along its eastern edge.

RESUME

Le long des zones de convergence les variations du couplage inter-plaque, de l'obliquité de la convergence, de l'état de contrainte de la plaque chevauchante sont considérées comme étant souvent à l'origine de l'individualisation de blocs qui s'échappent latéralement. Aux frontières des blocs continentaux individualisés par le processus d'échappement tectonique, se forment des basins en extension caractérisés par une forte subsidence. Le bassin du Golfe de Guayaquil-Tumbes (BGGT) est localisé à la terminaison méridionale de la frontière du bloc Nord Andin qui s'échappe vers le Nord à la vitesse de 1cm/an. L'ouverture en extension du BGGT est associée au fonctionnement du système décrochant dextre qui marque la frontière orientale du bloc Nord Andin, au travers de l'Equateur, de la Colombie et plus au Nord du Venezuela. Dans le Golfe de Guayaquil, le système de faille de Puna-Santa Clara est classiquement considéré comme la terminaison méridionale de la frontière du bloc Nord Andin. La localisation dans l'espace et dans le temps des failles et des déformations associées qui contrôlent l'évolution du BGGT sont encore discutées. Plus à l'Est, la formation de bassins intra-montagneux a été associée à l'échappement vers le Nord du Bloc Nord Andin.

L'interprétation de profils de sismiques multitraces et de données de forage (données Petroecuador pour l'Equateur et Perupetro pour le Pérou) montre que le domaine de la plate-forme continentale est séparé du domaine de la pente supérieure par le système de failles de Domito et du « Banco Peru » et le détachement de Talara. La pente supérieure est caractérisée depuis 15 à 10 Ma par un régime tectonique en extension qui est associé au régime tectonique de subduction-érosion. La plate-forme continentale est marquée par l'évolution du BGGT en deux grandes étapes : la première étape, d'âge Mio-Pliocène, se caractérise par un faible taux de subsidence ; la seconde étape, d'âge Pléistocène, se caractérise par une augmentation brutale du taux de subsidence. Durant cette seconde étape se dépose 3500 m de sédiment ce qui correspond au plus fort taux de subsidence jamais enregistré au cours des 10 derniers millions d'années dans les bassins avant-arc de l'Equateur et du Pérou. Cette forte subsidence et l'extension NS associée, localisées dans les bassins de La Esperanza , de Jambeli et de Tumbes, sont contrôlées par les détachements de Posorja, Jambeli et Tumbes. Le système de faille de Puna-Santa Clara est une faille de transfert qui accommode le jeu à vergence opposé des détachements de Jambeli (vers le Nord) et de Posorja (vers le Sud). De plus le système de faille de Puna-Santa Clara ne se prolonge pas vers le Nord, ni vers le Sud jusqu'à la fosse. Ce n'est donc pas la prolongation de la frontière orientale du Bloc Nord Andin comme communément acceptée. L'accélération du taux de subsidence dans le BGGT débute vers 1.8 -1.6 Ma. L'étroite relation qui existe entre l'échappement vers le Nord du bloc Andin et l'accélération de la subsidence dans le BGGT implique l'existence d'un changement important dans l'échappement du bloc Nord Andin à la limite Pliocéne-Pléistocéne inférieur. Cette accélération de l'échappement du bloc Nord Andin à la limite Pliocène-Pléistocène est probablement associée à l'arrivée en subduction de la ride de Carnegie. L'étirement total entre les détachements de Posorja et Tumbes atteint 13.5 à 20 km. Cet étirement est cohérent avec le taux de déplacement du BNA et l'ouverture principale du bassin au Pléistocène inférieur.

L'accélération de l'échappement du bloc Nord Andin ne se traduit pas par une forte subsidence dans le domaine du plateau continental. Nous suggérons que l'échappement tectonique est très sensible aux variations locales du couplage interplaque; ces variations sont probablement étroitement corrélées avec les zones de subsidence importante associées à l'échappement tectonique.

La modélisation du partitionnement de la convergence prenant en compte l'obliquité de la convergence, un couplage interplaque homogène et une résistance homogène de la plaque supérieure n'est pas satisfaisante quand on analyse l'évolution du BGGT. L'important amincissement crûstal au niveau du BGGT se traduit ainsi en terme de séismes par une baisse sensible de leur récurrence.

Les Andes centrales ont subi durant les 15 derniers Ma d'importantes phases d'extension qui ont donné naissance à l'ouverture de bassins intramontagneux. C'est ainsi que le long de structures andines pré-existantes se sont formés en Equateur, du Nord au Sud, les bassins de Cañar, Azogues et Santa Isabel. Tous ces bassins montrent une zone déformée vers l'est et une zone non déformée vers l'ouest. Cependant, les basins de Canar et d'Azogues sont caractérisés par un épisode de subsidence entre 15-9 Ma puis par un épisode compressif à 8.5-9 Ma tandis que le bassin de Santa Isabel est caractérisé par un épisode compressif ancien suivi par un épisode extensif depuis 15 Ma jusqu'à aujourd'hui. Ceci suggère que l'évolution du bassin de Santa Isabel correspond au bord libre d'un bloc rigide dont l'échappement provoque d'une part une subsidence au sud du bloc et d'autre part une déformation compressive diachrone le long de sa bordure orientale.

Remerciements

Je dédie ce travail à ma mère, ainsi, je la remercie de son soutien et de son courage grâce auxquels j'ai pu devenir ce qu'un jour elle a rêvé pour moi, ce travail a été fait en grande partie par ses propres mains. Merci pour tout cela, et pour avoir cru en moi. Je remercie ma famille pour son éternel appui. A vous tous mes mots d'admiration et de respect.

Je remercie et exprime mes sentiments de respect et admiration à mon directeur de thèse, Jacques Bourgois, pour son appui personnel et professionnel, pour son énorme intérêt a ma formation, pour avoir partagé avec moi ses connaissances et pour les avoir mis dans ce manuscrit, et pour avoir suivi de très près toutes les étapes de ma thèse, même avant de l'avoir commencé.

Je tiens a remercier les organismes qui ont financé cette thèse, le FUNDACYT, l'Ambassade de France en Equateur, l'Institut de Recherche pour le Développement, et Geosciences Azur.

A François Michaud, qui a commencé la direction de ce travail pendant mon DEA. Pour tout son appui, pour partager ses intérêts scientifiques avec moi, pour son enseignement et pour son ouverture.

Je remercie à Morgane, pour y être et pour m'avoir ouvert sa vie, pour son grand soutien niçois puis londonien, sans lequel cette thèse n'aurait jamais été couchée sur le papier, et surtout pour être tout ce qu'elle représente dans ma transplantation en terre française.

A Philippe Charvis pour son aide et son bon caractère.

Merci à tous ceux du laboratoire jaune du 2, Quai de la Darse, Martine, Véronique, Laure, Marie-Odile, Jean-François, Françoise, Sophie, pour leur soutien, qui montre qu'entre famille même le monstre administroscietinformatique apprend à sourire.

A tous mes amis du côté est, qui ont su plus donner que recevoir : Kevin, Alcinoe Valenti et Unai (parce que maintenant ils sont trois !!), Audrey, ma sœur Véronique, à Adelina, Agnes, Manal, Jerryl, Gueorgui, Eduardo, Steph, à vous tous mes remerciements, mon cœur, mes respects et mes meilleurs vœux de réussite……

A Alfonso Salguero, pour son aide, pour y croire, et pour être témoin de mon parcours parfois sinueux, et pour être témoin, et en français cette fois. Ce travail lui appartient aussi.

A tous mes amis du côté ouest, a tout le comité « pecho amarillo » du parc central de Santa Isabel : Alvaro, encore Alfonso, Pablo, Danilo, Camilo, Enriquito, Peter, encore Morgane, Lydia. A mes amis du côté ouest puis est, à Silvana, Fredy et Diego, et pour ce dernier : no me bajes los brazos, vamos todavia !!!

A tous mes professeurs de l'EPN, en spécial à Renan Cornejo et Arturo Eguez. Pour me guider et me préparer pendant et pour le futur de ma carrière.

Je remercie à la Famille Poulain, à Michel, Jacqueline, Johan, Isa, Romain et Martin.

A Petroecuador et Perupetro pour nous avoir permis d'utiliser leurs données.

Enfin mais pas en dernier, aux membres du jury de thèse pour avoir lu, discuté et amélioré ce travail.

Aix en Provence, le 19 Mars 2007

CONTENT

Figures

Chapter 1

Chapter 2

Chapter 3

Figure 3.3. a) Chronostratigraphic chart of southern Ecuador and fission track ages. **b)** Palinspatic reconstruction of southern Ecuador from middle to late Miocene times. From Hungerbüler et al. (2002).

Figure 3.4. a) Sketch of the central Ecuadorian Andean segment. **b)** N-W cross section of the Cañar basin. Modified from Lahuathe (2005). **c)** N-W cross section of the Azogues basin. **d)** Ages chart for the main intermountain basin filling. **e)** 86Sr/87Sr analysis of basal Biblian and Mangan Fms. c, d and e Modified from Verdezoto (2005).

Figure 3.5. Geological map of the Santa Isabel basin.

Figure 3.6. Key stratigraphic columns of the Santa Isabel basin.

Figure 3.7. The sedimentary formations of the Santa Isabel basin. **a)** The Jacapa Fm. **b)** The Red Mb. of the Burrohuaycu Fm. **c)** The Gray Mb. of the Burrohuaycu Fm. **d)** The mayor unconformity between the Jacapa Fm. and the Gray Mb. **e)** The Uchucay Fm. **f)** Carbonated alteration at the top of the Uchucay Fm.

Figure 3.8. a) S-E directed cross-section along the north segment of the Girón fault system. **b)** and **c)** Fault exposure zones at the Girón fault system. **d)** Alluvial deposits in front of the north segment of the Girón fault system.

Figure 3.9. a) S-E directed cross-section along the central segment of the Girón fault system. **b)** Vertical contact between the Saraguro Gp. and the Jacapa Fm. **c)** The highly deformed strata of the Jacapa Fm. at the range. **d)** Auto-breccia deposits along the Jacapa Fm. **e)** Major syncline formation along the Girón fault system. **f)** Normal fault plane at the contact between the Jacapa and Burrohuaycu Fms.

Figure 3.10. a) S-E directed cross-section along the south segment of the Girón fault system. **b)** Rupture surface along the Saraguro Gp. **c)** Trapezoidal-shaped hill-slopes at the contact between the Saraguro Gp. and the Jacapa Fm. **d)** The Corrales grouch. **e)** The La Cria anticline.

Figure 3.11. 1:25000 topographic map of the Girón fault system.

Figure 3.12. Cross sections of the Santa Isabel basin as proposed by Hungerbüler et al. (2002).

Figure 3.13. Evolution sketch on the intermountain basins of the central Ecuadorian Andean segment.

Chapter 4.

Figure 4.1. Evolution sketch of the Gulf of Guayaquil-Tumbes basin.

CHAPTER 1

INTRODUCTION

1.1 TECTONIC ESCAPE SYSTEMS

Collision-related strike-slip motion is a general process in continental evolution. Because buoyant continental (or arc) material generally moves during collision towards a nearby oceanic margin, where less buoyant lithosphere crops out, the process of major strike-slip dominated motion towards a 'free-face' is called 'tectonic escape' (Burke and Sengor, 1986). Active zones of tectonic escape have been recognized worldwide along active convergent margins. They normally involve oblique subduction systems and a detached upper plate sliver. Taking into account that the motion partitioning or migration of the sliver takes place at distances ranging normally from 100 to 150 km from the trench (Jarrard, 1986) they represent a major risk for highly populated cities. Two of the major earthquakes in the last ten years have occurred in partitioned systems, i.e. the 2002 Mw. 7.9 Denali Fault earthquake (i.e. Eberhart-Philips et al., 2003) and the 2004 Mw.>9 Sumatra earthquake (i.e. Subarya et al., 2006).

Several strike-slip systems, such as the Sumatra fault, the Japan median line, the Iñique-Ofqui fault system and the eastern frontier of the North Andean block have been considered as the major structures limiting the detached drifting block. In general, their geometrical disposition as well as their cinematic character is relatively well known in the continental zones. However, in almost all the cases, there is no consensus about the location and evolution of these structures along their ending tips (normally their prolongations become diffuse when these structures approach the continental margin). Probably the ending tip of the eastern frontier of the North Andean block is one of the most ambiguous in literature. Similarly, the literature offers few examples of works dealing specifically with the subsiding trailing edges of tectonic escape systems, most of them realized in the Indonesian subduction system (i.e. Huchon and Le Pichon, 1984; Lelgemann et al., 2000, Shang et al., 2002), or they have been immersed in wide geodynamic scenarios (Mann, 2002).

Since the work of Jarrard (1986), several works attempted to describe the phenomena controlling the tectonic escape in terms of obliquity, interplate coupling and overriding plate strength. However most of them analysed these aspects considering constant values for the entire subduction system (i.e. Jarrard, 1986; McCaffrey, 1992; Platt, 1993; Yu et al., 1993; Liu et al., 1995; Chemenda et al., 2000; Upton et al., 2003). On the other hand, the Andean chain has been considered as a well zone to develop constraints on escape tectonics (Burke and Sengor, 1986) since it promotes: (1) rifting and the formation of rift-basins with thinning of thickened crust; (2) pervasive strike-slip faulting late in

orogenic history which breaks up mountain belts across strike and may juxtapose unrelated sectors in cross-section; (3) localized compressional mountains and related foreland-trough basins.

This work attempts to place constraints on the evolution of one of the major tectonic escape systems and its related subsiding trailing edge, the North Andean block and the Gulf of Guayaquil, respectively. This analysis altogether with the stratigraphic and tectonic analysis of intermontane basins, located at the latitude of the Gulf of Guayaquil, allows to improve a wide regional model for escape tectonics along the southern Ecuadorian Andes and the southern Ecuadorian and northern Peruvian coastal zones.

1.2 GEODYNAMIC AND GEOLOGICAL SETTING

1.2.1 The subduction system

The Ecuadorian subduction system shows a complex history immersed in a broad scenario represented by the Galapagos Volcanic Province (GVP, Figure 1.1). The actual architecture of the Ecuadorian subduction system began to form ~26 Ma ago with the breakup of the Farallon plate (i.e. Handschumacher, 1976; Hey, 1977; Lonsdale and Klitgord, 1978). Afterwards, a combination of orthogonal to oblique convergence, hot-spot and asymmetrical spreading centre interaction, ridge subduction, roll-back subduction, among others, have controlled the tectonic evolution of the GVP.

1.2.1.1 Evolution models of the Farallon-Nazca-South America subduction system.

Several first-order constraints on the GVP evolution were obtained from intensive surveys combining seismic reflection, gravity, magnetic, and heat flow records (i.e., Malfait and Dinkleman, 1972; Rea and Malfait, 1974; Hey, 1977; Lonsdale, 1978; Lonsdale and Klitgord, 1978; Pilger, 1984; Wilson and Hey, 1995; Meschede and Barckhausen, 2000; Sallarès and Charvis, 2003). These works show that the Nazca plate has a complex plate tectonic history in relation with asymmetrical and complex tectonic history of the Cocos-Nazca spreading center. Aseismic ridges and their associated seamounts are not only the surficial manifestation of hot spot activity but also reflect regional tectonic events, including spreading centers jumps and migration.

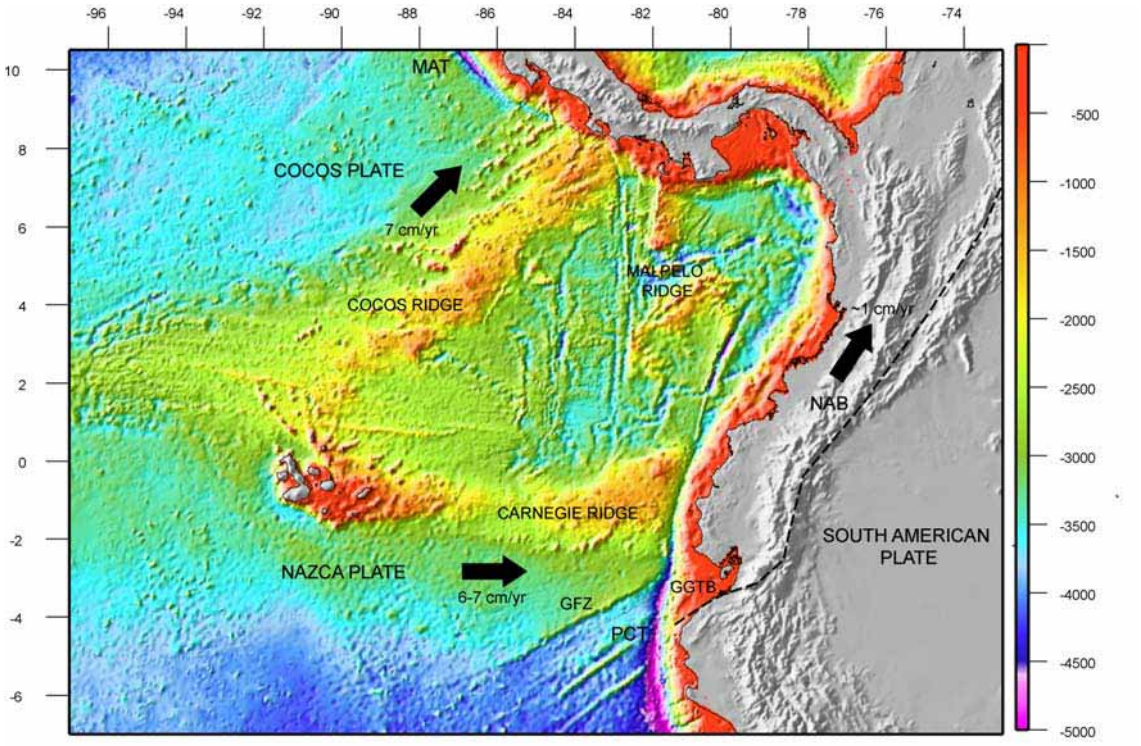

Figure 1.1. NGDC-NOA data showing the structure of the Galapagos volcanic province, the northern South America plate and the North Andean block. Average velocity vectors from, De Mets et al, (1990); Freymuller et al, (1993); Kellog and Vega, (1995); Trenkamp et al., (2002). GGTB, Gulf of Guayaquil-Tumbes basin; GFZ, Grijalva fracture zone; MAT, Mid-America trench; PCT, Peru-Chile trench; NAB, North Andean block.

Hey (1977) led to the conclusion that the Cocos-Nazca spreading center was born about 25 Ma as the Farallon plate broke apart along a pre-existing fracture zone to form the Cocos and Nazca plates (Figure 1.2). As a result of this breakup, subduction became approximately perpendicular to both the Mid-America and the Peru-Chile trenches. In this way, the original N-E trending system was reorganized into its present geometric configuration by about 23 Ma. Hey (1977) proposed that the Malpelo ridge may once have formed the northeastern extension of the Cocos ridge, which has been transferred to the Nazca plate by a discontinuous jump to the west of the Cocos-Nazca-Caribbean triple junction.

Similar conclusions were obtained by Lonsdale and Klitgord (1978). More recently, Sallarès and Charvis (2003) developed a quantitative model based on crustal thickness estimations along the Carnegie, Cocos and Malpelo ridges (Figure 1.3). Their results suggest that the Cocos-Nazca spreading centre has migrated with respect to the Galapagos hotspot (GHS) during the last 20 Ma (Figure 1.3). At ~20 Ma, the Galapagos hot spot was approximately ridge-centered.

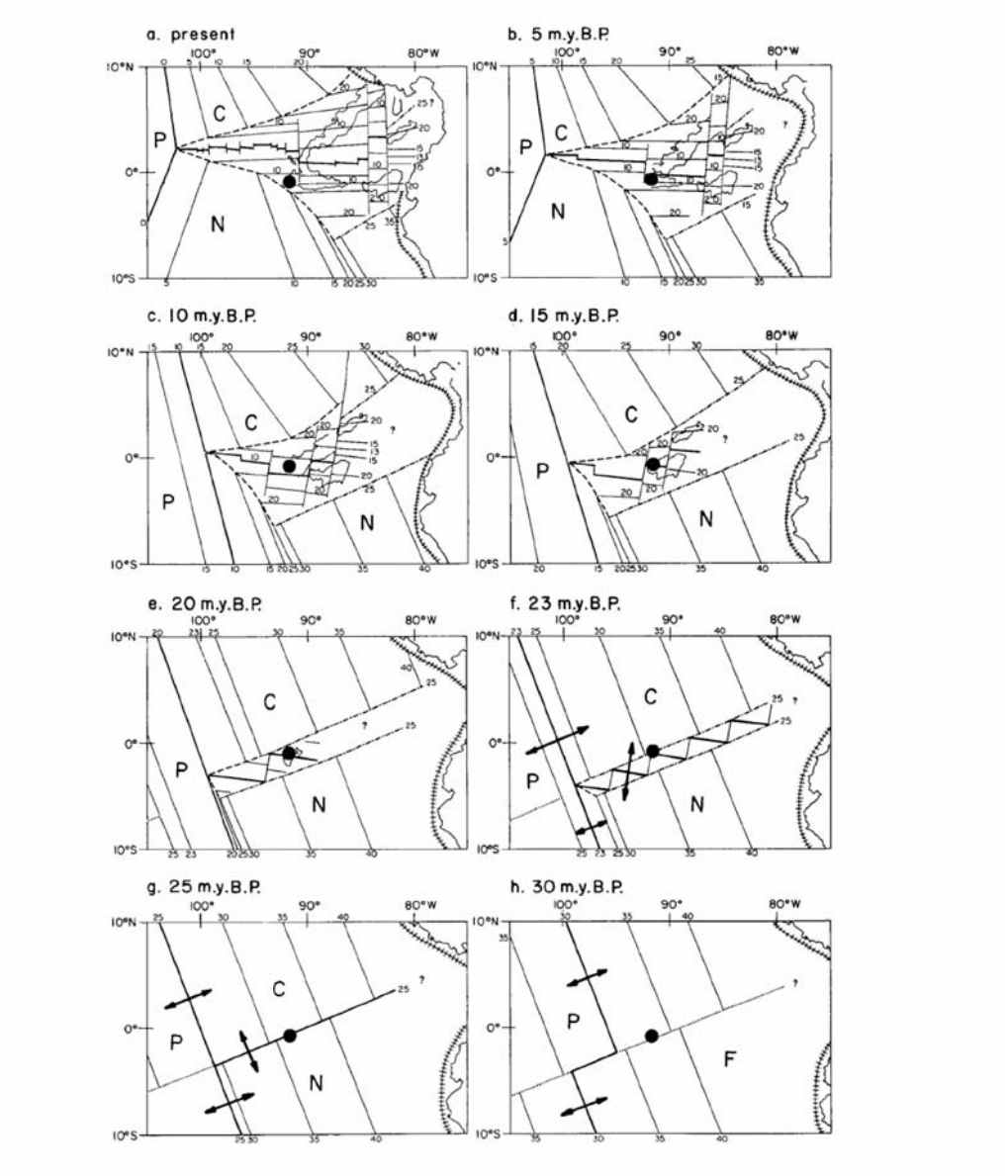

Figure 1.2. Schematic cartoon showing the evolution of the Galapagos volcanic province from 30 Ma to Present. From Hey (1977)

Subsequently, at ~11.5 Ma the hotspot was located ~105 km north of the spreading center while at present day it is located at ~190 km south. They used these results to reconstruct the relative position between the Galapagos hot spot and the Cocos-Nazca Spreading Center. The present configuration of the Galapagos Volcanic Province and the plate velocities are consistent with symmetric spreading with a mean full spreading rate of ~ 60 mm/yr along the Cocos-Nazca Spreading Center during the last 20 Ma. Sallarès and Charvis (2003) suggested that the subduction of the Cocos ridge beneath the Mid-America margin is recent (i.e. 2 Ma) while the older segments of the Carnegie ridge may subduct under the Ecuadorian margin at an age younger than 3-4 Ma.

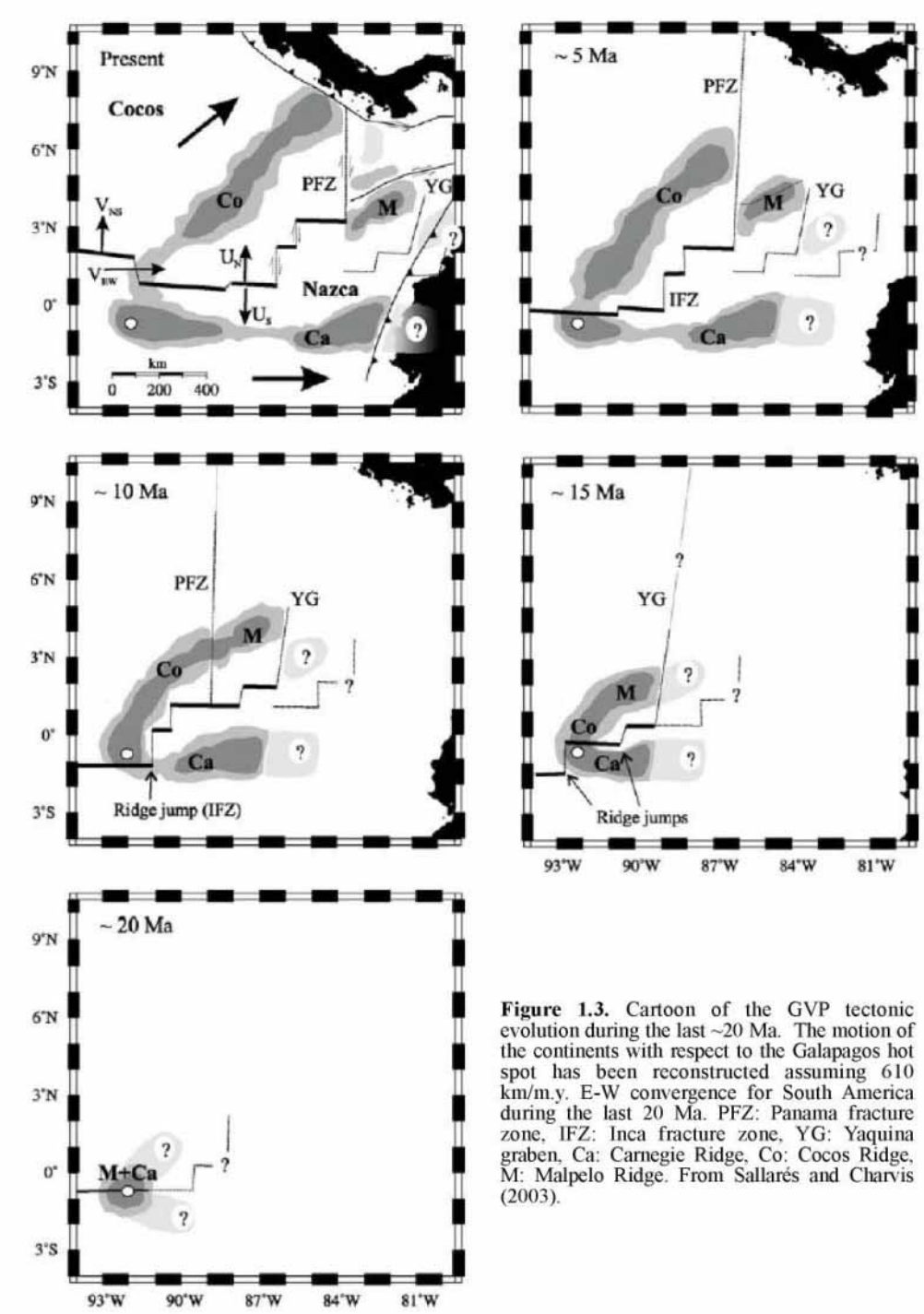

Figure 1.3. Cartoon of the GVP tectonic evolution during the last ~20 Ma. The motion of the continents with respect to the Galapagos hot spot has been reconstructed assuming 610 km/m.y. E-W convergence for South America during the last 20 Ma. PFZ: Panama fracture zone, IFZ: Inca fracture zone, YG: Yaquina graben, Ca: Carnegie Ridge, Co: Cocos Ridge, M: Malpelo Ridge. From Sallarés and Charvis (2003).

The oceanic plate that subducts under the South-America plate has been strongly controlled by the activity of the Galapagos hot spot and by the fragmentation of the Farallon plate. Geometric and magnetic reconstructions have been used to restore the relative motion of the Nazca plate from late Cretaceous time (Pilger, 1984; Pardo-Casas and Molnar, 1987; Somoza, 1998, Figure 1.2). The faster convergence (>100 mm/a) occurred between about 50 and 40 Ma and since 26-20 Ma. It has been related to large components of strike-slip deformation along the central part of the Andes and to the

formation of large transtensional basins in the Ecuadorian coastal area (Pardo-Casas and Molnar, 1987; Daly, 1989). The second step of fast convergence rate has been related to the fragmentation of the Farallon plate along the Grijalva fracture zone resulting in the formation of the Nazca and Cocos plates (Hey, 1977; Lonsdale and Klitgord, 1978,). At ~10 Ma the convergence rate showed a shallow decrease and remained constant to Present times (Pardo-Casas and Molnar, 1987). However a relatively strong decrease in convergence velocity has been proposed at 5 Ma at the northern Chile and northern Peru subduction zones (Somoza, 1998). These last three phases, at ~50, 26, and 10 Ma, coincide with phases of intense tectonic activity recognized in Peru and Ecuador: the late Eocene Inca phase and two of the Mio-Pliocene Quechua phases (Megard, 1984). On the other hand, the direction of the convergence showed a gradually reduction on dextral component since 60 Ma. However, the role of fragmentation and posterior accommodation of the Nazca South America system at ~25 Ma on the convergence direction is in debate (Pardo-Casas and Molnar, 1987; Somoza, 1998).

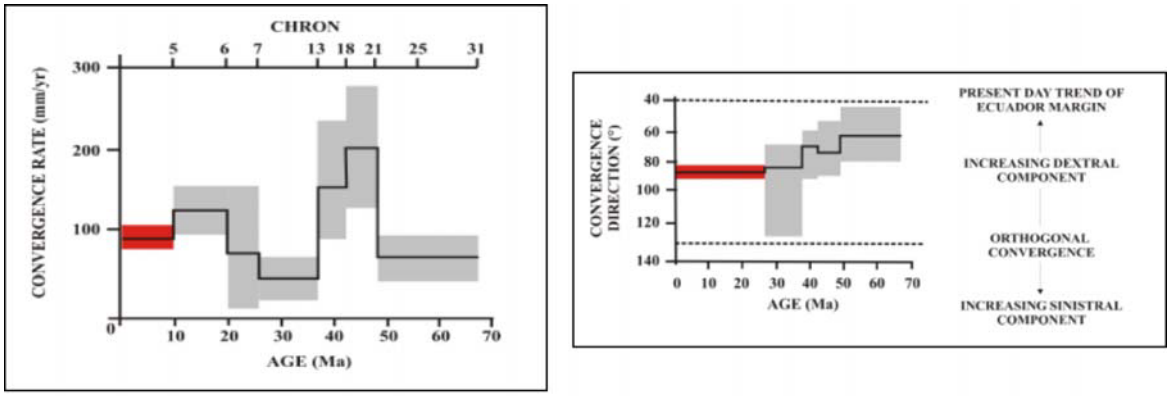

Figure 1.4. Convergence rate and direction (with uncertainty limits gray and red) for the Nazca South American plates system during Tertiary times. Note the constant convergence from 10 Ma to Present and constant convergence direction from 30 Ma to present. From Pardo-Casas and Molnar, 1987)

1.2.1.2 The current Nazca-South America plate structure

Along the Ecuadorian margin (2°N to 3°S), the Nazca plate subducts beneath the South American plate along a trench zone which convexity is turned to the west. The current convergence rate lies between 6 and 7 cm/yr with a main direction placed between N082 to N112 (De Mets et al, 1990; Freymuller et al, 1993; Kellog and Vega, 1995; Trenkamp, 2002). The analysis of the spatial distribution of seismicity obtained from temporal and global seismic stations data, allows to constraint the angle of the subducted slab from 25° to 35° from north to south of 2°N, respectively (Lonsdale, 1978; Alvarado, 1998; Guillier et al., 2001; Figure 1.5a). The convergence obliquity is not constant along the Ecuadorian trench. It shows an important change from N10E to N30 at ~0° latitude. This change in trend, and more specifically the existence of an important trench-parallel seismic moment

release, shows that motion partitioning takes place along the Ecuadorian trench (Ego et al., 1996). The elastic modeling of GPS-derived horizontal displacement suggests an apparent 50% of convergence locking at the subduction interface along the Carnegie ridge subduction zone, which enhanced strain accumulation along the Ecuadorian forearc zone (Trenkamp et al., 2002; White et al., 2003; Figure 1.5b). The strongest velocity vectors placed at the Ecuadorian forearc are interpreted as a strong transfer of movement from the subducting plate. On the other hand, the Carnegie ridge and the Grijalva fracture zone (GFZ) subduct beneath the Ecuadorian margin, influencing the subduction regime along the Ecuadorian trench.

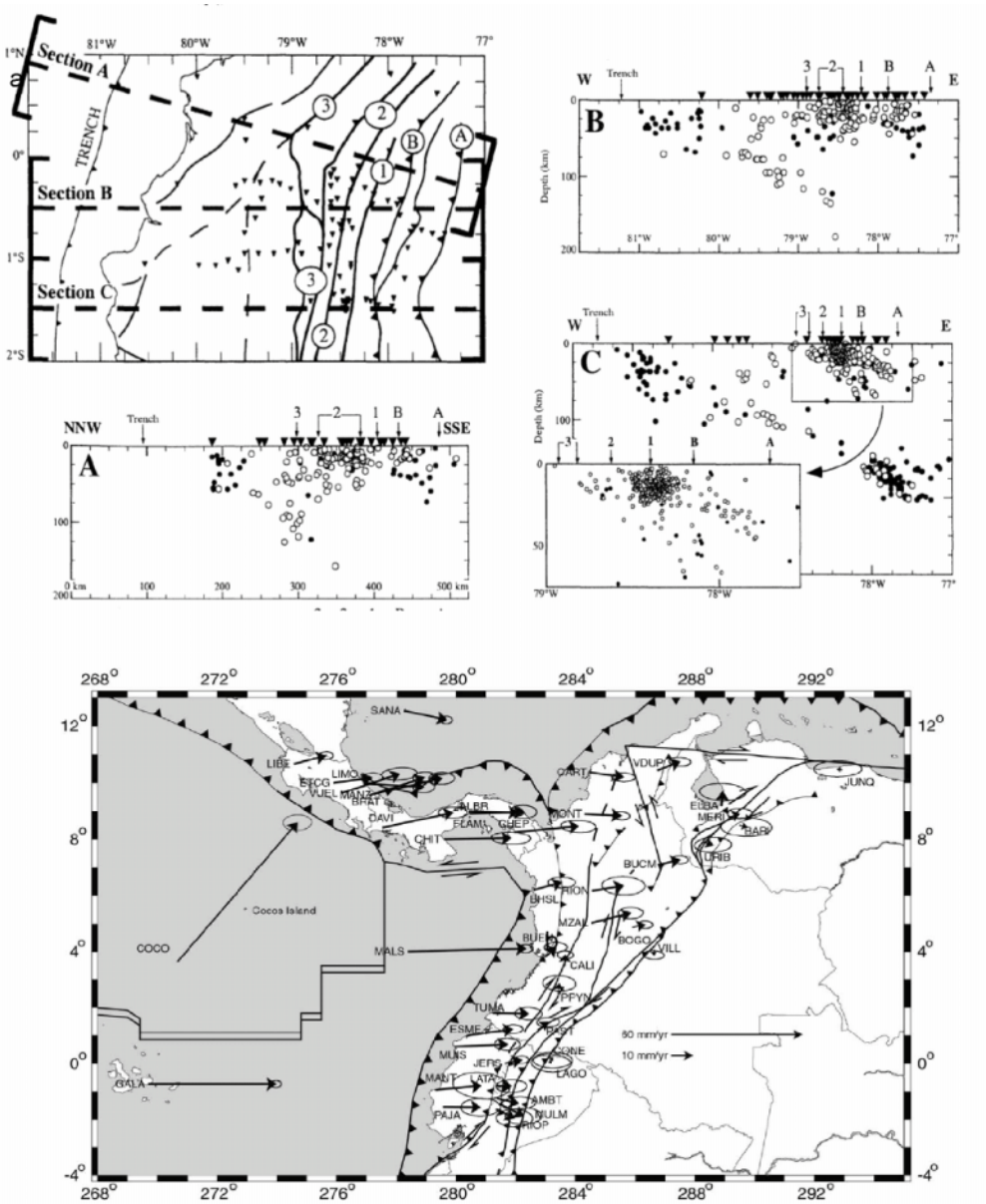

Figure 1.5. a) Maps showing the seismicity distribution in the range A, 0-25 km; B, 25-75 km; and C, 75-300 km. Open circles represent events using a temporary network data, from Guillier et al. (2001) **b)** Station velocity vectors relative to stable South America, from Trenkamp et al. (2002).

1.2.1.3 The Grijalva fracture zone

The Grijalva fracture zone (GFZ) subducts obliquely under the South-America plate near 3° S at the latitude of the Gulf of Guayaquil zone. It separates two different domains of age. To the south the Nazca plate is ~35 Ma, while to the north of the GFZ, the Nazca plate shows a 22-26 Ma age coherent with the proposed age for the break of the Farallon plate (Hey, 1977; Lonsdale and Klitgord, 1978). The GFZ is underlined by a ~700 m marine scarp trending in an N40-60 direction. (Hey, 1977; Lonsdale and Klitgord, 1978). The difference in age across the GFZ caused a regional change in basement depth of up to 700 m between the Carnegie platform and the Peru basin (Rea and Malfait, 1974). Dumont et al., (2004) have linked a period of tectonic inversion along structures observed in the Puná and Santa Clara islands to the GFZ subduction. This is almost the only model that relates upper-plate deformation to the subduction of the GFZ. However, the trench and forearc deformation related to the subduction of the GFZ remain poorly constrained. Probably the main aspect to analyze the relationship between the GFZ subduction and the deformation of the overriding plate is the migration of the collision zone due to the high angle between the GFZ and the trench. This geometrical aspect has been used to characterize the deformation zones along the Peruvian continental margin related to the incoming oblique Nazca ridge (i.e. Hampel et al., 2004). Taking into account an E-W directed convergence, a N10 trench direction and a N50 to N60 trending of the GFZ the zone of subduction of the GFZ might migrates to the south at ~30 to 45 mm/yr. However, no clear tectonic expression is observed in the continental margin as an expression of the GFZ subduction and its southward migration.

1.2.1.4 The Carnegie ridge.

The Carnegie ridge (CR) is the superficial expression of an over-thickened oceanic crust, of 15 km thick along its central part and 14 km along its southern flank (Sallarès and Charvis, 2003; Graindorge et al., 2004). It is proposed that the ridge is bounded to the north and south by large normal faults, which have vertical offsets of 200 to 500 m and were probably formed by differential contraction of varying thickness of cooling lithosphere (van Andel et al., 1971). In the eastern part of the ridge these faults enter the trench zone obliquely (Lonsdale, 1978). The axial trench profile shows the subducting ridge where the trench floor is about 1 and 1.5 km shallower than along southern Colombia and northern Peru, respectively. Recent evidence (Sage et al., 2006) shows that at the intersection with the underthrusting Carnegie Ridge, the thinning of the Ecuadorian margin basement is associated with pervasive seaward-dipping normal faults. Normal faults are caused by margin collapse associated with subduction erosion along a relatively low-friction plate interface under the continental slope (Sage et al., 2006). Where seamounts of the Carnegie Ridge enter the subduction zone, a marked subduction

channel structural patchiness may affect subduction erosion processes. In this area, several-kilometers-wide subducting sediment lenses retain large amount of fluids that cause overpressure as they are gradually underthrusted beneath the margin basement (Sage et al., 2006).

Seamount subduction has been proposed as a major element (among others factors) in the control of several aspects including: the increase of interplate coupling (Cloos, 1992; Scholz and Small, 1997), the location of uplift and subsidence along convergent margins (i.e. Gardner et al., 2001), the increase of subduction-erosion processes (i.e. Hampel et al., 2004), as a barrier on lateral earthquake rupture propagation (i.e. Kodaira et al., 2003) or as an inhibitor of thrust type subduction earthquakes (i.e. Bangs et al., 2006). Many of these aspects have been linked to the CR subduction. Even so, doubts persist about the fact that the subduction of the ride imprints a strong impact in the tectonic segmentation of the North Andean margin. Two major observations show that the CR is currently subducting beneath the South American continental margin: 1) direct observations based on wide-angle refraction data show that the CR has been subducting beneath the South-America plate for at least 1.4 my (Graindorge et al., 2004), and 2) a GPS-derived velocity model shows that the eastward convergence of the Nazca plate imprints a relatively strong eastward motion on the Ecuadorian forearc area. The increase of the velocity field in front of the CR subduction zone shows the high degree of interplate coupling occurring at this zone (Trenkamp et al., 2002; White et al., 2003; Figure 1.5b).

Generaly, models of the GPV evolution (Figures 1.2 and 1.3) suggest that ridge-trench collision occurred at the Pliocene–Pleistocene boundary (Rea and Malfait, 1974; Hey, 1977; Lonsdale, 1978; Lonsdale and Klitgord, 1978; Wilson and Hey, 1995). However, older ages for the ridge collision were proposed including the late Miocene (Pilger, 1984) and the early Miocene (Malfait and Dikleman, 1972).

The subduction of the CR has been one of the most used and, at the same time one of the most enigmatic features on Ecuadorian geology. Coastal uplift and subsidence, volcanic signatures, Andean construction, intermontane basin formation and other offshore and continental features have been considered as ridge induced, involving very different ages for the beginning of the ridge subduction. Some of these models include:

- Seismic reflexion profiles and bottom samples were used by Lonsdale (1978) to suggest a 2-Ma age for the beginning of the CR subduction. The subduction of the ridge is considered as the main factor in controlling the change of the trench axis direction from N10°E to N25°E.

- Graindorge et al. (2004) suggested that the strong normal stress related to the CR buoyancy, together with a larger surface involved in the subduction (inherent to the ridge itself), would locally

enhance the mechanical coupling between the plates and would therefore be responsible for an increase in the recurrence interval of large earthquakes.

- Regional and local works carried out in the whole Ecuadorian forearc region reach different conclusions about the ridge induced tectonic steps and their ages. Benitez (1995) suggests that the tectonic inversion of the Manabí basin (see Figure 1.8 for location of forearc basins) is triggered by the subduction of the ride in Quaternary times. Aalto and Miller (1999) suggest that a late Pliocene switch from trench-parallel extension to almost trench-orthogonal extension is possibly related to subduction erosion beneath the accretionary wedge, which probably resulted from the encroachment and collision of the leading edge of the continent with the thick crust of the CR. The origin and chronology of Pleistocene marine terraces and subsidence-uplift relations has been also used to constraint CR subduction. Cantalamessa and Di Celma (2004) propose that the encroachment and collision of the ridge with the Ecuadorian margin probably resulted in basal tectonic erosion beneath the upper plate favoring the emplacement of trench-normal extension and extremely rapid subsidence during the late Pliocene along the Ecuadorian coast. They suggest that after the late Pliocene subsidence progressively decreased as the CR subducted beneath the continental plate, favoring a subsequent regional uplift. A similar conclusion is presented by Pedoja et al. (2006) especially concerning the age of the subduction.

- Based on relations between basin subsidence and basement uplift in the frame of a southward ridge migration, Gustcher et al., (1999) suggest a ridge collision since 8 Ma involving at least 110 km of subducted ridge beyond the Ecuadorian continental forearc.

- Spikings et al. (2001) consider that fission-track derived cooling ages along the Cordillera Real are related with CR subduction. This model suggests that the collision of the ridge at the trench at ~15 Ma resulted in elevated cooling and exhumation rates in the north and extension in the south (i.e. south of 2°45S). This signal being stronger at ~9 Ma. More to the south, the inversion of the intermontane basins in the Cuenca and Loja areas has been also related to the subduction of the ridge at ~9 Ma (Steinmann et al., 1999; Hungerbühler et al., 2002).

- An adakitic imprint on the rocks of the current volcanic arc, combined with a flat-slab subduction model (Gustcher et al., 1999) is considered as a response to the subduction of the CR beneath the margin probably 5 Ma ago (i.e. Bourdon et al., 2003; Samaniego et al., 2002).

Some of these aspects described here may not have any relation to the CR subduction once a wider regional observation is considered (Witt et al., 2006; Michaud et al., in prep.).

1.3 THE CONTINENTAL MARGIN

Lonsdale (1978) obtained the first constraints of inner and outer disposition and evolution of the Ecuadorian trench. He argued that the Ecuadorian trench differs from most of the trenches in being very shallow, with an axis less than 3 km depth in average, in having unusually large normal-fault scarps on the lower oceanic slope and in lacking an along strike axis of turbidites. However, little was confirmed about the margin evolution upwards from the trench. Multichannel reflexion and wide angle refraction data obtained during the SISTEUR expedition offered a more detailed evolution of the entire Ecuadorian continental margin. Collot et al. (2002) charracterized the main aspects on margin architecture and evolution (Figure 1.6). Within 10-20 km of the trench, the shallow section of the plate interface separates vertically deformed margin rocks or accreted trench sediments from underlying sediments that appear to constitute the subduction channel (Figure 1.6). From the Carnegie ridge to the Gulf of Guayaquil latitude, the Ecuadorian margin shows seaward dipping reflectors and acoustic basement being truncated downward at the plate interface, suggesting that the margin underwent severe tectonic erosion.

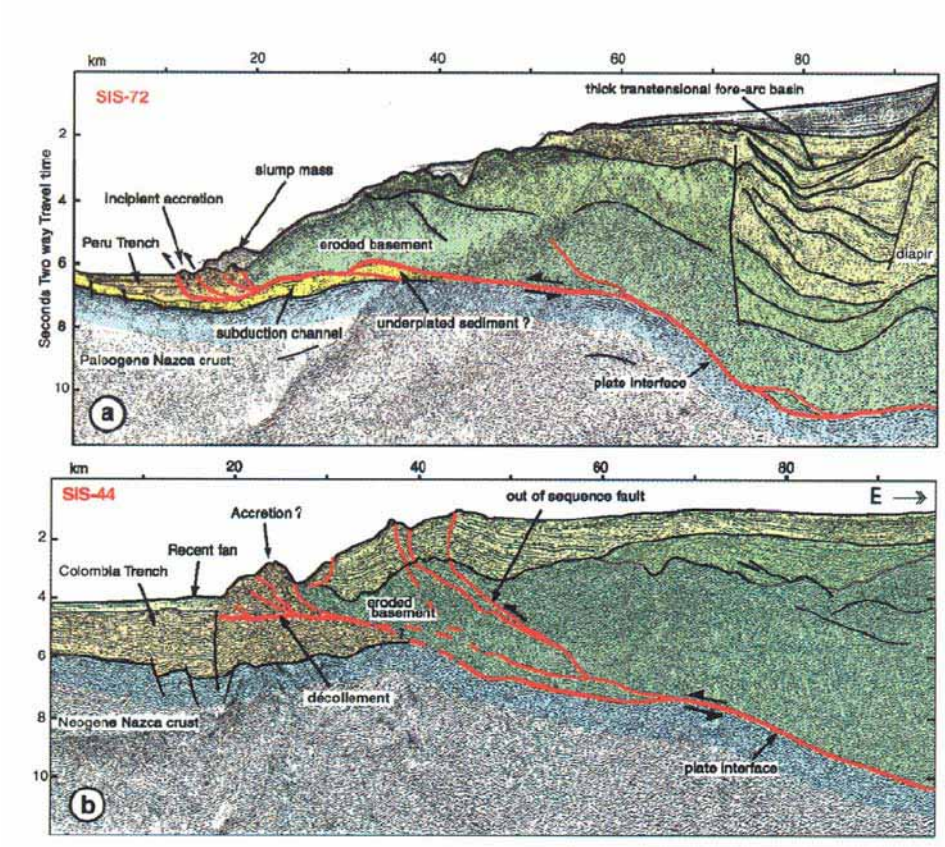

Figure 1.6. Seismic lines along the Ecuadorian continental margin. a) along the Gulf of Guayaquil latitude and b) along the Ecaudor-Colombia border. From Collot et al. (2002)

This tectonic erosion regime has been recently refined by Sage et al. (2006) who proposed that a patchiness character of the subduction channel modulates subduction erosion processes, by alternately favoring margin basement weakening and material removal. West of the Gulf of Guayaquil trench sediment offscrapping results in an incipient 8 km wide accretionary wedge which is locally overlain by mass wasting deposits, while the ~0.5 s TWTT thick Nazca plate pelagic sediments subduct beneath the margin over a minimum distance of ~25 km (see also section 2.1, Figure 2.2). On the opposite, in southern Colombia, a 30 km wide accretionary wedge has developed north of 3°N from a 1.2 s TWTT thick trench fill (Collot et al., 2006), suggesting along-trench variation in the subduction regime, from subduction-accretion to the north of 1°N to subduction-erosion south of ~1°S. The subduction erosion regime probably continues further south to the north Peruvian continental margin (Bourgois et al., 1988).

1.4 MAIN TECTONIC EVOLUTION FEATURES ALONG WESTERN ECUADOR

1.4.1 Accretionary processes.

The coastal zone corresponding to the Ecuadorian forearc, is a 100-150 km zone located between the shoreline and the foot of the Andes. The coast zone shows a flat morphology only contrasted by the E-W trending Cordillera Chongón-Colonche and the N-S trending Cordillera Costera. The Ecuadorian forearc basement, as well as the Cordillera Occidental, is composed of several tectono-stratigraphic units of oceanic origin. Mapping of these terranes allowed distinguishing several tectonic units, separated by major faults and characterized by distinct geological evolutions. For each terrane, stratigraphic studies led to identify major unconformities, which separate oceanic rocks devoid of detrital quartz (plateau basalts and dolerites, arc lavas and volcaniclastic rocks, radiolarian bearing cherts), from the overlying quartz-bearing clastic sediments (i.e. turbidites, marine shelf sandstones, subaerial conglomerates). The latter are interpreted as sealing the collision of the oceanic terrane with the continental margin (i.e. Jaillard et al. 2004), and therefore allow to date the accretion events. However, due to the variable lithology and nature of the rocks involved in the accretionary processes (Figure 1.7) it has been complex to propose a single stratigraphic and evolution model. In this way one to four accretionary periods have been proposed for coastal and Cordillera Occidental building.

Many works proposed different models which lead not only to different ages for the accretion processes but even to substantial differences in the involved stratigraphic units. A detailed review of the broad proposed models lies far away of the scope of this work. However, in a wide sense, two major accretionary events have been defined by almost all authors. From a wide variety of data and evolution-derived models (i.e. Bourgois et al., 1987 and 1990; Hughes and Pilatasig, 2002; Kerr et al.,

2003; Mamberti et al., 2003; Jaillard et al., 2004; Toro et al., 2005; Vallejo et al., 2006) these two major accretions events are: 1) a late Cretaceous (65-85 Ma) event involving the Pallatanga terrane (San Juan and Guaranda units) and 2) a middle-late Eocene event involving the Macuchi terrane (Macuchi and Naranjal units altogether with the Piñon Fm.). However, Kerr et al (2002) suggest that the Pallatanga terrane corresponds to the Caribean plateau originated over the Galapagos hot-spot while the Macuchi terrane (Figure 1.7) originated from a more southerly hot-spot region located at ~30°S. Subsequently, Kerr et al. (2005) re-define this interpretation, suggesting that the Pallatanga-Macuchi and Piñon terranes accreted together and that the late Eocene event occurs only along the northwestern zones of Ecuador (i.e. Naranajal unit). On the other hand, recently, Luzieux et al. (2006) suggest that only one acretional process at ~75-65 Ma is needed to explain the existence of all the blocks, this accreted material origination from the Caribbean plate.

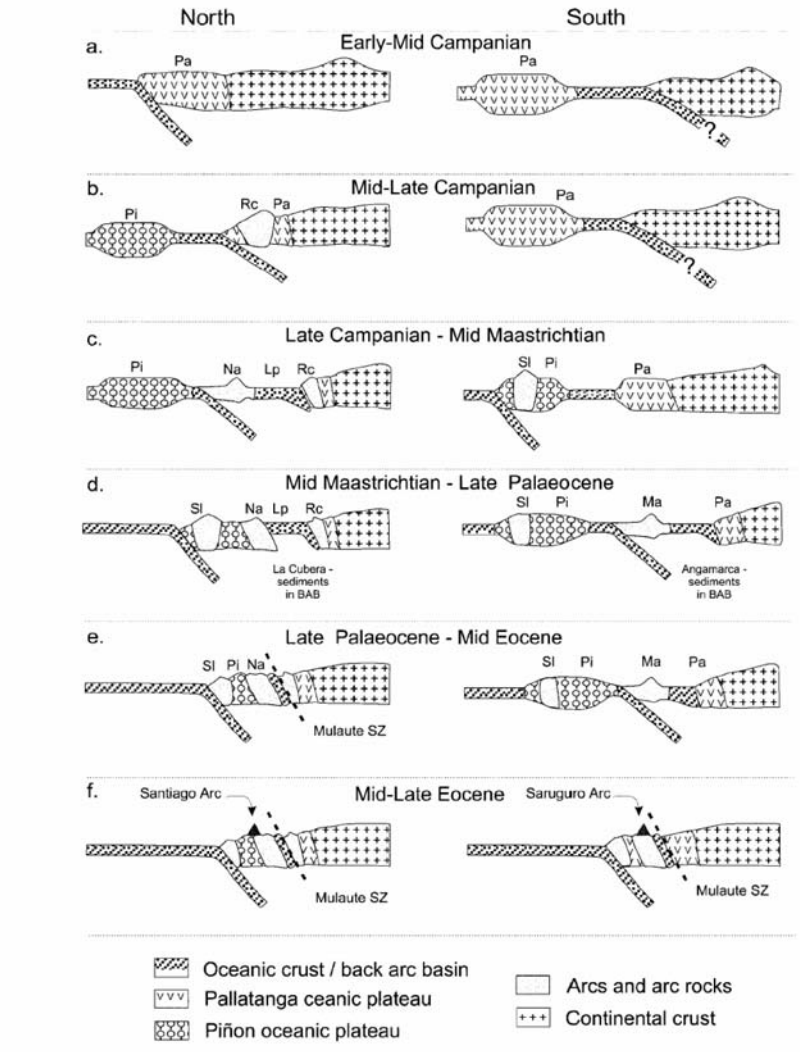

Figure 1.7. Schematic cross-sections (all from west to east) depicting the tectonic development of the Ecuadorian continental margin in the north (0°) and in the south (2°S). Pa, Pallatanga; Rc, Rio Cala; Lp, La Portada; Sl, San Lorenzo; Pi, Pinon; Ma, Macuchi; Na, Naranjal. BAB, back-arc basin; SZ, shear zone. From Kerr et al. (2002).

1.4.2 Forearc evolution

The Piñón Formation is regarded as the Cretaceous igneous basement of the Ecuadorian coast. It is made up of tholeiitic basalt-andesitic pillow basalts and massive flows, locally associated with pillow breccias, hyaloclastites and subordinate siliceous sediments (Goosens and Rose, 1973; Feininger and Bristow, 1980; Walrabe-Adams, 1990). This basement is interpreted as an accreted fragment of an overthickened and buoyant oceanic plateau (Reynaud et al., 1999). The age of the Piñón Formation remains controversial; Reynaud et al. (1999) propose an age of 123 Ma while more recently Luzieux et al. (2006) suggest a 87-90 Ma age. The differences between these ages have huge consequences on the interpretation of oceanic terranes accretions (see above). An early Paleocene to pre Middle Eocene deformation step is triggered by the collision and posterior accretion of the Piñón terrane, which is considered to take place during the Paleocene-early Eocene (Daly, 1989, Benitez et al., 1993; Benitez, 1995; Jaillard et al., 1997; Reynaud et al., 1999). The tectonic phases of Paleocene-Lower Eocene age coincide with major geodynamic reorganization (between 50 and 56 Ma) of the convergence direction (Pardo-Casas and Molnar, 1987). The accretion of the oceanic terranes has been related either to the change of the convergence direction of the paleo-Pacific plate from N-S or NNE to N-E (Benitez et al., 1993), or to overthickened characteristics of the oceanic plateau-related Piñón Fm. which prevents its normal subduction (Reynaud et al., 1999).

The post-collision period is considered as the formation of the forearc *sensu stricto* (Figures 1.8 c and d; Benitez, 1995) and more specifically the period after the reorganization of the Farallon plate at 24-26 Ma (i.e. Hey, 1977). From early Miocene to Present times, three main aspects (setting the Carnegie ridge subduction aside, see section 1.2.1.4) are relevant on the evolution of the Ecuadorian forearc: 1) the uplift of the Cordillera Costera which results in the emplacement of the actual drainage system, i.e. major input to the GGTB and the Esmeraldas areas, 2) the tectonic erosion of the continental margin and 3) the oblique subduction (i.e. Daly, 1989; Benitez, 1995; Jaillard et al., 1997).

The change of the convergence rates in the Lower Miocene is at the origin of the coastal forearc basin formation (Benitez, 1995). In this phase four major forearc basins are formed: the Borbón, Manabí, Progreso and Golfo de Guayaquil basins. The paroxysm of sedimentation is related with the Progreso and Angostura Fms, along the Progreso and Manabí-Borbón basins respectively. The basin formation has been related to dextral shear affecting the coastal region in response to oblique subduction at the Ecuadorian trench along pre-existing suture zones (Daly, 1989; Benitez, 1995). The Figures 1.8c and 1.8d show the progressive northward escape of a forearc sliver, resulting from oblique subduction. The stratigraphy and sedimentological features allow dividing the forearc evolution in a three steps development history (Deniaud, 2000). The firs step is marked by a

widespread fine marine transgressive sedimentation that affects the entire forearc area. The second stage turns to a marked sandy sedimentation with shallow water sedimentary structures. The third stage corresponds to the last sedimentary cycle that started at the beginning of the Pliocene and remains at present. It is marked by different tectono-sedimentary units with emergent and current subsidence zones. For Benitez (1995) the emersion phases are not related with major changes in convergence rate but to the arrival of oceanic asperities such as the Nazca and Carnegie ridge (Progreso and Manabí basins, respectively)

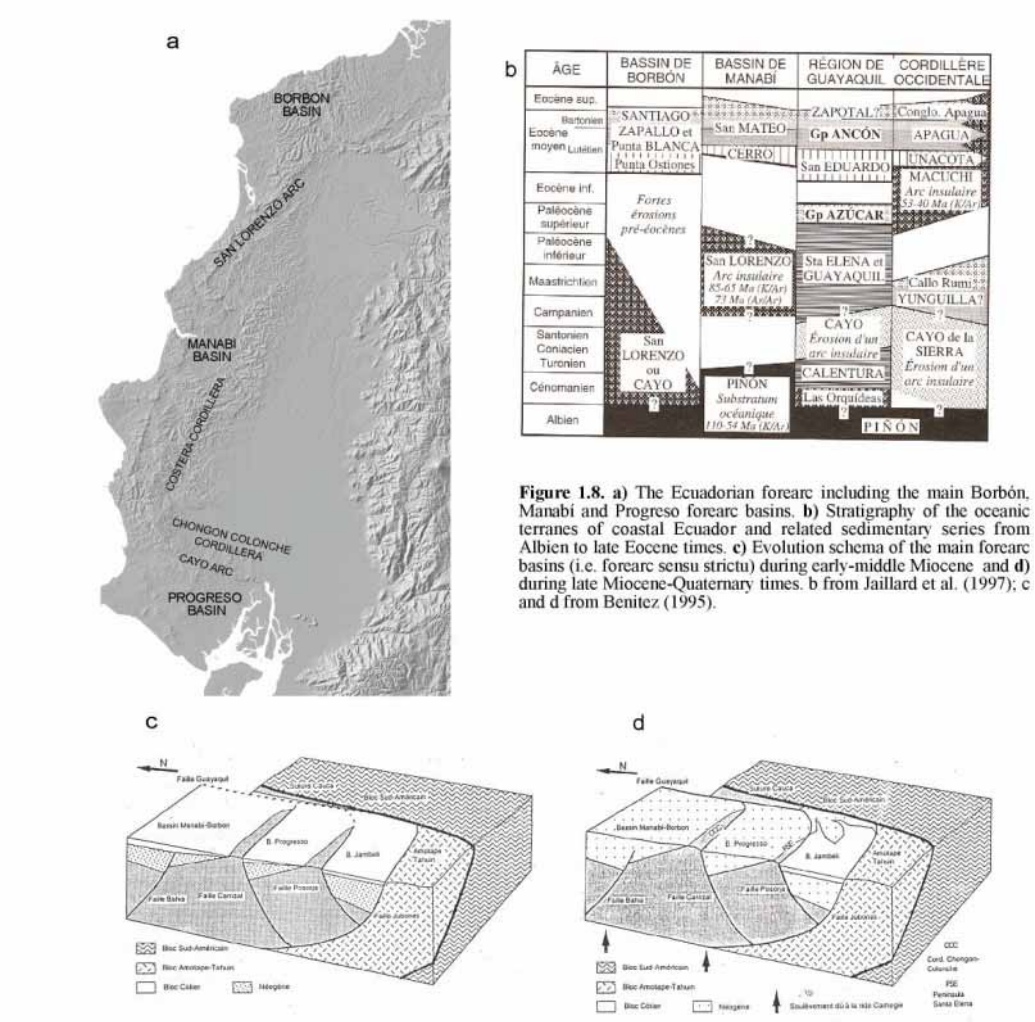

Figure 1.8. a) The Ecuadorian forearc including the main Borbón, Manabí and Progreso forearc basins. **b)** Stratigraphy of the oceanic terranes of coastal Ecuador and related sedimentary series from Albien to late Eocene times. **c)** Evolution schema of the main forearc basins (i.e. forearc sensu strictu) during early-middle Miocene and **d)** during late Miocene-Quaternary times. b from Jaillard et al. (1997); c and d from Benitez (1995).

1.4.3 The North Andean Block

The North Andean Block (NAB) is located along the northwestern zone of South America. The existence of this detached micro plate between the Nazca and South America plates (between Ecuador and Venezuela, Figure 1.9a) was first formally proposed by Pennington (1981). However, some approximations were already suggested by Case et al. (1973) and Campbell (1974), who first

proposed the now disused term of 'Dolores-Guayaquil fault system' to define the NAB eastern limit. The rate of NAB northward migration has been estimated between 0.6 to 1 cm/yr (Freymuller et al., 1993; Kellog and Vega, 1995; Trenkamp et al., 2002; White et al., 2003). Generally, all of the limits of the NAB are a matter of discussion.

The eastern boundary of the NAB is in debate. Seismicity distribution along the Ecuadorian Andes coincides with ancient suture zones suggesting reactivation or tectonic inversion of late Jurassic to early Tertiary east-dipping suture zones (Guillier et al., 2001). The reactivation of the suture zones was also proposed by Litherland and Aspden (1992). Nevertheless, the distribution of neotectonic structures (Eguez et al, 2003) does not always matches the ancient suture zones. Winter and Lavenu (1989), Soulas et al. (1991) and Ego et al. (1996) described the NAB limits as a major system of dextral faults crossing the Ecuadorian Andes through several active fault segments, such as the Pallatanga fault, the thrust faults along the Inter-Andean Valley, and the Chingual-La Sofia fault, from south to north (Figure 1.9 a). A complex array of structures accommodates the NAB migration along the Ecuadorian Andes. It seems that the system that accommodates the NAB northward migration is composed mainly of dextral transcurrent and reversal structures placed in the both Cordilleras, forming together a crustal restraining bend (Ego et al., 1996; Winkler et al., 2005).

The characterisation of the Pallatanga fault (or Calacalí-Pallatanga fault, Figure 1.9a and 1.9b) has been widely documented in Winter and Lavenu (1989 and 1989b); Lavenu (1990); Winter (1990) and Winter et al., (1993). They proposed that the Pallatanga fault extents from the Gulf of Guayaquil region to the south of the Chimborazo volcano. However, only the northern segment, which follows the Rio Pangor valley at elevations above 3600 m is prominent in the morphology. It displays clear morphological evidence of right lateral movement. The fault strikes N30E and dips 75° to the N-W while the slip vector projected on the fault plane shows a slight reverse component with a pitch of about 11.5° to the S-W. Offset morphological features, which can be inferred to be of early Holocene age indicate a main Holocene slip rate of 2.9-4.6 mm/yr. This rate is corroborated by long-term offsets related to the three last glacial terminations.

North of the Pallatanga fault the main Holocene strike-slip-related deformation is placed along two different corridors:

- The western corridor extends along the Occidental Cordillera. Evidences of Quaternary activity are located in the northern structures of the corridor. In Ecuador and southern Colombia regions (see Paris et al., 2000 and Eguez et al., 2003) the Nanegalito, El Angel and San Isidro faults connect north to the Buesaco Aranda fault (Romeral fault system). These faults have yielded strike-slip rates between 1 to 5 mm/yr (Figure 1.9b). In Colombia this

corridor extends along the Romeral fault system (i.e. the Paraiso, Piendamo and Rosas sections; Paris et al., 2000), which correspond to the most active parts of the Romeral system, yielding 0.2 to 1 mm/yr dextral slip rates.

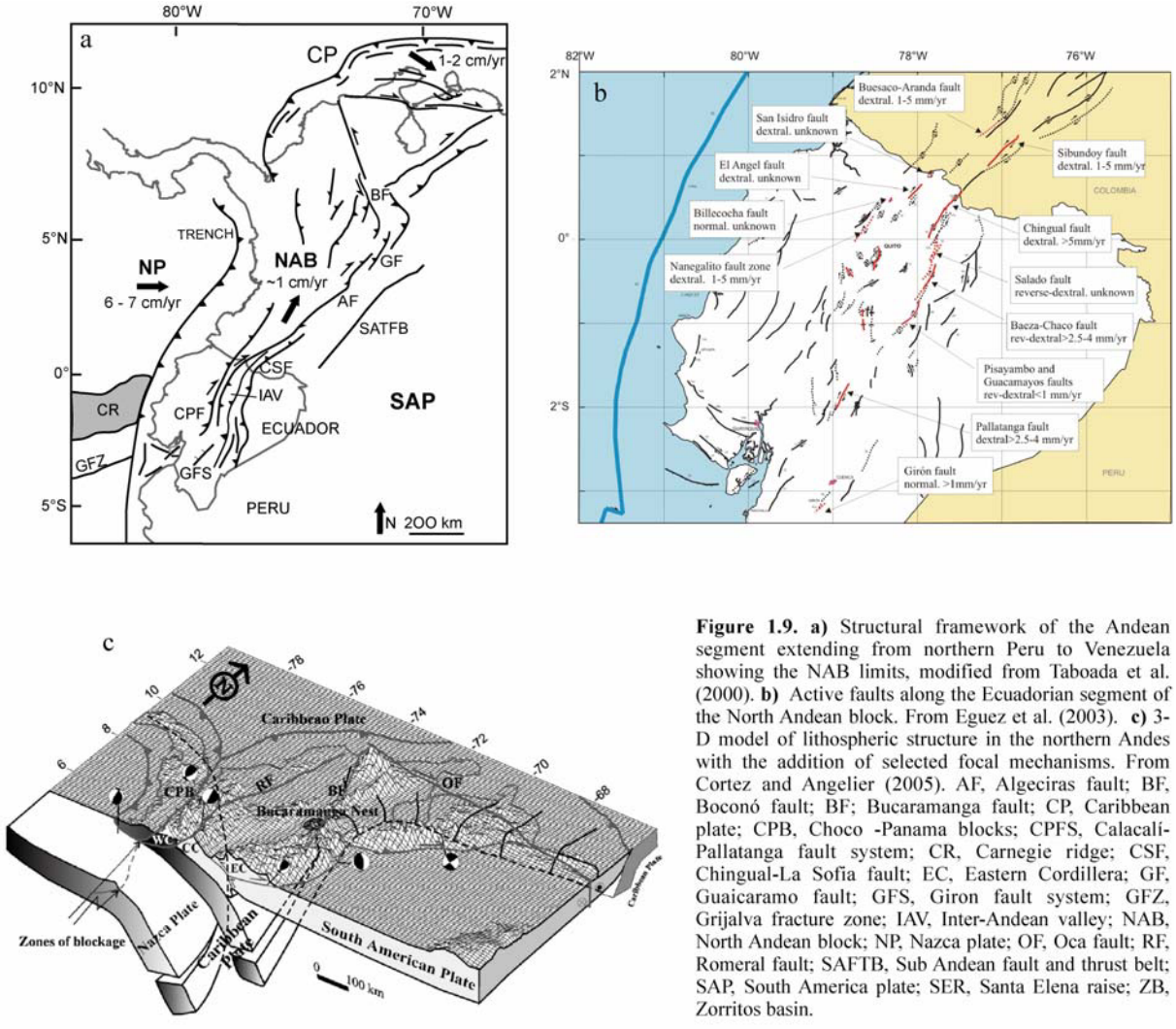

Figure 1.9. a) Structural framework of the Andean segment extending from northern Peru to Venezuela showing the NAB limits, modified from Taboada et al. (2000). **b)** Active faults along the Ecuadorian segment of the North Andean block. From Eguez et al. (2003). **c)** 3-D model of lithospheric structure in the northern Andes with the addition of selected focal mechanisms. From Cortez and Angelier (2005). AF, Algeciras fault; BF, Boconó fault; BF; Bucaramanga fault; CP, Caribbean plate; CPB, Choco -Panama blocks; CPFS, Calacalí-Pallatanga fault system; CR, Carnegie ridge; CSF, Chingual-La Sofia fault; EC, Eastern Cordillera; GF, Guaicaramo fault; GFS, Giron fault system; GFZ, Grijalva fracture zone; IAV, Inter-Andean valley; NAB, North Andean block; NP, Nazca plate; OF, Oca fault; RF, Romeral fault; SAFTB, Sub Andean fault and thrust belt; SAP, South America plate; SER, Santa Elena raise; ZB, Zorritos basin.

- The eastern corridor show longer and more linear Quaternary structures (see Paris et al., 2000 and Eguez et al., 2003). The Pisayambo, Baeza-Chaco, Salado and Chingual faults form the Ecuadorian section (Figure 1.9b). To the north this system extends along the Sigbundoy fault. Almost all these faults show 1-5 mm/yr slip rates. In Colombia along the so called 'Eastern front' all structures show dextral to reverse component of deformation yielding slip rates between 1-5 mm/yr.

It has been proposed that the coastal zone shows no important structure related to NAB migration since it acts as a rigid buttress transferring the stress from the subduction to the Andes (Guillier et al., 2001; Trenkamp et al., 2002). The southern Ecuadorian segment of the eastern boundary of the NAB has been considered as the structure that is at the origin of the Golfo de Guayaquil basin (i.e. Deniaud et al., 1999). The so called 'Puná fault' has been generally correlated directly with the Pallatanga fault.

The evolution of the Santa Isabel basin, as well as the evolution of the Cañar and Azogues basins have been also related, direct or indirectly, with the NAB northward drifting (Winter and Lavenu, 1989b; Hungerbühler et al., 2002; Bourgois et al., in prep).

Tectonic models suggest that the obliquity vector of convergence between the Nazca and South America plates is not fully partitioned throughout the NAB and that the Caribbean plate influenced mainly the area north of 5°N (Ego et al., 1996; Taboada et al., 2000; Corredor, 2003; Acosta et al., 2004; Cortés et al., 2005, Figure 1.9c). The transition zone being located along a major seismically E-W transform zone at ~5°N coincident with the Baudo range (Figure 1a) (Taboada et al., 2000). If only the region south of 5°N is influenced by the Nazca plate oblique convergence, which induces a right-lateral stress regime (i.e., northward drifting of the NAB) the accommodation of the deformation is more complicated than that involved in a single block moving northward as proposed from GPS data (Trenkamp et al., 2002).

Similarly the southern limit of the NAB is also a matter of debate, being directly related with the Gulf of Guayaquil evolution. This aspect is discussed in the section 2.1.

CHAPTER II

ANALYSIS OF THE TECTONIC DEFORMATION AT THE NORTH ANDEAN BLOCK TRAILING EDGE.

2.1 INTRODUCTION

The southern tip of the North Andean Block (NAB, i.e. its trailing edge), is characterised by several Neogene basins located in southwestern Ecuador and northwestern Peru. These basins include the Progreso, Esperanza, Jambelí and Tumbes basins. The 100-120 km long and 20-120 km wide Gulf of Guayaquil shelf zone (~3°S to 4°S) appears as the most prominent gulf of the Central and South American coasts, and constitutes the natural limit between the Ecuadorian coastal block (accreted oceanic basement) and the North Peru continental basement. It is a considerable subsiding area and sedimentary infill linked to the river Guayas major influx, which corresponds to one of the two major Ecuadorian drainage systems. The direct relationship between the NAB drifting and the opening and posterior evolution of the Gulf of Guayaquil-Tumbes basin was proposed in the 70's (Campbell, 1974). The combination between a high subsidence and a high sediment input produce locally the accumulation of at least 3500 m of Quaternary sediments in the area.

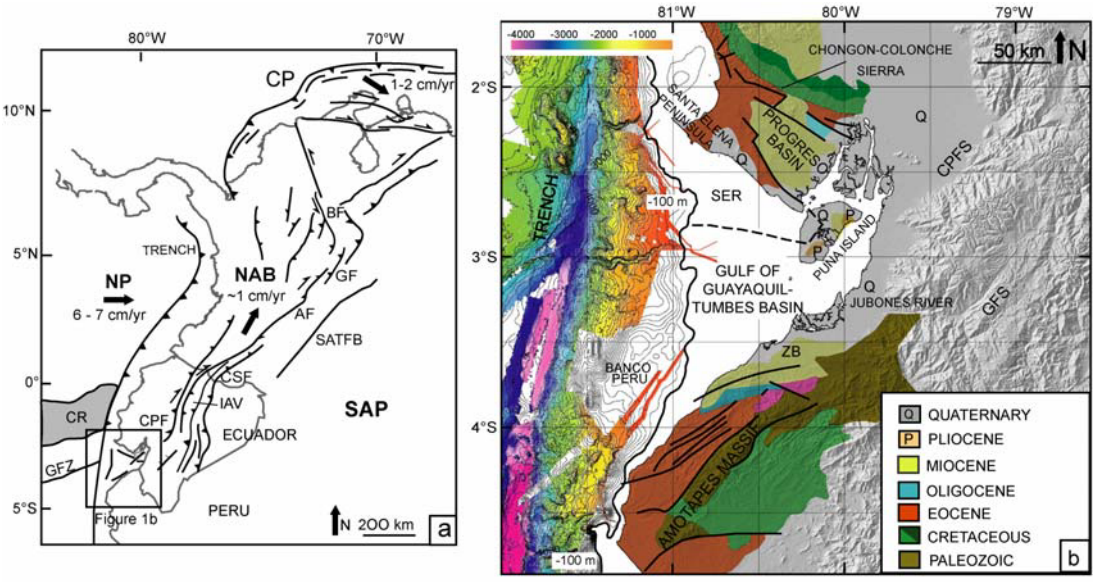

Figure 2.1. a) Structural framework of the Andean segment extending from northern Peru to Venezuela showing the NAB limits, modified from Taboada et al. (2000). **b)** Structural sketch of the Gulf of Guayaquil-Tumbes basin (GGTB) area, including the main continental features. Bathymetry of the continental margin and trench is a compilation of data from the Seaperc cruise of the R/V Jean Charcot and the Andinaut cruise of the R/V L'Atalante. Black line is the -100 m bathymetric contour that grossly follows the shelf-continental margin limit. Geology from, Zevallos (1970) and Benitez (1995). Legend is for both Figures 1a and 1b. AF, Algeciras fault; BF, Boconó fault; CP, Caribbean plate; CPFS, Calacalí-Pallatanga fault system; CR, Carnegie ridge; CSF, Chingual-La Sofia fault; GF, Guaicaramo fault; GFS, Giron fault system; GFZ, Grijalva fracture zone; IAV, Inter-Andean valley; NAB, North Andean block; NP, Nazca plate; SAFTB, Sub Andean fault and thrust belt; SAP, South America plate; SER, Santa Elena raise; ZB, Zorritos basin.

The northern edge of the Gulf of Guayaquil exhibits mafic and ultra-mafic Cretaceous rock basement that crops out extensively along the E-W trending Chongón-Colonche sierra (Figure 1b). This basement results from the accretion of oceanic terranes during late Cretaceous (Luzieux et al., 2006) or during Palaeocene-Eocene time (Benitez, 1995; Jaillard et al., 1997, and references therein). The oceanic basement is partially overlain by Palaeocene to Eocene series cropping out at the Santa Elena Peninsula and extending southward along the Santa Elena rise. Further south, sediments of Oligocene to Quaternary age accumulated along the Progreso basin, the GGTB and the Zorritos basin (ZB, Figures 1b and 2b). The southernmost edge of the Zorritos basin shows a Palaeozoic-Cretaceous metamorphic basement outcropping along the Amotapes massif. The metamorphic series show a varying metamorphism including some HP assemblages related to crustal thickening and exhumation during latest Jurassic-early Cretaceous accretional processes (Bosch et al., 2002, and references therein). Upper Cretaceous to Quaternary sediment dipping towards the GGTB unconformably overlies this basement.

2.2 PREVIOUS WORKS

First attempts to describe the evolution of the thick basins at the shelf and continental margin areas aimed at establishing constraints on hydrocarbon generation. Seismic records as well as several industrial drilling wells were done at the Esperanza and Tumbes basin during petroleum exploration at the beginning of the 80's. The main aspects of the studies carried out along the GGTB have dealed with the two major aspects of Gulf of Guayaquil evolution: the age of the subsidence steps and the location of the transcurrent structures being at the origin of this subsidence. Several theories as well as terminologies have been used in order to define the depocenter distribution along the NAB southern tip. The main proposed models include:

- The work of Sheperd and Moberly (1981) corresponds to the first work based on seismic data. They proposed that the Progreso pull-apart basin (i.e. Esperanza and Tumbes basins in this work) develops in response to NAB northward drifting during Neogene times. The escape tectonics-related pull-apart basin having its seaward transcurrent limit along the trench. However, seismic lines distribution (mostly along the continental margin) and depth (~1 km depth) resulted in misinterpretation of the structural aspects governing the evolution of the Esperanza and Tumbes basins located mainly along the shelf area.
- Benitez (1995) proposed a stratigraphic model based on occurrence on drilling records. He proposes a N-S directed extensional tectonic continuum affecting all the Ecuadorian forearc

basins. In this context he proposed that the Jambelí basin (i.e. Esperanza and Jambelí basins in this work) subsidence began in the middle Miocene.

- Using seismic lines Lyons (1995) proposes that the whole structure of the basin corresponds to a horst-tail structure, typical of ending tips of major transcurrent systems (i.e. the so called 'Dolores-Guayaquil system'). One trivial consequence of this model is that there is no need to connect the major NAB dextral boundary with the trench. Indeed the movement would be absorbed in the Gulf of Guayaquil area.

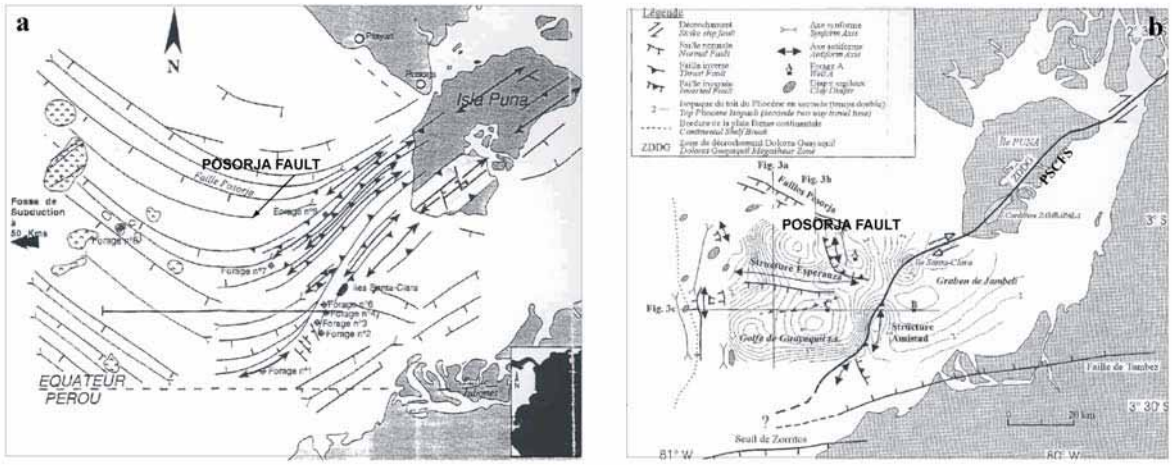

Figure 2.2. Cartography of the major structures of the Gulf of Guayaquil area (Ecuadorian side). **a)** Lyons, 1995; **b)** Deniaud et al., 1999. Both models derived from the same data used here(i.e. seismic lines and drilling).

- Deniaud et al. (1999) proposed a model based on seismic and drilling records. They proposed a pull-apart model in which the Esperanza basin developed in response to the dextral movement along the Dolores-Guayaquil fault system. Subsidence beginning in the Pliocene but major depocenters forming during Quaternary times. These authors suggested that the Dolores-Guayaquil fault system prolongates to the trench. In this way the pull-apart structure is similar to that proposed by Sheperd and Moberly (1981).
- A cinematic approach was used to determine the proposed linked evolution between the Gulf of Guayaquil and the so called 'Guayaquil-Caracas megashear' (Dumont et al., 2005). This work, based on the analysis of displaced marine terraces, beach deposits and offset channel morphologies as well as microtectonic observations along the Puná island (i.e. Zambapala fault), calculates a minimal mean slip rate of 5.8–8 mm/yr. This result allowed these authors to suggest that the Zambapala fault accommodates at least 60–80% of the slip motion of the 'Guayaquil Caracas megashear', an to propose that the NAB eastern limit extends from the Puná island to the Andean piedmont.

- More recently, Vega et al. (2005) proposed an evolution model for the Tumbes basin, which in terms of basin opening and depocenters age is partially based on the results obtained by Deniaud et al. (1999).

The deep structure of the Gulf of Guayaquil area (GG) along the south Ecuador convergent margin was investigated using marine multichannel seismic lines and wide-angle seismic (See section 1.3). The tectonic regime along the continental margin is clearly extensional (Figure 2.3). At the latitude of the GGTB these studies reveal that the South-Ecuadorian continental margin shows clues of subsidence, revealed by huge sedimentary basins (up to 7 km thick) related to normal and detachment faults (≥ 5 Ma). The Cretaceous oceanic substratum characterizing the lower part of overriding plate to the north may extend toward this area, despite significantly lower seismic velocities.

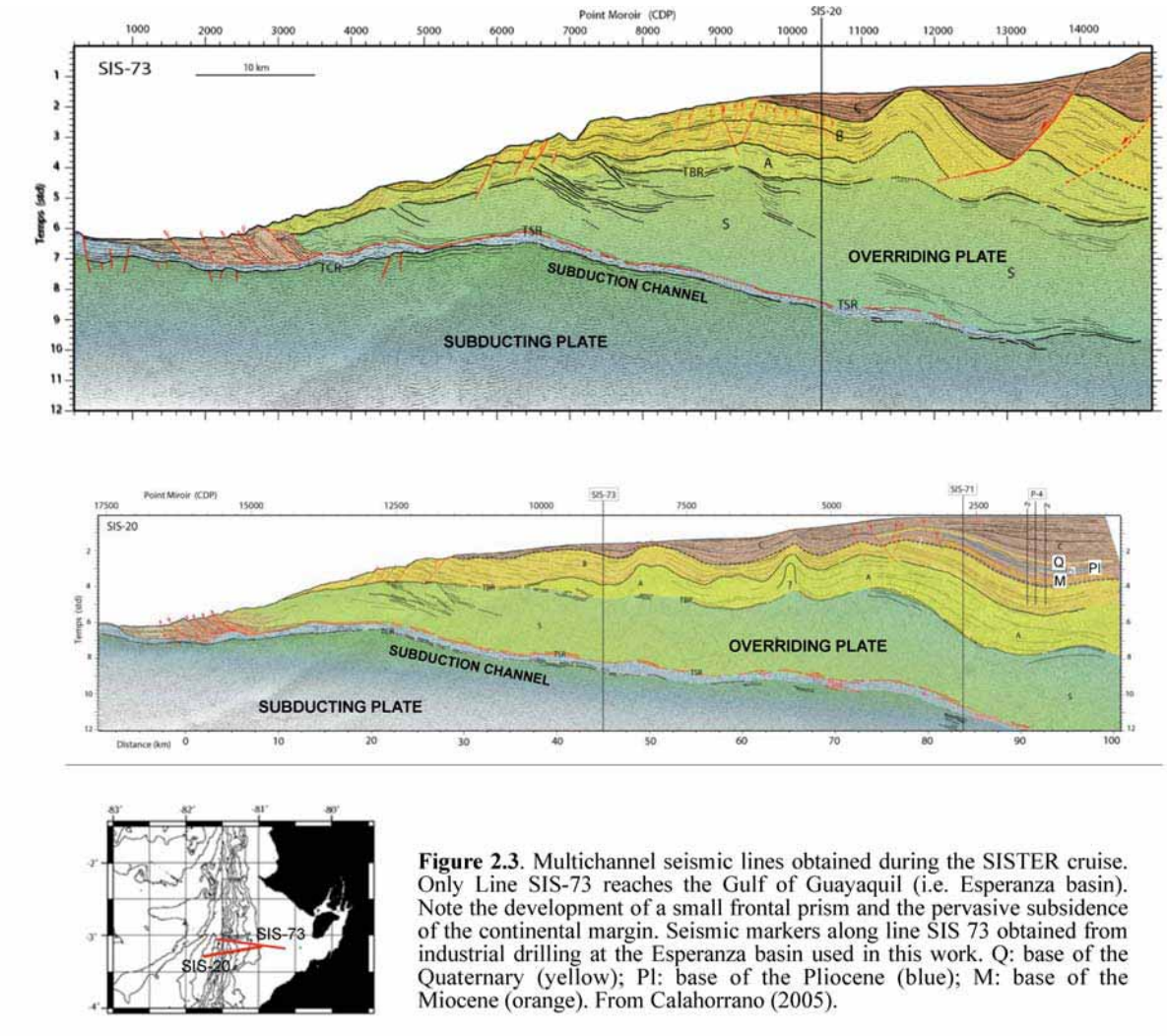

Figure 2.3. Multichannel seismic lines obtained during the SISTER cruise. Only Line SIS-73 reaches the Gulf of Guayaquil (i.e. Esperanza basin). Note the development of a small frontal prism and the pervasive subsidence of the continental margin. Seismic markers along line SIS 73 obtained from industrial drilling at the Esperanza basin used in this work. Q: base of the Quaternary (yellow); Pl: base of the Pliocene (blue); M: base of the Miocene (orange). From Calahorrano (2005).

The existence of a margin system limiting the major depocenters of the Esperanza and Tumbes basins is proposed using Ecuadorian (Petroecuador) and Peruvian (Perupetro) seismic lines (Witt et al., 2005; Witt et al., 2006a and b; Witt and Bourgois, submitted; two attached papers). This model proposes that two different tectonics control the Gulf of Guayaquil area evolution: 1) A Miocene (or older) to Present subduction-erosion regime controlling the upper and lower continental margin (Collot et al., 2002; Witt et al., 2005; Calahorrano, 2005) along N-S directed seaward dipping major normal faults, and 2) a major Quaternary extensional tectonic step leading to the major depocenters formation along the Esperanza, Tumbes and Jambelí basins controlled by the northward drifting of the NAB. The main NAB eastern limit does not cross the Puná island as it was previously proposed (Deniaud et al., 1999; Dumont et al., 2004). No connection between the NAB drifting related structures and the trench is needed to explain the evolution of the whole continental tectonics and shelf areas. A wide discussion of the local tectonics and its immersion in a whole geodynamic scenario as well as a comparison with other tectonic escape systems are proposed. Several geodynamic aspects such as: ridge subduction, subduction-erosion, interplate coupling and related upper-plate deformation, sediment bypassing or trapping as a result of subsidence and emersion are discussed.

Development of the Gulf of Guayaquil (Ecuador) during the Quaternary as an effect of the North Andean block tectonic escape

César Witt,[1,2] Jacques Bourgois,[1,2,3,4] François Michaud,[1,2] Martha Ordoñez,[5] Nelson Jiménez,[5] and Marc Sosson[1]

Received 5 August 2004; revised 27 December 2005; accepted 17 March 2006; published 21 June 2006.

[1] Interpretation of industrial multichannel seismic profiles and well data are used to identify the main tectonic features of the Gulf of Guayaquil (GG) area. These include two E-W trending major detachments: the Posorja and the Jambelí detachment systems, which represent half grabens with oppositely dipping detachments, to the south and to the north, respectively. The NE-SW trending Puná-Santa Clara fault system developed as a transfer fault system between the Posorja and the Jambelí detachments. The Esperanza and the Jambelí basins exhibit 3–4 km of sediment that accumulated during the past 1.6–1.8 Myr. The Puná-Santa Clara fault system bounds the Esperanza and the Jambelí basins, evidencing that the evolution of these basins is tightly controlled by the two detachments at depth. To the west, the N-S trending Domito fault system bounding the Posorja detachment system and the Esperanza basin to the west acted as a transfer zone between the shelf area and the continental slope. The Pliocene series show no significant variations in thickness throughout the Gulf of Guayaquil area suggesting that no important tectonic deformation occurred from 5.2 to 1.8–1.6 Ma. The major period of tectonic deformation in the Gulf of Guayaquil area occurred during the Pleistocene times. Three main tectonic steps are identified. From early Pleistocene to ~180 ka, major subsidence occurred along the Esperanza and Jambelí basins. From ~180 to ~140 ka, most of the Gulf of Guayaquil area was above sea level during the isotope substage 6 low stand. From ~140 ka to Present, tectonic activity is restricted along the normal faults bounding the Esperanza basin, the Tenguel fault, and the Puná-Santa Clara and Domito fault systems. A N-S trending tensional stress regime characterizes the Pleistocene times throughout. The northward drifting of the North Andean block is proposed to control the tectonic evolution and associated subsidence of the Gulf of Guayaquil area. It is also accepted that the collision of the Carnegie ridge with the trench axis has to play a major role in controlling the North Andean block northward drift. Because the Carnegie ridge subduction is possibly an ongoing process, which began prior to the Pliocene, we postulate the along-strike morphology of the ridge at the origin of interplate coupling variations. The subduction of an along-strike positive relief of the ridge is proposed at the origin of the major tectonic reorganization of the GG area occurring at ~1.8–1.6 Ma. **Citation:** Witt, C., J. Bourgois, F. Michaud, M. Ordoñez, N. Jiménez, and M. Sosson (2006), Development of the Gulf of Guayaquil (Ecuador) during the Quaternary as an effect of the North Andean block tectonic escape, *Tectonics*, *25*, TC3017, doi:10.1029/2004TC001723.

1. Introduction

[2] Active tectonic deformation in the Ecuadorian Andes has been the subject of many studies during the last 15 years [*Winter and Lavenu*, 1989; *Soulas et al.*, 1991; *Tibaldi and Ferrari*, 1992; *Winter et al.*, 1993; *Ego et al.*, 1996]. Nevertheless, few studies deal with the analyses of the coastal active tectonics and the evolution of the Gulf of Guayaquil (GG) area through time. In the GG area (Figure 1), the so-called Dolores-Guayaquil Fault System (DGFS) was considered to be part of the eastern active boundary of the North Andean block (NAB), the northward motion of which was proposed to be at the origin of the GG area subsidence [*Campbell*, 1974; *Shepherd and Moberly*, 1981]. *Deniaud et al.* [1999] interpreted the tectonic deformation of the GG area as a consequence of an extensional strain associated with the northward drifting of the NAB. They proposed that the first phase of subsidence took place in the GG area during the Pliocene, the GG area developing as a pull-apart basin along the NAB eastern limit. However, the evolution of the GG area and the role of the NAB eastern limit in its development remain poorly understood.

[3] On the basis of multichannel seismic reflection profiles and well data acquired by Petroecuador (Ecuadorian Petroleum Company) during the past two decades, we document the geodynamic evolution of the GG area for the past 2 Myr. The study area includes (Figure 1b) offshore zones located on either side of the Puná and Santa Clara

[1]UMR Geosciences Azur, Observatoire Océanologique de Villefranche-sur-Mer, Nice, France.
[2]Escuela Politécnica Nacional, Departamento de Geología, Quito, Ecuador.
[3]Centre National de la Recherche Scientifique, Paris, France.
[4]Institut de Recherche pour le Développement, Paris, France.
[5]Geological Research Centre of Guayaquil, Petroproducción, Guayaquil, Ecuador.

0278-7407/06/2004TC001723$12.00

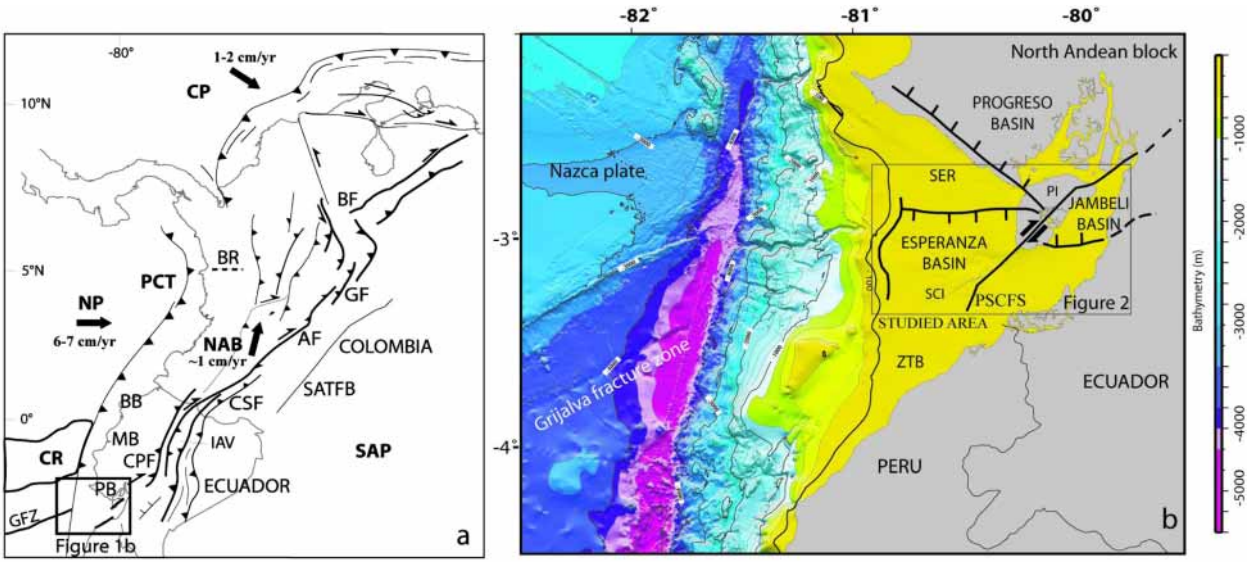

Figure 1. (a) Structural framework of the Andean segment extending from northern Peru to Venezuela showing the NAB limits and the forearc basins of the Ecuadorian segment, modified from *Taboada et al.* [2000]. (b) Structural sketch of the Gulf of Guayaquil area. Bathymetry of the continental margin and trench is a compilation of data from the Seaperc cruise (J. Bourgois chief scientist) of the R/V *Jean Charcot* and the Andinaut cruise (J. Bourgois chief scientist) of the R/V *L'Atalante*. Legend is for both Figures 1a and 1b. AF, Algeciras fault; BB, Borbón basin; BF, Boconó fault; BR, Baudo range; CP, Caribbean plate; CPF, Calacalí-Pallatanga fault; CR, Carnegie ridge; CSF, Chingual-La Sofia fault; GF, Guaicaramo fault; GFZ, Grijalva fracture zone; IAV, Inter-Andean valley; MB, Manabí basin; NAB, North Andean block; NP, Nazca plate; PB, Progreso basin; PCT, Peru-Chile trench; PI, Puná island; PSCFS, Puná-Santa Clara fault system; SAFTB, Sub Andean fault and thrust belt; SAP, South America plate; SCI, Santa Clara island; SER, Santa Elena rise; ZTB, Zorritos-Tumbes basin.

islands. Data are confined to above 100 m water depth, landward from the shelf slope break. We have identified three major tectonic features: the Esperanza and Jambelí basins and a diapiric zone located at the seaward edge of the continental platform. The evolution of these features is controlled by six main active fault systems (Figure 2), which include: the Puná-Santa Clara fault system (PSCFS), the Posorja detachment system (PDS), the Tenguel fault, the Domito fault system (DFS), the Esperanza graben, and the Jambelí detachment system (JDS). These major structures have been poorly characterized in previous studies. Their description improves available constraints on the tectonic reconstruction and subsidence history of the area. In addition, we present detailed mapping of the active structures and their evolution through time, and a geodynamic scenario for the Pliocene and Quaternary based on these constraints.

2. Geodynamics and Geologic Framework

[4] The Nazca plate (Figure 1) is subducting eastward beneath the South America plate at a rate of about 6–7 cm/yr in an E-W direction [*Freymueller et al.*, 1993; *Kellogg and Vega*, 1995; *Trenkamp et al.*, 2002]. The dip angle of subduction ranges between 25° and 35° [*Pennington*, 1981; *Guillier et al.*, 2001]. The Carnegie ridge is an approximately E-W trending bathymetric high of the Nazca plate entering the subduction between 1°N and 2°S latitude. Along the collision area of the Carnegie ridge with the trench, the Ecuadorian continental margin is being uplifted at Present [*Lonsdale*, 1978]. *Daly* [1989], *Benitez* [1995], *Aalto and Miller* [1999], *Pedoja* [2003], and *Cantalamessa and Di Celma* [2004] have proposed that the evolution of the forearc basins such as Borbón and Manabí basins were controlled by the Carnegie ridge subduction. Also the chemistry of the active volcanic arc [*Bourdon et al.*, 2003; *Samaniego et al.*, 2005] and cooling uplift-related Andean rates [*Steinmann et al.*, 1999; *Spikings et al.*, 2001] were related with the timing of arrival of the Carnegie ridge to the trench axis. The proposed ages for the ridge-trench collision lie in the range between 1 and 15 Ma (i.e., *Lonsdale* [1978] and *Spikings et al.* [2001], respectively, other ages lying in this range were also proposed by *Rea and Malfait* [1974], *Hey* [1977], *Lonsdale and Klitgord* [1978], and *Wilson and Hey* [1995]). A flat slab coincident with the zone of Carnegie ridge subduction was proposed from seismological global data [*Gutscher et al.*, 1999]. This flat slab configuration was first constrained by two events located at 250–300 km from the trench and then related to a model of adakitic volcanism generation [*Gutscher et al.*, 1999; *Bourdon et al.*, 2003]. Seismological studies using a dense network of 54 stations installed in northern Ecuador

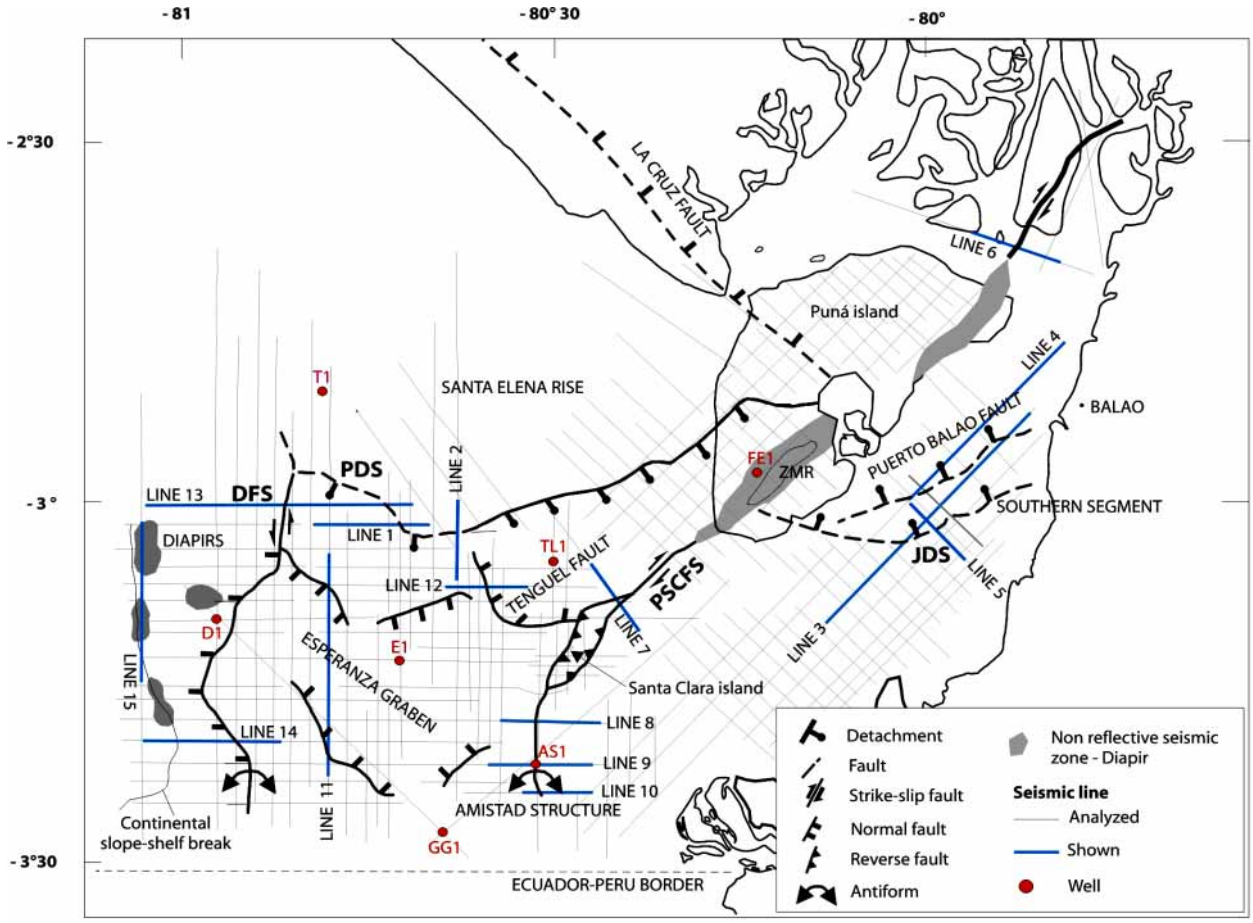

Figure 2. Structural map of the GG area. Solid line shows the active tectonic features. Dashed line shows the tectonic features with no clear activity today. The nonreflective seismic zones and diapirs are mapped down to 2 s TWTT. AS1, Amistad Sur 1 well; DFS, Domito fault system; D1, Domito 1 well; E1, Esperanza 1 well; FE1, Fe1 well; GG1, Golfo de Guayaquil 1 well; JDS, Jambelí detachment system; PDS, Posorja detachment system; PSCFS, Puná-Santa Clara fault system; T1, Tiburon 1 well; TL1, Tenguel 1 well; ZMR, Zambapala mountain range.

[*Guillier et al.*, 2001] do not reveal any major changes in the slab dip angle at depth associated with the Carnegie ridge.

[5] At ~1°N latitude, the trench axis exhibits a change in trend from N-S to the south to NNE to the north. North of 1°N, the convergence between the Nazca and South America plates is oblique and produces motion partitioning [*Ego et al.*, 1996]. The North Andean block (NAB) is migrating to the NE along a major right-lateral strike-slip system at a rate of 6 ± 2 mm/yr [*Trenkamp et al.*, 2002]. The oblique convergence and the subduction of the Carnegie ridge have been proposed to be at the origin of the northward drifting of the NAB [*Pennington*, 1981; *Ego et al.*, 1996]. Along the Ecuadorian coast the NAB exhibits mainly oceanic terrane accreted to the Andean continental margin. The obduction of these oceanic terranes occurred between the Late Cretaceous and the late Eocene [i.e., *Feininger and Bristow*, 1980; *Bourgois et al.*, 1982, 1987, 1990; *Benitez et al.*, 1993; *Jaillard et al.*, 1997; *Reynaud et al.*, 1999; *Lapierre et al.*, 2000; *Mamberti et al.*, 2003]. Even so, faults limiting continental crust tectonic units also accommodate NAB motion. *Winter and Lavenu* [1989], *Soulas et al.* [1991], and *Ego et al.* [1996] described the NAB eastern limits as a major system of dextral faults cutting across the Ecuadorian Andes through several active fault segments (Figure 1a) such as the Calacalí-Pallatanga fault, the thrust faults along the Inter-Andean valley, and the Chingual-La Sofia fault. Along the Inter-Andean valley this system would form a restraining bend along central and northern Ecuadorian Andes [*Ego et al.*, 1996; *Winkler et al.*, 2005]. In Colombia, the fault and thrust belt of the eastern front of the Oriental Cordillera (i.e., the Algeciras and Guaicaramo faults and the Pamplona indenter) connect to the north with the Boconó fault system in Venezuela. All these structures show features suggesting active deformation [*Boinet et al.*, 1985; *Bourgois et al.*, 1987, 1990; *Audemard*, 1997; *Taboada et al.*, 2000; *Dimate et al.*, 2003; *Velandia et al.*, 2005; *Dhont et al.*, 2005]. These fault systems show evidence of reactivation or tectonic inversion of older tectonic features and suture zones

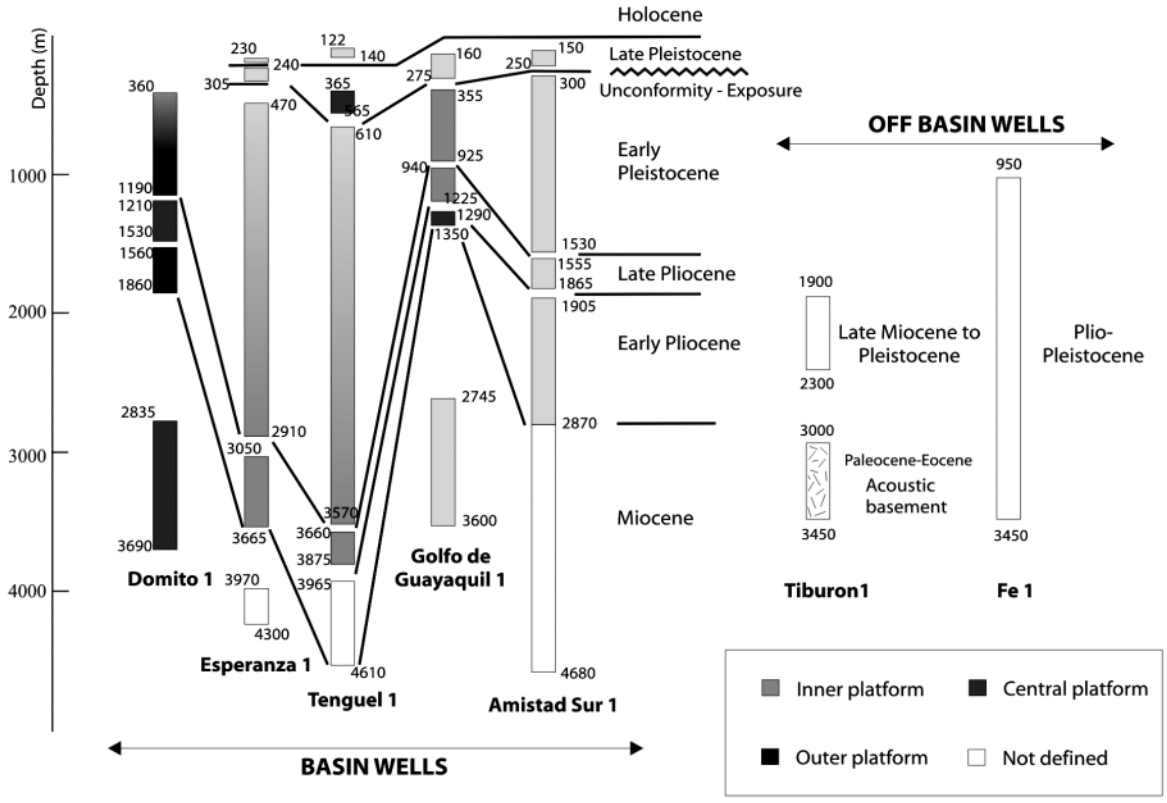

Figure 3. Stratigraphic columns from industrial wells drilled in the GG area. Age distribution is from micropaleontological and pollen assemblages. No well reached oceanic or continental basement. Tiburon 1 well is placed along the Santa Elena rise, away from the basin depocenters. The Tiburon 1 well data are used for basin basement correlations (acoustic basement along lines). See Figure 2 for well location. Numbers refer to depth below seafloor.

[*Audemard*, 1997; *Guillier et al.*, 2001; *Dimate et al.*, 2003; *Winkler et al.*, 2005]. Even so, other models suggest that the NAB does not act as a single block moving northward and that the accommodation of the deformation is more complicated since the Caribbean plate (Figure 1a) influences the area north of 4–5°N [*Ego et al.*, 1996; *Taboada et al.*, 2000; *Corredor*, 2003; *Acosta et al.*, 2004; *Cortés et al.*, 2005]. This model suggests that the zone of transition between the NE-ENE Nazca plate-related compression to the ESE Caribbean plate-related compression is placed at 4–5°N along an E-W trending transfer zone (i.e., the Baudo range, Figure 1a [*Taboada et al.*, 2000]).

[6] The forearc evolution is marked by the development of four main basins, from north to south these include: the Borbón, the Manabí, the Progreso, and the GG (Esperanza and Jambelí) basins. All of these basins show periods of shallowing or deepening of facies as they evolved through time [*Benitez*, 1995; *Deniaud*, 2000]. Except in the GG area, the subsidence of the other basins began approximately during the early Miocene. The sediment accumulation of the Esperanza and Jambelí basins is mainly composed of clastic deposits ranging in age from Mio-Pliocene (prerift sequences) to Pleistocene (synrift sequences). The Santa Elena rise separates the Miocene Progreso basin from the Pleistocene GG basins (Figures 1a and 2). The sediment accumulation of the GG area has recorded the tectonic and climatic signals of the adjacent continental areas. It includes the major continental crustal thinning of the GG area basement and the sediment coastal drainage and transport to the trench. Therefore the GG area is a key zone to develop analyses for constraining the tectonic evolution of the southern boundary of the NAB. Seaward of the GG area, the upper and middle continental slope are characterized by intense deformation along seaward dipping normal faults which constraint a subduction-erosion tectonic regime working at depth. At the toe of the continental slope, trench fill sediments are offscraped to form an incipient frontal accretionary prism [*Collot et al.*, 2002; *Calahorrano*, 2005].

3. Data

[7] This study considers the stratigraphy of seven industrial wells located at key sites (Figures 2 and 3). The data include determinations of microfossil and pollen associations as well as the environmental signature of sediment and rock petrology analyses. The selected wells such as Tenguel

1 and Esperanza 1 are located at sites where high subsidence rate is recorded. The Amistad Sur 1, Fe1, and Domito 1 wells on one side, and the Golfo de Guayaquil 1 and Tiburon 1 wells on the other side were selected because they are located above structural high and along transition zones, respectively. Only the Tiburon 1 well is used for acoustic basement correlations. This well is located away from zones of thick sediment filling, so we did not use it to correlate ages in those zones. The Fe1 well, which is located over a zone showing no clear seismic reflection resolution, also exhibits poorly defined stratigraphic data. As a consequence, no correlation of the Fe1 well data with records from the GG area is possible.

[8] The sediment accumulation of the Esperanza and Jambelí basins is mainly composed of clastic deposits ranging in age from Mio-Pliocene (prerift sequences) to Pleistocene (synrift sequences). The early middle Miocene sequences (Subibaja Formation) accumulate in an outer platform to continental environment. The middle to late Miocene transitional sequences (Progreso Formation) and the Pliocene-Pleistocene marine sequences (Lower and Upper Puná formations) were deposited in an inner platform environment [*Benitez*, 1995, and references therein]. *Deniaud et al.* [1999] identified at least four subsidence phases for the GG area: (1) a phase of low subsidence–low sedimentation rates during Mio-Pliocene, (2) a phase of high subsidence–high sediment deposition rates during early Pleistocene, (3) a phase of low subsidence–low sediment accumulation rates in the late Pleistocene, and (4) a phase of relatively high subsidence–high sediment accumulation rates during the Holocene. No evidence of stratigraphic age exists for phases 3 and 4. In this work, we assume that the GG area evolved through two main steps. The first one, during the Mio-Pliocene is characterized by low subsidence–low sedimentation rates, and the second one, during the Pleistocene, exhibits high subsidence and sedimentation rates that a short exposure phase of the GG area interrupted.

[9] The seismic lines used in this work were collected and processed by different companies between 1980 and 1983. We have analyzed about 100 of them for a total of ~4000 km (Figure 2). Only 15 key lines are presented in this work. All profiles have been treated using a conventional processing sequence including deconvolution and migration. The analyzed seismic lines show high-quality seismic reflections down to 4–5 s two-way traveltime (TWTT). The poor quality of seismic reflections does not offer proper constraints on the tectonic history of the deeper series.

4. Interpretation

[10] The GG area (Figure 2) shows three main zones exhibiting different origin and style of tectonic deformation. The central zone exhibits the Esperanza basin, which developed south of the Posorja detachment system (PDS). The Domito fault system (DFS) and the Puná-Santa Clara fault system (PSCFS) bound this basin to the west and to the east, respectively. The Jambelí basin develops east of the PSCFS. The Jambelí detachment system (JDS) bounds the Jambelí basin to the south. The upper continental slope extends west of the DFS.

4.1. Posorja Detachment System

[11] The Posorja detachment system (PDS) bounds the Esperanza basin to the north. It corresponds to the boundary between the Santa Elena rise and the Esperanza basin, which separates the Paleocene–early Miocene acoustic basement to the north from the Pliocene-Quaternary basin infill to the south (Figure 2). It exhibits a strong signature on profiles at depth ranging from 2 to 5 s TWTT. Once corrected for the ~2.5 vertical exaggeration, this discontinuity dips to the south with an angle of about 20°. The seismic profiles reveal that the direction of the PDS changes from E-W to NE-SW along trend. A southward increasing subsidence rate and a rollover fold developing to the south is associated with the development of this major tectonic discontinuity. Consequently, the PDS is a low-angle flat ramp. The seismic profiles show that this detachment controlled the subsidence all along the system during the Quaternary. The subsidence is limited to the west by the DFS and to the east by the PSCFS (Figure 2). Along line 1, the lower series shows a normal drag fold pattern with highest subsidence zones placed close to the discontinuity. This tectonic signature resembles that of a simple normal fault along the NW-SE segments of the PDS (line 1, Figure 4). Along line 2, subsidence is weaker but the highest subsidence of Quaternary series is located away from the tectonic discontinuity suggesting that southward subsidence was controlled by the detachment structure. We consider that high subsidence and normal drag fold subsidence related pattern observed close to the tectonic discontinuity of the PDS along line1 is a local signature related to change in its trending direction. This change in trend possibly plays an important role in the amount of subsidence generated by the PDS at this zone. In contrast, the shallow Quaternary series shows a rollover reverse drag fold pattern (lines 1 and 2). We assume that this tectonic feature is related to the major dip change of the detachment from subhorizontal to the north to about 20° to the south making necessary the rollover fold to develop. The rollover folding placed above the horizontal surface along line 1 probably results from the slip of an eastern or northern fault. Even so this fault has not been observed in seismic lines. The northern flank of the rollover fold is characterized by the development of normal faults (lines 1 and 2). These faults located above the flat ramp of the detachment accommodate the rollover deformation in this area. Because global compilations of normal fault focal mechanisms show only a small fraction of events with nodal plane dipping less than 30°, doubt persists that faults either initiate or slip at shallow dips. However, geologic reconstructions and seismic reflection profiling indicate that initiation and slip on low-angle normal faults in the upper crust are common in the geologic record [i.e., *Wernicke*, 1981; *Angelier and Coletta*, 1983; *Spencer*, 1984; *Buck*, 1988].

[12] The deeper series observed along the seismic profiles along the western part of the PDS (lines 1 and 2) tend to

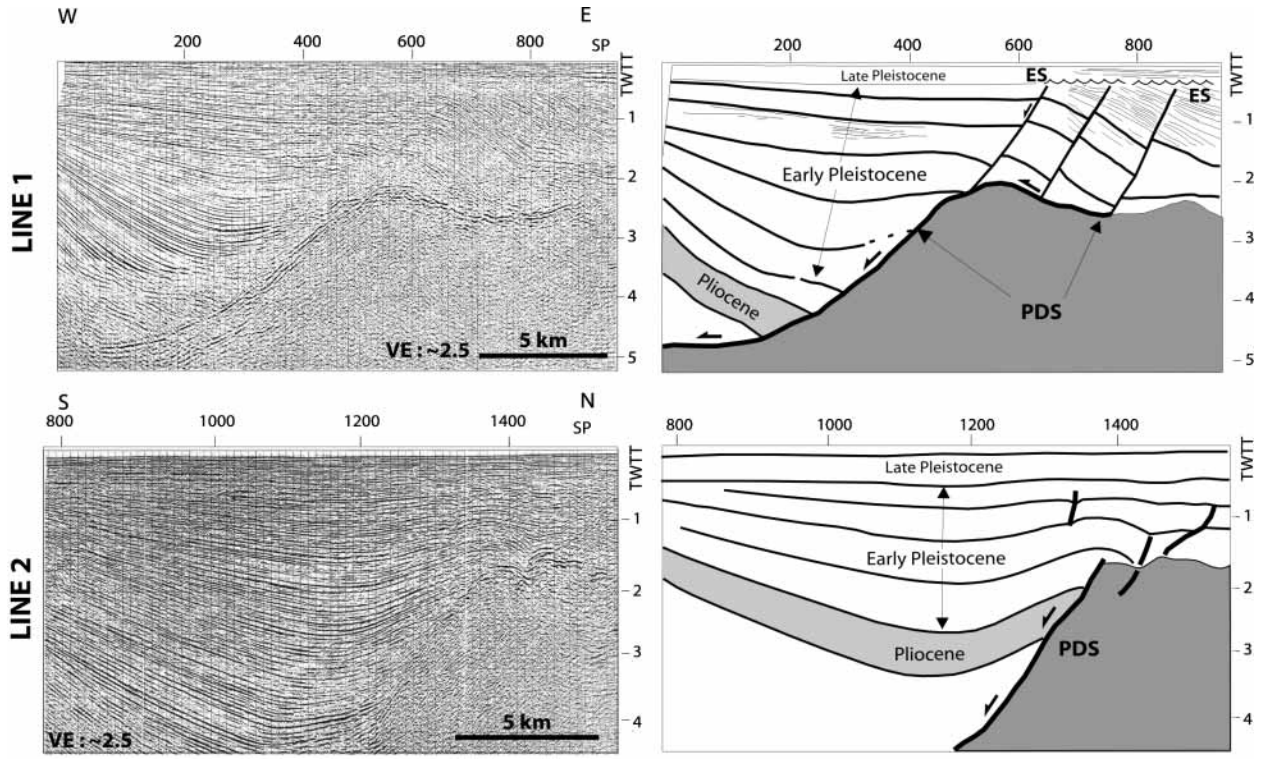

Figure 4. Posorja detachment system (PDS). (top) Line 1. Note that the development of the PDS controlled the accumulation of sediment along the hanging wall. Also a rollover fold developed as the flat ramp of the detachment developed. The late Pleistocene unconformably overlies the rollover fold. The ES unconformity is associated with an exposure occurring during the isotope substage 6 low stand. No active subsidence related to the detachment is observed above the ES unconformity. (bottom) Line 2. Thickening of the syntectonic sequences show that the flat ramp of the PDS was mainly active during the early Pleistocene. Note the presence of a rollover fold. Dark grey shows the basement (i.e., Paleocene–early Miocene sequence of the Santa Elena rise). Light grey shows the Pliocene. ES, exposure surface, unconformity. See Figure 2 for location of lines.

thicken near the ramp, indicating that sedimentation occurred during tectonic deformation along the detachment. This began possibly during the Pliocene (the Pliocene series along line 1 lies on the zone where seismic reflections become unclear) in the western part of the system. To the east (line 2) the Pliocene shows no thickness variation. The main subsidence event took place in the early Pleistocene. Because the late Pleistocene unconformably overlies (ES in Figure 4) the related rollover fold deformation, we consider that the PDS has no significant activity since that time.

[13] A thinner sequence of late Pleistocene age unconformably overlies the thick syntectonic sediment accumulation. We assume that after this episode the PDS shows no significant activity. Even so, minor extensional activity has been observed in the segment placed near the Puná island (Figure 2). There, the observed deformation is not related to the detachment but to a growth fault that developed between the flat ramp and the sedimentary cover.

4.2. Jambelí Detachment System

[14] The Jambelí detachment system (JDS) and the associated Jambelí basin (Figure 2) are characterized by a complex array of old (pre-Quaternary) and recent structures. The projection of data from the Tiburon 1 well to the east and the seismic facies interpretation from line to line allows us to identify the Jambelí basin basement to be probably of Paleocene–early Miocene age. The base of the early Pleistocene facies has been projected from the Amistad Sur 1 well, using N-E and N-W trending seismic lines (line 5, Figure 5).

[15] The JDS includes two major faults: a southern normal fault and a northern low-angle slip surface both dipping to the north. The northern fault (i.e., the Puerto Balao fault) connects the detachment at depth (line 3). The Jambelí basin exhibits a 2–3 km thick accumulation of sediment. This accumulation is mainly controlled by the Puerto Balao fault development. The Puerto Balao fault shows a complex geometry. In line 3 it dips almost vertically close to the seafloor. It flattens downward to be almost horizontal as it connects to the southern segment at depth. The Puerto Balao fault marks the southern limit of the main early Pleistocene subsidence in the Jambelí basin. Along this fault, subsidence is also controlled by a series of antithetic normal faults developing above the active slip

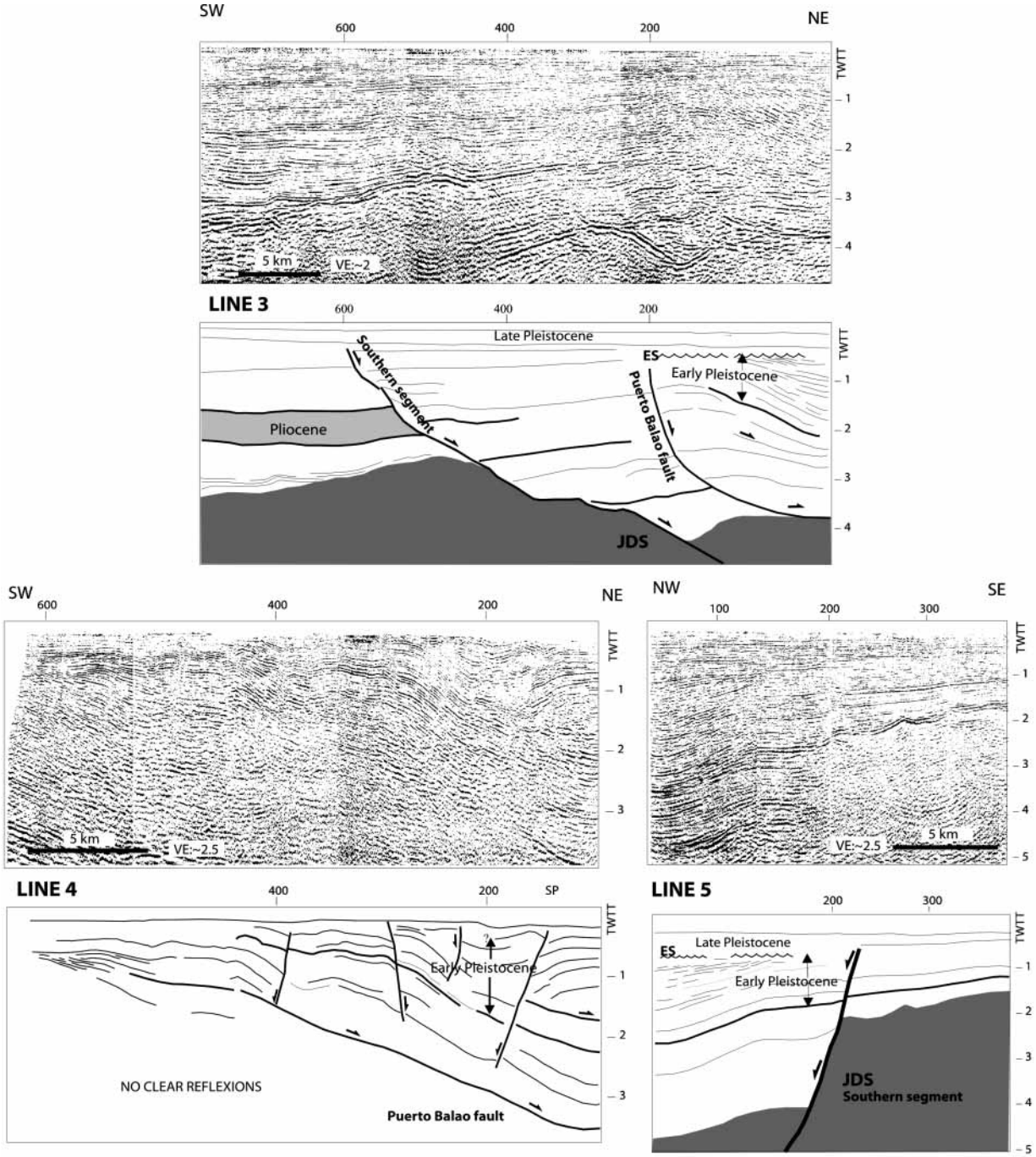

Figure 5. Jambelí detachment system (JDS). (top) Line 3. Age interpretation is from Amistad Sur 1 well data projected to the Jambelí area. Main subsidence phase occurred during the early Pleistocene times. (bottom left) Line 4, rollover folding developed in association with the flat ramp of the JDS. Note that the synthetic and antithetic faults only developed above the flat ramps. (bottom right) Line 5, note the ES unconformity that is coeval with that identified along line 3. Dark grey shows the basement. Light grey shows the Pliocene. ES, exposure surface, unconformity. See Figure 2 for location of lines.

zone (line 4). Also rollover folds developed in these areas of high subsidence rate indicating the presence of low-angle slip working at depth (lines 3 and 4). The sites showing the highest subsidence are those located in the limit between the offshore and onshore seismic lines enhancing a lack of data that prevents an accurate analysis of this zone.

[16] The southern fault of the JDS exhibits an E-W trending direction, roughly parallel to the Puerto Balao fault (Figure 2). The almost horizontal attitude of the sedimentary sequences located between the two faults (line 3) reflects the low tectonic activity of the southern segment. The recent activity of this southern segment is characterized by low-amplitude vertical displacement, which is associated with low subsidence in the sedimentary cover (lines 3 and 5, Figure 5). On the other hand, the basement of the Jambelí basin exhibits a greater displacement along the fault (lines 3 and 5, Figure 5). The difference in displacement observed between the recent and older sequences is possibly related to a recent reactivation of the fault in the early Pleistocene (Figure 5). Subsequently, no tectonic deformation exists during the development of an erosional unconformity (ES in lines 3 and 5, Figure 5) overlying older sequences. This unconformity is associated with a general subaerial exposure of the GG area occurring between 182 and 329 ka (section 5.2).

4.3. Puná-Santa Clara Fault System

[17] On the basis of the available seismic profiles, we have identified three main segments along the Puná-Santa Clara fault system (PSCFS), from NE to SW it includes (Figure 2): the Puná segment, the Santa Clara platform segment, and the southern Amistad structure.

[18] To the north, along the Puná segment, the PSCFS shows weak compressional deformation (line 6, Figure 6). The deeper sequences show no syntectonic features related to the formation of this structure, indicating that deformation began recently. No evidence exists onshore for the PSCFS having a prolongation to the north. Northeast of the Puná island the seismic profiles show an elongated 5–7 km wide nonreflective zone (Figure 2). Close to this zone the acoustic signature of the upper layers (profile not shown) shows major tectonic disruption also suggesting that recent compressive activity occurred. The seismic profiles allowed us to follow this nonreflective zone (Figure 2) to the south, across the Puná island and below the Zambapala mountain range (300 m above sea level). Unfortunately, the loss of seismic reflections and the uncertain correlation with the ages obtained from well data prevent constraining properly the chronology of the tectonic activity within the area.

[19] Southward, along the segment of the Santa Clara platform (Figure 2) the seismic profiles reveal a pop-up compressional structure (line 7, Figure 6). At that site, the seafloor exhibits a 4–17 m high scarp, indicating that the structure is active. On either side of the PSCFS, the thickness of the early Pleistocene-Pliocene sequences shows no significant variation, suggesting that the pop-up structure formed afterward. Because the syntectonic on-lap deposits, unconformably overlying the raised series, are of late Pleistocene age, we assume that deformation began at the early late Pleistocene boundary.

[20] The southern prolongation of the PSCFS corresponds to an antiform, the so-called Amistad structure (line 8, Figure 7). No Pliocene thickness variation is observed crossing of the Amistad structure documenting that no significant tectonic activity existed during the Pliocene at that site (lines 8, 9, and 10, Figure 7). Paleontological markers from the Amistad Sur 1 well, combined with seismic facies signatures; show that Quaternary subsidence was more important west of the structure than to the east. Instead to record the tectonic activity of the PSCFS, this variation in thickness recorded the subsidence history of the Esperanza basin that began in the early Pleistocene. Indeed, the western segments of lines 8 and 9 (Figures 2 and 7) are located at the eastern edge of the Esperanza basin. The late Pleistocene on-lap sedimentation unconformably overlying raised up series of early Pleistocene age (line 8, Figure 7) documents a compressional tectonic event that affected this basin limit at the early late Pleistocene boundary. More to the south (line 9, Figure 7), as the antiform broadens the on-lap syntectonic deposits thin, which suggests that the edge of the basin is almost not affected by the late Pleistocene compressional deformation at that site. The southernmost profile (line 10, Figure 7) shows that no deformation exists in this area. At this point, the southern edge of the Esperanza basin has no clear expression. The main activity of the PSCFS has taken place during the Quaternary. At that time the tectonic activity along the Amistad structure propagates 6–7 km to the south in a gentle flexure structure. Three to four km to the south, line 10 shows no tectonic structure or sediment thickness variation in the prolongation of the Amistad structure. Therefore the PSCFS exhibits no prolongation south of $\sim 3°25'$S.

4.4. Esperanza Graben

[21] The Esperanza graben is located in the central part of the GG area. It trends roughly perpendicular to the PSCFS and the DFS (Figure 2). The Esperanza graben is bounded to the north and to the south by a series of major normal faults dipping toward the graben axis (line 11, Figure 8). The trend of the system changes from ESE to the west to ENE to the east. The faults that limit the graben are among the most active tectonic features in the GG area. Also, these faults record the most significant dip-slip component observed from the available data. This graben is the area of the GG where subsidence was the second greatest. Here the Quaternary series are more than 3000 m thick. During the late Pleistocene, no tectonic inversion is observed along the faults bounding the graben. An antiform trending approximately E-W developed between the active limits of the graben. The uniform thickness of the Pliocene throughout the graben area (line 11) associated with the early Pleistocene highest subsidence rates along faults indicate that this antiform formed during the early Pleistocene time. Because this antiform is associated with major normal faults we assume that it develops either as a rollover

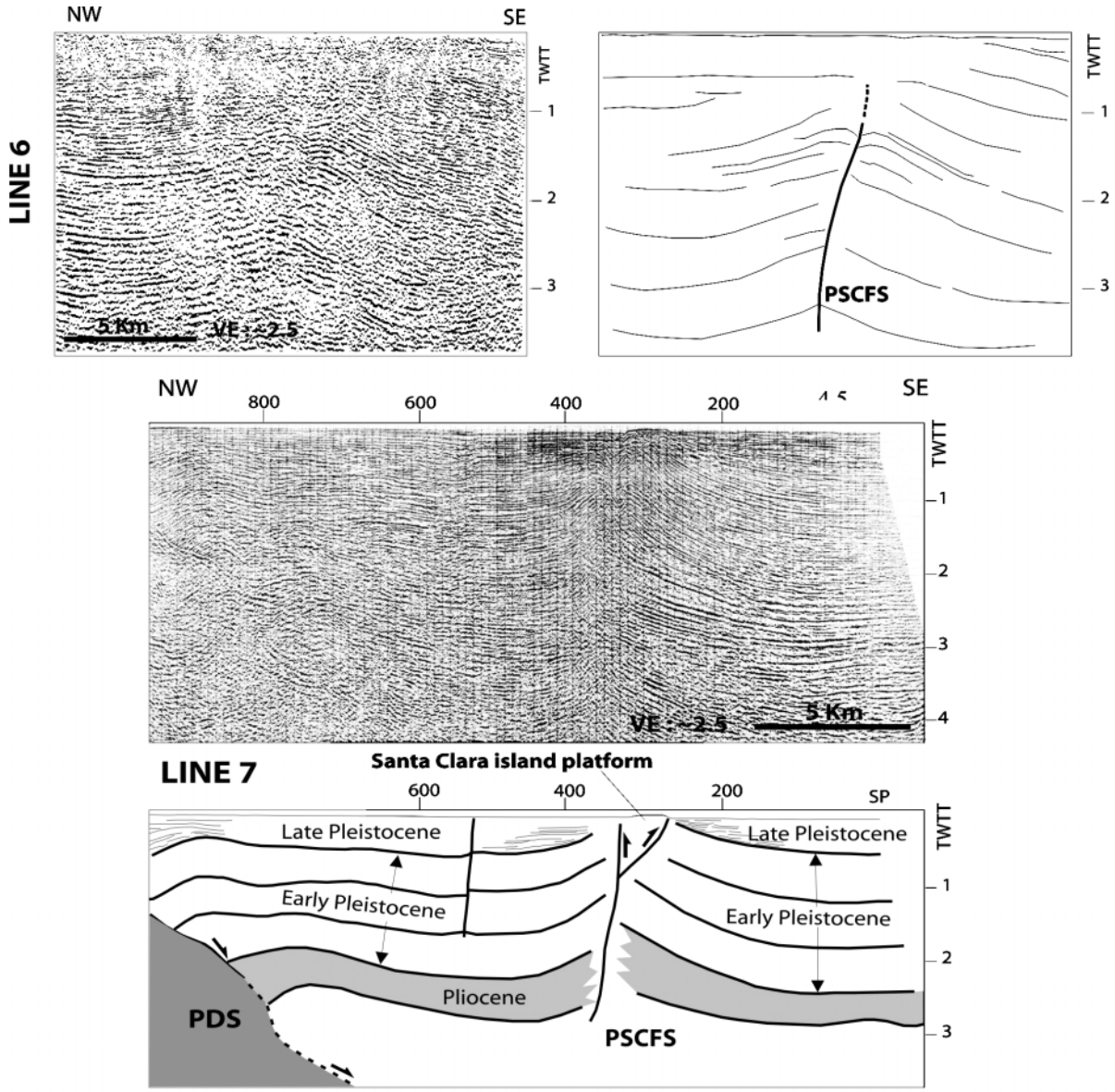

Figure 6. Puná-Santa Clara fault system (PSCFS). (top) Line 6, northeastern segment of PSCFS. No age correlation is possible in this area. Seismic record shows moderate contraction. The lost of seismic signal upward prevents to characterize the most recent deformation. Sequences show no variation in thickness on either side of the PSCFS suggesting that tectonic deformation occurred recently. (bottom) Line 7, the Santa Clara island segment of PSCFS. The thickness of the Pliocene–early Pleistocene sequence shows no variation crossing the fault system. Fault activity began in the late Pleistocene. The rollover fold to the NW is related to the PDS development. Dark grey shows the basement. Light grey shows the Pliocene. See Figure 2 for location of lines.

fold along a detachment fault at depth or as the signature of a lateral strike-slip component along the normal faults bounding the graben.

4.5. Tenguel Fault

[22] The Tenguel fault (line 12, Figure 8) shows a major change of its trending direction, from N-S to the north to E-W to the south. It is a normal fault and its evolution is recorded by 3600 m of Quaternary sediments. This is the highest sedimentation rate known in the GG area. The seismic profile (line 12, Figure 8) exhibits at least two faults. A scarp on the seafloor indicating that tectonic deformation is active underlines the main fault to the west. The two faults together and an antiform feature placed between them form a positive flower type structure located

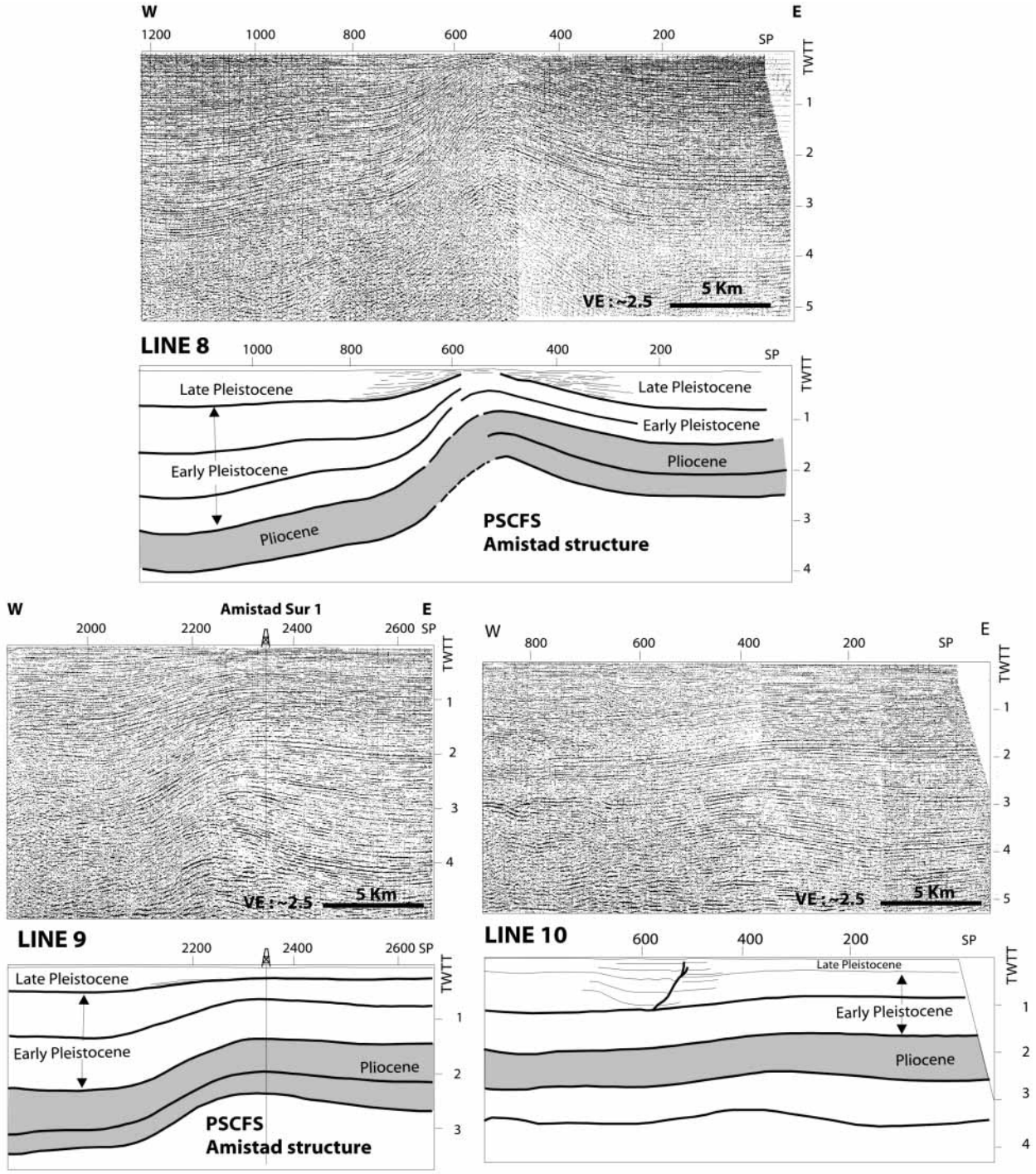

Figure 7. Southern segment of the Puná-Santa Clara fault system (PSCFS). (top) Line 8. The so-called Amistad structure shows no significant variation in thickness of the Pliocene sediment, the antiform structure formed afterward. (bottom left) Line 9. The Amistad structure flattens southward. (bottom right) Line 10. More to the south, no tectonic deformation exists in the prolongation of the Amistad structure. See Figure 2 for location of lines.

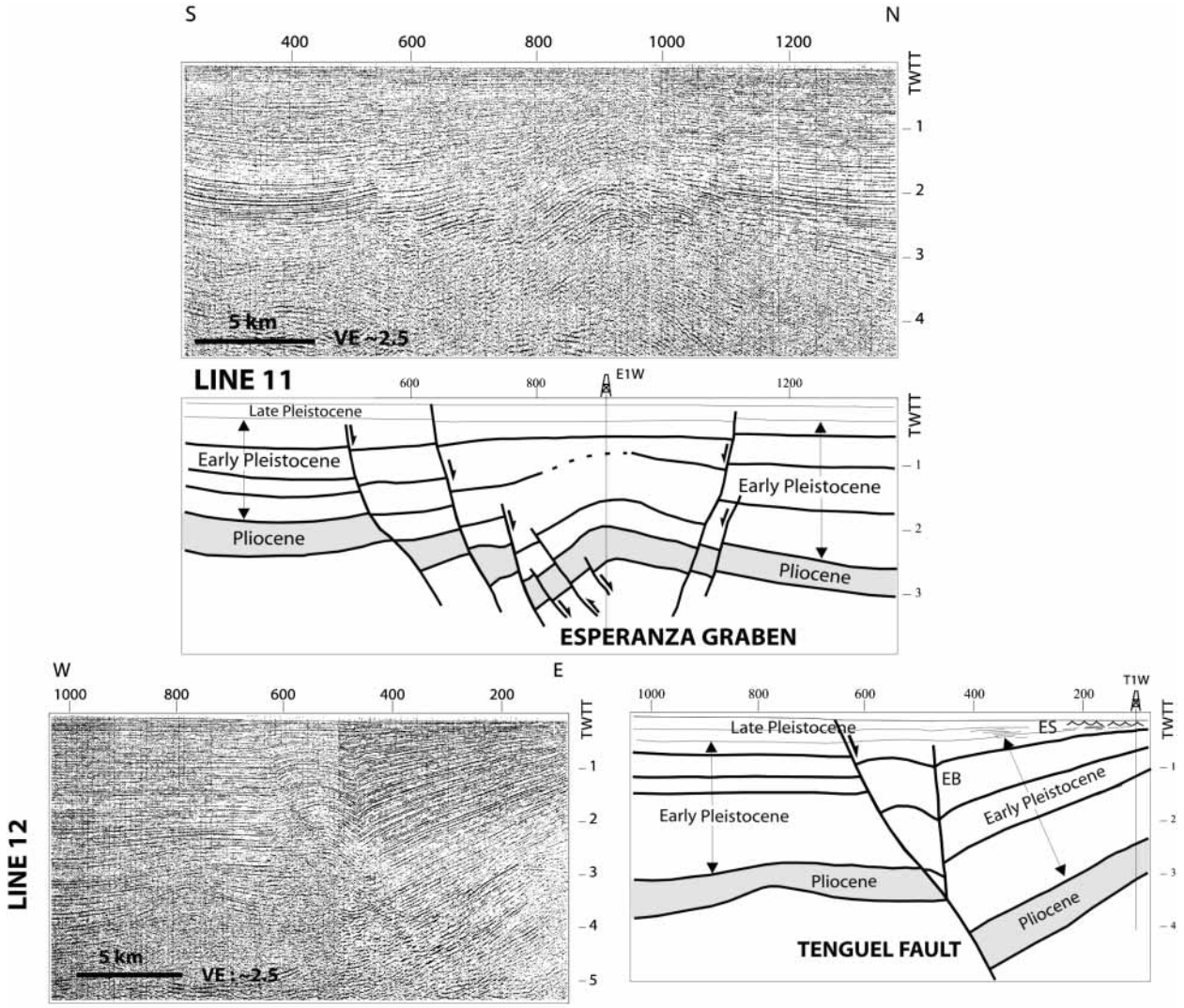

Figure 8. Esperanza graben and the Tenguel fault. (top) Line 11. The syntectonic series are of early Pleistocene age. Note the antiform at the center of the line. It may originate either from strike-slip induced deformation or rollover folding related to PDS at depth. Age controls are from the industrial E1 well located 8 km off line. (bottom) Line 12. The Tenguel fault evolved as a normal fault during the early Pleistocene. The vertical eastern branch of the fault (EB) possibly originated from late Pleistocene compression. At Present, the Tenguel fault is under tensional stress. Age controls are from the industrial T1 well located 8 km off line. ES, exposure surface, unconformity. See Figure 2 for location of lines.

in the central part of the system. The Tenguel fault evolved through three tectonic episodes:

[23] 1. During the early Pleistocene the southwestward dropping and the thickened sedimentary series close to the Tenguel fault suggest that a major normal faulting event occurred. The main accumulation of sediment occurred at that time as the flat normal Tenguel fault evolved.

[24] 2. The formation of the antiform occurred in late Pleistocene times. This feature is associated with a transpressive component of deformation along the Tenguel fault and/or to space problems arising during downward movement of the hanging wall block. This effect is probably due to the curvature of the fault at depth and to the drastic change in trend which push-up the hanging wall block (Figures 2 and 8). Seismic lines do not allow us to constraint a single model for the antiform formation. Even so, if there is a compressive episode, the compressive deformation does not significantly displace reflections as compared to the $\sim$1 km down throw, which occurred during the previous tensional episode. The tectonic inversion episode is a local and minor event.

[25] 3. Subsequently, an extensional tectonic episode occurred along the Tenguel fault. This tectonic event is associated with the development of a normal fault, which

displaced the seafloor along an 11 to 40 m high scarp. This suggests that extensional processes controlled the tectonic evolution of the Tenguel fault during the late Pleistocene. The Tenguel fault, located above the PDS, appears as a second-order tectonic feature associated with the first-order PDS located at depth. We consider that the Tenguel fault is an antithetic tectonic feature that developed in close associated with the PDS at depth.

4.6. Domito Fault System

[26] The Domito fault system (DFS) is roughly located along the shelf break, which bounds to the west the continental platform from the upper continental slope. Also, it marks the limit of the Esperanza basin to the west (Figures 2 and 9). Westward, from the DFS, the continental slope exhibits a series of N-S trending structures with strong signature both in bathymetric and seismic records. These seaward dipping tectonic features are listric normal faults (lines 13 and 14, Figure 9) accommodating the tensional tectonic regime along this area. The tectonic style and deformation along the continental slope is different than those identified to the east along the Esperanza basin.

[27] Along the DFS the deepest deformed reflectors in the northern part of the system are observed at 3.5–4 s TWTT below seafloor. The thickening of the sedimentary sequences toward the DFS indicates the occurrence of syntectonic sedimentation suggesting that this fault system was mainly active during Miocene to Pliocene time (lines 13 and 14, Figure 9). To the south, close to the Peru-Ecuador border, the eastern fault of the DFS is associated with a N-S trending fold. We suggest that strike-slip motion occurred along the fault (Figure 2). The roughly N-S trending PSCFS and DFS bound the Esperanza basin to the east and to the west, respectively. As the PSCFS, the DFS acted as a transfer fault during Pleistocene time. Evidences including the presence of seafloor escarpments along the DFS show that the system is active at Present.

[28] Several mud diapirs exist along the seaward break of the continental platform (line 15, Figure 9). These mud diapirs underline the DFS. Instead of being related to the fault zone, *Deniaud et al.* [1999] proposed that the emplacement of the diapirs originated from Quaternary sediment having high sedimentation rate. We found no direct relationship between the zones of high Quaternary subsidence rate and the emplacement of the diapirs. As a matter of fact no diapirs are observed in areas of highest subsidence rates (i.e., inside the Esperanza basin). The diapirs are only observed along the upper continental slope, and their emplacement is tectonically controlled by N-S trending normal faults. The roots of the diapirs are not identified in the seismic lines, indicating that the undercompacted mud material from which they originated is located deeper than 5 s TWTT below seafloor (i.e., deeper than 5000–6000 m below seafloor). Deep marine multichannel seismic reflection profiles acquired across the western part of the GG and the continental platform [*Collot et al.*, 2002] show that diapirs possibly root at the main unconformity between the basement and the sedimentary cover at 6–8 s TWTT depth below seafloor [*Calahorrano*, 2005]. None of the diapirs identified in this area pierce through to the seafloor suggesting that the process is currently inactive (line 15, Figure 9). Because the late Pleistocene unconformably overlies the diapir structures, they probably remained inactive since that time.

5. Gulf of Guayaquil Area Evolution

[29] During the Miocene-Pliocene the GG shelf-slope break was probably located farther east than today. The N-S trending DFS and associated seaward dipping normal faults (line 14, Figure 9) that controlled the high subsidence rate were situated along the upper and middle continental slopes during this period. The 2 to 7 s TWTT thick Mio-Pliocene (or older) sediment identified in this area recorded an E-W trending tensional tectonic step (Figure 10a). This tectonic regime that induced trench parallel seaward dipping normal faults is widely recognized along active margins where subduction-erosion is working at depth [*Scholl et al.*, 1980; *Bourgois et al.*, 1984, 1988; *von Huene and Scholl*, 1991]. In this western area of the GG, we assume that subduction related processes controlled sediment accumulation during the Mio-Pliocene time. Indeed subsidence was active along the DFS at least since the late Miocene. Moreover, evidences show that the DFS connects southward to Banco Peru and farther south to the Talara detachment [*Witt et al.*, 2006] both structures being associated with westward dipping N-S trending normal faults. Along the northern Peruvian margin subduction erosion working at depth has been considered as the driving mechanism of subsidence of the continental margin since the middle Miocene [*von Huene et al.*, 1988]. The tectonic regime identified along the continental margin of southern Ecuador (off the Gulf of Guayaquil) extended farther to the south off northern Peru.

[30] On the basis of the occurrence of Mio-Pliocene series in well data, *Benitez* [1995] proposed a Mio-Pliocene age for the GG area opening. However, the model of *Benitez* [1995] was not supported by seismic data. The Pliocene sediment accumulation shows no major difference in thickness throughout the GG area, suggesting that most of the major tectonic features, which characterize the area, were inactive during the Pliocene (Figure 10a). *Calahorrano* [2005] reached the same conclusion using 15 s TWTT length MCS records acquired along the western Esperanza basin area during the Sisteur cruise [*Collot et al.*, 2002]. The synrift series along the Esperanza basin traverse are of early Pleistocene age.

[31] However, along seismic lines a weak opening pulse of the Esperanza basin occurred locally during Pliocene time. It is recorded along the PDS western segment (Figure 10a) showing a low subsidence rate and is likely not related to the PSCFS. Indeed, we found no evidence for the PSCFS to exist at that time. Minor subsidence events are also observed along what will be the JDS. This period of minor Pliocene subsidence was also observed by *Deniaud et al.* [1999].

[32] Regarding the pre-Quaternary evolution, well data of the GG area (Figures 2 and 3) show that the Miocene and

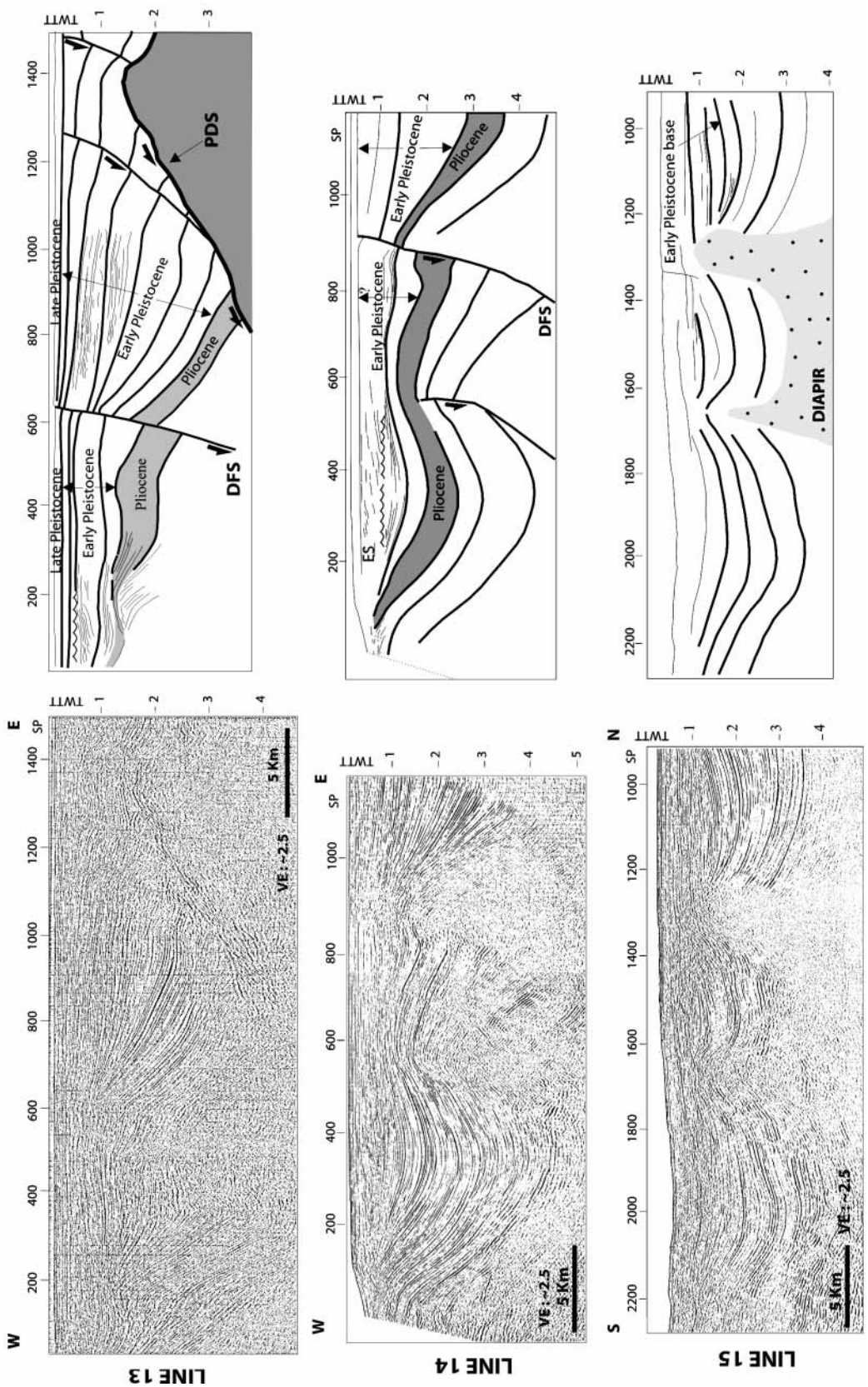

Figure 9. Domito fault system (DFS). E-W trending tensional stress west of DFS is associated with the tectonic evolution of the upper continental slope. (top) Line 13. Upper continental slope east of DFS, note that seaward dipping normal faults are still active in the late Pleistocene. (middle) Line 14. The main subsidence phase occurred during Miocene-Pliocene time along seaward dipping normal fault. (bottom) Line 15. Diapir emplacement along the upper continental slope occurred in early Pleistocene time. Dark grey shows Santa Elena rise basement. Light grey shows Pliocene. Light grey with dots shows diapir. ES, emersion surface, unconformity. See Figure 2 for location of lines.

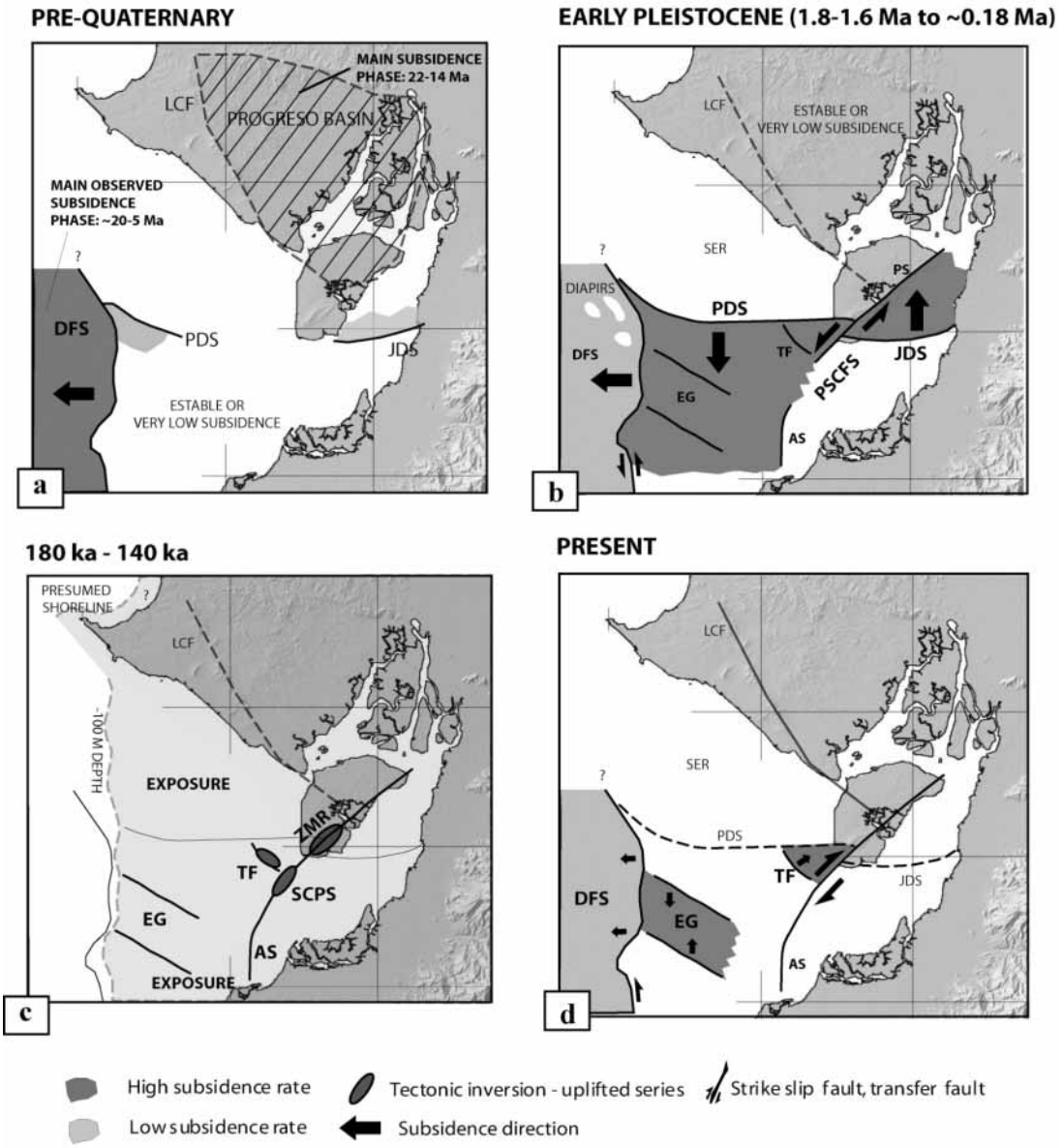

Figure 10. Reconstruction of the tectonic history of the GG area. The coastline is considered only as a geographic reference frame. Dashed line shows the currently inactive features. (a) Pre-Quaternary time, main subsidence periods are shown; (b) early Pleistocene time; (c) Exposure of the GG area during isotope substage 6 low stand; and (d) Present time. DFS, Domito fault system; EG, Esperanza graben; JDS, Jambelí detachment system; LCF, La Cruz fault; PDS, Posorja detachment system; PSCFS, Puná-Santa Clara fault system (including AS, Amistad structure; PS, Puná segment; SCPS, Santa Clara platform segment; ZMR, Zambapala mountain range); SER, Santa Elena rise; TF, Tenguel fault. See text for more detail.

Pliocene facies described along the Progreso forearc basin (Figure 1) extend southward along the GG area, including below the thick Quaternary sediment, which accumulated along the Esperanza basin. It is of importance to note that the paroxysm of subsidence along the Progreso basin is significantly older than along the GG area. Main subsidence-related sedimentation rates along the Progreso basin occurred during ~23–14 Ma [*Benitez*, 1995; *Deniaud*, 2000]. Subsequently, a stable or very low subsidence period is installed from 14 Ma to present times, a period during which NAB drifting probably begins [*Winkler et al.*, 2005]. Even so, minor change occurred during the Pliocene, the stable subsidence phase of the GG area was from ~5 to ~2 Ma [*Deniaud*, 2000]. At 2 Ma the subsidence-related sediment accumulation rate increased drastically being ~6 times greater than that recorded during the Pliocene. In comparison with the Progresso basin, the GG sediment accumulation rate during the Quaternary is 3–5 and 20 times greater for the Miocene (23–14 Ma) and the Quaternary times, respectively. High subsidence rate along the GG during the Quaternary define the most important tectonic event in the Ecuadorian forearc for at least the past 10 Myr. To consider that the GG developed above a precursor Progreso basin, or if the Domito fault system extended landward, cannot be resolved with our seismic lines. However, we consider that the major change in the subsidence and deformation style during the early Pleistocene time is the signature of a major reorganization along the NAB southern limits.

[33] It is possible that the major geodynamic reorganization of Pleistocene-Holocene age documented along the GG area extended to the north across the Progresso basin area. However, the reorganization along the Progreso basin was much less significant than along the GG area where the major PDS slip motion maintained the GG area below sea level. This evolution of the GG area developed through three main tectonosedimentary steps: the first one and the last one characterized by major extensional tectonic events and high subsidence-sediment accumulation rates and the second one by an extensive and short-lived emergence of the GG area in relation with an eustatic sea level low stand.

5.1. Early Pleistocene Step

[34] Major subsidence in the GG area occurred during the early Pleistocene. Along the Esperanza basin the southward dipping PDS controlled this subsidence phase. The early Pleistocene subsidence phase identified in the Jambelí basin developed in relation to the northward dipping JDS. This major flat detachment dips in the opposite direction to that of the PDS (Figure 10b). Therefore during Pleistocene time, the Puná segment of the PSCFS has to develop as a transfer fault (PS in Figure 10b) in order to accommodate the opposite motion of the two opposite verging detachment systems. The maximum of tectonic deformation to accommodate the transfer of motion from one side to another has to be located along the segment of PSCFS, which connects the two detachments (i.e., along the Zambapala mountain range of the southern Puná island, Figure 2). Indeed this segment of the PSCFS is the site of major deformation as evidenced by the loss of reflections over a 5–7 km wide corridor following the PSCFS across southern Puná island (Figure 2). This strip of tectonic deformation, deeply rooted at depth is interpreted to be a major highly fractured zone that defines a left-lateral transform zone. Unfortunately, no age can be projected from the Fe1 well data to this zone due to the loss of reflections. In accordance with our transfer fault model, the age of deformation along the southern Puná segment of PSCFS must be coeval with the early Pleistocene age of the southward and northward slip motions documented along the two detachment systems.

[35] The Esperanza and Jambelí basins evolved through a N-S trending tensional regime. We assume that this regime is related to the NAB northward drifting. The roughly N-S trending PSCFS and DFS bound the Esperanza basin to the east and to the west, respectively. This implies that the DFS participates in the accommodation of the NAB northward drifting. The major depocenters with the highest subsidence rates are controlled by the Tenguel fault and the normal faults, which bound the Esperanza graben. The development of these faults during Pleistocene time was controlled by the PDS at depth.

5.2. Short Period of Uplift and Exposure

[36] A pervasive unconformity marks the end of the early Pleistocene subsidence phase, which occurred along the Posorja and Jambelí detachment systems. Early and late Pleistocene are locally used to refer to the sequences located below and above the strong reflections that underline the unconformity. Because about 3000 m of sediment accumulated during the so-called early Pleistocene in the subsiding zones of the GG area, it is widely accepted that it was about 1 Myr in duration leading to an accumulation rate of ~3 mm/yr. As a consequence the so-called late Pleistocene would be about 600–800 kyr in duration. Accepting this gross interpretation, we assume that the exposure of the GG area has to occur during one of the four sea level low stand known during the past 600 kyr, i.e., at ~21, ~140, ~350, and ~450 kyr [*Porter*, 1989; *Shackleton*, 1997; *Tzedakis et al.*, 1997; *Lambeck et al.*, 2002]. During these past glaciations, sea level was lower by 120–140 m than today. Because these sea level low stands are 30 to 40 kyr in duration [*Winograd et al.*, 1997], we assume that the exposure of the GG area was short in duration, ~20–50 kyr with respect to the location site. West of the Esperanza basin the unconformity is at a depth of ~0.4–0.6 s TWTT (i.e., ~350 to ~500 m) below seafloor in water depth ranging from 150 to 200 m. Taking into account that sea level was ~140 m below than today, the unconformity, which underlines the exposure subsided between 310 and 560 m in this area located more than 100 km west of the Present coastline. Considering that (1) the NAB escape to the north is recognized as a major leading factor controlling the GG tectonics and (2) the kinematic situation allowing the NAB to drift northward has been stable since the base of the Pleistocene at ~1.6–1.8 Ma, we assume that subsidence rate in the GG area has no reason to experience major change originating from kinematics constraint. In addition, the exposure was short in duration. Therefore it makes sense to

apply to the GG area a main subsidence rate for the past 1.6–1.8 Myr, whether or not it was below sea level. In that way, we calculate that the western Esperanza basin subsided at a mean rate of about 1.7 mm/yr since the early Pleistocene time. Using this rate value we infer that the exposure should have occurred between 182 and 329 ka. Since glacial sea level falls occurred from 180 to 140 (isotopic substage 6e) and from 380 to 350 ka (isotopic substage 10c), respectively, we assume that the low stand isotopic substage 6e is the better candidate for the GG area exposure. Indeed the entire GG is <100 m depth, it should have been exposed during every glacial maximum (i.e., ~21, ~140, ~350, and ~450 kyr [*Porter*, 1989; *Shackleton*, 1997; *Tzedakis et al.*, 1997; *Lambeck et al.*, 2002]). However, only the ~180–140 ka glacial maximum related erosion is observed. This could be explained by the following: (1) other exposure surfaces are not imaged since the frequency used in the industrial seismic lines allows to image the basin architecture at depth and not the sedimentary processes of the shallower series and (2) considering that sea level was 120–140 m lower than today, it is probable that shorelines involved in the ~21, ~350, and ~450 ka low stands are placed farther west of the available set of lines.

[37] Evidence of compression exists at three zones in the GG area. It includes the Santa Clara platform, the southern Puná island (both located along the PSCFS), and the central segment of the Tenguel fault (Figure 10c). Moreover, marine beds of Pleistocene age were documented on the top of the Zambapala mountain range indicating that uplift of the cordillera occurred afterward [*Deniaud et al.*, 1999; *Dumont et al.*, 2005]. These compressional events, which are roughly coeval with the short-period exposure, show local restricted extension both in space and time. It is difficult to explain the existing compressional tectonic features in the general frame of the kinematics situation with the NAB drifting to the north. In this context, only tensional deformation is expected along the GG area. Because (1) only short segments of the PSCFS and the Tenguel fault show compressional tectonics with low amplitude if compared with the deeply rooted tensional deformation (i.e., low tectonic inversion ratio), (2) no such compressional features exist along other faults trending in the same direction, and (3) subsidence exists along the PDS (line 7, Figure 6) coeval with uplift along the PSCFS at the Santa Clara island platform, we consider that compression observed in the GG area is minor and local. In addition, the structures that exhibit the weak compressive deformation in late Pleistocene times (i.e., Tenguel fault and Santa Clara platform) show a pervasive tensional deformation at Present. We conclude that an extensional stress regime characterizes the Pleistocene evolution of the GG throughout.

5.3. Postexposure Tectonics

[38] Currently, tensional tectonic activity takes place along the DFS, the Esperanza graben and the Tenguel fault (Figure 10d). The PDS and JDS show no evidence for ongoing extension today. This process implies a southward migration of the tectonic activity from the PDS to the fault bounding the Esperanza graben to the north. A major reorganization of the basin limits is occurring at Present (Figure 10d). However, minor deformation has been observed along the eastern segment of the PDS. The tectonic activity takes place along a growth fault, which developed between the ramp and the sedimentary cover. We propose that the tectonic deformation associated with this fault is not directly related to the PDS flat ramp, but accommodates the motion produced by the currently active PSCFS and Tenguel fault (Figure 2). Extensional tectonics controls the evolution of the GG area at Present.

[39] It is quite difficult to recognize strike-slip deformation from seismic records because this type of data allows only the vertical motion to be quantified. Moreover, recognition of strike-slip movement may be particularly difficult in young fault systems with small cumulated displacement, where oblique slip or trending slip occurs, and where high rates of contemporaneous sedimentation blankets the evolving deeper structures. This is the case of the PSCFS along which major change in deformation style occurs. It includes seafloor displacements, "pop-up" systems, flower structures and highly fractured vertical zones along trend. These tectonic features demonstrate that the PSCFS is a wrench fault. Taking into account the nature of the detachment zones (i.e., a basement rock along which the sedimentary cover slips) and the slip direction of the detached sedimentary series, we assumed that a left-lateral strike-slip component developed along the southern Puná segment (i.e., between the junction of PDS and JDS with the PSCFS) during the main subsidence phase in early Pleistocene times. Subsequently, the end of the activity along the PDS and JDS modifies the slip direction along the PSCFS. When tectonic activity stopped along the PDS and JDS, the PSCFS accommodated the dextral slip originating from the Tenguel fault, still active at Present. This is in agreement with the right-lateral transtensional deformation during the late Pleistocene described along the Zambapala mountain range [*Deniaud et al.*, 1999; *Dumont et al.*, 2005].

[40] Along the coastal plain southeast of Guayaquil and the Balao area (Figure 2), no morphotectonic feature is identified suggesting that active fault exists in both the northward prolongation of the PSCFS [*Eguez et al.*, 2003] and the eastward prolongation of the two faults of the JDS. We thus assume that the PSCFS and/or the JDS do not connect directly to the Calacalí-Pallatanga fault at present time. The transfer of the partitioning motion between the NAB and the South American plate is not related to a simple fault system cutting across the coastal plain area. In addition, part of the present-day NAB motion must also be accommodated along the seaward side of the continental platform, along the DFS, and across the Esperanza graben.

6. Discussion

[41] The NAB northward drifting was proposed to originate from both the obliquity of the convergence between Nazca and South America plates [*Ego et al.*, 1996] and the Carnegie ridge subduction supposed to increase the interplate coupling [*Pennington*, 1981]. We thus postulate that one of these two factors or both were at the origin of the

main reorganization occurring south of the NAB (i.e., along the GG area) at the Pliocene-early Pleistocene boundary (i.e., at ~1.6–1.8 Ma [*Berggreen et al.*, 1985; *Haq et al.*, 1988; *Cande and Kent*, 1995]). We also postulate that NAB northward drift exerts important feedback coupling to tectonic behavior and evolution of the GG area. Because no significant plate reorganization has been identified during the past 5 Myr [*Pardo-Casas and Molnar*, 1987], we assume that no major change in the obliquity of the convergence occurred at ~1.6–1.8 Ma. Therefore, accepting seamount subduction as a major factor in the increase of interplate coupling [*Cloos*, 1992; *Scholz and Small*, 1997], it is reasonable to accept the Carnegie ridge subduction as the main source of coupling between Nazca and South America plates along the Ecuadorian segment of the Peru-Chile trench. We thus postulate the Carnegie ridge subduction as being the major factor that induced the NAB northward drifting to increase at the Pliocene–early Pleistocene boundary, and in this manner controlling the GG area evolution.

6.1. Stress Regime Evolution

[42] Along the continental margin west of the GG, we document a pervasive Miocene-Pleistocene extensional tectonics associated with seaward dipping normal faults paralleling the N-S trending DFS. This normal faulting along active margins is considered as the signature of subduction erosion working at depth [*Scholl et al.*, 1980; *Aubouin et al.*, 1982, 1984; *Bourgois et al.*, 1984, 1988; *von Huene et al.*, 1989; *von Huene and Scholl*, 1991].

[43] In early Pleistocene times the subsidence in the Esperanza and Jambelí basins began. The N-S verging detachment structures related to the northward escape of the NAB triggered off the subsidence. Consequently, the DFS marks the limit between a zone strongly controlled by margin processes along the upper continental slope and the continental platform controlled by the northward tectonic escape of the NAB. This reflects that part of the partitioning motion is accommodated along the DFS.

[44] The major period of deformation in the GG area occurred in early Pleistocene times. At that time a major change in the tensional stress regime occurred from ~E-W (DFS) to ~N-S (PDS and JDS) inducing a major reorganization of the NAB southern limits. Accepting that the subsidence along the GG area is controlled by the northward drifting of the NAB during Quaternary times, we thus conclude that the Pliocene–early Pleistocene boundary is associated with a major increase in the northward migration rate of the NAB.

6.2. North Andean Block Drifting

[45] Tectonic models suggest that the obliquity vector of convergence between the Nazca and South America plates is not fully partitioned throughout the NAB and that the Caribbean plate influenced mainly the area north of 5°N [*Ego et al.*, 1996; *Taboada et al.*, 2000; *Corredor*, 2003; *Acosta et al.*, 2004; *Cortés et al.*, 2005]. The zone of transition being placed along a major seismically defined E-W transform zone at ~5°N coincident with the Baudo range (Figure 1a) [*Taboada et al.*, 2000]. If only the region south of 5°N is influenced by the Nazca plate oblique convergence, which induces a right-lateral stress regime (i.e., northward drifting of the NAB) the accommodation of the deformation is more complicated than that involved in a single block moving northward as proposed from GPS data [*Trenkamp et al.*, 2002]. Our data do not allow us to speculate the northernmost extensions of the NAB. For this reason, we only correlate the evolution of the GG area with the proposed NAB limits south of the postulated [*Taboada et al.*, 2000] transition zone at ~5°N.

[46] The age of the NAB northward drifting has been constrained considering mainly the age of the bounding tectonic features. In Colombia the NAB drifting is accommodated along the Guaicaramo-Algeciras fault [i.e., *Velandia et al.*, 2005; *Dimate et al.*, 2003]. Quaternary tectonic features are documented along this fault but no timing for the beginning of the tectonic deformation is proposed. In Ecuador, *Lavenu et al.* [1995] and *Winkler et al.* [2005] suggest that the Inter-Andean basins developed in a transpressive tectonic regime related to NAB northward drifting during the past 5–6 Myr. Even so, *Lavenu et al.* [1995] argue that although the formation of the Inter-Andean valley probably began in the late Miocene, the structural analysis demonstrates that it was subjected to major E-W shortening between 1.85 and 1.21 Ma. Furthermore, in the zone where the NAB eastern limit swings to the GG area a major pull-apart basin formed along a transtensional-releasing bend. This pull-apart basin began to form ~2.5 Myr ago [*Winter and Lavenu*, 1989]. Similarly, *Winkler et al.* [2005] defined a major phase of compression younger that 2.9 Ma along the northern Inter-Andean valley. These results support our interpretation that a major reorganization of the NAB limits took place at the Plio-Quaternary boundary. Furthermore, roughly dated Quaternary changes in the tectonic regime of the central part of the Inter-Andean valley has been related to major changes in the slip of the faults bounding the NAB [*Tibaldi and Ferrari*, 1992; *Villagomez et al.*, 2002].

[47] East of the GG area, the Andean foothills of the Western Cordillera underline a ~100 km displaced zone (southernmost prolongation of the Calacalí-Pallatanga fault) that has been linked with the dextral slip at the origin of the GG area [*Steinmann et al.*, 1999; *Hungerbühler et al.*, 2002]. To consider that the opening of the GG is of Quaternary age combined with the ~1 cm/yr rate of NAB northward drifting only ~20 km of northward drifting of the NAB may account for Quaternary times. Mainly on the basis of paleogeographic reconstructions and facies correlations *Steinmann et al.* [1999] and *Hungerbühler et al.* [2002] suggest a direct connection between the Manabí and Progreso coastal basins and the Inter-Andean basins, prior to the uplift of the Andes. They propose that opening of the GG area occurred ~10 Myr ago and that the opening of the GG area is related to the ~100 km offset of the Andean foothills along the Calacalí-Pallatanga fault. This interpretation of data allows them to properly match the postulated ~100 km offset and the NAB migration with a 10 Myr ongoing dextral displacement. Following *Steinmann et al.* [1999] and *Hungerbühler et al.* [2002], the GG area

subsidence has to start during the late Miocene. Our data do not allow us to speculate about the connection between the forearc and Inter-Andean basins. However, our data of the GG area document a major discrepancy with this model: the main subsidence of the GG depocenters began during the early Pleistocene following a stable Pliocene period during which no significant tectonic deformation occurred. We thus consider that the ~100 km of right-lateral slip along the so-called Calacalí-Pallatanga fault zone cumulated northward drifting from tectonic events as old as the Paleocene [*Dunkley and Gaibor*, 1997; *Pecora et al.*, 1999; *Hughes and Pilatasig*, 2002; *Kerr et al.*, 2002]. Furthermore, the ~20 km NAB northward drifting that occurred during the Quaternary time is consistent with the total net lengthening calculated across a N-S section from the Santa Elena rise (Ecuador) to the Amotape massif (Peru) [*Witt et al.*, 2006]. Whatever the old terrane accretion phases are, the modern construction of NAB limits (i.e., since early Pleistocene) started from reactivation of ancient suture zones as previously proposed along northern NAB boundaries [*Audemard*, 1997; *Guillier et al.*, 2001; *Dimate et al.*, 2003; *Winkler et al.*, 2005]. However, our conclusions leave an open question regarding the origin of the Pliocene stable tectonic phase. An understanding of this point could be achieved considering the along trend morphology of the Carnegie ridge which show a major central saddle associated with a ridge necking at about 85–86°W longitude. Such a lowering and associated necking of the Carnegie ridge relief entering the subduction may be related with low coupling at the plate interface and consequently with lower rates of NAB drifting.

6.3. Carnegie Ridge History

[48] On the basis of onshore offshore wide-angle seismic data, a minimum age of 1.4 Ma for the Carnegie ridge subduction was proposed [*Graindorge et al.*, 2004]. Ages for the Carnegie ridge collision with the trench axis were proposed from onshore offshore geophysical studies. Several first-order constraints were obtained from intensive surveys of the Galapagos igneous province combining seismic reflection, gravity, magnetic, and heat flow records [i.e., *Malfait and Dinkelman*, 1972; *Rea and Malfait*, 1974; *Hey*, 1977; *Lonsdale*, 1978; *Lonsdale and Klitgord*, 1978; *Pilger*, 1984; *Wilson and Hey*, 1995; *Meschede and Barckhausen*, 2000; *Sallarès and Charvis*, 2003]. These works provide constraints to show that the Nazca plate has a complex plate tectonic history in relation with asymmetrical and complex tectonic history of the Cocos-Nazca spreading center. Aseismic ridges and their associated seamounts are not only the surficial manifestation of hot spot activity but also reflect regional tectonic events including spreading centers jumps and migration. As a consequence, no simple relation between distance and convergence rate can be established to date the arrival of the Carnegie ridge to the trench axis. Models have been proposed suggesting that ridge-trench collision occurred at the Pliocene–early Pleistocene boundary [*Rea and Malfait*, 1974; *Hey*, 1977; *Lonsdale*, 1978; *Lonsdale and Klitgord*, 1978; *Wilson and Hey*, 1995]. However, older ages for the ridge collision were proposed including the late Miocene [*Pilger*, 1984] and the early Miocene [*Malfait and Dikleman*, 1972].

6.4. Slab Geometry

[49] *Daly* [1989] explored the possible relationship between slab geometry and the evolution of the forearc area. During the late Miocene, the Carnegie ridge subduction may have triggered a regional tectonic inversion along the forearc. However, he noted that the Carnegie ridge subduction occurred too late to be the unique factor responsible for the inversion. *Benitez* [1995] proposed an extensive analysis of the forearc stratigraphy and deformation. He shows that the uplift of the forearc area, including the Manabí and Progresso basins originated from a tectonic inversion, which occurred during the Quaternary time. He thus favored a Quaternary age for the ridge subduction. Subsequently, *Deniaud* [2000] minimized the unconformity documented at the base of the Pleistocene [*Benitez*, 1995; this work]. On the basis of this assumption they proposed an older age for the Carnegie ridge subduction to begin. Recently, analyses of marine terrace uplift allowed *Pedoja* [2003] and *Cantalamessa and Di Celma.* [2004] to argue that ridge subduction began at the late Pliocene–early Pleistocene limit. Similarly, an important post-Pliocene change of the extensional tectonic regime that characterized the Borbón basin was associated with the subduction of the ridge by *Aalto and Miller* [1999]; they also proposed a Quaternary age for the ridge subduction.

[50] Other models such as *Gutscher et al* [1999] suggest that the Carnegie ridge subduction began 8 Myr ago. Those models imply the subducted ridge segments to extend far to the east beneath the Andes. They argue from three major points including (1) a suggested feedback mechanism between uplift and subsidence related to the southward migration of the ridge along the forearc, (2) a seismic gap of intermediate seismicity (flat slab model), and (3) the existence of an adakite volcanism. More recent works dealing specifically with each of these three particular points [*Guillier et al.*, 2001; *Pedoja*, 2003; *Cantalamessa and Di Celma*, 2004; *Garrison and Davidson*, 2003; *Stern*, 2004; *Samaniego et al.*, 2005; *Kay*, 2005] have presented evidences against the flat slab model and the related 8 Ma age for ridge subduction initiation. The adakite volcanism extensively recognized along the broad Ecuador volcanic arc was proposed to either originate from lithospheric tears separating the flat Carnegie ridge from the steeper adjacent segments or the slab flattening itself. It is postulated that higher degrees of slab melting can be obtained from higher geothermal gradient originating from ridge flattening [*Samaniego et al.*, 2002]. In that manner, the adakitic signal, which occurred since 1.5 Ma has been interpreted as ridge induced. Consequently, the ridge collision with the trench was proposed to occur at ~5 Myr ago. Recently, *Samaniego et al.* [2005] related an increase in adakitic products at about 0.4 Ma with the arrival of the Carnegie ridge to the trench axis. Also extensive evidence was presented from numerous studies documenting that adakites in the Andes can be explained by equilibration of mantle wedge derived arc magma with thickened garnet-bearing continental crust

rather than by melting of subducted oceanic slabs [*Garrison and Davidson*, 2003; *Stern*, 2004; *Kay*, 2005, and references therein].

[51] Along-strike segmentation of the thermal and tectonic response along the Eastern Cordillera of the Ecuadorian Andes [*Spikings et al.*, 2001] was also attributed to differing along-strike subducted slab age, strength and composition. North of 1°30S, the development of higher topography and elevated cooling rates at ~15 Ma (north highest rates up to 50°C/Myr i.e., ~1.4–1.5 mm/yr uplift rate) and ~9 Ma (south highest rates up to 30°C/Myr i.e., ~0.8–1 mm/yr uplift rate) are associated with the presence of the postulated subducted flat slab at depth. It is suggested that Carnegie ridge collided with the trench at ~15 Ma and that subsequent interplate coupling produced the high 9 Ma exhumation rates. Beyond the uncertainty of the flat slab at depth, the along-strike segmentation of the Andean chain is questionable. In the southern Ecuadorian Andes (south of 2°30′S), *Steinmann et al.* [1999], *Hungerbühler et al.* [2002] have defined a high cooling rate at ~9 Ma coeval with that documented north of 1°30′S [*Spikings et al.*, 2001]. Interestingly, *Hungerbühler et al.* [2002] defined a ~0.7 mm/yr high uplift rate south of 2°30'S from 9 Ma to Present. Instead of being located far to the south, this uplift phase is also related with the Carnegie ridge subduction. Furthermore, southward along the Huayhuash Cordillera in northern Peru (~10°S) the same 9–10 Ma cooling period was documented from the same termochronometric approach [*Garver et al.*, 2005]. Here no ridge exists, and the area is located far away from the Nazca Ridge collision zone [*Hampel*, 2002]. Similarly, along the Eastern Cordillera of Colombia a comparable cooling event (with series cooling from temperatures of about 100°–150°C) of late Miocene age was also inferred from fission track analyses [*Gomez et al.*, 2003, 2005]. An extensive review of the uplift history of the central and northern Andes suggest that the 10–15 Ma uplift period was also important in the Bolivia and Chile cordilleras [*Gregory-Wodzicki*, 2000]. In addition, younger cooling steps have been identified in Ecuador between 3 and 5 Ma, as a regional event south of 2°45'S [*Steinmann et al.*, 1999; *Hungerbühler et al.*, 2002] and as a local imprint north of 2°45'S [*Spikings and Crowhurst*, 2004]. The Plio-Quaternary cooling event was also documented in the Eastern Cordillera of Colombia and in the Mérida Andes of Venezuela [*Gregory-Wodzicki*, 2000; *Audemard*, 2003; *Gomez et al.*, 2003, 2005]. Widespread cooling events have been observed in the Andes for at least the past 25 Myr and possibly represent an ongoing process. There appears to be no distinct cooling period linked with the Carnegie ridge subduction area or with its landward postulated prolongation at depth.

[52] As describes above, a late Miocene (~8–10 Ma) and a late Pliocene–Quaternary (~3–2 Ma) are the two main proposed ages for the collision of the Carnegie ridge with the trench axis. Along the Ecuadorian forearc, the GG area is the zone of greatest deformation occurring during Quaternary. Since the oblique convergence remains constant for at least the past 5 Myr and because the evolution of the GG area is strictly controlled by the northward migration of the NAB we assume that a major reorganization of the NAB northward drifting occurs at the Pliocene–early Pleistocene boundary. We assume that the subduction of the Carnegie ridge is at the origin of the increase of the interplate coupling involved in the acceleration of the NAB migration. At present times an elastic locking of ~50% of the convergence movement is taking place along the subduction zone [*White et al.*, 2003]. This locking matches the NAB displacement rate of ~1 cm/yr [*Trenkamp et al.*, 2002; *White et al.*, 2003]. Moreover, the Carnegie ridge is ~10 km thicker than the surrounding oceanic crust [*Gallier*, 2005]. Following the *Scholz and Small* [1997] model, this excess of crust thickness would induce an increase interplate coupling of at least ~200 MPa (buoyancy not included). We consider that such an interplate coupling increase is high enough to modify the kinematics of a wide zone, especially if the NAB is considered as a rigid block [*Guillier et al.*, 2001; *Trenkamp et al.*, 2002; *White et al.*, 2003]. Therefore we consider that the GG area has recorded the history of plate coupling in relation to the Carnegie ridge collision. In the GG area, the main tectonic deformation and related subsidence began by the beginning of early Pleistocene suggesting that the Carnegie ridge collision or the collision of an along-strike positive did not begin much earlier than at that time (i.e., ~1.8–1.6 Ma). If subduction of the Carnegie ridge has been a constant process since late Miocene times [*Pilger*, 1984; *Spikings et al.*, 2001] the subduction of a positive relief would explain the documented major reorganizations in the forearc deformation regime during the Plio-Quaternary limit [*Deniaud et al.*, 1999; *Aalto and Miller*, 1999; *Pedoja*, 2003; *Cantalamessa and Di Celma*, 2004] including NAB northward drifting acceleration.

7. Conclusions

[53] The tectonic analysis of the GG area allows us to identify two major detachment systems: the Posorja (PDS) and the Jambelí (JDS) detachment systems. These two detachments exhibits opposite verging slip direction, to the south and to the north, respectively. The N-S trending Puná-Santa Clara fault system (PSCFS), developed as a transfer fault system between the PDS and the JDS. It accommodated the opposite motion of the two opposite verging detachment systems. It thus exhibits no prolongation to the north and to the south. The Esperanza and the Jambelí basins exhibit 3–4 km of sediment that accumulated during the past 1.6–1.8 Myr. The PSCFS bound the Esperanza and the Jambelí basins, evidencing that the evolution of these basins is strictly controlled by the two Posorja and Jambelí detachment systems. To the west, the N-S trending Domito fault system (DFS) acted as a transfer zone between the shelf area and the continental slope. The DFS bounds the PDS and the Esperanza basin to the west.

[54] The Pliocene series observed in the Esperanza and Jambelí basin areas show no significant variations in thickness throughout the GG area suggesting that no substantial deformation occurred from 5.2 to 1.6–1.8 Ma. By contrast, a pervasive Miocene-Pliocene extensional tectonics is observed west the DFS in conjunction with N-S trending

normal faults dipping seaward. These faults are considered as related to subduction erosion working at depth as demonstrated elsewhere along convergent margins [*Scholl et al.*, 1980; *Aubouin et al.*, 1982, 1984; *Bourgois et al.*, 1984, 1988; *von Huene et al.*, 1989]. An E-W tensional stress regime prevailed along the continental margin since Miocene time. In early Pleistocene time the E-W trending PDS and JDS controlled the subsidence of the Esperanza and Jambelí basins. Therefore a N-S tensional stress regime characterized the GG shelf area during the past 1.6–1.8 Myr. As previously proposed, we consider that the N-S tensional stress regime of the GG area is the effect of the NAB northward drift. The DFS marks the limit between an area strongly controlled by margin processes (i.e., the upper continental slope) and another one (i.e., the shelf area) strongly controlled by the tectonic escape of the NAB. This reflects that part of the partitioning motion is accommodated along the DFS. The major period of deformation in the GG area occurred in early Pleistocene times. Taking into account the strong dependence of the subsidence in the GG area with respect to the northward drifting of the NAB, we assume that the Pliocene–early Pleistocene boundary is associated with a major change in the northward migration rate of the NAB. No major kinematic reorganization occurred along the Nazca-South America plate boundary since the Pliocene (5.2 Ma) that would explain the higher rate of the NAB northward drifting during early Pleistocene time. Therefore we postulate that the collision of the Carnegie ridge with the trench axis must play a major role in controlling the NAB northward drift. Because evidences exist for northward drift of the NAB prior to Miocene time, we assume that the increase of the interplate coupling at the Pliocene–early Pleistocene boundary originated from the Carnegie ridge itself. We postulate that the along-strike morphology of the ridge is possibly at the origin of interplate coupling variations.

[55] A major exposure of the GG area occurred during glacial sea level fall of isotopic substage 6e (between 180 and 140 ka). This exposure induced the accumulation of marine sediment to stop. Also this major paleogeographic change probably caused local strain changes able to have tectonic signatures. These are the so-called late Pleistocene compressional deformations confined to two small segments of the PSCFS and the central segment of the Tenguel fault. We consider that these local contractive tectonic features (inversion) have local causes. Indeed no cinematic reorganization at plate boundaries existed at that time. Therefore we assume that no major change in the general tectonic regime existed during the Quaternary evolution of the GG area. The GG area has been in an extensional stress regime since the early Pleistocene. At Present time, the tectonics of the studied area is dominantly extensional. In the GG area it is concentrated along the Esperanza graben and along the Tenguel fault. The DFS shows reactivation as a normal fault in recent times while the Posorja and Jambelí detachments are no longer active.

[56] Detrital material discharges from the two major Ecuadorian Andean-coastal drainage basins provide great sediment input to the GG area. During the isotopic substage 6 low stand, the exposure of the GG area allows the sediments to reach the trench axis instead of being trapped in the GG area. It has been shown elsewhere [i.e., *von Huene and Scholl*, 1991; *Bourgois et al.*, 2000] that sediment supply to the trench axis is a major cause for the tectonic regime to switch from subduction-erosion to subduction-accretion. This reflects the potential importance of the GG area in controlling the tectonic regime along the southern Ecuadorian margin. Indeed the turbidite trench fill has recently accreted against the margin backstop off the GG area [*Collot et al.*, 2002]. During the cold period of isotopic substage 6, the detrital material bypassing the GG allows rapid increase in trench deposition. Instead a postulated asperity subduction, variation in the sediment supply to the trench axis could explain more convincingly the tectonic regime of the margin to switch from subduction erosion to subduction accretion.

[57] **Acknowledgments.** This study was supported by the Fundacyt (Ecuador), the French Embassy in Quito, the Institut de Recherche pour le Developpement (IRD, France), and the Centre National de la Recherche Scientifique (CNRS, France). We are grateful to Petroproduccion for providing the basic data for this work including drilling and seismic records. We thank Wilfred Winkler and Richard Spikings for their critical and constructive reviews. Their comments greatly improved the original manuscript.

References

Aalto, K. R., and W. Miller (1999), Sedimentology of the Pliocene Upper Onzole Formation, an inner-trench slope succession in northwestern Ecuador, *J. S. Am. Earth Sci.*, *12*, 69–85.

Acosta, J., L. Lonergana, and M. P. Coward (2004), Oblique transpression in the western thrust front of the Colombian Eastern Cordillera, *J. S. Am. Earth Sci.*, *17*, 181–194.

Angelier, J., and B. Coletta (1983), Tension fractures and extensional tectonics, *Nature*, *301*, 49–51.

Aubouin, J., et al. (1982), Leg 84 of the Deep Sea Drilling Project: Subduction without accretion: Middle America Trench off Guatemala, *Nature*, *297*, 458–460.

Aubouin, J., J. Bourgois, and J. Azéma (1984), A new type of active margin: The convergent-extensional margin, as exemplified by the Middle America Trench off Guatemala, *Earth Planet. Sci. Lett.*, *67*, 211–218.

Audemard, F. (1997), Holocene and historical earthquakes on the Boconó fault system, southern Venezuelan Andes: Trench confirmation, *J. Geodyn.*, *24*, 155–167.

Audemard, F. (2003), Geomorphic and geologic evidence of ongoing uplift and deformation in the Mérida Andes, Venezuela, *Quat. Int.*, *101–102*, 43–65.

Benitez, S. (1995), Évolution géodynamique de la province côtière sud-équatorienne au Crétacé supérieur Tertiaire, Ph.D. thesis, 221 pp, Univ. Grenoble 1, Grenoble, France, 11 July.

Benitez, S., E. Jaillard. M. Ordoñez, and N. Jimenez (1993), Late Cretaceous to Eocene tectonic sedimentary evolution of southern coastal Ecuador: Geodynamic implications, paper presented at 2nd International Symposium of Andean Geodynamics, Inst. de Rech. pour le Dev., Oxford, U.K., 21–23 Sept.

Berggreen, W. A., D. V. Kent, and J. J. Flynn (1985), Paleogene geochronology and chronostratigraphy, the chronology of the geological record, *Mem. Geol. Soc. Am.*, *10*, 141–195.

Boinet, T., J. Bourgois, H. Mendoza, and R. Vargas (1985), Le poinçon de Pamplona (Colombie): Un jalon de la frontière méridionale de la plaque Caraïbe, *Bull. Soc. Géol. Fr.*, *8*(1), 403–413.

Bourdon, E., J. P. Eissen, M. A. Gutscher, M. Monzier, M. L. Hall, and J. Cotten (2003), Magmatic response to early aseismic ridge subduction: The Ecuadorian margin case (South America), *Earth Planet. Sci. Lett.*, *205*, 123–138.

Bourgois, J., B. Calle, J. Tournon, and J. F. Toussaint (1982), The Andean ophiolitic megastructures on the Buga-Buenaventura transverse (Western Cordillera–Valle, Colombia), *Tectonophysics*, *82*, 207–229.

Bourgois, J., J. Azéma, P. O. Baumgartner, J. Tournon, A. Desmet, and J. Aubouin (1984), The geologic history of the Caribbean-Cocos plate boundary with special reference to the Nicoya ophiolite complex (Costa Rica) and D.S.D.P. (legs 67 and 84 off Guatemala): A synthesis, *Tectonophysics*, *108*, 1–32.

Bourgois, J., J. F. Toussaint, H. Gonzalez, J. Azéma, B. Calle, A. Desmet, L. A. Murcia, A. P. Acevedo, E. Parra, and J. Tournon (1987), Geological history of the Cretaceous ophiolitic complexes of northwestern South America (Western and Central cordilleras of the Colombia Andes), *Tectonophysics*, *143*, 307–327.

Bourgois, J., et al. (1988), Seabeam and seismic reflexion imaging of the tectonic regime of the Andean continental margin off Peru (4°S to 10°S), *Earth Planet. Sci. Lett.*, *87*, 111–126.

Bourgois, J., A. Eguez, J. Butterlin, and P. De Wever (1990), Evolution géodynamique de la Cordillère Occidentale des Andes d'Equateur: La découverte de la Formation éocène d'Apagua, *C. R. Acad. Sci.*, *311*(2), 173–180.

Bourgois, J., C. Guivel, Y. Lagabrielle, T. Calmus, J. Boulègue, and V. Daux (2000), Glacial-interglacial trench supply variation, spreading-ridge subduction, and feedback controls on the Andean margin development at the Chile triple junction area (45–48°S), *J. Geophys. Res.*, *105*, 8355–8386.

Buck, W. R. (1988), Flexural rotation of normal faults, *Tectonics*, *7*, 959–973.

Calahorrano, A. (2005), Structure de la marge du Golfe de Guayaquil (Equateur) et propriété physique du chenal de subduction, à partir de données de sismique marine réflexion et réfraction, Ph.D. thesis, 227 pp, Univ. Paris VI, Paris.

Campbell, C. J. (1974), Ecuadorian Andes, in *Mesozoic Cenozoic Orogenic Belts: Data for Orogenic Studies*, edited by A. M. Spencer, *Geol. Soc. Spec. Publ.*, *4*, 725–732.

Cande, S. C., and D. V. Kent (1995), Revised calibration of the geomagnetic polarity time scale for the Late Cretaceous and Cenozoic, *J. Geophys. Res.*, *100*, 6093–6095.

Cantalamessa, G., and C. Di Celma (2004), Origin and chronology of Pleistocene marine terraces of Isla de la Plata and of flat, gently dipping surfaces of the southern coast of Cabo San Lorenzo (Manabí, Ecuador), *J. S. Am. Earth Sci.*, *16*, 633–648.

Cloos, M. (1992), Thrust-type subduction-zone earthquakes and seamount asperities: A physical model for seismic rupture, *Geology*, *20*, 601–604.

Collot, J. Y., P. Charvis, M. Gutscher, and E. Operto (2002), Exploring the Ecuador-Colombia active margin and inter-plate seismogenic zone, *Eos Trans. AGU*, *83*(17), 185, 189–190.

Corredor, F. (2003), Seismic strain rates and distributed continental deformation in the northern Andes and three-dimensional seismotectonics of the northwestern South America, *Tectonophysics*, *372*, 147–166.

Cortés, M., J. Angelier, and B. Colletta (2005), Paleostress evolution of the northern Andes (Eastern Cordillera of Colombia): Implications on plate kinematics of the south Caribbean region, *Tectonics*, *24*, TC1008, doi:10.1029/2003TC001551.

Daly, M. C. (1989), Correlations between Nazca-Farallon plate kynematics and forearc basin evolution in Ecuador, *Tectonics*, *8*, 769–790.

Deniaud, Y. (2000), Enregistrements sédimentaire et structurale de l'évolution géodynamique des Andes équatoriennes au cours du Néogène: Étude des bassins d'avant-arc et bilans de masse, Ph.D. thesis, 157 pp, Univ. Grenoble 1, Grenoble, France.

Deniaud, Y., P. Baby, C. Basile, M. Ordoñez, G. Montenegro, and G. Mascle (1999), Ouverture et évolution tectono-sedimentaire du Golfe de Guayaquil: Basin d'avant arc néogène et quaternaire du Sud des Andes équatoriennes, *C. R. Acad. Sci.*, *328*(3), 181–187.

Dhont, D., G. Backé, and Y. Hervoüet (2005), Plio-Quaternary extension in the Venezuelan Andes: Mapping from SAR JERS imagery, *Tectonophysics*, *399*, 293–312.

Dimate, C., L. Rivera, A. Taboada, B. Delouis, A. Osorio, E. Jimenez, A. Fuenzalida, A. Cisternas, and I. Gomez (2003), The 19 January 1995 Tauramena (Colombia) earthquake: Geometry and stress regime, *Tectonophysics*, *363*, 159–180.

Dumont, J., E. Santana, and W. Vilema (2005), Morphologic evidence of active motion of the Zambapala Fault, Gulf of Guayaquil (Ecuador), *Geomorphology*, *65*, 223–239.

Dunkley, P., and A. Gaibor (1997), Geology of the Cordillera Occidental of Ecuador between 2–3°S, Proyecto de Desarrollo Miner. y Control Ambiental, Programa de Inf. Cartog. y Geol., CODIGEM-BGS, Quito, Equador.

Ego, F., M. Sébrier, A. Lavenu, H. Yepes, and A. Eguez (1996), Quaternary state of stress in the northern Andes and the restraining bend model for the Ecuadorian Andes, *Tectonophysics*, *259*, 101–116.

Eguez, A., A. Alvarado, H. Yepes, M. Machette, C. Costa, and R. Dart (2003), Database and map of Quaternary faults and folds of Ecuador and its offshore regions, *U.S. Geol. Surv. Open File Rep., 03-289*.

Feininger, T., and C. R. Bristow (1980), Cretaceous and Palaeogene geologic history of coastal Ecuador, *Geol. Rundsch.*, *69*, 849–874.

Freymueller, J. T., J. Kellog, and V. Vega (1993), Plate motions in the north Andean region, *J. Geophys. Res.*, *98*, 21,853–21,863.

Gallier, A. (2005), Structure de la marge d'Equateur–Colombie par modélisation des données de sismique grand angle marines: Influence sur le fonctionnement de la subduction et la sismicité, Ph.D. thesis, Univ. Nice-Sophia Antipolis, Nice, France.

Garrison, J., and J. Davidson (2003), Dubious case of slab melting in the northern volcanic zone of the Andes, *Geology*, *31*, 565–568.

Garver, J. I., P. W. Reiners, L. Walker, J. Ramage, and S. E. Perry (2005), Implications for timing of Andean uplift from thermal resetting of radiation-damaged Zircon in the Cordillera Huayhuash, northern Peru, *J. Geol.*, *113*, 117–138.

Gomez, E., T. E. Jordan, R. W. Allmendinger, K. Hegarty, S. Kelleey, and M. Heizler (2003), Controls on architecture of the Late Cretaceous to Cenozoic southern Middle Magdalena Valley Basin, Colombia, *Geol. Soc. Am. Bull.*, *115*, 131–147.

Gomez, E., T. E. Jordan, R. W. Allmendinger, K. Hegarty, and S. Kelleey (2005), Syntectonic Cenozoic sedimentation in the northern middle Magdalena Valley Basin of Colombia and implications for exhumation of the northern Andes, *Geol. Soc. Am. Bull.*, *117*, 547–569.

Graindorge, D., A. Calahorrano, P. Charvis, J. Y. Collot, and N. Bethoux (2004), Deep structures of the Ecuador convergent margin and the Carnegie Ridge, possible consequence on great earthquakes recurrence interval, *Geophys. Res. Lett.*, *31*, L04603, doi:10.1029/2003GL018803.

Gregory-Wodzicki, K. (2000), Uplift history of the central and northern Andes: A review, *Geol. Soc. Am. Bull.*, *112*, 1091–1105.

Guillier, B., J. L. Chatelain, E. Jaillard, H. Yepes, G. Poupinet, and J. F. Fels (2001), Seismological evidence on the geometry of the orogenic system in central-northern Ecuador (South America), *Geophys. Res. Lett.*, *28*(19), 3749–3752.

Gutscher, M. A., J. Malavieille, S. Lallemand, and J. Y. Collot (1999), Tectonic segmentation of the north Andean margin: Impact of the Carnegie ridge collision, *Earth Planet. Sci. Lett.*, *168*, 255–270.

Hampel, A. (2002), The migration history of the Nazca Ridge along the Peruvian active margin: A re-evaluation, *Earth Planet. Sci. Lett.*, *203*, 665–679.

Haq, B. U., J. Hardenbold, and P. R. Vail (1988), Mesozoic and Cenozoic chronostratigraphy and cycles of sea-level change, *Spec. Publ. Soc. Econ. Paleontol. Mineral.*, *42*, 71–108.

Hey, R. (1977), Tectonic evolution of the Cocos-Nazca spreading center, *Geol. Soc. Am. Bull.*, *88*, 1404–1420.

Hughes, R., and L. Pilatasig (2002), Cretaceous and Tertiary terrane accretion in the Cordillera Occidental of the Andes of Ecuador, *Tectonophysics*, *345*, 29–48.

Hungerbühler, D., M. Steinmann, W. Winkler, D. Seward, A. Eguez, D. E. Peterson, U. Helg, and C. Hammer (2002), Neogene stratigraphy and Andean geodynamics of southern Ecuador, *Earth. Sci. Rev.*, *57*, 75–124.

Jaillard, E., S. Benítez, and G. Mascle (1997), Les déformations paléogènes de la zone d'avant-arc sud-équatorienne en relation avec l'évolution géodynamique, *Bull. Soc. Geol. Fr.*, *168*(4), 403–412.

Kay, S. M. (2005), Andean adakites from slab melting, forearc subduction erosion and crustal thickening, paper presented at 12th Congreso Latinoamericano de Geologia, Col. de Ing. Géol. De Pichincha, Quito, Ecuador.

Kellogg, J. N., and V. Vega (1995), Tectonic development of Panama, Costa Rica and the Colombian Andes: Constraints from Global Positioning System (GPS) geodetic studies and gravity, in *Geologic and Tectonic Development of the Caribbean Plate Boundary in Southern Central America*, edited by P. Mann, *Spec. Pap. Geol. Soc. Am.*, *295*, 75–90.

Kerr, A., J. Aspden, J. Tarney, and L. Pilatasig (2002), The nature and provenance of accreted oceanic terranes in western Ecuador: Geochemical and tectonic constraints, *J. Geol. Soc. London*, *159*, 577–594.

Lambeck, K., Y. Yokoyama, and T. Purcell (2002), Into and out of the Last Glacial Maximum: Sea level change during oxygen isotope stage 3 and 2, *Quat. Sci. Rev.*, *21*, 343–360.

Lapierre, H., et al. (2000), Multiple plume events in the genesis of the peri-Caribbean Cretaceous oceanic plateau province, *J. Geophys. Res.*, *105*, 8403–8421.

Lavenu, A., T. Winter, and F. Dávila (1995), A Pliocene-Quaternary compressional basin in the Interandean depression, central Ecuador, *Geophys. J. Int.*, *121*, 279–300.

Lonsdale, P. (1978), The Ecuadorian subduction system, *AAPG. Bull.*, *62*, 2454–2477.

Lonsdale, P., and K. Klitgord (1978), Structure and tectonic history of the eastern Panama Basin, *Geol. Soc. Am. Bull.*, *89*, 981–999.

Malfait, B. T., and M. G. Dinkelman (1972), Circum-Caribbean tectonic and igneous activity and the evolution of the Caribbean plate, *Geol. Soc. Am. Bull.*, *83*, 251–272.

Mamberti, M., H. Lapierre, D. Bosch, E. Jaillard, R. Ethien, J. Hernandez, and M. Polvé (2003), Accreted fragments of the Late Cretaceous Caribbean–Colombian Plateau in Ecuador, *Lithos*, *66*, 173–199.

Meschede, M., and U. Barckhausen (2000), Plate tectonic evolution of the Cocos-Nazca spreading center, *Proc. Ocean Drill. Program, Sci. Results*, *170*, 1–10.

Pardo-Casas, F., and P. Molnar (1987), Relative motion of the Nazca (Farallon) and South America plate since late Cretaceous times, *Tectonics*, *6*, 233–248.

Pecora, L., E. Jaillard, and H. Lapierre (1999), Accrétion paléogene et décrochement dextre d'un terrain océanique dans le Nord du Perou, *C. R. Acad. Sci.*, *329*(6), 389–396.

Pedoja, K. (2003), Les terrasses marines de la marge Nord Andine (Equateur et Nord Pérou): Relations avec le contexte géodynamique, Ph.D. thesis, 413 pp, Univ. Paris VI, Paris.

Pennington, W. D. (1981), Subduction of the eastern Panama Basin and seismotectonics of northwestern South America, *J. Geophys. Res.*, *86*, 10,753–10,770.

Pilger, R. H. (1984), Cenozoic plate kinematics, subduction and magmatism: South American Andes, *J. Geol. Soc. London*, *141*, 793–802.

Porter, S. C. (1989), Some geological implications of average Quaternary glacial conditions, *Quat. Res.*, *32*, 245–261.

Rea, D. K., and B. T. Malfait (1974), Geologic evolution of the northern Nazca Plate, *Geology*, *2*, 317–320.

Reynaud, C., E. Jaillard, H. Lapierre, G. Mascle, and V. Dupuis (1999), Oceanic plateau and island arcs of southwestern Ecuador: Their place in the geodynamic evolution of the northwestern America, *Tectonophysics*, *307*, 235–254.

Sallarès, V., and P. Charvis (2003), Crustal thickness constraints on the geodynamic evolution of the Galapagos Volcanic Province, *Earth Planet. Sci. Lett.*, *214*, 545–559.

Samaniego, P., H. Martin, C. Robin, and M. Monzier (2002), Transition from calc-alkalic to adakitic magmatism at Cayambe volcano, Ecuador: Insight into slab melts and mantle wedge interactions, *Geology*, *30*, 967–970.

Samaniego, P., H. Martin, M. Monzier, C. Robin, M. Fornari, J. P. Eissen, and J. Cotten (2005), Temporal evolution of magmatism in the northern volcanic zone of the Andes: The geology and petrology of Cayambe Volcanic Complex (Ecuador), *J. Petrol.*, *46*(11), 2225–2252, doi:10.1093/petrology/egi053.

Scholl, D., R. von Huene, T. Vallier, and D. Howell (1980), Sedimentary masses and concepts about tectonic processes at underthrust ocean margins, *Geology*, *8*, 564–568.

Scholz, C., and C. Small (1997), The effect of seamount subduction on seismic coupling, *Geology*, *25*, 487–490.

Shackleton, N. J. (1997), The deep sea sediment record at the Pliocene-Pleistocene boundary, *Quat. Int.*, *40*, 33–35.

Shepherd, G. L., and R. Moberly (1981), Coastal structure of the continental margin northwest Peru and southwest Ecuador, in *Nazca Plate: Crustal Formation and Andean Convergence*, edited by L. D. Kulm et al., *Mem. Geol. Soc. Am.*, *154*, 351–391.

Soulas, J. P., A. Eguez, H. Yepes, and V. Perez (1991), Tectónica activa y riesgo sismico en los Andes ecuatorianos y el extremo sur de Colombia, *Bol. Geol. Ecuat.*, *2*(1), 3–11.

Spencer, J. E. (1984), Role of tectonic denudation in warping and uplift of low angle normal faults, *Geology*, *12*, 95–98.

Spikings, R. A., and P. V. Crowhurst (2004), (U-Th)/He termochronometric constraints on the Late Miocene-Pliocene tectonic development of the northern Cordillera Real and the Interandean depression, Ecuador, *J. South Am. Earth Sci.*, *17*, 239–251.

Spikings, R. A., A. Winkler, D. Seward, and R. Handler (2001), Along-strike variations in the thermal and tectonic response of the continental Ecuadorian Andes to the collision with heterogeneous oceanic crust, *Earth Planet. Sci. Lett.*, *186*, 57–73.

Steinmann, M., D. Hungerbühler, D. Seward, and W. Winkler (1999), Neogene tectonic evolution and exhumation of the southern Ecuadorian Andes: A combined stratigraphy and fission track approach, *Tectonophysics*, *307*, 255–276.

Stern, C. R. (2004), Active Andean volcanism: Its geologic and tectonic setting, *Rev. Geol. Chile*, *31*, 161–206.

Taboada, A., L. Rivera, A. Fuenzalida, A. Cisternas, H. Philip, H. Bjwaard, J. Olaya, and C. Rivera (2000), Geodynamics of the northern Andes: Subduction and intracontinental deformation (Colombia), *Tectonics*, *19*, 787–873.

Tibaldi, A., and L. Ferrari (1992), Latest Pleistocene-Holocene tectonics on the Ecuadorian Andes, *Tectonophysics*, *205*, 109–125.

Trenkamp, R., J. N. Kellogg, T. Freymuller, and P. H. Mora (2002), Wide plate margin deformation, southern Central America and northwestern South America, CASA GPS observations, *J. South Am. Earth Sci.*, *15*, 157–171.

Tzedakis, P. C., et al. (1997), Comparison of terrestrial and marine records of changing climate of the last 500,000 years, *Earth Planet. Sci. Lett.*, *150*, 171–176.

Velandia, F., J. Acosta, R. Terraza, and H. Villegas (2005), The current tectonic motion of the northern Andes along the Algeciras Fault System in SW Colombia, *Tectonophysics*, *399*, 313–329.

Villagomez, D., A. Eguez, W. Winkler, and R. Spikings (2002), Plio-Quaternary sedimentary and tectonic evolution of the central Inter-Andean Valley in Ecuador, paper presented at 4th International Symposium on Andean Geodynamics (ISAG), Inst. de Rech. pour le Dév., Toulouse, France, 16–18 Sept.

von Huene, R., and D. Scholl (1991), Observations at convergent margins concerning sediment subduction, subduction erosion, and the growth of continental crust, *Rev. Geophys.*, *29*(3), 279–316.

von Huene, R., E. Suess, and the Leg 112 Shipboard Scientists (1988), Ocean Drilling Program Leg 112, Peru continental margin: Part 1, Tectonic history, *Geology*, *16*, 934–938.

von Huene, R., J. Bourgois, J. Miller, and G. Pautot (1989), A large tsunamogenic landslide and debris along the Peru Trench, *J. Geophys. Res.*, *94*, 1703–1714.

Wernicke, B. (1981), Low-angle faults in the Basin and Range province: Nape tectonics in an extending orogen, *Nature*, *291*, 645–648.

White, S., R. Trenkamp, and J. Kellog (2003), Recent crustal deformation and the earthquake cycle along the Ecuador-Colombia subduction zone, *Earth Planet. Sci. Lett.*, *216*, 231–242.

Wilson, D. S., and R. Hey (1995), History of rift propagation and magnetization intensity for the Cocos-Nazca spreading center, *J. Geophys. Res.*, *100*, 10,041–10,056.

Winkler, W., D. Villagomez, R. Spikings, P. Abegglen, St. Tobler, and A. Eguez (2005), The Chota basin and its significance for the inception and tectonic setting of the inter-Andean depression in Ecuador, *J. South Am. Earth Sci.*, *19*, 5–19.

Winograd, I. J., J. M. Landwehr, K. R. Ludwig, T. B. Tyler, and A. C. Riggs (1997), Duration and structure of the past four interglaciations, *Quat. Res.*, *48*, 141–154.

Winter, T., and A. Lavenu (1989), Morphological and microtectonic evidence for a major active right-lateral strike-slip fault across central Ecuador (South America), *Ann. Tect.*, *3*(2), 123–139.

Winter, T., J. Avouac, and A. Lavenu (1993), Late Quaternary kinematics of the Pallatanga strike slip fault (central Ecuador) from topographic measurements of displaced morphological features, *Geophys. J. Int.*, *115*, 905–920.

Witt, C., J. Bourgois, and F. Michaud (2006), Quaternary tectonic history of the Gulf of Guayaquil-Tumbes basin as the signature of the North Andean block tectonic escape, paper presented at the Backbone of the Americas, Geol. Soc. of Am., Mendoza, Argentina, 3–7 April.

J. Bourgois, F. Michaud, M. Sosson, and C. Witt, Geosciences Azur, La Darse BP. 48, F-06230 Villefranche-sur-Mer, France. (bourgois@ecua.net.ec; micho@obs-vlfr.fr; sosson@obs-vlfr.fr; witt@obs-vlfr.fr)

N. Jiménez and M. Ordoñez, Labogeo Petroproduccion, Via a Salinas, km 6 1/2, Guayaquil, Ecuador. (cigg@telconet.net; marthaleonor5@hotmail.com)

The Gulf of Guayaquil-Tumbes basin at the North Andean block trailing tail: a forearc basin originating from trench-parallel extension

Submitted to GSA Bulletin

Keywords: Ecuador, Peru, tectonic escape, interplate coupling, detachment faulting

César Witt [a, b], and Jacques Bourgois [a, b, c, d]

a Géosciences Azur, UMR 6526, Observatoire Océanologique de Villefranche-sur-Mer, France

b Escuela Politecnica Nacional, Andalucia n/s, C. P. 17-01-2759, Quito, Ecuador

c Institut de Recherche pour le Développement (IRD)

d Centre National de la Recherche Scientifique (CNRS), France

ABSTRACT

The Gulf of Guayaquil-Tumbes basin (GGTB) evolution controlled trench-parallel extensional strain that results from the North Andean block (NAB) northward drifting. Interpretation of industrial multichannel seismic and well data shows that low-angle detachment normal faults, the Posorja, Jambelí and Tumbes detachment systems, accommodate the main subsidence step along the shelf area during early Pleistocene (i.e. 1.8-1.6 Ma). These detachment systems are limited seaward by a major transfer system roughly located at the continental margin shelf break extending from the Domito faults system to the Banco Peru fault. The Tumbes detachment system corresponds to the master fault of basin evolution. It probably connects with the continental structures assumed to define part of the eastern frontier of the NAB. The total lengthening of a complete N-S transect between the

Posorja and Tumbes detachments ranges between 13.5 and 20 km. This lengthening is coherent with the documented NAB drifting rate combined with an early Pleistocene age for GGTB main opening pulse. The subsidence related to NAB drifting is almost entirely located at the shelf. The continental margin is unaffected by the escape tectonic process because of low coupling along the interplate contact. The GGTB, as well as other subsident-related trailing edges of tectonic escape systems seem to be characterized by low seismic release. It is proposed that the subsidence and related lengthening along the GGTB tends to weak the crust preventing the capacity to restore elastic strain to be released during seismic events.

INTRODUCTION

The current northward migration of the North Andean block (NAB, Figure 1a) triggers trench parallel extension that produces subsidence and related basin formation along its trailing tail (i.e. southernmost tip). From north to south the structures at the NAB trail includes the Miocene Progreso basin, the Eocene to Paleocene Santa Elena rise and the Quaternary Esperanza and Jambelí basins, both of them located along the Gulf of Guayaquil area, Ecuador. This system extends southward to the Quaternary Tumbes basin, the Miocene on-shore Zorritos basin and the Banco Peru, in the Peruvian side (Figure 1b and 2b). The Tumbes basin (northwestern Peru) is the southern part (Figure 1) of the Gulf of Guayaquil (GG), which extends on both sides of the Ecuador-Peru border at 3°20'S latitude. Indeed, Travis et al. (1974) and Shepherd and Moberly (1981) have long ago identified the Tumbes basin as the southern segment of the GG. Here we use the term Gulf of Guayaquil-Tumbes basin (GGTB) to define the conjunction of the Esperanza, Jambelí and Tumbes basins. The GGTB is proposed to evolve in response to the NAB northward drifting. In this context the GGTB has been generally described as a pull-apart basin, which formed between the eastern NAB boundaries and the trench (Shepherd and Moberly, 1981; Deniaud et al., 1999).

The southern Ecuador–northern Peru subduction zone extends along the western margin of South America and accommodates the ~6-7 cm/yr eastward convergence of the Nazca plate with the South America plate (DeMets et al., 1990; Freymuller et al., 1993; Kellog and Vega,

1995; Trenkamp et al., 2002). Along Ecuador, the dip angle of the Benioff zone ranges between 25° to 35° (Pennington, 1981; Guillier et al., 2001). The Carnegie ridge and the Grijalva fracture zone are currently subducting along the Ecuadorian margin (Figure 1a). At ~2° S the trench axis exhibits a change in trend from N-S to the south to NNE to the north. This change in trend would have enhanced oblique convergence between the Nazca and South America plates producing motion partitioning and the migration of an upper-plate sliver (Ego et al., 1996), the so called 'North Andean block' (NAB). Actually the NAB is migrating to the NNE at a rate of ~1 cm/yr along a major right-lateral strike-slip system that extends from Ecuador to Colombia and probably to Venezuela (Kellog and Vega, 1995; Trenkamp et al., 2002, Figure 1a). This scenario predicts at least 50% of locking of the convergence movement at the Carnegie ridge subduction zone (Trenkamp et al., 2002; White et al., 2003) defining the high degree of coupling between the subducting and overriding plates during at least the current seismic cycle. Both, the oblique convergence-related partitioning and the subduction of the Carnegie ridge have been proposed to be at the origin of the northward drifting of the NAB (Lonsdale, 1978; Pennington, 1981; Ego et al., 1996; Witt et al., 2006).

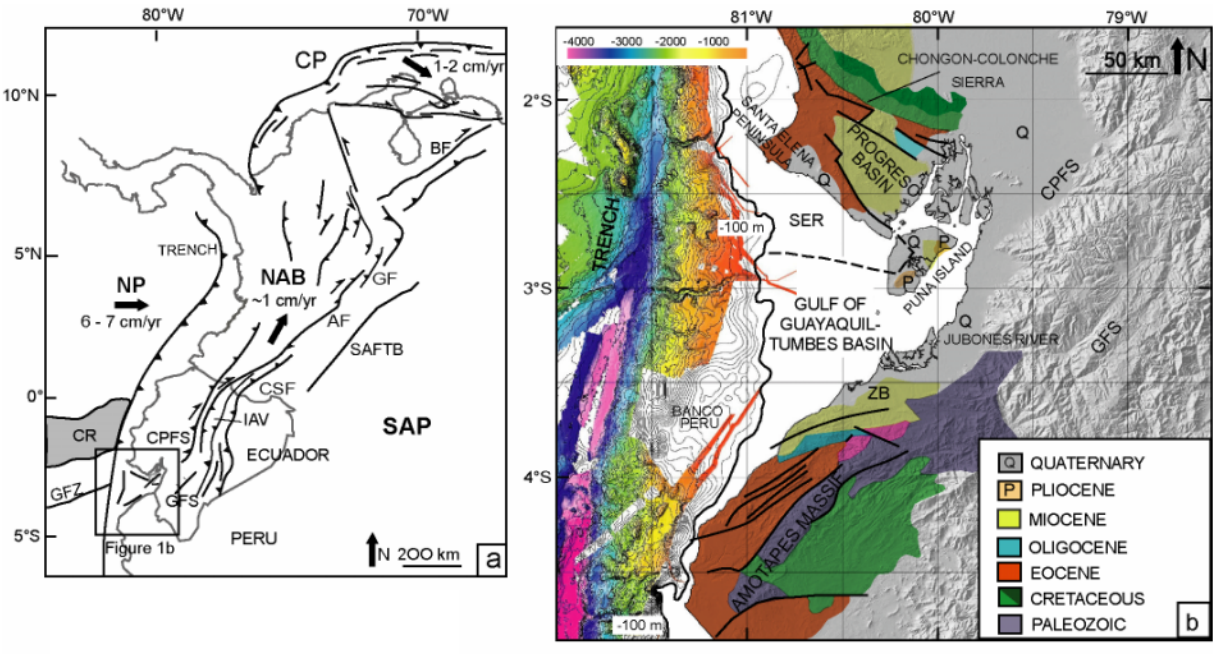

Figure 1. a) Structural framework of the Andean segment extending from northern Peru to Venezuela showing the NAB limits, modified from Taboada et al. (2000). **b)** Structural sketch of the Gulf of Guayaquil-Tumbes basin (GGTB) area, including the main continental features. Bathymetry of the continental margin and trench is a compilation of data from the Seaperc cruise (J.B. chief scientist) of the R/V Jean Charcot and the Andinaut cruise (J.B. Chief scientist) of the R/V L'Atalante. Black line is the -100 m bathymetric contour that grossly follows the shelf-continental margin limit. Geology from, Zevallos (1970) and Benitez (1995). Legend is for both Figures 1a and 1b. AF, Algeciras fault; BF, Boconó fault; CP, Caribbean plate; CPFS, Calacalí-Pallatanga fault system; CR, Carnegie ridge; CSF, Chingual-La Sofía fault; GF, Guaicaramo fault; GFS, Giron fault system; GFZ, Grijalva fracture zone; IAV, Inter-Andean valley; NAB, North Andean block; NP, Nazca plate; SAFTB, Sub Andean fault and thrust belt; SAP, South America plate; SER, Santa Elena rise; ZB, Zorritos basin.

Because the GGTB is located along the continental shelf, it recorded the tectonic and climatic signals of the adjacent continental area as it evolved through time. It includes, the tectonic record of the NAB northward drifting, the major continental crust thinning of the GGTB basement at depth and the sediment coastal drainage and transport to the trench. The GGTB is a key zone to develop analyses for constraining the tectonic evolution of the southern boundary of the NAB as well as the major tectonic decoupling occurring along the upper slope-shelf boundary. However, the southern Ecuadorian and northern Peruvian margin and shelf have been poorly studied. Most works concentrate in the central and southern segments of the Peruvian margin. This work investigates the northern Peru margin and continental shelf from unpublished industrial multi-channel reflection lines provided by Perupetro. First order correlations between the Ecuadorian and Peruvian continental margin and shelf are proposed in order to constraint a tectonic model for the GGTB evolution.

GEOLOGICAL CONSTRAINTS

The northern edge of the Gulf of Guayaquil exhibits mafic and ultra-mafic Cretaceous rock basement that crops out extensively along the E-W trending Chongón-Colonche sierra (Figure 1b). This basement resulted from the accretion of oceanic terranes. There is no consensus regarding the nature and age of the accretional phases. Ages ranging from late Cretaceous to Eocene time were proposed (i.e. Benitez, 1995; Jaillard et al., 1997; Luzieux et al., 2006). The oceanic basement is partially overlaid by Palaeocene to Eocene series cropping out along the Santa Elena Peninsula and extending offshore to the south along the Santa Elena rise (Figures 1b and 2b). Further south, sediments of Oligocene to Quaternary age accumulated along the Progreso basin, the GGTB and the on-shore Zorritos basin. The southernmost edge of the Zorritos basin shows metamorphic basement of Paleozoic age outcropping along the Amotapes massif (northern Peru). The metamorphic series show a varying metamorphism including some HP assemblages related to crustal thickening and exhumation during latest Jurassic-early Cretaceous time (Bosch et al., 2002, and references therein). Late Cretaceous to Quaternary sediment dipping towards the GGTB unconformably overlies this basement.

Off northern Peru, between 3°30’ and 7°30’S, the continental margin is characterized by the absence of contractile structures. Extensional tectonic features trending N-S extend not only throughout the middle and upper slopes, but also along the lower slope (Sheperd and Moberly, 1981; Bourgois et al., 1988; von Huene et al., 1989; Bourgois et al., 1993). They appear to result from the down-slope forces imparted by gravity as the continental margin over steepened. Active subsidence takes place along seaward dipping low angle (20 to 30°) detachments deep rooted in the basement (von Huene et al., 1989; Bourgois et al., 1993; Bourgois et al., 2007). Such tectonic conditions require decoupling along the subduction zone as well as subduction-erosion working at depth (i.e. Wang and Hu, 2006). The subduction-erosion regime extends northward to the Ecuadorian margin at the latitude of the GG (Calahorrano, 2005; Witt et al., 2006) and farther north to the latitude of the southern flank of the Carnegie ridge (Sage et al., 2006) where current seaward dipping normal faulting is at least partially related to subduction erosion processes. Normal faulting and massive subsidence are characteristics of the northern Peru-southern Ecuador margin. However, off Ecuador, the lower slope shows the local development of a small frontal prism (Collot et al., 2002) indicating that inner wall trench conditions probably changed along strike.

Based on industrial seismic line analysis, Witt et al. (2006) evidence that the northward drifting of the NAB controlled the main subsidence period of the GG area during at least the past 2 Myr (Figure 3). It includes the development of major detachments trending E-W, perpendicular to the N-S trending normal faults of the continental margin. This situation suggests that the continental margin tectonics is subduction-related meanwhile the NAB northward drifting controls the evolution of the GG along the shelf area. On the other hand, the Puná-Santa Clara fault system which has been considered as the main NAB frontier along the GG (Deniaud et al., 1999; Dumont et al., 2005) was defined as a local transform fault system between the Posorja and Jambelí detachment systems dipping to the south and to the north, respectively (Figure 2). The main period of NAB drifting is inferred from the high rates of subsidence and related sedimentation beginning at 1.8-1.6 Ma. Taking into account the strong dependence of the subsidence in the GGTB area with respect to the northward drifting of the NAB, we assume that the Pliocene–early Pleistocene boundary is associated with a major change in the northward migration rate of the NAB produced by the increase of the interplate coupling probably caused by the Carnegie ridge subduction.

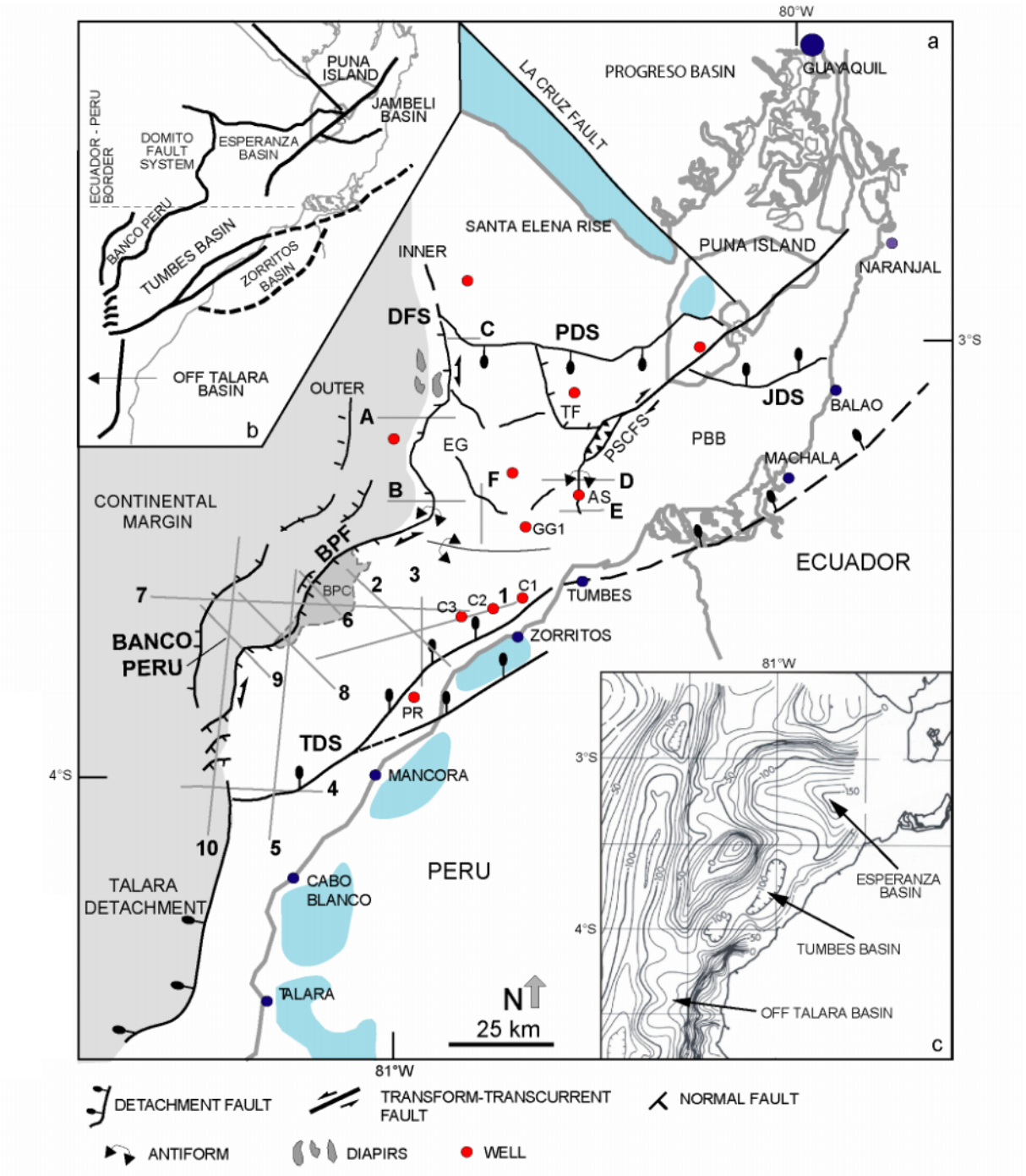

Figure 2. a) Structural map of the Gulf of Guayaquil-Tumbes basin (i.e. the southern tip of the NAB). The diapirs are identified down to 2 s TWTT. Minor normal faulting observed along the Tumbes basin and the central part of the Esperanza graben is not considered on this sketch. Note that the TDS exhibits an onland prolongation to the east. Light blue areas show zones where coastal uplift have been active at least since 200 kyr (data from, Pedoja et al., 2006 and Bourgois et al., 2007). A to F, seismic lines shown on Figure 3; 1 to 10, seismic lines shown on Figures 4 to 8; BPC, Banco Peru canyon; BPF, Banco Peru fault; DFS, Domito fault system; C1, C2 and C3, Corvina wells; EG, Esperanza graben; GG1, Golfo de Guayaquil 1 well; JDS, Jambelí detachment system; PBB; Puerto Bolivar block; PDS, Posorja detachment system; PR, Piedra Redonda well; PSCFS, Puná-Santa Clara fault system; TDS; Tumbes detachment system; TF, Tenguel fault. For description of wells north of the Ecuador-Peru border see Witt et al. (2006). **b)** Main tectonic features. **c)** Free-air gravity anomaly map (10 mgal contours), from Sheperd and Moberly (1981).

CONTINENTAL MARGIN AND SHELF STRUCTURES OF NORTHWESTERN PERU

We have analyzed about 3000 km of closely spaced industrial seismic lines (complete set of lines not shown on Figure 2a) covering the lower to upper continental slope and shelf between the Ecuador-Peru border at 3°25'S and Talara at ~4°40'S. This area includes the Tumbes basin, the Banco Peru, and the Eocene off-shore Talara basin. This work concentrates on the analyses of recent depocenter formation and associated record of tectonic deformation. Interpretation has been done on hardcopy profiles. All the profiles have been treated using a conventional processing sequence until migration. All the lines in this present work show a ~2.5 vertical exaggeration. Additionally, stratigraphic record from industrial wells is used to constrain age correlation of seismic markers throughout the studied area. The chronology of tectonic deformation was also done following first order correlations with GG area structures (Witt et al., 2006) where off-shore well stratigraphic record is best differentiated for the Plio-Quaternary period. An E-W directed antiform limits the Esperanza basin depocenter to the north from the Tumbes basin depocenter to the south (Figures 2 and 3). To minimize errors in projecting the data, seismic facies and stratigraphic correlations are proposed only for neighbor zones exhibiting low amplitude tectonic deformation.

Between the Santa Elena peninsula (Ecuador) and the Amotapes massif (northern Peru), the GGTB exhibits several km thick accumulation of Miocene to Quaternary sediment. This is also documented from free-air gravity anomalies (Figure 2c, Shepherd and Moberly, 1981). The 5-6 km thick sedimentary infilling of the GGTB extends southward along the Tumbes basin to about the latitude of Cabo Blanco at 4°S. South of 4°S, N-S steep positive gravity anomaly gradients, which underline the narrow shelf area, are the signatures of the seaward prolongation of the dense Paleozoic rocks of the metamorphic continental basement. Here gravity anomaly includes the signature of the thick accumulation of Eocene sediments. At 3°30'S, a contrasting gravity high underlies a shallow water flat-topped bank located 40-50 km seaward from the shelf: the so called Banco Peru. This strong anomaly connects northward to the Santa Elena Peninsula gravity anomaly (Ecuador) suggesting that mafic basement extends south to Banco Peru as first proposed by Sheperd and Moberly (1981). They proposed that Banco Peru is composed by rocks having density signature of mafic to ultramafic rock. If this issue is accepted, the low gravity minima, which underlie the GGTB

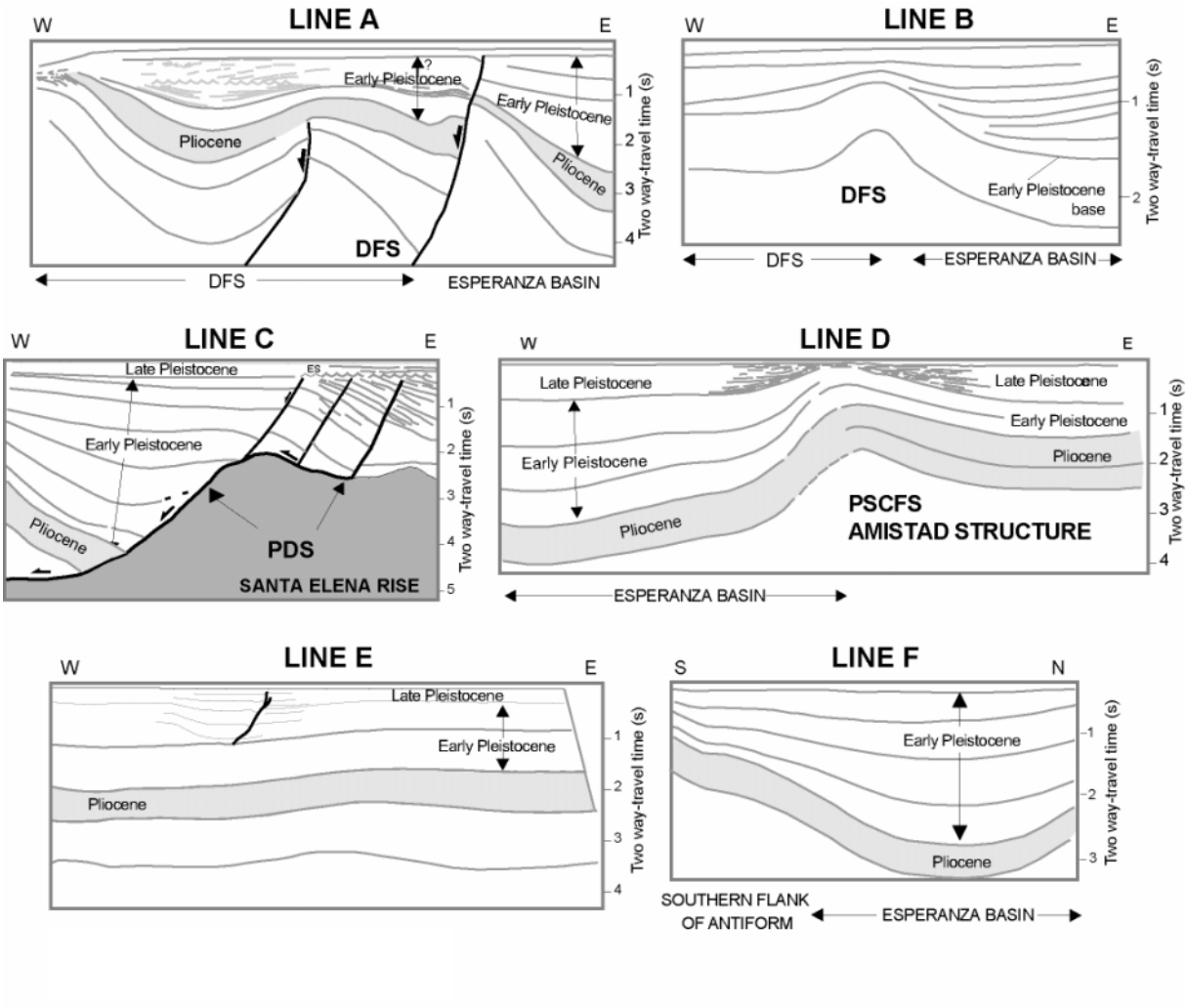

Figure 3. Key multichannel seismic lines of the Gulf of Guayaquil area (after Witt et al., 2006). Although a relatively thick Mio-Pliocene sedimentation exists beneath the main depocenters of the Eperanza basin the early Pleistocene is the period of major subsidence and depocenter individualization in the GG area. The GG area developed in relation with the northward escape of the NAB, in agreement with the evolution of extensional tectonic features bounding the main depocenters. The northward drifting of the NAB controlled the location of depocenters and associated subsidence that occurred along the GG during the past 1.6-1.8 Ma. Lines A and B, Domito fault system (DFS); Line C, Posorja detachment system (PDS), dark grey zones show the Paleocene-Eocene acoustic basement of the Esperanza basin; Line D and E, the Amistad structure, showing that the Puná-Santa Clara fault system (PSCFS) has no prolongation to the south (i.e. south of the Ecuador-Peru border); Line F, the southward raised reflectors define the southern flank of the antiform located at the transition between the Tumbes and Esperanza basins, the synforme placed in the centre of Line F defines the main Esperanza basin depocenter. Note that the Pliocene shows no variation in thickness throughout the Gulf of Guayaquil area suggesting that the main structures controlling the Pleistocene subsidence were not active previously. See Figure 2 for location of lines. Vertical exaggeration of lines ~2.5.

would be roughly located along the boundary between mafic Cretaceous basement to the north and metamorphic continental basement to the south (Figure 2c). This major limit located at depth is probably inherited from the tectonic suture of accreted ophiolitic material against the South America continent. Between 3°25' and 4°10'S a strong gradient in the free air gravity anomaly defines the eastern limit of Banco Peru. We assume that the connection between the inner Banco Peru and the DFS (Domito fault system) follows the -60 to -70 mgal contours. Indeed, seismic lines show that this connection takes place along a transcurrent

zone that connects the eastern limit of the Banco Peru (the Banco Peru fault, BPF) with the eastern normal fault of the DFS (Figure 2). Off southern Ecuador, along the continental margin, the basement is formed by oceanic rocks having low seismic velocities (Gailler, 2005). This low velocities basement extends to the north to the southern flank of the Carnegie ridge (Sage et al., 2006). The anomalous low velocities of the oceanic basement seem to be an effect of severe faulting and fracturing (Gailler, 2005). These evidences suggest that the transition between continental basement to the south and oceanic basement to the north takes place under the GGTB not far from the shoreline of northern Peru.

Stratigraphic constraint

We use data obtained from industrial wells drilled along the northern Peruvian shelf: the Corvina wells (CORV wells) and the Piedra Redonda (PR) well (data provided by PERUPETRO, Figures 2, 4a and 4c). These wells allow us to place first order constraints for Tumbes basin depocenter age and evolution. We have made no attempt to infer the tectonic history using sedimentary data. The CORV wells show a stratigraphic column that crosses the early Miocene to Quaternary sequences including the Heath, Zorritos, Cardalitos, Tumbes, Mal Pelo and La Cruz Formations. However, no precise stratigraphic records exist for the upper 900-1100 m of the section. Younger ages obtained from the CORV wells are generally defined as Plio-Pleistocene (Mal Pelo and La Cruz Formations.). North of the Ecuador-Peru border, in the GG area, the GG1 well record permits to identify the limit between the Pliocene and the Quaternary series. The nearness of the CORV and GG1 wells makes possible to project the stratigraphy established on the Ecuadorian side to that of the Peruvian side. Indeed, between the CORV and GG1 wells, the antiform, which defines the transition from the Esperanza basin to the Tumbes basin (Figure 2) is symmetric and wide open. The upper series defined as Plio-Pleistocene extend from 740 to 940 m below sea floor at CORV1 and CORV3, respectively (Figure 4c). At the GG1 well, the Pleistocene of the upper Puná Formation is clearly defined. It exhibits ~900 m thick accumulation of sediment, the base of which is characterized in seismic lines by weak to medium amplitude reflectors. In the GG1 well area the late Pliocene exhibits in seismic lines a series of strong reflections overlying poor continuity and low amplitude reflections in its lower part. Because these seismic signatures are roughly similar to those recorded along the eastern section of Line 1 we extend the seismic stratigraphy identified on the Ecuadorian side to the Peruvian side.

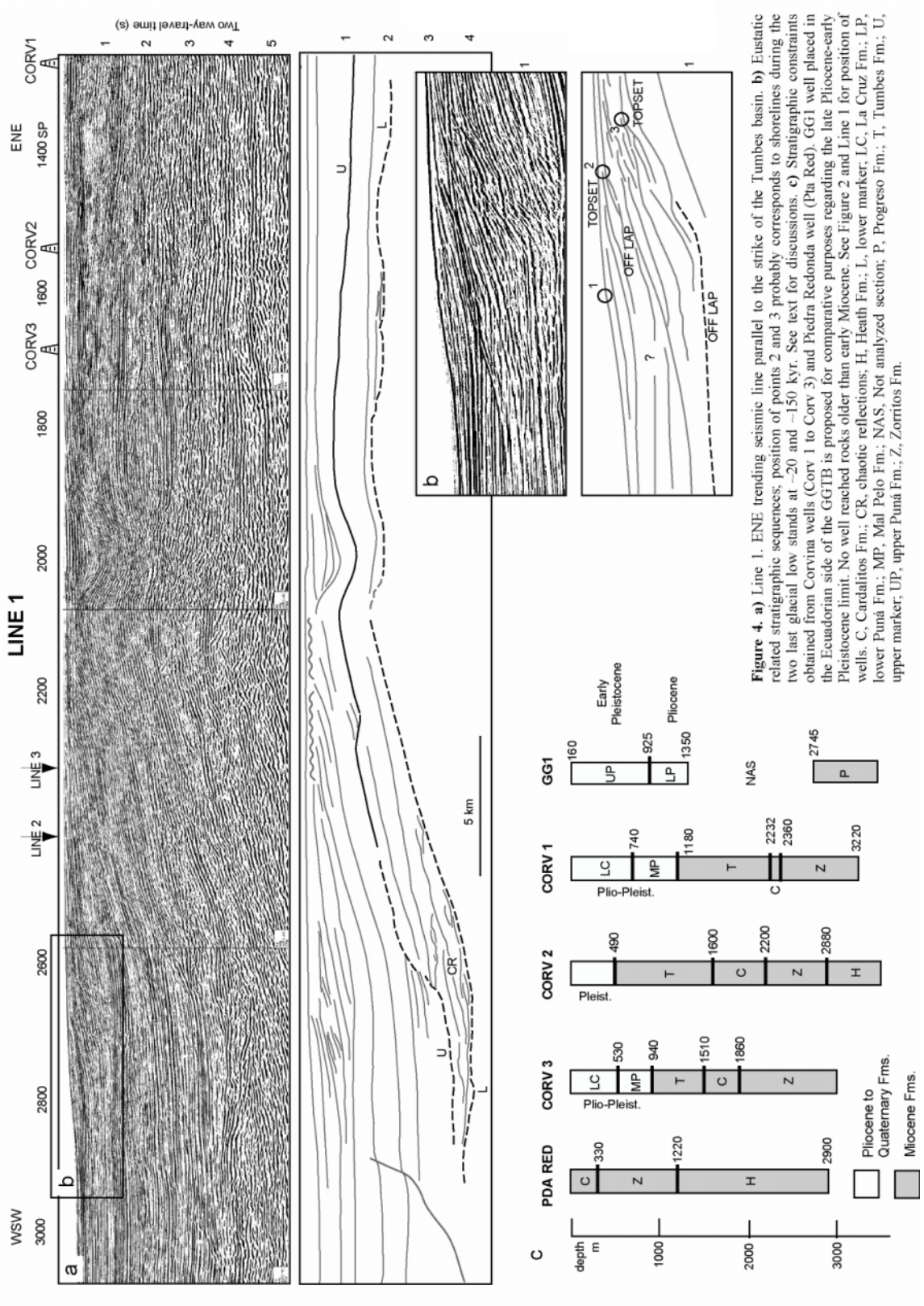

Figure 4. a) Line 1. ENE trending seismic line parallel to the strike of the Tumbes basin. **b)** Eustatic related stratigraphic sequences; position of points 2 and 3 probably corresponds to shorelines during the two last glacial low stands at ~20 and ~150 Kyr. See text for discussions. **c)** Stratigraphic constraints obtained from Corvina wells (Corv 1 to Corv 3) and Piedra Redonda well (Pta Red). GG1 well placed in the Ecuadorian side of the GGTB is proposed for comparative purposes regarding the late Pliocene-early Pleistocene limit. No well reached rocks older than early Miocene. See Figure 2 and Line 1 for position of wells. C, Cardalitos Fm.; CR, chaotic reflections; H, Heath Fm.; L, lower marker; LC, La Cruz Fm.; LP, lower Puná Fm.; MP, Mal Pelo Fm.; NAS, Not analyzed section; P, Progreso Fm.; T, Tumbes Fm.; U, upper marker; UP, upper Puná Fm.; Z, Zorritos Fm.

Considering the strong similarities in thickness and seismic signature we assume that the stratigraphic section defined as Plio-Quaternary on the Peruvian side, is an equivalent of

the upper Puná Formation, defined as late Pliocene to Pleistocene along the Ecuadorian side. More to the south, the Piedra Redonda well exhibits ~ 2500 m of Miocene sediments of the Carrizal, Zorritos and Heath Formations (Figure 4c) and defines the zones where sediment accumulation is Miocene in age.

Two seismic markers are relevant to reconstruct the chronology and steps of tectonic deformation along the Tumbes basin, it includes: a deep regional unconformity of middle Miocene age (the L marker, Figure 4a) and a shallower late Pliocene-early Pleistocene limit (the U marker, Figure 4a). The L marker probably corresponds to the unconformity at the limit between the Zorritos and the on-lapping Cardalitos Formation defined by Vega et al. (2005). We have made no attempt to describe other deeper unconformities observed along Line 1, which are probably older than Miocene. A precise characterization of these older depositional sequences in northern Peru was done using offshore seismic and onshore field data (Vega et al., 2005). The central segment of the Line 1 (at SP 2000, Figure 4) shows a canyon-type morphology with horizontal infilling of sediment. It separates the Line 1 into two segments. The eastern one displays parallel and horizontal seismic facies configurations. As opposed, the western segment exhibits markers that deepen to the SW. At this location the prolongation of the U marker coincides with an unconformity surface located above a zone where chaotic reflections exist (CR in Figure 4). We consider that this unconformity is the signature of a major tectonic event. Because this tectonic event is younger than the U marker, it occurred after the upper Pliocene. Indeed, the base of the Pleistocene sequence shows clear on-lap configurations (SP 2600, Figure 4a) pinching out toward the east. On the other hand, the projection of the U marker to the Lines 2 and 3, matches the early stages of tectonic activity along the Tumbes detachment system (TDS). We assume that the late Pliocene-early Pleistocene U marker predated the very early stage of the Tumbes basin formation. The Tumbes basin subsidence initiated at the limit between the late Pliocene and the early Pleistocene. Consequently, the Tumbes basin infilling is Pleistocene in age. Because the U marker recorded an erosive event increasing to the west, including the development of an erosion scarp facing seaward at about 2600 SP and 3 s TWTT depth (Figure 4a), we assume that this erosional event is also related with the early steps of basin formation. In this area, the erosion incised the sediment down to the L marker. As a result the vertical distance between L and U unconformities is drastically reduced, or in some cases, only the U unconformity exists west of Line 1.

On the other hand, the western shallow segment of Line 1 shows the development of clinoform sets defined by relatively deep off lap surfaces and shallow flat top surfaces (Figures 4a and 4b). Considering its present depth (i.e. shallow than 1 s TWTT), we assume that these clinoform sets are related to sea level fluctuations during the Pleistocene. We identified at least two sequences documenting two steps of sea level fall followed by sea level rise. Since the zone where these sequences are observed is located above the 100 m bathymetric contour, the two shallower sequences, shorelines 2 and 3 in Figure 4a, might be the signature of the two last documented low stands at ~20 kyr and ~150 kyr, respectively (Porter, 1989; Shackleton, 1997, and references therein).

The interpretation of the seismic lines used here allows us to recognize three major tectonic systems controlling the evolution of the margin and shelf of north-western Peru: the Tumbes detachment system (TDS), the Banco Peru (including the outer fault system and the inner Banco Peru fault, BPF) and the Talara detachment (Figure 2).

The Tumbes detachment system (TDS)

Well-defined normal faults occur along the northern Peru shelf area between Tumbes and Cabo Blanco (Figure 2a). They generally exhibit a strong signature on profiles. The most spectacular of these faults in seismic reflection profiles are gently dipping normal faults flattening to subhorizontal decollements at depth as exemplified by the TDS in Lines 2 and 3 (Figures 5 and 6, respectively). Considering that the profiles exhibit a ~2.5 vertical exaggeration these faults dip seaward (i.e. to the N-NW) at angles varying from 10 to 20°. These faults exhibit the signature of detachments. They developed as growth faults in association with roll-over folds, which accommodate fault nearest subsidence constraining the low-angle slip at depth. All major extensional faults are located within the 10-15 km of the shelf area close to the coastline.

For all major listric faults, a correlation can be made both in age and location, with the more currently active structures located closer to the coastline. Each detachment is characterized by regular growth strata, which indicate continuous development through time. The evolution of each of the TD1, TD2 and TD3 listric faults is associated with the development of a roll-over fold as evidenced by hanging wall growth strata. Each of the three

roll-over folds exhibit a hinge characterized by the development of an erosional surface, ES1 to ES3 from north to south and from older to younger, respectively (Figures 5 and 6). It documents a ~10 km landward migration of the tectonic deformation. We assume that Pleistocene sea level low stands favor the development of these erosion surfaces. Whether or not related to eustatic variations the evolution of the TDS tectonic activity documents a landward migration of the Tumbes basin depocenters.

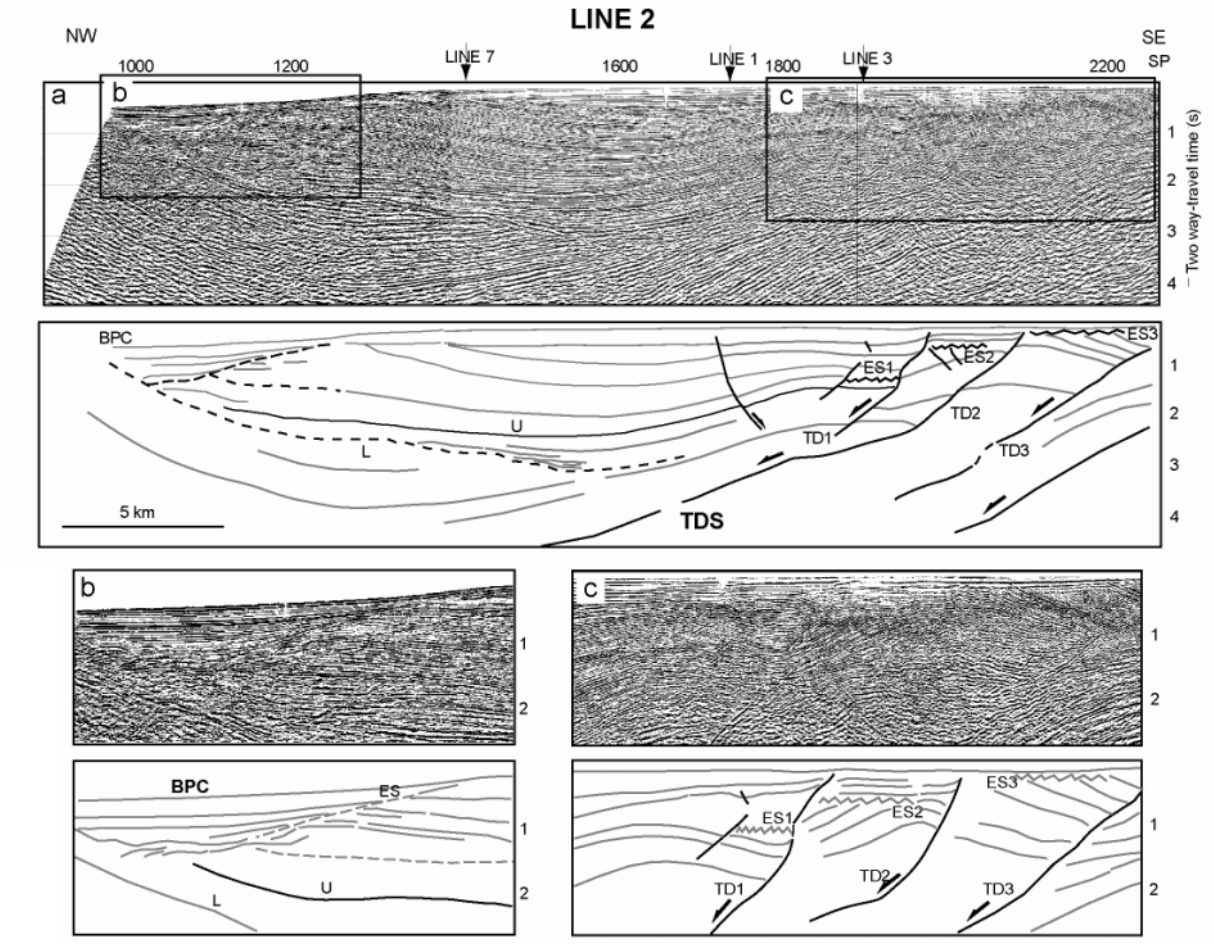

Figure 5. a) The Tumbes detachment system (TDS). The U seismic marker developped during the first step of activity along the TDS (i.e. the Plio-Pleistocene boundary). **b)** The Banco Peru canyon (BPC) cutting the U marker and defining this way the Quaternary age of the canyon. ES, Erosive surface. **c)** The landward (southward) migration of the tectonic activity along the TDS is defined by the TD1 (older) to TD3 (younger) fault segments. The ES1 to ES3 related erosive surfaces placed at the hinge of the roll-over faults define the end of main active tectonic step along the TD1 to TD3 segments. Location of Line 2 on Figure 2. Vertical exaggeration ~2.5.

To the south the Tumbes basin shows well stratified seismic facies. The accumulation of sediments is 3-4 s TWTT thick. Data from Line 1 projected along Line 5 (Figure 7) allows identifying the U marker at depth ranging from 3-4 s TWTT. Normal antithetic and synthetic faulting participates in basin subsidence. In the southern zone of Line 5 the development of a

growth fold along the TDS documents the tectonic activity of this major detachment. The westward limit of the Tumbes basin occurs along the complex triple junction between the Banco Peru fault (BPF) the TDS and the Talara detachment. This junction of three major fault systems may explain the complicated tectonic signature as well as the deepening water depth along the southernmost segment of the Tumbes basin.

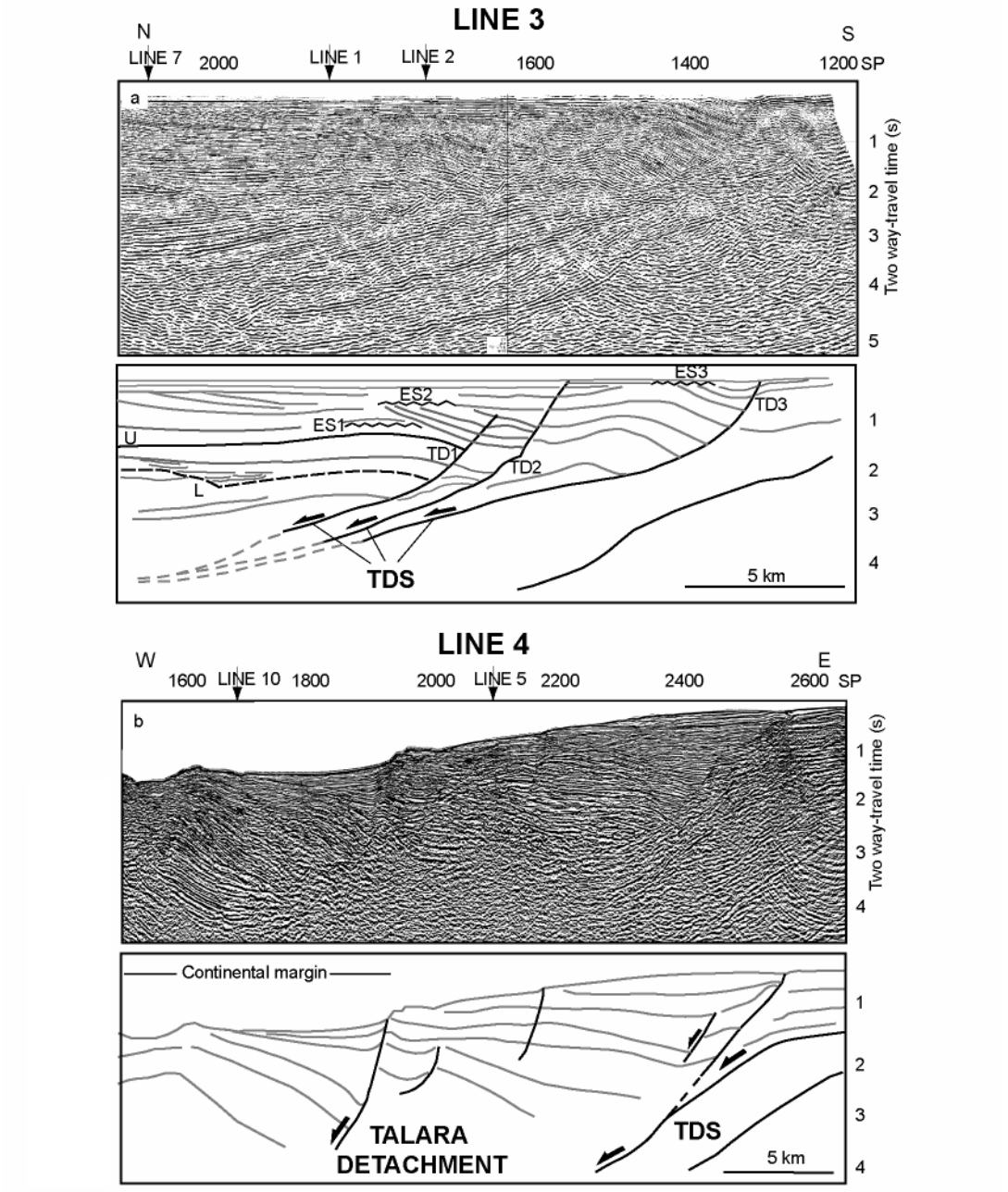

Figure 6. a) The Tumbes detachment system (TDS). Note the low angle (less than 20°) of the slip surfaces and the flattening of those surfaces at depth below 2-3 (s) TWTT. Evolution of TD1 to TD3 detachments and ES1 to ES3 erosion surfaces similar to that documented along Line 2. **b)** The Talara detachment controls deposition of Eocene to Pliocene (?) thick accumulation of sediments. Location of lines on Figure 2. Vertical exaggeration ~2.5

The initiation of the TDS-related subsidence can be inferred from identification of the depocenters and thickness variation of growth strata involved in the detachment fault activity (Figures 5 and 6). The early pulses of subsidence (Line 2, Figure 5) coincide with the base of a depocenter (at ~1.8 s TWTT) located away from the detachment zone. Additionally, in the Line 3 (Figure 6) first steps of TDS activity can be inferred from the older growth sediments placed near the fault plane. Correlation with Line 1 shows that these surfaces (i.e. base depocenter along Line 2 and base of the growth strata along Line 3) are late Pliocene-Pleistocene in age. The U marker, which connects to the U unconformity, is coeval with the beginning of the main step of the Tumbes basin subsidence. We assume that the late Pliocene-early Pleistocene first step of subsidence is controlled by the initiation of tectonic activity along the TDS controlling this way the Tumbes basin formation. The geometry configuration of the TDS slip zone, which parallels the strata of the early Miocene formations, suggests that clay mineral composition of particular beds may control the tectonic pathway of detachment. Recently, Vega et al. (2005) have suggested that the TDS correspond to a raft-gravity driven structure, the decollement zone extending along the top of the Heath Formation where the TD1 to TD3 flatten at depth. It is likely that the low angle geometry of the TDS is controlled by the presence of Miocene strata along its footwall segment. As Lines 4 and 5 show, no low angle geometry exists when footwall sediment is Eocene in age (Figures 1, 5 and 6).

Banco Peru.

Banco Peru is a flat shallow-depth bathymetric high located 30-50 km seaward from the coastline of northern Peru. The Tumbes basin, which exhibits a N-E trending axis, more or less parallel to the coastline, develops east of Banco Peru. A major landward-dipping normal fault (i.e. the Banco Peru fault, BPF, Figure 2) bounds the inner flank of Banco Peru to the east. The BPF controls the extension of the Tumbes basin to the west. Seaward dipping normal faults bound the outer flank of Banco Peru. These N-S trending faults parallel the trench axis and control the subsidence of the continental margin. The BPF displaces the sea floor along a 50-150 m high scarp. This scarps clearly documents that BPF is active (Lines 5, 6 and 7, Figure 7 and Line 9, Figure 8).

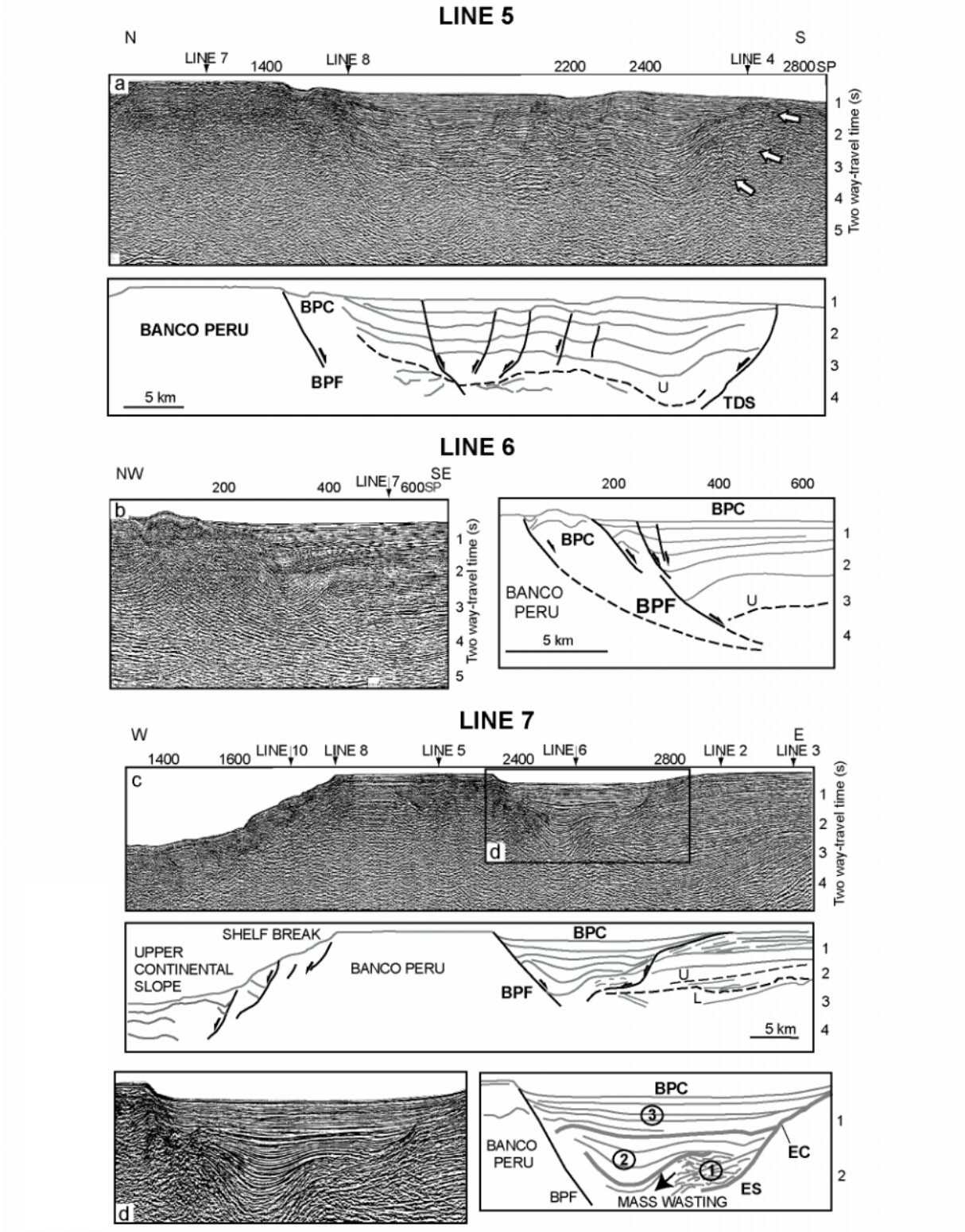

Figure 7. a) N-S transect of the south-western segment of the Tumbes basin from Banco Peru to the north to the TDS to the south. Synthetic and antithetic faulting affect the sediment infill of the basin. The TDS (white arrows in Line 5) shows a complex geometry along its southern segments as approaching the Talara basin. **b)** Transpressive structure defining a strike-slip component of deformation along BPF northern segments. **c)** E-W transect of Banco Peru. Seaward dipping normal faults define the limit between Banco Peru and the upper continental slope. Landward, the Banco Peru eastern limit (BPF), which acts as a normal fault, corresponds to the limit between the Banco Peru and the Tumbes basin. **d)** The Banco Peru canyon. 1 to 3 show the canyon filling sequences. EC, erosive cliff; ES, erosive surface. See text for further explanation. Location of lines on Figure 2. Vertical exxageration of lines ~2.5

A V-shaped canyon develops between the BPF and the Tumbes basin depocenter, the so called 'Banco Peru canyon' (BPC, Figures 2 and 7). Along BPF, clear seismic reflections characterize the BPC infilling down to 2-2.5 s TWTT, below this depth no clear seismic reflection exists. Three sequences (1 to 3 defining the lower, central and upper sequences, Figure 7d) define the canyon infilling along Line 7. An erosive surface bounds to the east the 1 to 3 sequences. Abrupt dip changes along this erosive surface probably correspond to ancient erosive wave-cut cliffs. The lower sequence is defined by very chaotic reflections located along the eastern wedge of the canyon. We assume that the chaotic reflection signal is the signature of important deformation and mass wasting processes. It is likely that these chaotic reflections extend northward and reaches the surface where Line 6 crosses the BPF (Figure 7). At depth, a convex erosive surface separates the lower and central sequences. The non deformed well stratified central sequence on-lap this erosive surface and extends farther up to ~1 s TWTT. The transition between the central and upper sequences is less abrupt. It is marked by an almost horizontal surface. However, minor on-lapping of the basal upper series is also observed. Considering that the upper section of the erosive surface, that limits the canyon to the east, crosses the most recent sediments of the GGTB, it is most likely that canyon formation took place during the past documented low-stands at ~20, ~140, ~350~, and ~450 ka (i.e. Porter, 1989; Shackleton, 1997). We assume that canyon filling and subsequent erosion of infilling sediments are coeval with high-stands and low-stands, respectively. The BPC shows a complex geometry defined by a strong along-strike variation of width and depth. Along its northern segment (Line 2) the canyon is 5 to 7 km wide with deeper expressions placed down to 1 s TWTT. More to the south, along Line 7, it is 15 km wide with seismic signature reaching 2.5 s TWTT. Along Lines 5 and 7 the seismic signature of the canyon reduced drastically in width. Along the N-S trending Line 10 no BPC signature exists.

The Line 6 (Figure 7) shows three major normal fault segments which probably connect downward to a single slip plane. Two antiforms exist between these normal fault segments. At ~SP 200 (Line 6, Figure 7) horizontal reflectors unconformably overlie one of these antiforms. We consider that these antiforms define a component of transpressive motion. The BPF geometry along Line 6 is that of a negative flower structure resulting from the succession of extensive and transpressive deformation and/or tectonic inversion along the normal fault segments. Along Line 7, tectonic activity takes place along a single normal fault

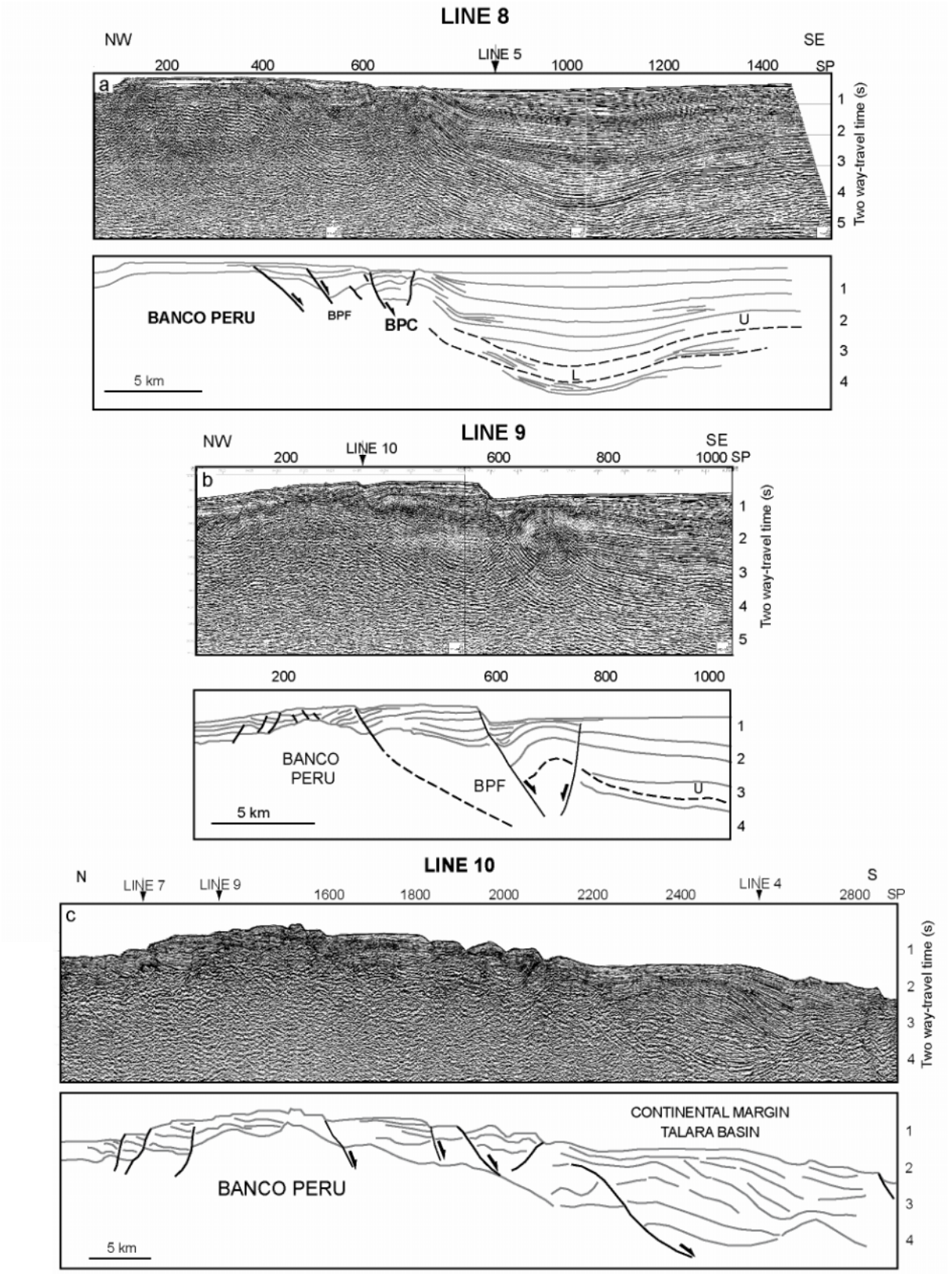

Figure 8. **a)** N-W directed line across the BPF. Note the weak deformation along BPF similar to that observed along Line 5 (Figure 7). **b)** Great extensive activity along the BPF defined by a roll-over fold. **c)** N-S transect of the upper continental margin. Complex geometry at the junction between the Banco Peru and the Talara basin. Note that no seismic signature of the Tumbes basin is observed. Location of lines on Figure 2. Vertical exaggeration of lines ~2.5.

segment. Recent tectonic activity is relatively weaker, since the upper section of the canyon filling is not disturbed by the fault. More to the south, the slip along BPF is probably transmitted from the single segment observed on Line 7 to at least three basinward dipping fault segments along Line 8. Further south, fault activity takes place along two major fault segments (Line 9, Figure 8). Here, roll-over folding accommodates the extensional deformation triggered by the fault. This is probably related to active low angle slip surfaces working at depth. Here the U marker deepens as it approaches to the BPF and is involved in roll-over fold deformation defining the Quaternary age for BPF activity. The along-strike and vertical differences in the style and amount of deformation show that a component of strike-slip deformation took place along BPF. On the other hand, along the seaward limit of the Esperanza basin (Ecuadorian side) the DFS exhibits a transcurrent component of deformation (Witt et al., 2006). This suggests that the strike slip motion of the inner DFS extends southward to the BPF, the complex connection between the landward segment of the DFS and the BPF is located along the N-S trending axis of the major antiform identified along Line B (Figure 3).

The formation of Banco Peru has been directly associated to the opening of the GGTB. It has been interpreted as a detached zone of ophiolitic basement left at its Present location during the northward drifting of the NAB (Shepherd and Moberly, 1981). Higley (2004) proposed that the Banco Peru was a part of the Santa Elena rise (if correct the Banco Peru series have to be of Palaeocene-Eocene age). We think that the origin of Banco Peru can not be well constrained due to the lack of age data of Banco Peru series.

The Talara detachment

The Talara detachment trends in a N-S direction from 4 to ~5° S (Figure 2a). To the south it swings to connect an E-W trending valley to reach the trench axis. This suggests that this detachment connects the subduction channel at depth (Bourgois et al., 2007). These authors propose that the Talara detachment corresponds to a sub-surface signature of subduction erosion working at depth. The Talara detachment is a seaward gently dipping normal fault, which displaces the continental basement of the Peruvian continental margin. In the shallow zones, fault activity displaced sea floor along a 150–200 m high scarp. Seismic makers along the fault show normal drag fold deformation indicative of subsidence down to

3.5 TWTT (Line 4, Figure 6). A series of relay-ramp normal faults connect the Talara detachment and the Banco Peru (Line 10, Figure 8).

DISCUSSION

Tectonic regimes and GGTB structure

The evolution of the southern Ecuadorian and northern Peruvian continental margin and shelf is controlled by two tectonic regimes showing different styles and ages. The extensional regime along the shelf area is NAB drifting-related while the extensional regime along the continental margin results from tectonic erosion working at depth.

The upper slope of the continental margin evolved controlled by normal faulting, which extends upslope to the outer DFS, the outer Banco Peru and the Talara detachment, from north to south. The outer Banco Peru is the southern prolongation of the outer DFS. The Talara detachment connects southward to the trench at ~5° S. The DFS and the Talara fault control the margin tectonic history in the southern Ecuador and northern Peru continental margins from Miocene to Present times. These extensional structures develop in response to subduction erosion working at depth (von Huene et al., 1989; Bourgois et al., 1993; Calahorrano, 2005; Witt el al., 2006; Sage et al., 2006; Bourgois et al., 2007). The complex geometry of the BPF and the inner DFS is interpreted as the result of a transcurrent component of motion. The direction of motion is quite difficult to constraint using seismic lines. However, it is possible that the sense of motion along this transfer system, which bounds the GGTB to the west, is controlled by the detachment systems controlling GGTB subsidence. The connection between the inner DFS and the BPF is located along a N-S trending folding zone. It accommodates the different motion between the seaward dip of the inner DFS and the landward dip of the BPF. The seaward limit of the GGTB is clearly defined by this transfer system. It limits to the west the zones where subsidence results from NAB drifting. No diffuse deformation exists at the southernmost seaward limit of the NAB.

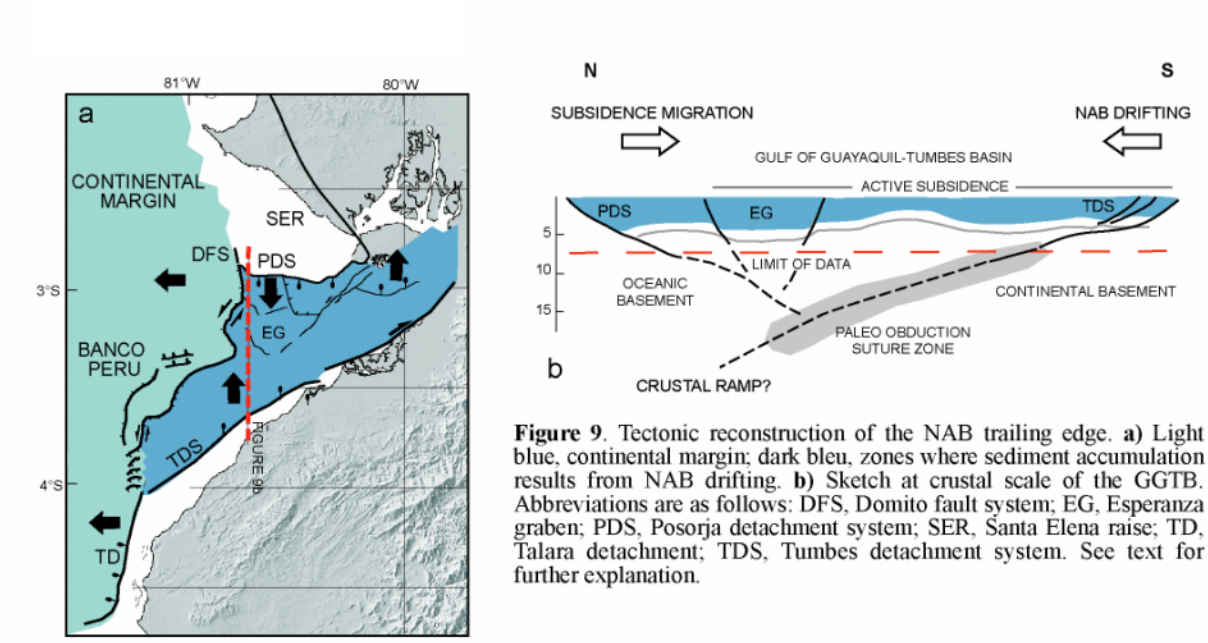

Figure 9. Tectonic reconstruction of the NAB trailing edge. **a)** Light blue, continental margin; dark bleu, zones where sediment accumulation results from NAB drifting. **b)** Sketch at crustal scale of the GGTB. Abbreviations are as follows: DFS, Domito fault system; EG, Esperanza graben; PDS, Posorja detachment system; SER, Santa Elena raise; TD, Talara detachment; TDS, Tumbes detachment system. See text for further explanation.

The GGTB shows two main subsidence and related-sedimentation phases: a Mio-Pliocene period showing low subsidence and low sedimentation rates followed by an early Pleistocene phase showing high subsidence and high sediment accumulation rates. A relatively thick Mio-Pliocene accumulation of sediments occurred along the shelf, including beneath the main early Pleistocene depocenters of the GGTB. Nevertheless, no major pre-Quaternary structure exists at the GGTB. The only pre-Quaternary fault-related activity along the GGTB area occurred along the western segments of the PDS, where deep growth faulting accommodates Mio-Pliocene subsidence. As opposed, the eastern segments of the PDS show deep on-lapping of the Mio-Pliocene series above the Paleocene-Eocene series of the Santa Elena rise. It seems that the western section of the Santa Elena rise acted as a horst-type structure while the eastern one was a topographic barrier. During Mio-Pliocene deposition this barrier separates the Progreso basin and the GGTB. On the other hand, the Miocene L unconformity is not identified at depth along the Esperanza basin. During Miocene times the southward wedge of the GGTB (i.e. the Tumbes basin) was subjected to stronger deformation and erosion pulses than the northern edge (i.e. the Esperanza basin) where sedimentation occurred in a more protected environment. To the south of the main TDS, along the Zorritos basin, the sedimentary series are predominantly Miocene in age. It includes the Tumbes, Cardalitos and Zorritos Formations. From the shoreline to 10 to 20 km landwards from Zorritos and Mancora (Zorritos basin, Figure 2a) the Miocene strata dips northwards exhibiting pervasive closely spaced low-angle normal faults. These faults, which

are probably active, trend E-W and dip to the north. This tectonic deformation suggests that an on-shore detachment structure located between the Zorritos basin and the Amotapes massif controlled the subsidence during Miocene times. This scenario suggests that a roughly N-S directed strain was acting before major depocenters formation in early Pleistocene times, a similar scenario was first proposed by Benitez (1995).

During the early Pleistocene the subsidence rate increases drastically. The E-W trending PDS and JDS controlled the subsidence of the Esperanza and Jambelí basins, respectively. More to the south, the N-E trending TDS triggered subsidence for the Tumbes basin evolution during the same period of time (Figure 9). The BPF participated also in subsidence accommodation. However, activity along the BPF was less important, local, and is probably more related to a transtensional component of deformation. Therefore, a ~N-S tensional stress regime characterized the GGTB shelf area during Quaternary times. The PDS and the TDS extent only until the inner DFS and the complex zone of the junction between BPF and the Talara detachment, respectively. The subsidence related to the NAB northward drifting being at the origin of the GGTB is mainly confined to the shelf zone (Figure 9a). No connection exists between the NAB limits and the trench.

Detachment faults are common in zones of high extensional strain and often accommodated great displacement (i.e. Axen, 1992; Wernicke, 1995). However, almost no active low angle normal faults have been documented in zones of tectonic escape. Doubts persist if low angle normal faults originated and slipped at close to their current dips or if they originate at high angles which are later rotated flexurally to shallow angles as slip increases (i.e. Spencer, 1984; Buck, 1988; Wernicke and Axen, 1988; Brun et al., 1994; Gartrell, 1997). The main subject of debate is that being detachment faults at high angle to the main vertical strain, resolved strain along the slip plane tends to be small, enhancing slip to occur. Nevertheless, at low-angle normal faults principal stress might be rotated at depth, allowing slip to occur (i.e. Bartley and Glazner, 1985; Bradshaw and Zoback, 1988). Such rotation exists if there is a significant contrast of pressure or viscosity between faulted and unfaulted strata (i.e. if the faults are weaker than its surroundings Bartley and Glazner, 1985; Axen, 1992). Furthermore, overpressured low-angle normal-slip growth faults are well known from delta depositional environments where elevated pore pressure can be contained by sedimentary layering (i.e. Cobbold et al., 2004 and references therein). The TDS has been

interpreted as a raft structure (Vega et al., 2005). The lowest angles along the TDS occur where the TDS footwall-block consists of Miocene strata. The parallel dip of the TDS slip zones and the Miocene strata suggest that stratigraphy could exert a major control on fault evolution. Even so, the major PDS, in the opposite side of the GGTB, is a low-angle normal fault, which slip zone is not related to a stratigraphic plane. This suggests that raft tectonics can not be the only factor controlling the low-angle geometry of the structures governing the GGTB architecture. Abnormal gradients of pressure have been measured in the CORV 2 well during drilling operations. A high pressure zone is located at ~2600 m. It nearly matches at depth the décollement zone of the TDS (as it is observed along a N-S directed line that cross the Corv 2 well, line not shown due to poor quality shallow seismic markers). However, it is difficult to assume a high pressure layer extending all over the TDS at depth, because no pressure record exists for the CORV 1 and 3 wells. On the other hand, active low-angle normal faulting has been observed at shallower depths along the Zorritos basin suggesting that low-angle normal fault formation may not be related to a single over pressured plane along which slip occurs. To the north, the PDS shows its lowest angles close to the DFS, not far from the diapir emplacement zone seaward from the DFS, suggesting that probably high pressure conditions also took place along the PDS. It is difficult to clearly define the low-angle nature of the structures governing the GGTB evolution because evidences are contradictory. However, one critical point to characterize kinematics of the GGTB is that detachment faults formed in response to a vertical strain but also to a N-S directed main horizontal strain related to NAB drifting. It is probable that the N-S directed horizontal strain exerts an important control on the origin and evolution of the main extensional systems. It has been proposed that similar magnitudes of the two vertical and horizontal principal strains are related with weak faults which in turn favor low-angle normal fault formation (Axen, 1992).

Classical pull-apart basins develops preferably along strike-slip bend or strike-slip stepover, whether they form along one or two major transcurrent faults, respectively (i.e. Christie-Blick and Biddle, 1985). Pull-apart basin formation along releasing joints and fault-ending-tails has been also proposed (Bertoluzza and Perotti, 1997). The architecture of the GGTB does not fit the classic pull-apart basin model in which subsidence develops in response to slip difference along one or two offset transcurrent structures. Indeed, transcurrent structures (i.e. the inner DFS, the BPF-Talara detachment junction zone and the

PSCFS) accommodate at the GGTB the motion related to the extensional detachment structures. This is exactly the opposite to pull-apart basins, where extensional structures develop in response to the difference in the strike-slip character of transcurrent systems. The development of the GGTB as a pull-apart-basin limited seaward by the trench, which acts as one of the major transcurrent faults of the pull-apart system (Sheperd and Moberly, 1981), is inconsistent with the tectonic deformation as recorded along the shelf and the continental margin. Furthermore, the transcurrent structures at the GGTB itself (i.e. the PSCFS) do not define the major NAB limits as it was previously proposed (Deniaud et al., 1999; Dumont et al., 2005). At the scale of a major-crustal transcurrent system (i.e. the eastern boundary of the NAB) the graben structure of the GGTB is a fault-ending trail.

The PDS and the TDS extend from 50 to ~100 km (no major segmentation is observed in seismic lines) and developed in response to the drifting of an upper-plate sliver. Along continental settings 20 km length faults are assumed to cut across all the seismogenic crust (Jackson, 1987). Typically the PDS and the TDS must penetrate deep into the crust down to the interplate interface, located at ~20 km beneath sea bottom at the shelf break (Calahorrano, 2005). No direct evidence exists to identify the master fault that controlled the basin evolution. However, several points should be considered: 1) the Progreso basin and the Santa Elena rise show no major subsidence in Quaternary times. Furthermore, the PDS is not active at present time (Witt et al., 2006). The southward migration of activity from the PDS to the Esperanza graben is probably the response to progressive slip blocking northwards and the subsequent creation of a southward free border along the TDS. 2) The PDS is limited landward by the PSCFS (i.e a length approximately twice smaller than the TDS). 3) The N-E trending of the TDS, similar to that of the continental structures in northwestern Peru and the coastline between Cabo Blanco and Tumbes suggest that this system exerts a strong control on coastline location. Along the eastern zones of the shelf (i.e. the Puerto Bolivar block, Figure 2a) seaward subsidence is located above a pervasive seaward dipping unconformity zone, showing a geometry strongly similar to the TDS. It seems that this block evolved controlled by the landward segments of the TDS suggesting that the TDS extends onshore. This is supported by vibro zeiss data that evidence a detachment structure along the coastal plain between Machala and Balao (Figures 2a and 4). The TDS is the southward boundary of the extensional deformation accommodation at the NAB trailing edge and it probably connects northward to right lateral or normal faults, such as the Calacalí-Pallatanga fault

system or the Girón fault system (Figure 1b), assumed to define part of the eastern frontier of the NAB. We consider that the shallower tectonic escape architecture of the GGTB does not differ from that of other continental rift basins: a master normal fault or detachment evolving with antithetic and synthetic faulting in the hanging wall resulting in a graben structure (Figure 9). We consider that the TDS is the master fault of basin evolution.

Considering that the GGTTB is bounded by Cretaceous oceanic terranes to the north and Paleozoic continental basement to the south, the role of the old suture zone between these terranes in controlling the location of the GGTB has been evaluated in many works (i.e. Calahorrano, 2005; Gallier, 2006). However, there is no consensus about the location of the suture zone under the thick sedimentary cover of the GGTB. Indeed, at the shelf break the basement of the GGTB shows weak seismic velocities, which have been considered as the signature of continental basement (Calahorrano, 2005) or as the signature of highly fractured oceanic basement (Gallier, 2006). Modeling of the gravity data obtained by Sheperd and Moberly (1981) leads to poor results about the deep structure of the basin. Indeed, considering a 6-7 km thick sedimentary layer and a ~20 km thick basement, the gravity signal matches only if we consider very similar densities for both, oceanic and continental basements. Modeling does not allow imaging the geometry of the suture zone. However, it is important to consider that the oceanic basement is currently drifting northwards along the limit of the NAB while the continental basement is considered as fixed (with respect to the South American plate). Whether the suture zone plays an important role in GGTB tectonics, we assume that a northward dipping crustal ramp (Figure 9b) may exist along the suture between oceanic and continental basement. The TDS (i.e. the master fault of basin evolution) would be the shallower signature of this suture zone. In that manner, the PDS probably evolve controlled at depth by the northward dipping slip surface of the TDS. This is consistent with models of ramp-flat-ramp subsidence, which predict more subsident zones not necessarily placed above the master fault but near to the main antithetic fault (Gibbs, 2002 and references therein). This is the case of the GGTB where main subsidence is located along the Esperanza basin close to the main PDS antithetic fault.

Horizontal drifting of a sliver of the overriding plate triggers arc-parallel extension which has been considered as a major factor controlling exhumation of metamorphic rocks along the so called ‘metamorphic core complexes’ (i.e. McCaffrey, 1996; Avé Lallemant and

Oldow, 2000). One of the most remarkable features of metamorphic core complexes is that they are all bounded by low-angle normal faults and that they appear to be related with previously thickened crust (i.e. Wernicke and Axen, 1988; Smith et al., 2006). Large displacements on low-angle normal faults results in isostatic uplift of the lower plate in response to tectonic denudation (Spencer, 1984). In its modeling Spencer (1984) observed important warping of the lower plate and antiform formation with axes perpendicular to the direction of extension for amounts of extension of ~20 km. This warping and antiform formation is normally accompanied by uplift of metamorphic and plutonic rocks. Furthermore, Spencer's model have four structural domains all separated by low-angle normal faults. Taking into account that emplacement, over-thickening and uplift of HP and other metamorphic rocks along the Amotapes massif could be as old as Jurassic-early Cretaceous (Bosch et al., 2001 and references there in) and that the whole structure of this HP assemblages is controlled by E-W directed structures is tempting to think that NAB northward migration and GGTB opening may increase recent exhumation rates of metamorphic rocks of the Amotapes massif.

Interplate mechanical and seismological coupling constraints

Models of tectonic escape along oblique convergence margins attempt to explain the existence of motion partitioning and the drifting of an upper plate sliver in terms of convergence obliquity, mechanical coupling between the subducting and overriding plates and strength of the overriding plate (Jarrard, 1986; McCaffrey, 1992; Platt, 1993; Yu et al., 1993; Liu et al., 1995; Chemenda et al., 2000; Upton et al., 2003). However, the nature of these aspects, especially if the expulsion of the sliver results from strong or weak interplate coupling, are in debate. Nevertheless, the frictional properties along the interplate limit and overriding plate strength have been considered and modelled as homogenous features in a large setting that includes all the subduction system: the trench, the arc and even the back-arc systems. On the other hand, observed patterns of interplate seismicity are consistent with differences in interplate coupling; the weaker coupling indicating a lack of seismogenic potential and a low probability for large earthquakes occurrence (Huang et al., 1997). The

northern South American subduction zone segment, between 1°N and 8°S, shows no occurrence of great earthquakes (Lay and Kanamori, 1982; Swenson and Beck, 1996). Based on trench parallel gravity variations (Song and Simons, 2003) predict low elastic strain accumulation between 1°N to 3°S and higher elastic strain accumulation from 4°S to 8°S. However, the continental margin segment between 1°N and 3°S shows strong segmentation, it includes the Carnegie ridge subduction zone and the GGTB, which must be analyzed separately in terms of strain accumulation. In fact, the frictional interplate limit properties are not constant at the GGTB.

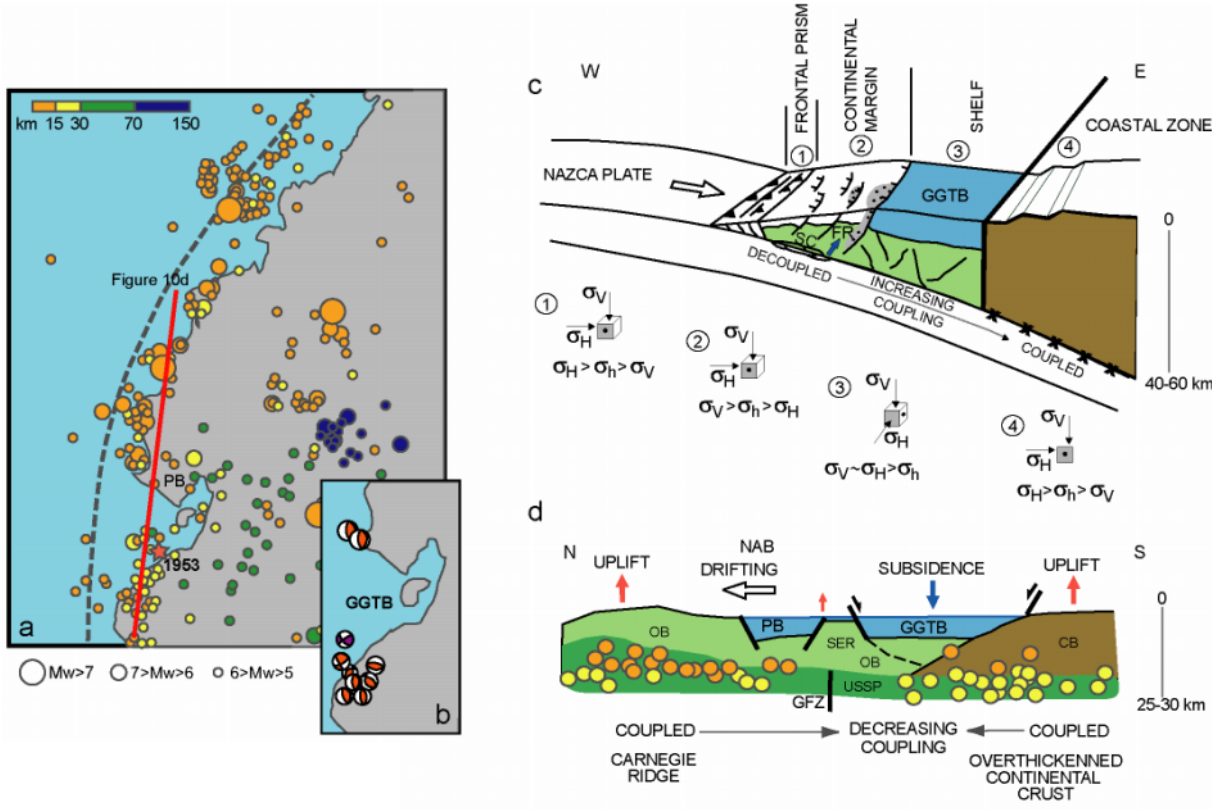

Figure 10. **a)** Seismic events location along the Andean segment from southern Colombia to northern Peru, data from the USGS-NEIC catalogue. Location of the 1953 Mw. 7.3 event (red start) from Silgado (1957) **b)** Focal mechanisms of 5>Mw>6 along the GGTB and neighbour zones, data obtained from the Harvard centroid catalogue. **c)** E-W schematic transect of the subduction system at the GGTB latitude. Spatial distribution of strain is proposed for each segment. **d)** Schematic N-S transect between the Carnegie ridge subduction zone to the Amotapes massif (overthickenned continental crust). Circles corresponds to Mw>5 events as represented in Figure 10a. GGTB, Gulf of Guayaquil-Tumbes basin; CB, continental basement; FR, fluid release; OB, oceanic basement; PB, Progreso basin; SC, subduction channel; USSP, upper section of the subducting plate. See text for further explanations.

The subsidence of the GGTB, which results from the tectonic escape of the NAB is a major factor in controlling the subduction tectonic regime of the continental margin area. Indeed, the sediment input to the trench is a major control feature on the nature of the subduction regime under the continental margin. It has been shown elsewhere (i.e. von

Huene and Scholl, 1991; Bourgois et al., 2000; Clift and Vanucci, 2004) that an increase of the sediment supply to the trench axis is a major cause for the continental margin tectonic regime to switch from subduction-erosion to subduction-accretion. A relatively thin sediment cover below the trench favours the subduction of sediments rather that the construction of an accretionary prism (Clift and Vanucci, 2004). The GGTB plays a major role in controlling the trench sediment input since subsidence along the GGTB favors the sediment to be trapped at the shelf instead of reaching the continental margin and the trench axis. Most of the GGTB area is less than 100 m water depth, therefore it emerges during Pleistocene low-stands increasing the sediment input to the trench axis.

The southern Ecuadorian and northern Peruvian continental margins are defined by westward dipping normal faults (the outer DFS and the outer Banco Peru; Bourgois et al., 1993; Collot et al., 2002; Calahorrano, 2005; Witt et al., 2006; Bourgois et al., 2007). The absence of significant contractional structures or bending along the southern Ecuadorian and northern Peruvian continental margin confirms that compressional strain build up is low reflecting this way the high degree of long-term decoupling between the continental margin and the subducting plate. Beneath the lower and middle slope, an interplate seismic channel where overpressured sediments are being subducted is imaged on seismic lines (Calahorrano, 2005). The overpressured fluids are released at ~ 20 km landward from the trench, this release promoting a landward increase of interplate coupling (Calahorrano, 2005). No realistic geophysical data exist to constraint the nature of the interplate interface under the GGTB. However, if a great amount of fluids is expelled it means that friction increases to the east, below the GGTB, increasing this way the mechanical coupling between the plates. However, the landward increase of interplate coupling may be gradual. The transition between decoupled (or partially coupled) and coupled interplate limit takes place not far from the TDS (Bourgois et al., 2007). It seems that a gradual increase of interplate coupling takes place from the trench to the coastal zone (Figure 9b). In this scenario we suggest that the continental margin does not react to the tectonic escape because of low interplate coupling.

The seismic data used here represents a complete N-S transect of the GGTB. We calculate the lengthening along the basin as the sum of the horizontal extension calculated for each major fault. Assuming: 1) an uniform fault dip. 2) that slip is essentially orthogonal to the structures (coherent with the observed low angle slip surfaces). 3) that no important

rotations exists, and 4) that compaction of sediments is negligible compared with the tectonic-related basin subsidence, or that this value is compensated by the displacement along minor closely-spaced normal faults (Walsh et al., 1991), the early Pleistocene total lengthening between the PDS and the TDS ranges between 13.5 and 20 km (~5 to 10% net lengthening). Furthermore, a 13.5 to 20 km total lengthening is in good agreement with the ~1 cm/yr calculated rate for the northward NAB migration rate (i.e. Kellog and Vega, 1995; Trenkamp et al., 2002) combined with an early Pleistocene age (1.8 to 1.6 Ma) for GGTB area main opening pulse. This lengthening probably increases taking into account a longer transect between the Santa Elena rise and the Amotapes (i.e. the older Mio-Pliocene basin formation). We did not calculate the lengthening related to this subsidence step because almost no structure has been observed in seismic lines for this period. However, if we assume that there must be a direct correlation between lengthening and subsidence, and considering that major depocenter formation in the GGTB in early Pleistocene (3-3.5 km) corresponds only to 5 to 10% net lengthening, it is most likely that Mio-Pliocene lengthening might be quite smaller. The GGTB evolved bounded westward by the inner DFS and the BPF and eastward probably by the Andean piedmont. These limits remain in a relatively stable location through time. Consequently, considering a simple geometry and assuming that rock volume must be constant the crustal thinning must be roughly equivalent to the amount of horizontal lengthening, i.e. 5 to 10% of the initial thickness. The crustal thinning along the GGTB seems to be quite smaller than the expected for a 5-6 km deep basin (at least 80-100% of crustal thinning, McKenzie, 1978). It is probably that additional crustal thinning beneath the GGTB is related to subduction-erosion working at depth beneath the basin. However, account the crustal thinning originated from the subduction-erosion process itself is difficult to measure because it is proposed to be largely controlled by the roughness of the subducting plate (Clift and Vanucci, 2004).

Seismological data of the USGS-NEIC, catalogue from 1973 to present times shows that the GGTB is a zone where earthquake occurrence is low (Figure 10a and 10d, see also Engdahl et al., 1988). Furthermore, the low occurrence of seismic events at the GGTB seems not to be related to the subduction megathrust as revealed by focal mechanisms of the Harvard Centroid Catalogue (Figure 10b), which define dextral transcurrent slip motion. The GGTB is bounded to the north and to the south by zones along which high recurrence of earthquake occurs ($5<Mw<7$), all defining subduction-type thrusting events along the

subduction interface. To the north it corresponds to the southern flank of the Carnegie ridge. To the south it occurs along the coastal plain of northern Peru (Figure 10a). The northward limit of the high recurrence seismic zone at coastal Peru roughly follows the shoreline (i.e. not far from the TDS). It corresponds to the zone where the great 12 December 1953, Mw 7.3 earthquake occurred (the epicentre was located at 3°40' S and 80°30' W, Silgado, 1957; i.e. not far from the TDS). However, no seismic evidences exist for the 1953 event to originate from the subduction contact or the TDS either. These evidences suggest that low seismogenic coupling takes place at the interplate limit beneath the GGTB, while strong coupling takes place northward, along the Carnegie ridge subduction zone, and southward, along the overthickenned crust of the Amotapes massif (Figure 10). Seismogenesis occurs where the upper plate is coherent and sufficiently thick to store the elastic strain released during earthquakes (McCaffrey and Goldfinger, 1995; von Huene et al., 2004). From a global examination of subduction zones (McCaffrey and Goldfinger, 1995) suggest that upper plate sliver drifting limits the maximum size of thrust subduction earthquakes. As pointed out before, the crustal thinning beneath the GGTB depocenter may be related to both tectonic escape and subduction erosion processes. The subsidence along the GGTB tends to weak the crust preventing the capacity to store elastic strain, which in turn favors the tectonic erosion of the overriding plate. If the overriding plate is not capable to restore elastic strain the capacity of generating earthquakes decreases even if the mechanical coupling between the subducting and overriding plates is high because an increase in deformation would promote increasing fracturing rather than flexing.

Similarities with other tectonic escape trailing edges

Global data of the USGS-NEIC catalogue show that the trailing edges of tectonic escape systems are characterized by low earthquake occurrence. The Golfo de Penas (Chile), the Bussol strait (Japon) and the Sunda strait (Indonesia) have been documented as the subsidence-related trailing edges of partitioned systems (oblique convergence or ridge subduction induced) taking place at the southern Chile, Kuril and Sunda-Sumatra subduction systems, respectively (i.e. Huchon and LePichon, 1984; Forshyte and Nelson, 1985; Kimura, 1986). These zones, approximately located along zones where convergence changes from orthogonal to oblique, show no occurrence of Mw>7 subduction-related seismic events (supplementary data). Furthermore, they all define a relatively seismic gap of Mw>6 seismic

events. Mw>6 seismic events occurrence increases along the direction of sliver migration. This is an interesting similarity between the GGTB and other majors subsiding zones formed in response to escape tectonics. This scenario is probably also suitable at the Aleutians (Amukta and Amlia basins, Geist et al., 1988), where low seismic occurrence has been also recorded in the zones where convergence changes from orthogonal to oblique. Global analysis of seismological data is often not sufficient to characterize the seismological behavior of subduction zones. However, we consider that the data analyzed here takes into account the epicenter location of relatively well-located high magnitude (Mw>6) seismic events. Further work is needed to determinate if the absence of major earthquakes along the zones described above responds to a feedback behavior between tectonic escape and others aspects such as slab age, slab dip angle or variations in interplate physical processes. Even so, we point out that the clear segmentation of Mw>6 and the complete absence of Mw>7 seismic events obtained from global seismological data suggest that low seismic release exists at escape tectonics trailing edges.

The GGTB represents a zone of major change in geodynamic cinematics from normal subduction off the GGTB to oblique subduction northwards. From 1°N to 1°S the oblique subduction is strongly influenced by the subduction of the Carnegie ridge. However, seismic slip vectors show that this segment acts as a typical partitioned segment (Ego et al., 1996). Indeed, slip vectors indicate a right lateral slip component on the subduction plane which results in subduction with less obliquity. This aspect, combined with GPS migration rates (see above), are the major features showing that partitioning of convergence takes place actually along the Ecuadorian trench. At the latitude of the GGTB no obliquity of convergence exists, it increases northwards to ~30° at ~1°S. The Pallatanga fault, proposed as the southernmost transcurrent continental limit of the NAB, is also located in front of a zone where obliquity is very small. A trivial consequence of the existence of this transcurrent deformation is that, at the Ecuadorian margin, partitioning is currently taking place in zones where obliquity is negligible. Several similarities exist between the GGTB and the Sunda Strait where subsidence developed in response to trench parallel extension along the oblique convergent motion of the Indian-Australian and Eurasian plates. The Sumatra fault which probably ends at the Sunda Strait is considered as the major strike-slip system that accommodates motion partitioning along this subduction system (Huchon and LePichon, 1984; Malod et al., 1995). The Sunda Strait is located along the shelf area and the structures controlling basin subsidence seem not to reach the trench. Here a trench parallel transcurrent

system, the Mentawai fault, is considered as a second accommodation zone related to oblique convergence partitioning (Diament et al., 1992; Malod et al., 1995). Furthermore, the trailing edge of the forearc sliver is defined by strong trench-parallel and trench-orthogonal variations in interplate coupling (Baroux et al., 1998). The existence of the Sunda Strait and the Mentawai fault have been also explained in terms of changes on the along and across strike interplate mechanical coupling. Furthermore, as pointed out before no major earthquake recurrence exist at the Sunda Strait and the partitioned system develops in a zone where convergence is orthogonal suggesting that slip at the Sumatra fault develops in zones of low obliquity.

CONCLUSIONS

The GGTB evolution is controlled by the trench-parallel extension that results from the NAB northward drifting. Low-angle normal faults, the TDS, the PDS and the JDS, accommodate the subsidence along the shelf area. The main opening pulse along the GGTB took place during early Pleistocene. The TDS is the master fault of basin evolution and probably corresponds to the shallow expression of a paleo obduction suture zone. It bounds to the south the main GGTB depocenter. It extends to the continent and probably connects with the major transcurrent or normal structures, assumed to define part of the eastern frontier of the NAB. The early Pleistocene total lengthening of the GGTB ranges between 13.5 and 20 km, in good agreement with the ~1 cm/yr postulated rate for NAB migration combined with an early Pleistocene age (i.e. 1.8-1.6 Ma) for GGTB area main opening pulse.

The subsidence resulting from NAB drifting is mainly concentrated along the shelf area. The detachment systems controlling subsidence along the GGTB are limited seaward by the inner DFS and the BPF, which act as a major transfer system. Transcurrent faulting along the basin limits and along the basin depocenters develops in response to the extensional structures. These aspects suggest that the GGTB does not correspond to a classical pull-apart basin as it was previously suggested.

The continental margin is unaffected by the escape tectonic process because of the low coupling along the interplate contact. We suggest that tectonic escape systems are highly sensitive to local interplate coupling variations, and that these variations are important to

define the zones where subsidence results from escape tectonics. The modeling of convergence partitioning in terms of convergence obliquity, constant interplate coupling and constant overriding plate strength at the scale of the whole subduction system seems to be insufficient when analyzing the trailing edge of the tectonic escape system. The GGTB, as well as other subsident-related trailing edges of tectonic escape systems seem to be characterized by low seismic release. It is proposed that the subsidence and related lengthening along the GGTB tends to weak the crust preventing the capacity to restore elastic strain to be released during seismic events.

REFERENCES

Avé-Lallemant, H., and Oldow, J., 2000, Active displacement partitioning and arc-parallel extension of the Aleutian volcanic arc based on Global Positioning System geodesy and kynematic analysis: Geology, v. 28, p. 739-742.

Axen , G., 1992, Pore pressure, stress increase, and fault weakening in low-angle normal faulting: Journal of Geophysical Research, v. 97, p. 8979-8991.

Bartley, J., and Glazner, F., 1985, Hydrothermal systems and tertiary low-angle normal faulting in the south-western United States: Geology, v. 13, p. 562-564.

Baroux, E., Avouac, P., Bellier, O., and Sebrier, M., 1998, Slip-partitioning and forearc deformation at the Sunda trench, Indonesia: Terra Nova, v. 10, p. 139-144.

Benitez, S., 1995, Évolution géodynamique de la province côtière sud-équatorienne au Crétacé supérieur -Tertiaire : Géologie Alpine, v. 71, p. 5-163.

Bertoluzza, L., and Perotti, C., 1997, A finite-element model of the stress field in strike-slip basins: implications for the Permian tectonics of the Southern Alps (Italy): Tectonophysics, v. 280, p. 185-197.

Bilek, L., and Lay, T., 1999, Rigidity variations with depth along interplate megathrust faults in subduction zones: Nature, v. 400, p. 443-446.

Bourgois, J., Pautot, G., Bandy, W., Boinet, T., Chotin, P., Huchon, P., Mercier de Lepinay, B., Monge, F., Monlau, J., Pelletier, B., Sosson, M., and von Huene, R., 1988, Seabeam and seismic reflection imaging of the tectonic regime of the Andean continental margin off Peru (4°S to 10°S): Earth and Planetary Science Letters, v. 87, p. 111-126.

Bourgois, J., Lagabrielle, Y., De Wever, P., Suess, E. and NAUTIPERC team, 1993, Tectonic history of the northern Peru convergent margin during the past 400 ka: Geology, v. 21, p. 531-534.

Bourgois, J., Guivel, C., Lagabrielle, Y., Calmus, T., Boulègue, J., and Daux, V., 2000, Glacial-interglacial trench supply variation, spreading-ridge subduction, and feedback controls on the Andean margin development at the Chile triple junction area (45-48°S): Journal of Geophysical Research, v. 105, p. 8355-8386.

Bourgois, J., Bigot-Cormier, F., Bourles, D., Braucher, R., Dauteuil, O., Witt, C., and Michaud, F., 2007, Tectonic records of strain buildup and abrupt co-seismic stress release across the northwestern Peru coastal plain, shelf, and continental slope during the past 200 kyr: Journal of Geophysical Research, v. 112, B04104, doi:10.1029/2006JB004491.

Bosch, D., Gabriele, P., Lapierre, H., Malfere, J.L., and Jaillard, E., 2002, Geodynamic significance of the Raspas Metamorphic Complex (SW Ecuador): geochemical and isotopic constraints: Tectonophysics, v. 345, p. 83-102.

Bradshaw, G.A., and Zoback, M., 1988, Listric normal faulting, stress refraction, and the state of stress in the Gulf Coast basin: Geology, v. 16, p. 271-274.

Brun , J.P., Sokoutis, D., Van Den Driessche, J., 1994, Analogue modeling of detachment fault systems and core complexes: Geology, v. 22, p. 319-322.

Buck, W.R. ,1988, Flexural rotation of normal faults: Tectonics, v. 7, p. 959-973.

Calahorrano, A., 2005, Structure de la marge du Golfe de Guayaquil (Equateur) et propriété physique du chenal de subduction, à partir de données de sismique marine réflexion et réfraction: Université Paris VI, Paris. Ph.d. thesis, 227 p.

Chemenda, A., Lallemand, S., and Bokun, A., 2000, Strain partitioning and interplate friction in oblique subduction zones: constraints provided by experimental modelling: Journal of Geophysical Research, v. 105, p. 5567-5581.

Clift, P., and Vannucchi, P., 2004, Controls on tectonic accretion versus erosion in subduction zones: Implications for the origin and recycling of the continental crust: Review of Geophysics, v. 42, RG2001, doi:10.1029/2003RG000127.

Cobbold, P.R., Mourgues, R., and Boyd, K., 2004, Mechanism of thin-skinned detachment in the Amazon Fan: assessing the importance of fluid overpressure and hydrocarbon generation: Marine and Petroleum Geology, v. 21, p. 1013-1025.

Collot J.Y., Charvis P., Gutscher M. and Operto E., 2002, Exploring the Ecuador-Colombia active margin and inter-plate seismogenic zone: Eos, Transactions. American Geophysical Union, v. 83, p. 189-190.

Christie-Blick, N., and Biddle, K.T., 1985, Deformation and basin formation along strike-slip faults: In: Biddle, K.T., Christie-Blick, N. (Eds.), Strike-slip Deformation, Basin Formation, and Sedimentation. Society of Economy, Paleontology and Mineralogy Special Publication, v. 37, p. 1-34.

DeMets, C., Gordon, R.G., Angus, D.F., and Stein, C., 1990, Current plate motions: Geophysical Journal International, v. 101, p. 425-478.

Deniaud, Y., Baby, P., Basile, C., Ordoñez, M., Montentegro, G., and Mascle, G., 1999, Ouverture et évolution tectono-sedimentaire du Golfe de Guayaquil: basin d'avant arc néogène et quaternaire du Sud des Andes équatoriennes: Comptes Rendus de l'Académie de Sciences Paris, v. 328, p. 181-187.

Denaiud, Y., 2000, Enregistrements sédimentaire et structurale de l'évolution géodynamique des Andes équatoriennes au cours du Neogene: Etude des bassins d'avant arc et bilans de masse, Pd.D. thesis, 157 pp., Université Grenoble 1, France.

Dumont, J., Santana, E. and Vilema, W., 2005, Morphologic evidence of active motion of the Zambapala Fault, Gulf of Guayaquil (Ecuador): Geomorphology, 65, 223-239.

Diament, M., Harjono, H., Karta, K., Deplus, C., Dahrin, D., Zen, T., Gerard, M., Lassal, O., Martin, A., and Malod, J., 1992, Mentawai fault zone off Sumatra: A new key to the geodynamics of western Indonesia: Geology, v. 20, p. 259-262.

Ego, F., Sébrier, M., Lavenu, A., Yepes, H., and Eguez, A., 1996, Quaternary state of stress in the Northern Andes and the restraining bend model for the Ecuadorian Andes: Tectonophysics, v. 259, p. 101-116.

Engdahl, E.R., Van der Hilst, R.P., and Buland, R.P., 1998, Global teleseismic earthquake relocation with improved travel times and procedures for depth determination: Bulletin of the Seismological Society of America, v. 88, p. 722-743.

Forsythe, R. D., and E. P. Nelson, 1985, Geological manifestations of ridge collision: Evidence from the Golfo de Penas-Taitao basin, southern Chile: Tectonics, v. 4, p. 477 – 495.

Freymueller, J.T., Kellog, J., and Vega, V., 1993, Plate motions in the North Andean region: Journal of Geophysical Research, v. 98, p. 21853-21863.

Gailler, A., 2005, Structure de la marge d'Equateur-Colombie par modélisation des données de sismique grand angle marines: Influence sur le fonctionement de la subduction et la sismicité : Ph.D. thesis, Univ. Nice-Sophia Antipolis, Nice, France.

Gartrell, A.P., 1997, Evolution of rift basins and low-angle detachments in multilayer analog models: Geology, v. 25, p. 615-618.

Geist, E.L., Childs, J.R., and Scholl, D.W., 1988. Evolution and petroleum geology of Amlia and Amukta intra–arc summit basins, Aleutian Ridge: Marine and Petroleum Geology, v. 4,

p. 334–352.

Gibbs, A.D., 2002, Structural evolution of extensional basin margins: from Holdsworth, R. and Turner, J. (compilers). Extensional Tectonics: Faulting and related processes: The Geological Society, Key issues in Earth sciences v. 2, p. 13-24.

Guillier, B., Chatelain, J-L., Jaillard, E., Yepes, H., Poupinet, G., and Fels, J.F., 2001, Seismological evidence on the geometry of the orogenic system in central-northern Ecuador (South America): Geophysical Research Letters, v. 28, p. 3749-3752.

Higley, D., 2004, The Progreso basin province of northwestern Peru and southwestern Ecuador: Neogene and Cretaceous-Paleogene total petroleum systems: open file, U.S. Geological Survey Bulletin 2206-B, 25 p. Available at URL http://pubs.usgs.gov/bul/b2206-b/

Huang S., Sacks, I., and Snoke J.A., 1997, Topographic and seismic effects of long-term coupling between the subducting and overriding plates beneath Northeast Japan: Tectonophysics, v. 269, p. 279-297.

Huchon, P., and Le Pichon, X., 1984, Sunda strait and central Sumatra fault: Geology, v. 12, p. 668-672.

Jaillard, E., Benitez, S., and Mascle, G., 1997, Les déformations paléogènes de la zone d'avant-arc sud-équatorienne en relation avec l'évolution géodynamique: Bulletin Société Géologique de France, v. 168, p. 403-412.

Jarrard, R.D., 1986, Terrane motion by strike-slip faulting of forearc slivers: Geology, v. 14, p. 780-783.

Kellogg, J.N., and Vega, V., 1995, Tectonic development of Panama, Costa Rica and the Colombian Andes: Constraints from Global Positioning System (GPS) geodetic studies and gravity: Geologic and tectonic development of the Caribbean plate boundary in southern Central America, edited by P. Mann, Special Publication Geological Society of America, v. 295, p. 75-90.

Kimura, G., 1986, Oblique subduction and collision: forearc tectonics and the Kuril Arc: Geology, v. 14, p. 404-407.

Lay, T., Kanamori, H., and Ruff, L., 1982, The asperity model and the nature of large subduction zone earthquakes: Earthquake Prediction Research, v. 1, p. 3-71.

Liu, X., McNally, C., and Shen, K., 1995, Evidence for a rol of the downgoing slab in earthquake slip partitioning at oblique subduction zones: Journal of Geophysical Research, v. 100, p. 15351-15372.

Lonsdale, P., 1978, The Ecuadorian subduction system: American Association Petroleum Geologist Bulletin, v. 62, p. 2454-2477.

Malod, J., Karta, K., Beslier, M.O., and Zen, M., 1995, From normal to oblique subduction: tectonic relationships between Java and Sumatra: Journal of Southeast Earth Sciences, v 12, p. 85-93.

McCaffrey, R., 1992, Oblique plate convergence, slip vectors, and forearc deformation: Journal of Geophysical Research, v. 97, p. 8905-8915.

McCaffrey, R., and Goldfinger, C., 1995, Forearc deformation and great subduction earthquakes: implications for Cascadia offshore earthquake potential: Science, v. 267, p. 856-859.

McCaffrey, R., 1996, Estimates of modern arc-parallel strain rates in fore arcs: Geology, v. 24, p. 27-30.

McKenzie, D., 1978, Some remarks on the development of sedimentary basins: Earth and Planetary Sciences Letters, v. 40, p. 25-32.

Pedoja, K., Ortlieb, L., Dumont, J.F., Lamothe, M., Ghaleb, B., Auclair, M. and Labrousse, B., 2006, Quaternary coastal uplift along the Talara Arc (Ecuador, Northern Peru) from new marine terrace data, Marine Geology, v. 228, p. 73-91.

Pennington, W.D., 1981, Subduction of the eastern Panama Basin and seismotectonics of northwestern South America: Journal of Geophysical Research, v. 86, p. 10753-10770.

Platt, J.P., 1993, Mechanics of oblique convergence: Journal of Geophysical Research, v. 98, p. 16239-16256.

Porter, S.C., 1989, Some geological implications of average Quaternary glacial conditions: Quaternary Research, v. 32, p. 245-261.

Sage, F., Collot, J.Y., and Ranero, C., 2006, Interplate patchiness and subduction-erosion mechanisms: Evidence from depth migrated seismic images at the central Ecuador convergent margin: Geology, accepted.

Shackleton, N.J., 1997, The deep sea sediment record at the Pliocene-Pleistocene boundary: Quaternary International, v. 40, p. 33-35.

Sheperd, G.L., and Moberly, R., 1981, Coastal structure of the continental margin northwest Peru and southwest Ecuador: In L.D. Kulm et al. (Editors), Nazca Plate: crustal formation and Andean convergence, Geological Society of America Memory, v. 154, p. 351-391.

Silgado, E., 1957, El movimiento sismico del 12 de Diciembre de 1953: Paper presented at the Primer Congreso Nacional de Geologia, Peru, v. 32, p. 225-238.

Smith, D., R., Cann, J., and E Escartine, Widespread active detachment faulting and core complex formation near 138N on the Mid-Atlantic Ridge: Nature, v. 442, p. 440-443.

Song, T. and M. Simons, 2003, Large Trench-Parallel Gravity Variations Predict Seismogenic Behavior in Subduction Zones: Science v. 301, p. 630-633.

Spencer, J., 1984, Role of tectonic denudation in warping and uplift of low-angle normal faults: Geology, v. 12, p. 95-98.

Swenson, J., and Beck, S., 1996, Historical 1942 Ecuador and 1942 Peru subduction earthquakes, and earthquake cycles along Colombia, Ecuador and Peru subduction segments: Pure and Applied Geophysics, v. 146, p. 67-101.

Taboada, A., Rivera, L., Fuenzalida, A., Cisternas, A., Philip, H., Bjwaard, H., Olaya, J., and Rivera, C., 2000, Geodynamics of the northern Andes: subductions and intracontinental deformation (Colombia): Tectonics, v. 19, p. 787-873.

Travis, R.B., Gonzales, G., and Pardo, A., 1976, Hydrocarbon potential of coastal basins of Peru. In: M.T. Halbouty, J.C. Maher and H.M. Lian (Editors), Circum Pacific Energy and Mineral resources, American Association Petroleum Geologist Memory, v. 25, p. 331-338.

Trenkamp, R., Kellogg, J.N., Freymuller, T., and Mora, P.H., 2002, Wide plate margin deformation, southern Central America and northwestern South America, CASA GPS observations: Journal of South American Earth Sciences, v. 15, p. 157-171.

Upton, P., and Koons, P., 2003, Extention and partitioning in an oblique subduction zone, New Zealand: Constraints from three-dimensional numerical modelling: Tectonics, v. 22, doi:10.1029/2002TC001431.

Vega, M., Baby, P., Brusset, S., Vega, N., Monges, C., Bolanos, R., and Marocco, R., 2005, Structural and stratigraphic architecture of the Tumbes forearc basin (northern Peru): 6th International Symposium on Andean Geodynamics (ISAG), Barcelone, p. 776-778.

von Huene, R., and D. Scholl (1991), Observations at convergent margins concerning sediment subduction, subduction erosion, and the growth of continental crust, Review of Geophysics, v. 29, p. 279-316.

von Huene, R., Bourgois, J., Miller, J., and Pautot, G., 1989, A large Tsunamogenic landslide and debris along the Peru Trench: Journal of Geophysical Research, v. 94, p. 1703-1714.

von Huene, R., Ranero, C., and Vanucchi, P., 2004, Generic model of subduction erosion: Geology, v. 32, p. 913-916.

Walsh, J., Watterson, J., and Yielding, G., 1991, The importance of small-scale faulting in regional extension: Nature, v. 351, p. 391-393.

Wang, K., and Hu, Y., 2006, Accretionary prisms in subduction earthquakes cycles: the theory of dinamyc Coulomb wedge: Journal of Geophysical Research, v. 11, B06410, doi:10.1029/2005JB004094.

Wernicke, B., and Axen, G., 1988, On the role of isostasy in the evolution of normal fault systems: Geology, v. 16, p. 848-851.

Wernicke, B., 1995, Low-angle normal faults and seismicity: a review: Journal of Geophysical Research, v. 100, p. 20159-20174.

White, S., Trenkamp, R., and Kellogg, J., 2003, Recent crustal deformation and the earthquake cycle along the Ecuador–Colombia subduction zone: Earth and Planetary Science Letters, v. 216, p. 231-242.

Witt C., Bourgois J., Michaud F., Ordoñez M., Jimenez N., and Sosson M., 2006, Development of the Golfo de Guayaquil (Ecuador) as an effect of the North Andean Block tectonic escape since the Lower Pleistocene: Tectonics, v. 25, TC3017, doi:10.1029/2004TC001723.

Yu, G., Wesnousky, G., and Extrom, G., 1993, Slip partitioning along major convergent plate boundaries: Pure and Applied Geophysics, v. 140, p. 183-210.

Zevallos, O., 1970, Petróleo en rocas del basamento. Primer Congreso Latinoamericano de Geología, v. 2, p. 30-62.

CHAPTER 3

TECTONIC EVOLUTION OF THE INTERMONTANE BASINS OF SOUTHERN ECUADOR BETWEEN 2°20' S TO 3°25' S.

3.1. INTRODUCTION

The evolution of the Santa Isabel basin, as well as the evolution of the Cañar and Azogues basins have been related direct or indirectly with the NAB northward drifting (Winter and Lavenu, 1989b; Hungerbühler et al., 2002).

The central and northern Ecuadorian Andean chain consists of two N-S directed mountain chains separated by a central inter-Andean valley or depression. The eastern mountain chain (i.e the Cordillera Real) comprises metamorphic rocks units intruded by early to middle-Mesozoic granitoids (i.e. Aspden and Litherland, 1992; Litherland et al., 1994). Some of these units resulting from the accretion of oceanic terranes during Jurassic times. To the west of the inter-Andean valley, the western mountain chain (i.e. the Cordillera Occidental) consists predominantly of fault-bounded Cretaceous-Tertiary accreted oceanic terranes comprising basaltic, volcanic and volcaniclastic rocks (i.e. Feininger and Bristow, 1980; Mamberti et al., 2003; Hughes and Pilatasig, 2002; Kerr et al., 2002; Jaillard et al., 2004). Several theories attempted to constraint the age and the nature of the terranes involved in the accretionary events in the Coast and the Occidental Cordillera. Due to the variable nature of the rocks implicated in the accretionary processes, many different models have been proposed. From a wide variety of data (i.e. Hughes and Pilatasig, 2002; Kerr et al., 2002; Mamberti et al., 2003; Jaillard et al., 2004; Toro and Jaillard, 2005; Vallejo et al., 2006) two major accretion events seem to be relevant: 1) a late Cretaceous (65-85 Ma) event involving the Pallatanga terrane (San Juan and Guaranda units), and 2) a middle-late Eocene event involving the Macuchi terrane (Macuchi and Naranjal units, see unit 1.5.1, Figure 1.8) The accreted oceanic terranes extend south to ~3°20' S. Further south, the Ecuadorian Andean chain shows a Paleozoic basement that probably corresponds to the southern prolongations of the Cordillera Real. The contact between metamorphic basement and oceanic accreted terranes roughly follows the Jubones river (Figure 3.1). An interesting aspect on the Ecuadorian Andean evolution is that after accretion subsequent marginal parallel transport of these terranes had probably continued throughout much of the Paleocene to Present times (i.e. Pecora et al., 1999; Kerr et al., 2002).

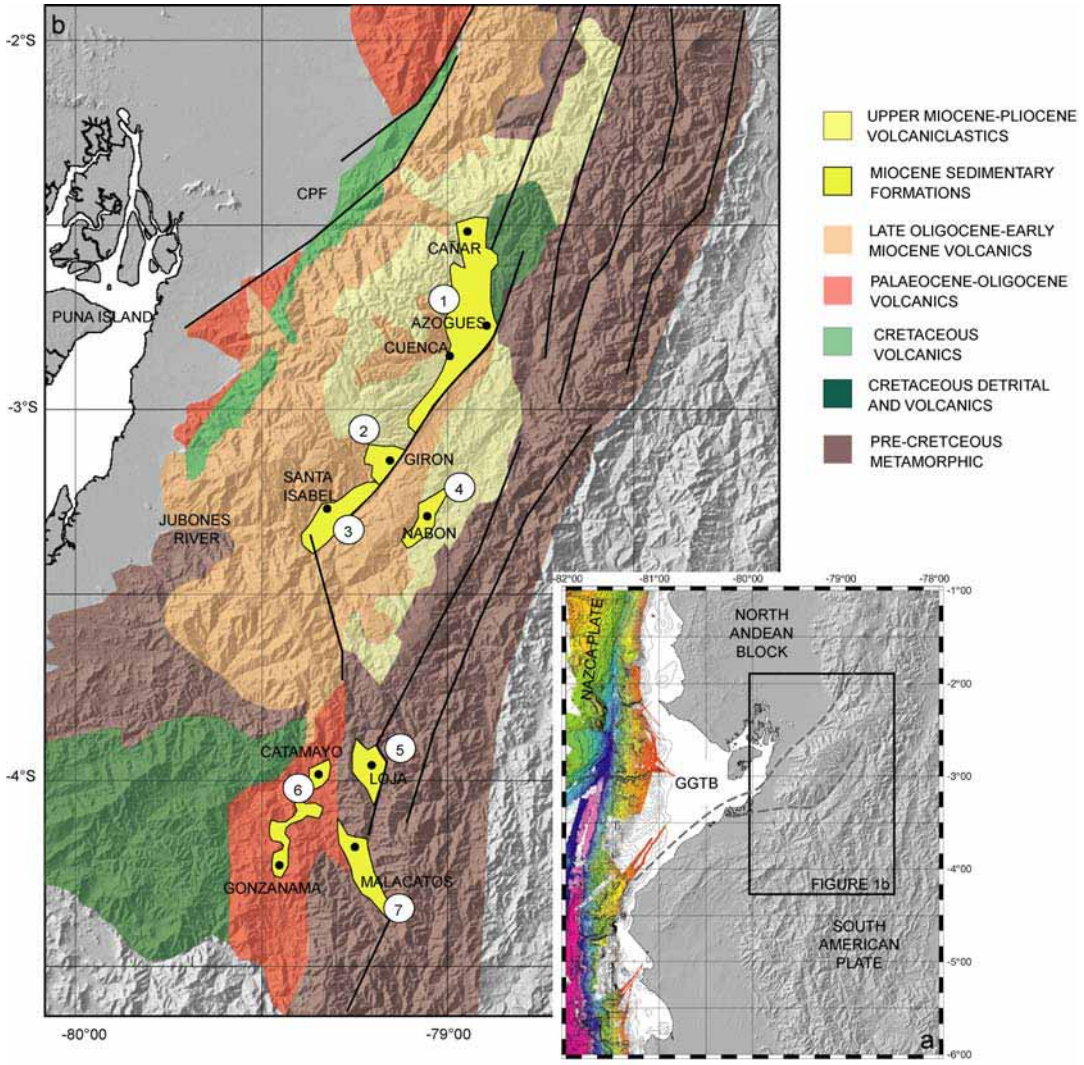

Figure 3.1. a) Regional sketch of the northern Peruvian and southern and central Ecuadorian Andean chain. **b)** Geological sketch of the central and southern Ecuadorian Andes and location of intermountain basins. From 1 to 7 they include: 1, Cuenca basin; 2,3 Girón-Santa Isabel basin; 4, Nabón basin; 5, Loja basin; 6, Catamayo-Gonzanamá basin; 7, Malacatos-Vilcabamba basin. Modified from, Hungerbuhler et al. (2002).

During late Cretaceous times, the marine Yunguilla Fm. deposits above the previously accreted Pallatanga terrane (Eguez et al., 1993; Dunkley and Gaibor, 1997). The Macuchi island arc develops during Paleocene-late Eocene times while the first volcanic pulse of the Saraguro continental arc began in Eocene times (Dunkley and Gaibor, 1997; Kerr et al., 2002). A hiatus in volcanism as well as a deformation step along the older (Eocene) southern rocks of the Saraguro Gp. is attributed to the docking of the Macuchi terrane against the margin in the late Eocene (Dunkley and Gaibor, 1997; Hughes and Pilatasig, 2002). Subsequently, the break of the Farallon plate at 25-26 Ma (i.e. Hey, 1977, see section 1.2.1.1) results in a strong increase of intermediate andesitic volcanic activity along the Saraguro arc (Dunkley and Gaibor, 1997). Almost all the processes describe above imprint a ~N-S to N-E segmentation of the Andean chain (i.e. Andean trending, N-S to N-E directed structures).

Subsequently, the Miocene corresponds to the period of intermontane basin formation with basins developing along Andean trending reactivated directed structures.

The active Quaternary structures trend in an NNE to N-E direction. They comprise from north to south the Paute and Gualaceo faults and the Girón fault system (GFS, Eguez et al., 2003). The Paute and Gualaceo faults seem to border the western margin of the Cordillera Real. The tectonic activity of these faults is not clear but they have been considered as currently active showing a slip-rate lower than 1 mm/yr (Eguez et al., 2003). The GFS trends in a constant N-E direction and extends from the south of Cuenca to the south of Santa Isabel, and probably further south. The total length of the GFS lies in the range of 45-50 km.

3.2 STRATIGRAPHIC AND TECTONIC MODELS PROPOSED FOR THE SOUTHERN ECUADORIAN INTERMONTANE BASINS

Several Tertiary intermontane basins such as the Cuenca, Girón-Santa Isabel, Nabón, Loja Malacatos, and Vilcabamba basins (Figure 3.1) developed along the central and southern Ecuadorian Andean chain (i.e. Bristow, 1973; Lavenu et al., 1992 and 1995a; Steinmann et al., 1999; Hungerbühler et al., 2002). Generally, the intermontane basin fill unconformably overlies the Eocene-lower Miocene volcanic formations. South of 3°30'S the Eocene-Oligocene Loma Blanca Fm. corresponds to basin basement of the Loja, Malacatos-Vilcabamba and Catamayo-Gonzanama basins. To the north of 3°30'S, the early Oligocene-early Miocene Saraguro Gp. corresponds to the basin basement of the Cuenca, Girón, Santa Isabel, and Nabón basins. Two highly incompatible origins, continental and marine-continental sediment input models have been proposed for the Tertiary sediments of these basins. The two proposed models having their own tectonic implications.

It has been long suggested that during late Tertiary a thick continental sedimentation spreads along the intermontane basins of the southern Andes of Ecuador (Kenerley et al., 1973; Lavenu et al 1992 and 1995a). The continental type sedimentation has been proposed in various works carried out in the Cuenca, Girón-Santa Isabel, Nabón and Malacatos basins (Lavenu and Noblet, 1989, Noblet et al, 1988; Lavenue et al., 1992a and 1995) as well as in some detailed unpublished works (Fierro, 1991; Izquierdo, 1991; Mediavilla, 1991). These authors consider that the cycle of sedimentation is composed of two sequences along all the basins. The first sequence (M1, Figure 3.2a, adapted for the Cuenca and Loja Malacatos basins) consists of 600-1500 m of proximal (alluvial) to distal (lacustrine) deposits. This upward fining and thinning sequence resulting from the deepening related to large tectonic subsidence, which marks the opening period of the basins. The second sequence (M2, Figure 3.2a) shows a reverse sequence that ranges from distal (lacustrine) to proximal (alluvial) sediments.

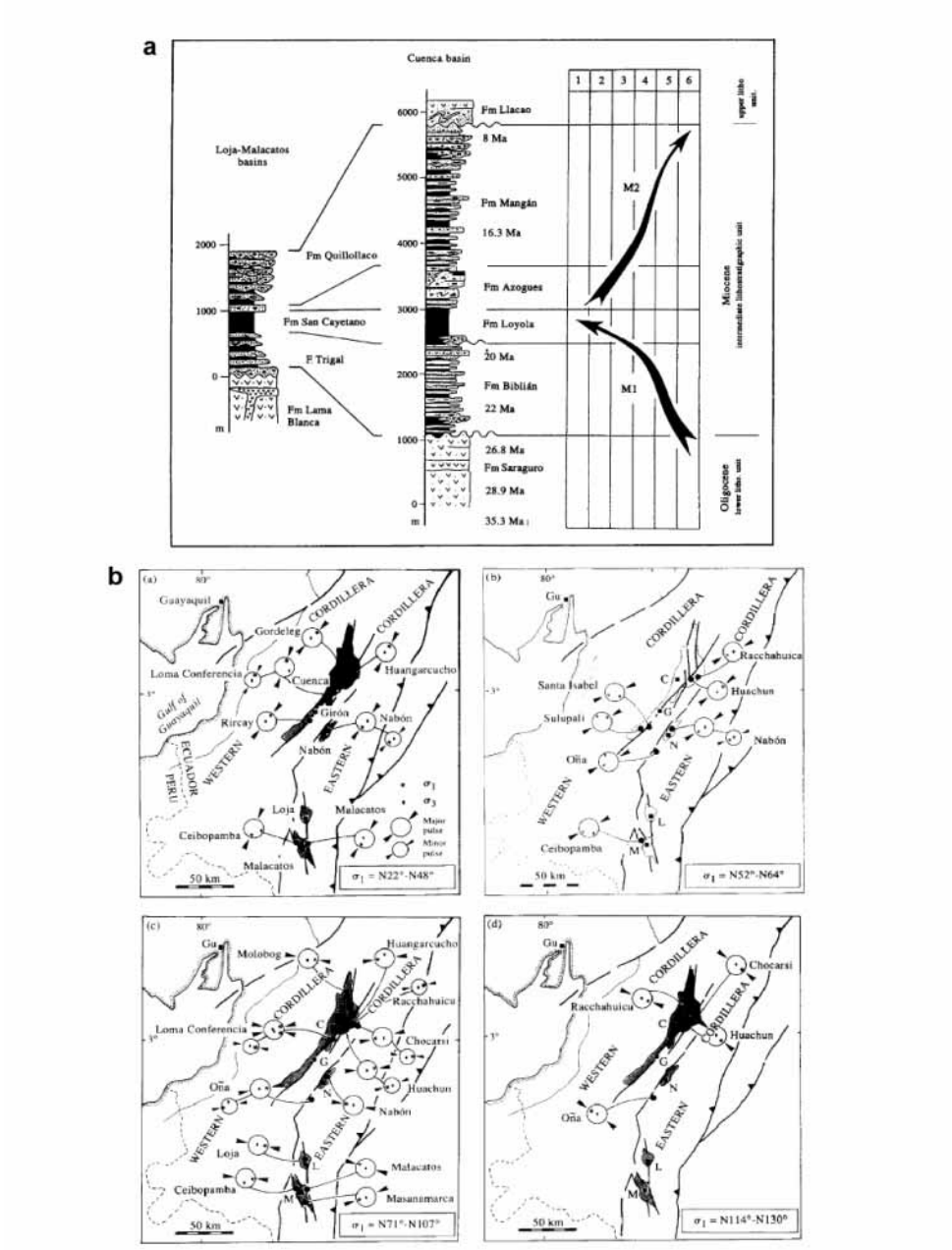

Figure 3.2. a) Stratigraphic columns of the Cuenca and Loja-Malacatos basins. The megasequence M1 corresponds to the opening of the basins while the megasequence M2 corresponds to their closing. **b)** Principal commpresional stress directions deduced from kinematics of reverse and strike-slip faults of early to late Miocene. From Lavenu et al. (1995a).

This upward coarsing and thickening sequence; which would represent the tectonic closing of the basins is 300-1000 m thick. This model suggests active deposition on the intermontane basins from ~22 Ma to 8 Ma. Combined studies of stratigraphy, sedimentology, syn-sedimentary deformation and microtectonics (Noblet et al, 1988; Noblet and Marocco, 1989; Lavenue et al., 1992 and 1995) allow proposing that a compressive continuous deformation affected all the intermontane basins during the entire Miocene period (i.e. after the break of the Farallon plate). During Miocene to Pliocene, the evolution of the basins is the consequence of the dextral displacement along the main basin margins. Following their observations they propose that a NNE directed compressive strain controls the basin

opening (M1 sequence Figure 3.2b), which is transformed in a dextral strike slip movement along N-S trending faults and dextral normal movement along N20-N40 trending faults. A posterior continuum clockwise rotation to an E-W directed compressive strain controls the posterior evolution and closing of the basins (Figure 3.2b). The chronology of the compressive phases is generally established from dating on regional unconformities. The compressive pulses are dated as Late Oligocene, early Miocene (20 to 16 Ma) and late Miocene (8 to 7.1 Ma); the Miocene tectonic pulses being related with rapid Neogene convergence. Bristow (1973) suggested that the basal Loyola Fm. shows a slight marine fauna. Considering that this fauna is not recorded further west, he speculated the possibility of a westward-directed marine ingression (i.e. from the Oriente basin) during early Miocene times. However, this argument was very briefly discussed. He argued that the change from marine to continental-derived deposits takes place along the red-beds and conglomerates of the Santa Rosa Fm. (see Figure 3.3a for stratigraphic position). No provenance or depositional ambient of the stratigraphic series in the time spam between the Loyola and Santa Rosa Fms. was suggested. More recently, the sedimentation on these basins have been divided in two main stages: 1) from 15 to 9 Ma, the so called "Pacific coastal stage", leads to widespread deposition of marine sediments prior to Andean exhumation (Steinmann et al., 1999) or linked to massive extensional collapse of the Inter-Andean zone (Hungerbühler et al., 2002). Marine delta environments, which are described in fonction of fauna descriptions or from facies associations, correspond to the Catamayo, Gonzanamá, San Jose, Santo Domingo, La Banda, Trigal, Belen, Loyola, Azogues and Mangan Fms (Figure 3.3a). 2) from 9.5 to 8 Ma, the so called 'Intermontane stage' defines a period of E-W directed compression which results in a major exhumation period and more restricted sediment deposition. The two proposed stages are separated by a major sediment unconformity at about 9 Ma. Steinmann et al. (1999) and Hungerbühler et al. (2002) propose that two major embayments related with marine ingression controls the marine sedimentation along the area: the Cuenca and Loja embayments, to the north and to the south, respectively. The Girón-Santa Isabel area, where continental-type sedimentation prevailed fulltime, separates these two embayments. The proposed shallow marine nature of the sedimentary series dated from 15 to 9 Ma (Steinmann et al., 1999; Hungerbühler et al., 2002) leads to a more complicated evolution model (Figure 3.3b). Considering that a low topography profile that allows marine ingressions is needed, it is suggested that basin formation predates Western Cordillera uplift (Steinmann et al., 1999) or, that it is related to major collapse of the Western Cordillera (Hungerbühler et al., 2002). According to this preceding model, the crustal colapse woul have caused a loss of support due to the crustal thinning caused by the drifting of the upper-plate sliver. Both of these models propose that the ~100 Km displaced zone coincident with the Calacali Pallatanga fault (Figures, 4.1 and 4.3b) could be restored palinspaticly considering, 1) modern North Andean block drifting rates (i.e. ~1 cm/yr), and 2) a 10 Ma age (Benitez, 1995) for the Gulf of Guayaquil opening. This reconstruction matches the Loja and Progreso basins to the south and the Manabí and Cuenca basins to the north, both separated by the Santa Isabel and Santa Rosa-Saraguro highs (Figure 3.3b).

Following this scenario, the Loja and Cuenca basins would represent the shallower sections of the Progreso and Manabí basins, respectively. The collision of the Carnegie ridge (from 15 Ma to 9 Ma) is proposed to be the major feature controlling the evolution of the basins, first enhancing the major northward expulsion of the coastal block (15-9 Ma) and subsequently increasing compression along the intermontane basins at 9-8 Ma (Steinmann et al., 1999; Hungerbühler et al., 2002).

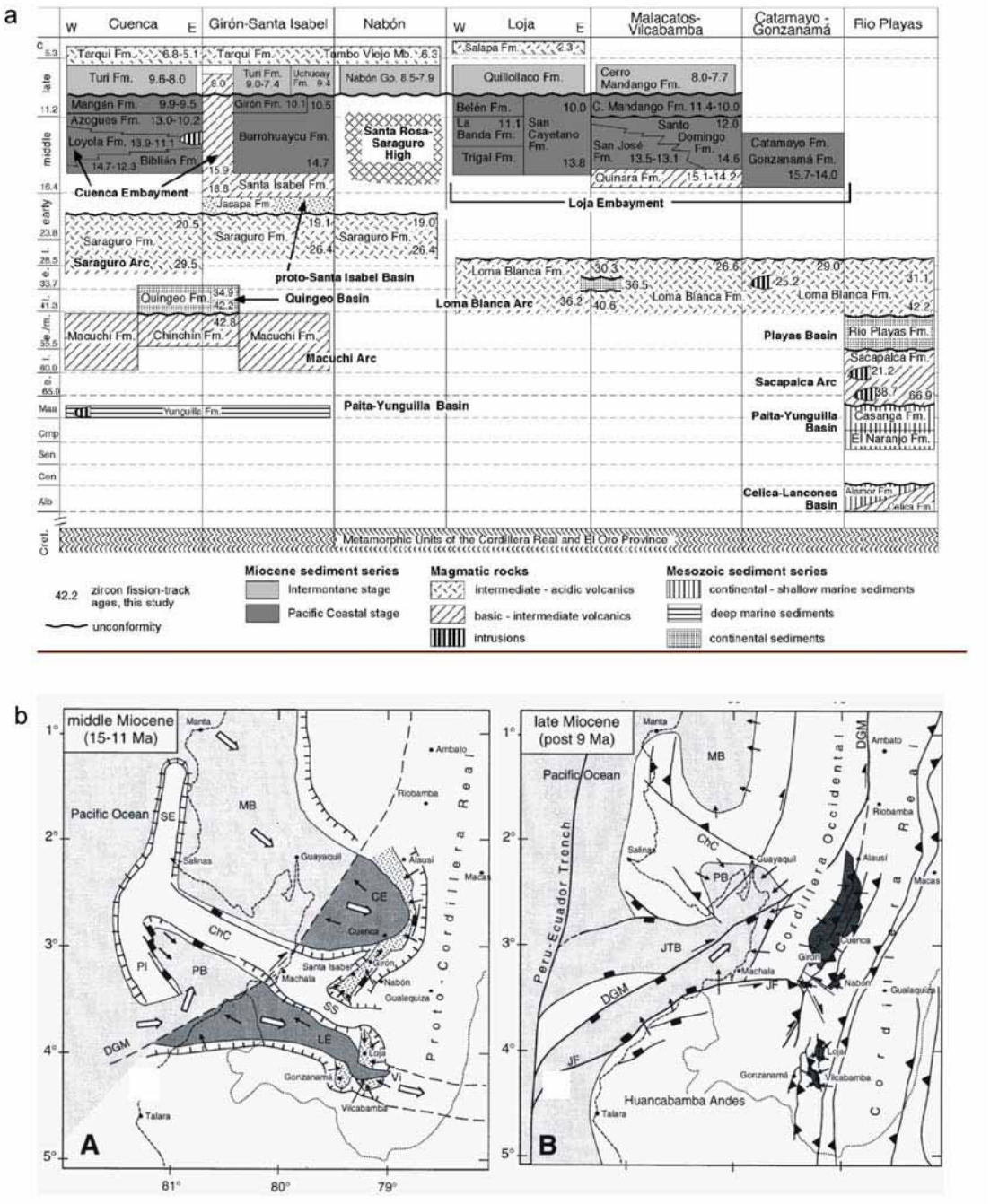

Figure 3.3. a) Chronotratigraphic chart of southern Ecuador and fission-track ages. **b)** Proposed palinspatic rcconstruction of southern Ecuador from middle to late Miocene times. a and b from Hugerbuhler et al. (2002). Abbreviations: BLAFZ, Baños-Las Aradas Fault Zone., ChC, Chongon-Colonche High., CE, Cuenca Embayment., CPFZ, Calacali-Pallatanga Fault Zone., JF, Jubones Fault., JTB, Jambelí-Tumbes Basin., LE, Loja Embayment., MB, Manabí Basin., Pl, Playas High., PB, Progreso Basin., SE, Santa Elena High., SS, Santa Rosa-Saraguro High.

3.3 NEW STRATIGRAPHIC AND CHRONOLOGIC DATA OF THE CAÑAR AND AZOGUES BASINS.

During 2002-2005 extensive field work funded by the IRD was carried out along the Andean zones between 2°30' S to 2°50' S in the context of the 'Dolores-Guayaquil project'. This work deals with the stratigraphic and tectonic evolution of the intermontane basins of Cañar and Azogues (Lahuathe, 2005; Bourgois et al., 2006; Verdezoto, 2006; Bourgois et al., in prep), which correspond to the northward prolongation of the Cuenca basin. The evolution of these basins takes place along three major tectonic units showing different lithologies and tectonic development. From east to west they include: the Cocha Huma-Azogues the Ingapirca-Toray, and the Cañar-Deleg units (Figure 3.4) all bounded by major ~N-S trending fault systems.

The eastern Cocha Huma-Azogues unit develops to the east of the Toray-Ingapirca fault (TIF). It corresponds along the Cañar basin to the late Cretaceous-Eocene deformed series mainly represented by the Yunguilla Gp. This unit extends to the south to the old series of the Yunguilla and Saraguro Gps., which bond the main depocenters of the Azogues basin. However, at this site they are overlain by relatively thin series of the Biblian, Loyola and Azogues Formations (Figure 3.4).

The central corridor, the Toray-Ingapirca unit, is bounded by the Toray-Ingapirca fault (TIF) and the Honorato Vasquez-Deleg fault (HVDF) to the east and to the west, respectively. The TIF and the HVDF correspond to the master faults of basin development along the Cañar and Azogues basins, respectively. The central corridor corresponds to the major Miocene infill of the Cañar and Azogues basins, which extends along major N-S trending antiform structures. The Biblian, Azogues (only along the Azogues basin), Loyola and Mangan Formations outcrop along the central corridor. New Ar/Ar age data combined with published ages (Olade, 1980; Barberi et al., 1988; Lavenu et al., 1992; Steinmann et al., 1999) as well as field stratigraphic relationships allow redefining the individual periods of deposition for each formation (Figure 3.3, Verdezoto, 2006).

The western corridor, the Cañar-Deleg unit, is limited to the east by the HVDF (Figure 3.4). These formations on-lap the Saraguro Gp to the west and are in turn overlain by volcanic deposits of the Tarqui Mb (Llacao and Tarqui Fms.). It defines the zone of younger periods of basin infilling, i.e. the Mangan and Turi Fms. The upper sequences depositional area is limited to the east by the major antiforms developing along the central corridor.

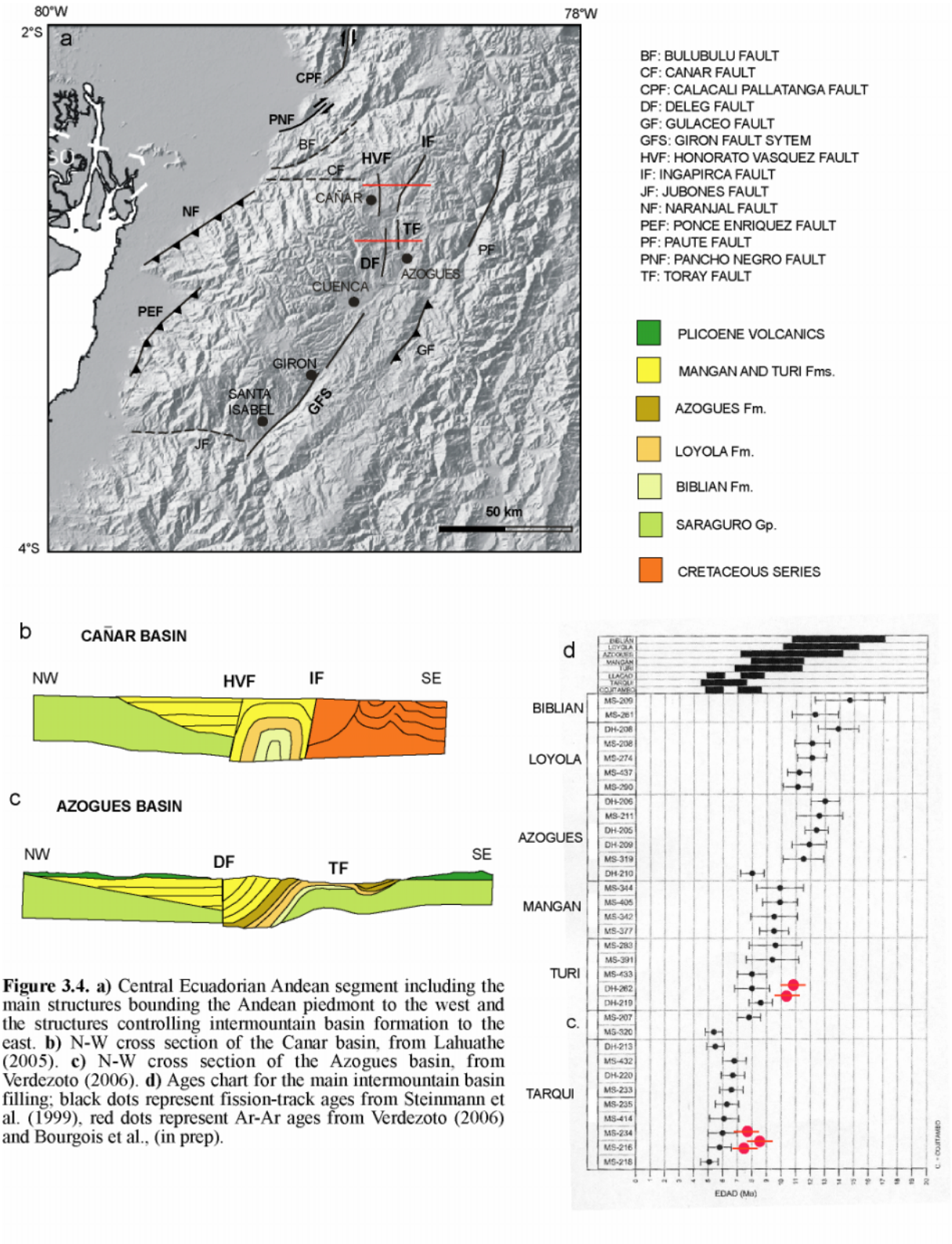

Figure 3.4. a) Central Ecuadorian Andean segment including the main structures bounding the Andean piedmont to the west and the structures controlling intermountain basin formation to the east. **b)** N-W cross section of the Canar basin, from Lahuathe (2005). **c)** N-W cross section of the Azogues basin, from Verdezoto (2006). **d)** Ages chart for the main intermountain basin filling; black dots represent fission-track ages from Steinmann et al. (1999), red dots represent Ar-Ar ages from Verdezoto (2006) and Bourgois et al., (in prep).

The evolution of the sedimentary infill of the Cañar and Azogues basins follows two major steps during Miocene times. The first one, characterized by major subsidence periods, led to depocenters formation, and the second one related to compressive deformation was related to tectonic

inversion. The stratigraphic sequence finishes upwards with the deposition of clastic and volcano-clastic strata, which unconformably overlies the basin infilling.

3.3.1 The Miocene subsidence step.

The Miocene evolution of the Cañar basin (Lahuathe, 2005; Bourgois et al., 2006) seems controlled by contemporaneous transcurrent and normal faults. During early-middle Miocene the TIF develops at the eastern side of the ancient deformed series, which correspond to the Cañar basin basement. It acts as a normal fault controlling deposition of the Biblian and Loyola Fms. During late Miocene subsidence migrated to the west. The HVDF controled subsidence of a western sub-basin formed mainly by deposits of the Mangan and Turi Fms. To the south, along the Azogues basin, an early Miocene E-W directed extension led to reactivation of ancient structures including the HVDF, which controls deposition of the Biblian, Loyola and Azogues Fms., involving a subsidence rate of 4 mm/yr (Verdezoto, 2006). During late Miocene a graben-type structure develops between the HVDF and the ITF controlling the deposition of the Mangan Fm. However, this step marks a decrease in tectonic activity along the HVDF.

3.3.2 The late Miocene contractional step.

The stratigraphic sequences along the Ingapirca-Deleg unit are strongly deformed along N-S directed antiformes and faults. Two major antiforms develop along the Cañar and Azogues basins, the Ingapirca and Biblian antiforms. Compressive deformation is mainly accommodated along the TIF. This compressive step produces stretching measured about 60% and 30% for the Cañar and Azogues basins, respectively. Considering that the deformation period corresponds to the time span between the deposition of the Turi Fm. (deformed) and the overlying undeformed volcanic formations (Tarqui and Callao Mbs.) an age of 8.7-8 Ma is proposed (Verdezoto, 2006). This date is in agreement with other models that proposed a tectonic inversion period at ~9 Ma (Steinmann et al., 1997; Hungerbühler et al., 2002). However, the Ingapirca-Deleg unit is not deformed by this compressive event. Along the Cañar basin, the differences in deformation between the Cañar-Azogues and Ingapirca-Deleg units are probably related to the strength of the basement (Lahuathe, 2005). The basement of the western Ingapirca-Deleg unit (i.e. the Saraguro Gp.) acting like a buttress enhancing its overlying sequences to be affected by the compressive event. A more or less similar mechanism is proposed for the late Miocene evolution of the Azogues basin (Verdezoto, 2006). Here, the highly deformed Cañar-Azogues unit lies next to the undeformed Ingapirca-Deleg unit. The antiform which formed during

deposition of the Turi Mb. acted as a topographic barrier limiting the deposition of Santa Rosa Mb. along a sub-basin which forms to the west of the antiform.

From 8 Ma intense volcanic activity led to the deposition of the Tarqui Mb., which discordantly overlies the previously deformed series of the basin infilling along the central corridor. The most important aspect of basin architecture is that both, the Cañar and the Azogues basins show a westward-undeformed section of late Miocene-Pliocene age, which is limited to the east by the Honorato Vasquez and Deleg faults.

3.4 THE SANTA ISABEL BASIN.

3.4.1. General location.

The Santa Isabel basin (SIB) trends in a N-E direction from ~3° S to 3°25' S (Figure 3.5). The SIB is infilled by Miocene continental clastic sediments, which unconformably overlies the basin basement defined by the Eocene-Oligocene rocks of the volcanic Saraguro Gp. (Kenerley et al., 1973; Pratt et al., 1997; Hungerbühler et al., 2002; Dunkley and Gaibor, 1997). Two different formal subdivisions for the SIB sediments have been proposed: Kennerley et al. (1973) grouped the major section of sedimentary rocks of the Santa Isabel area together with the Santa Rosa and Mangan Fms. of the Cuenca basin in a broad Group, the so-called 'Ayancay Group'. This group being overlain by rocks of the Uchucay Fm. Recent cartographic works use this terminology (Pratt et al., 1997; Dunkley and Gaibor, in prep). Contrary, Hungerbühler et al. (2002) subdivide the stratigraphic series in three main formations, including the Jacapa, Burrohuaycu (major depocenter), and Uchucay Fms. In this work, we use the formal subdivision proposed by Hungerbühler et al. (2002) which is more exhaustive for the description of the stratigraphic events occurring locally at the SIB.

A regional range front extending from the south of Cuenca to the Sumaypamba area bounds to the east the continental series of the SIB (Figures 3.4 and 3.5). The structure of the range results from compressive and extensional tectonics. Near to Girón the sedimentary infilling of the SIB is overlain by the clastic and volcanic sediments corresponding to the Turi Fm. This formation is also bounded eastward by the range. This section of the work corresponds to the analysys stratigraphic evolution and the record of tectonic deformation from 3°15' S to 3°25' S (Figure 3.5) including the evolution of the southernmost section of the range (i.e. the La Cria anticline) and the evolution of the Girón Fault System (GFS). Sedimentary and tectonic events dated along basins located further north (i.e. Cañar and Azogues basins) as well as local published data are used to date the stratigraphic and tectonic events along the SIB.

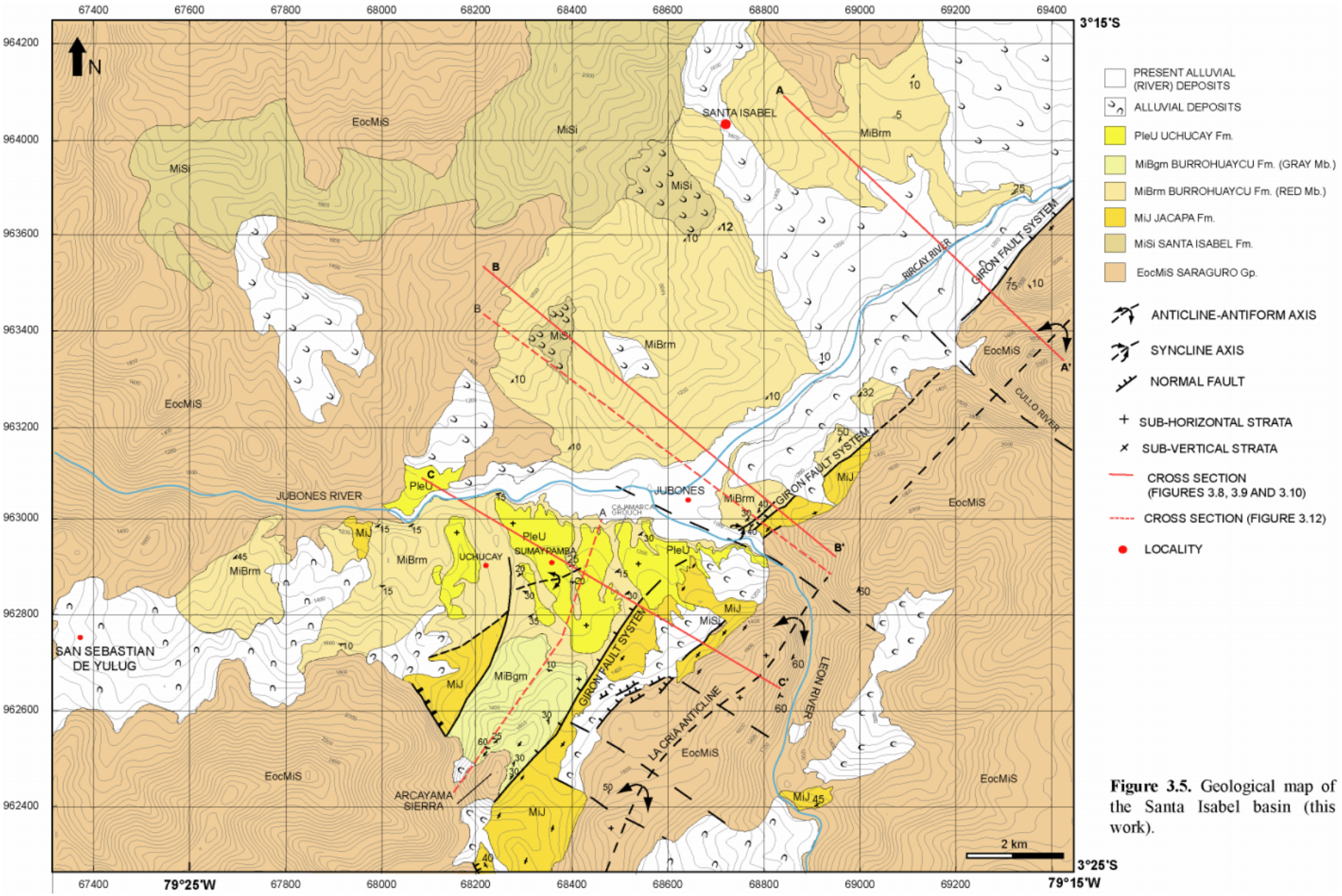

Figure 3.5. Geological map of the Santa Isabel basin (this work).

3.4.2. Stratigraphic record of the Santa Isabel basin

3.4.2.1 The Saraguro Gp.

The Saraguro Gp. corresponds to the SIB basement. It is the formation of greatest areal extent in the studied area. It bounds to the N-W and to the S-E the basin infilling of the SIB. The Saraguro Gp. contains a great number of formations and informal units, which comprises 500-2000 m thick of intermediate to acidic volcanic rocks of middle Eocene to early Miocene age (Dunkley and Gaibor, 1997; Pratt et al., 1997; Hungerbühler et al., 2002). The Saraguro Gp. shows a complex stratigraphic record of more than 20 Myr of volcanic activity and local short-term fluvial to lacustrine deposition. Along southern Ecuador, from 3°5'S to 3°20'S, the Saraguro Gp. includes at least four formations: the Las Trancas, Plancharumi, Jubones, and La Paz Fms. (Dunkley and Gaibor, 1997; Pratt et al., 1997). However, at the Santa Isabel area, most of the Saraguro Gp. outcrops have been not differentiated in cartographic works. The differentiation of the Saraguro Gp. is far from the scope of this work. Here we use the term 'Saraguro Gp.' to describe all the undifferentiated volcanic series of late-middle Eocene to Miocene age outcropping the Santa Isabel area.

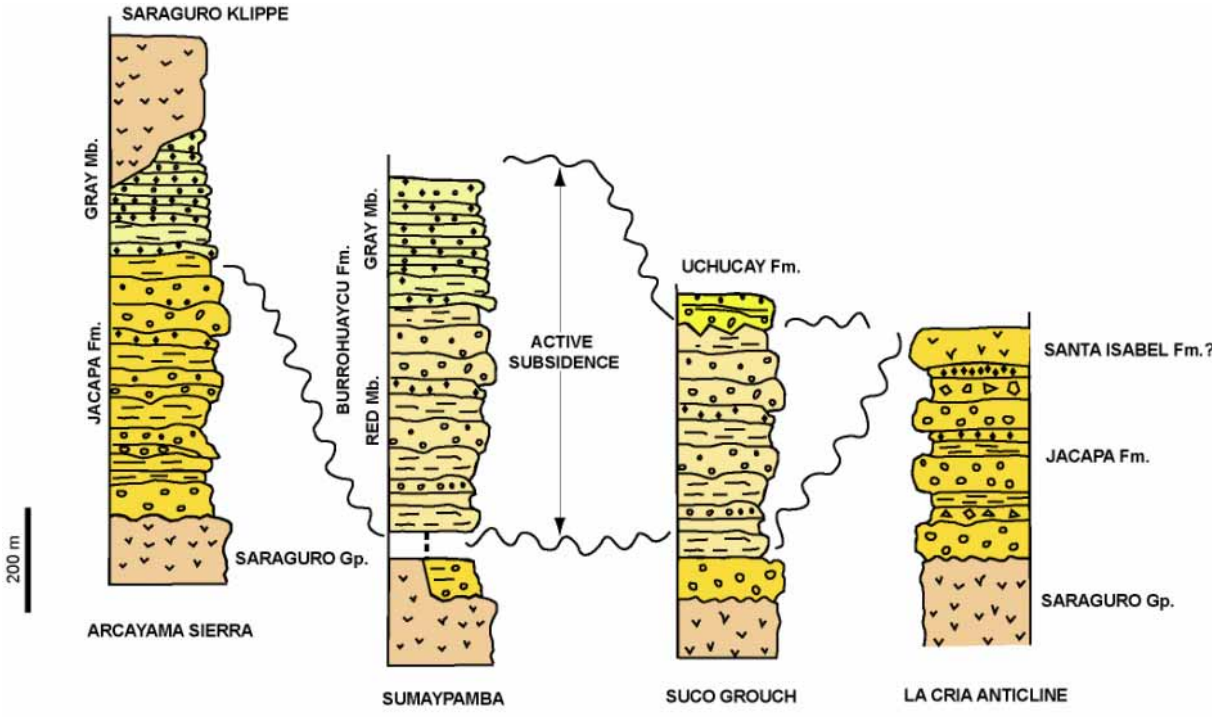

Figure 3.6. Key stratigraphic columns of the SIB. From left to right they include the Arcayama sierra, Sumaypamba, Suco grouch and La Cría anticline sections. Fission-track dating of the Red Mb. sequence yielded ages between 10.5 to 14.7 Ma (Hungerbüler et al. (2002). Two major angular unconformities exist: a major unconformity between the Jacapa and Burrohuaycu Fms and a minor one between the Burohuaycu and Uchucay Fms.

3.4.2.2 The Jacapa Fm.

Initially considered as part of the Ayancay Gp. (Kenerley, 1973), the Jacapa Fm. was defined by Hungerbühler et al. (2002) to distinguish the deformed series observed along the SE border of the SIB. The main outcropping zone lies in the west flank of the La Cria anticline along a 400 to 2000 m wide NE trending strip. Along this strip, it reaches a maximum thickness of 600-800 m in the southern limits (i.e. Cajamarca grouch) and no more than 400 m in the northern limits (i.e. next to the locality of Jubones). The Jacapa Fm. extends to the Jubones locality and is not observed further north. The formation also outcrops to the east of the Leon River. Here, a 50-100 m thick E-W elongated band outcrops along the eastern flank of the La Cria anticline. The prolongation of the Jacapa Fm. to the east of the main depocenter of the SIB led Pratt (1997) to argue that severe erosion may lead to the loss of a thick section of the Jacapa Fm. to the east of the Leon river.

The clastic Jacapa Fm. is exclusively formed by rocks originating from the Saraguro Gp. It consists of up to 15 m of gray well-bedded poorly-sorted conglomerate layers. This sequence is interbeded with up to 10 m fine to coarse red and gray sandstone and siltstone layers. The thicker and broader conglomerate layers are located at the base of the formation (UTM 832-230, Figure 3.6). The sequence fines and thins upwards. The origin is fluvial to lacustrine. Imbrication measures suggest that sediment supply originated from a southward source (Mediavilla, 1991). Channel formation and related incision of the top of the Jacapa Fm. suggest that the top of the formation is directed to the north. However, due to the high degree of deformation, it is difficult to establish if all outcrops follow this sedimentary pattern. The stratigraphic series are highly deformed along the N-E directed strip and along the small outcrop observed east of the Leon river. Dip angles normally range between 70° to vertical. One of the main aspects of the Jacapa Fm. sequence is the presence of angular breccia deposits interbedded in the fluvial series (Figure 3.10). Breccia layers show intermediate to acid volcanic rocks input, being the only zone where acid blocks have been observed. It is probable that deposition of the Jacapa Fm. occurred during the deformation period that led to the formation of the La Cria anticline and pervasive folding of the Saraguro Gp. (i.e. formation of the range). Several aspects as auto-breccia layer deposition (Figure 3.9d) point out to a tectonically disrturbed depositional environment. However, this hypothesis could not be properly tested in the field. At the UTM 687000-9628500, several volcanic layers are intercalated along the upper series of the Jacapa Fm. These volcanic layers have been attributed to the Santa Isabel Fm. (Hammer, 1997; Hungerbühler et al., 2002). In this way, these authors assumed an early Miocene age for the the Jacapa Fm.

The Jacapa Fm. was initially considered as a strip limiting to the west the La Cria anticline (Hungerbühler et al., 2002). However, to the west of the anticline, we consider that several 50-200 m

thick sections of clastic sediments unconformably overlying the Saraguro Gp may be attributed to the Jacapa Fm. These series are deformed and unconformably overlain by younger sediments of the Burrohuaycu Fm. We suggest that the Jacapa Fm. extends further west than previously proposed (Figure 3.5).

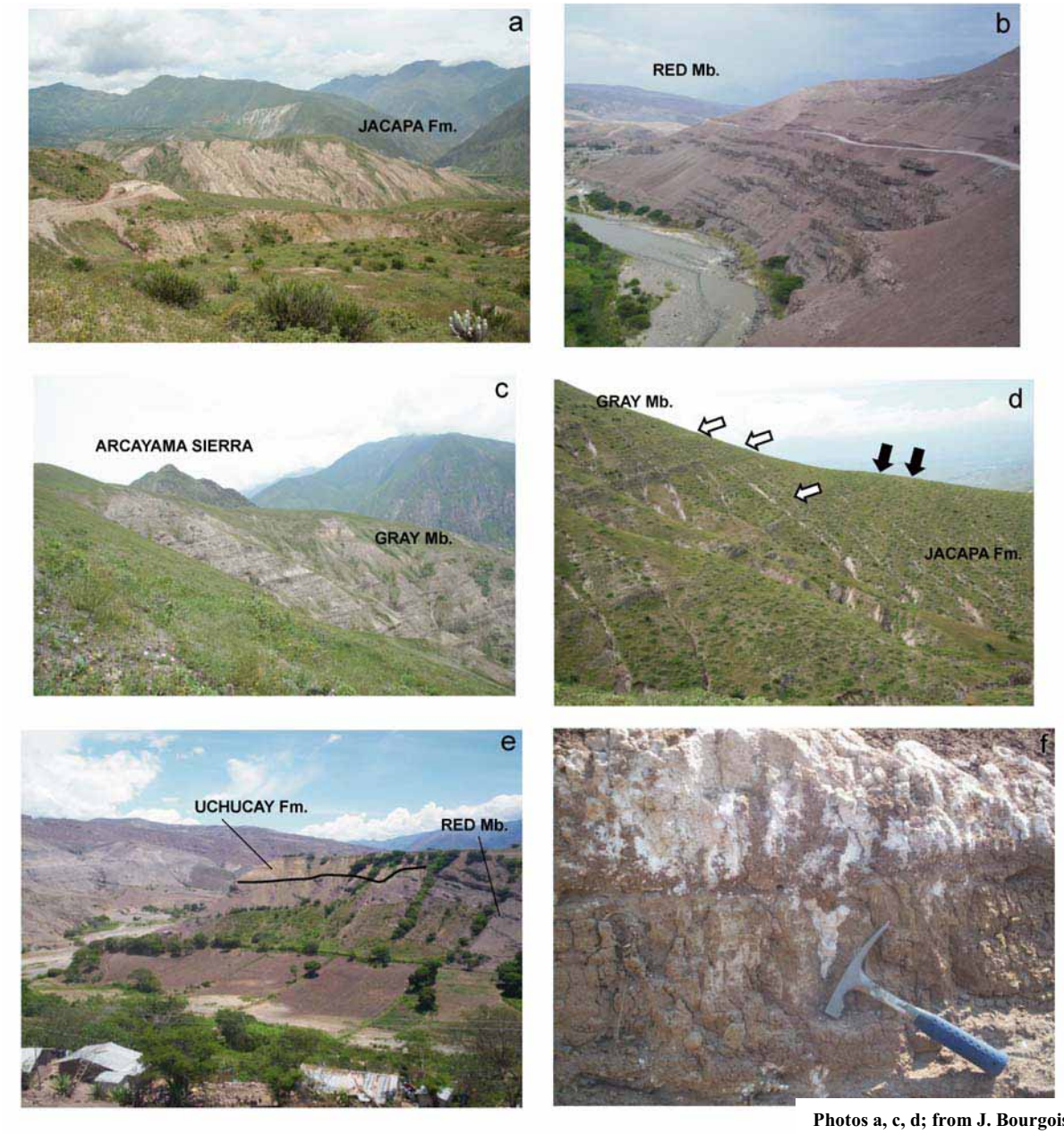

Photos a, c, d; from J. Bourgois

Figure 3.7. a) Sub-vertical strata of the Jacapa Fm. outcropping at the southeastern section of the SIB. **b)** The Red Mb. of the Burrohuaycu Fm. at the southern edge of the Jubones river. **c)** Undeformed sequence of the Gray Mb. **d)** The strong angular unconformity between the Jacapa Fm. and the Gray Mb. of the Burrohuaycu Fm. **e)** The unconformity between the Uchucay Fm. and the Red Mb. **f)** Carbonated alteration (white layer) at the top of the Uchucay Fm. Note the soil horizon located above and below of the white layer.

3.4.2.3 The Santa Isabel Fm.

The Santa Isabel Fm. (Pratt et al., 1997; Hugerbuhler, 1997) outcrops mainly in the N-W zone of the studied area. Dominant lithologies include intermediate lava flows and volcanic breccias. Thickness is variable ranging between 500 and 1500 m (Hungerbühler et al., 2002). Fission track ages range between 21.1 and 18.4 Ma (Hungerbühler et al., 2002) for the Santa Isabel area and up to 8 Ma for the Girón area. This suggests that the Santa Isabel Fm. could be contemporaneous with the Burrohuaycu Fm. Furthermore, small bands of vertical volcanic series outcropping next to the Jacapa Fm. (UTM: 686500-9627500) attributed to the Santa Isabel Fm. (Hammer, 1997) suggest that the Santa Isabel Fm. could be also contemporaneous with the upper section of the Jacapa Fm. Stratigraphic relationships between the Santa Isabel Fm. and the Jacapa and Burrohuaycu Fms are not clear.

3.4.2.4 The Burrohuaycu Fm.

The Burrohuaycu Fm. corresponds to the main infilling of the SIB. It extends from the SW of Girón to the south of Sumaypamba (Figure 3.5). It was initially defined as part of the Ayancay Gp. (Kenerley et al., 1973) suggesting that the Burrohuaycu Fm. corresponds to the southern prolongations of the Mangan and Santa Rosa Fms. observed along the Cuenca and Azogues areas. The Burrohuaycu Fm. unconformably overlies the Saraguro Gp. and in some places the Jacapa Fm. Upwards, in the Girón area, the formation is conformably overlain by the Turi Fm.

The Burrohuaycu Fm. shows two main different members at the SIB (other works propose a two to five members subdivision (i.e, Mediavilla, 1991; Helg, 1998; Hammer, 1998; Hungerbühler et al., 2002). The lower (Red Mb.) overlies discordantly the Jacapa Fm. and in some places the Saraguro Gp. It mainly consists of well-bedded 5-9 m of coarse to fine channelized conglomerate gray layers interbedded with up to 6-8 m thick red siltstone bodies (Figure 3.7b). An upward layer thinning and a general variation in grain size from coarse to thin is observed from the base to the top of the member and from south to north. The northernmost observed outcrops, to the east of Santa Isabel, consist of a thinly alternation of sandstones and siltstones. The thickness of the Red Mb. is between 400-600 m at the southernmost tip of the SIB (i.e. Uchucay-Sumaypamba area) but it can reach 700-800 m at the whole basin. The series dip gently (10-20°) to the S-SE but dip increases generaly to 30° next to the GFS. Local variations in dip are related to local processes as along the small ~E-W directed antiform developing near to Sumaypamaba (UTM: 68300-962900, Figure 3.5) and along the northernmost segments of the studied zone. Along this sector, the Red Mb. dips gently to the north. The change in dip direction is mostly due to massive landslide typical of this zone.

The Red Mb. interfingers with the concordantly overlying Gray Mb (Figure 3.7d). It consists of 2-3 m gray sandstone and conglomerate bodies outcropping between Sumaypamba and the Arcayama sierra. The Gray Mb. unconformably overlies the Jacapa Fm. The series of the Gray Mb. lie sub-horizontaly to gently dipping to the west. Local high perturbations of the gently dipping pattern are observed at the top of the Arcayama sierra. It is difficult to obtain fresh volcanic layers from both Red and Grey members. Volcanic horizons are often reworked. Fission-track ages obtained mostly from tephra layers yielded in the range between 10.5 to 14.7 Ma (Hungerbühler et al., 2002).

3.4.2.5 The Uchucay Fm.

The Uchucay Fm. defines a 20 to 100 m thick of coarse to fine yellow boulder deposited discordantly over the Red Mb of the Burrohuaycu Fm. The Uchucay Fm. extends to both sides of the Jubones river. The broader section outcrops at the Sumaypamba locality (Figure 3.7e). Here the base of the stratigraphic column consists of 20-30 m of coarse boulder. Upwards (i.e. to the north of Sumaypamba) the thinnest series show cross-bedding fine layers intercalated with sandstone and medium to fine conglomerates. It has been suggested that deposition occurred in a lake which had a high detrital input (Hammer, 1998 in Hungerbühler et al., 2002). A maximum thick of 100 m is measured. The northern outcrop, placed in the northern edge of the Jubones river, consists of a ~50m thick of up to 4m cross-bedding fine layers intercalated with sandstone and medium to fine conglomerates. These series are similar to those observed to the north of Sumaypamba but strike correlations are difficult to establish.

Initially considered as Pleistocene (DGGM, 1974) more recently, a single reworked tephra layer (UTM: 682810-9629759) obtained from the top of the coarser section yielded a ~9.5 Ma age (Hungerbühler et al., 2002). However, this layer is not placed inside the sedimentary sequence. It corresponds rather to a highly carbonated non-consolidated white layer extending superficially in the top of the formation all over the Sumaypamba area (Figure 3.7f). Its position (inside the soil horizon) and composition seems to be rather related to a pedogenic-type alteration.

3.4.2.6 Alluvial deposits

A great area of the SIB is covered by alluvial deposition. The nature and age of these deposits is quite different, being the response to tectonic or erosional driving mechanisms. The major area extent of alluvial is observed in the northeastern section of the mapped area and is coincident with the most active segments of the GFS (see below). It shows matrix supported medium to poorly rounded decimetric blocks. The freshness of the materials involved in the coluvial leads to think that the deposit is relatively young. An organic sample was collected; it is being dated with the 14 C method.

The alluvial zones placed along the southern flank of the Rircay river are made up of coarse, sometimes metric, blocks of the Saraguro Gp. The second major area of coluvial deposits concentration corresponds to the flanks of the La Cria anticline. Coalescence of these deposits forms the bajada morphology between the Saraguro Fm. and the Corrales grouch. Other alluvial deposit may be contemporaneous with the Saraguro Gp. (UTM: 830-320) while the big extent alluvial zone of the San Francisco zone is mostly related to erosion of the Saraguro Gp.

3.4.3 Main structures of the Santa Isabel basin

The SIB is a semi-arid to arid extensional continental basin where an axial river is situated and flanking piedmonts classified as either pediments or alluvial fans interact with it. The SIB develops next to the range that controls the direction of the valley of the Rircay and Girón rivers. The main normal fault of the Girón fault system (GFS) represents the westward limit of this range, it separates the sediments of the Burrohuaycu and Turi Fms. to the west from the range front to the east (Figures 3.4 and 3.5). The SIB corresponds to a half-graben basin. Several structural arguments such as basin and fold formation have been used to evaluate the structure of the GFS. However, the tectonic character of the structure as well as the relationships between the sedimentation of the Burrohuaycu and Turi Fms. and the activity of the GFS are in debate. Some models consider that the GFS develops in a pure extensive tectonic regime. In this scenario, the GFS has been interpreted as a normal fault (Kenerley et al., 1973; Winter and Lavenue, 1989; Mediavilla, 1991). The main aspects used in this interpretation are: 1) the closely related disposition between depocenters formation and fault location (i.e. Burrohuaycu and Turi Fms. depocenters), and 2) a strong current extensional activity along the escarps bounding the range in front of the Santa Isabel locality. An extensional pulse (coincident with the deposition of the Jacapa and Burrohuaycu Fms.) followed by a pure reverse fault mechanism has been also proposed recently (Hungerbühler et al., 2002; Dunkley and Gaibor, in prep). However, Dunkley and Gaibor (in prep.) consider that the first pulses of extensional activity are difficult to constraint due to extreme erosion of the involved subsiding series. In the Ecuadorian database of Quaternary faults, the GFS is considered as an active normal fault, which slip rate is roughly measured as > 0.5 mm/yr (Eguez et al., 2003).

Two main deformation periods lead to the current architecture of the GFS. A compressive period deforming the Saraguro Gp. and the Jacapa Fm. (i.e. formation of the range) and a more recent extensional step that triggers subsidence for accumulation of the Burrohuaycu Fm.

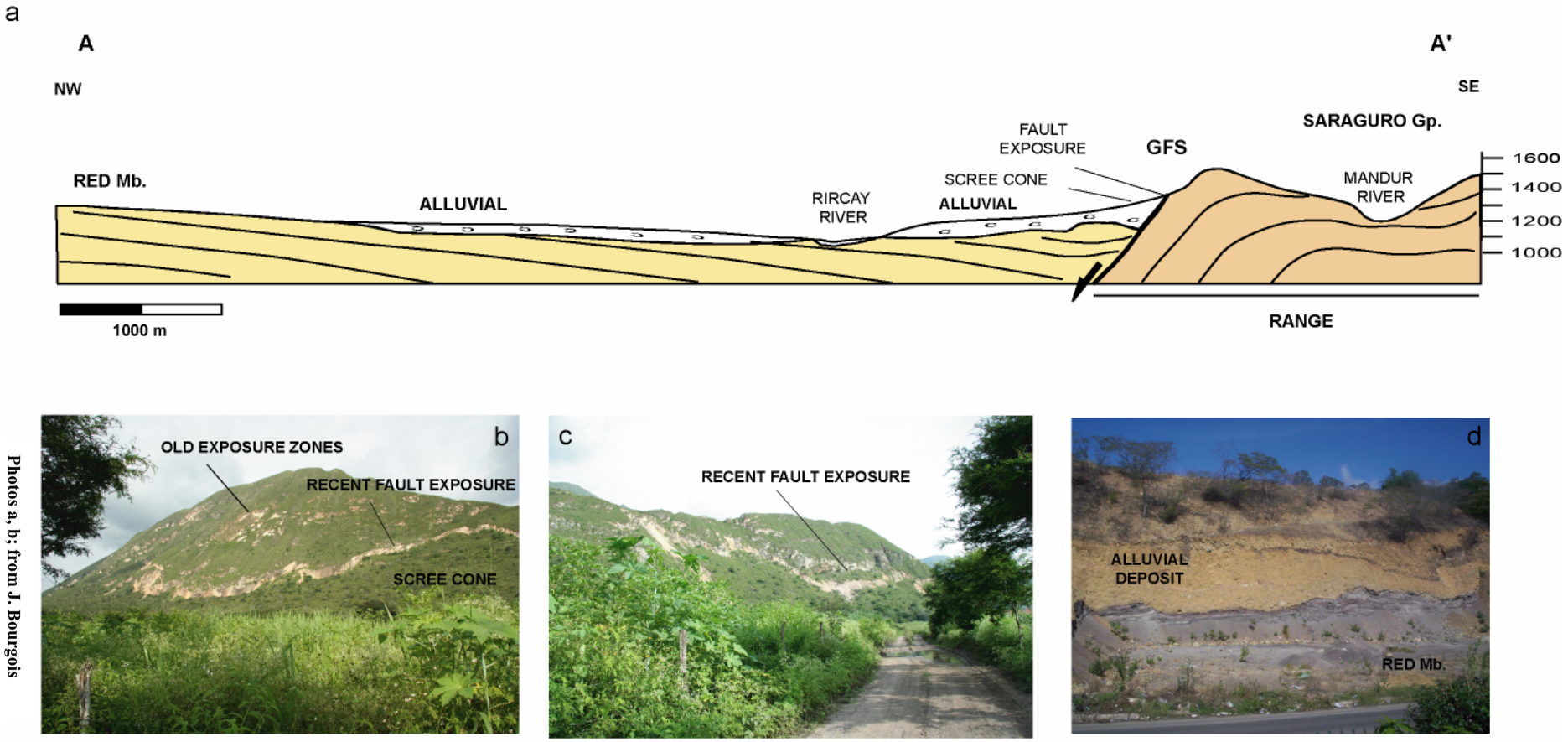

Photos a, b; from J. Bourgois

Figure 3.8. a) S-E directed cross-section of the SIB along the north segment of the GFS (no vertical exageration) **b)** Main scarp of the GFS. Note the old exposure zones and the elongated recent fault exposure. **c)** The most recent exposure or fault rupture zone extends at least 1000 m along the north segment of the GFS.**d)** Main alluvial deposition in front of the more active zones of the GFS. See text for further explanations.

3.4.3.1 The range: La Cria anticline

At the SIB the range mainly consists of rocks of the Saraguro Gp. It reaches altitudes of 300-700 m above the valley floor. Important flexing and folding of the Saraguro Gp. along the range limit is interpreted as evidence of a N-W verging compressive step (Hungerbühler et al., 2002; Dunkley and Gaibor, in prep.). The northern segments of the range, (Figure 3.8) do not offer good outcrops since the range front is totally covered by alluvial deposits (Figure 3.8a). On the opposite, along both flanks of the Leon river the range structure is easily observed. At the Jubones locality, good outcrops expose the range structure, which is formed by the Saraguro Gp. and the Jacapa Fm. A major vertical plane separates these sequences (Figure 3.9b). Stratigraphic planes are sub-vertical at both sides of the plane. This high parallelism leads to think that there is no major fault at the Saraguro Gp. and the Jacapa Fm. We consider that this surface corresponds to a major stratigraphic plane. Sliding plains, which seem active at the boundary between these two formations, are considered to be minor tectonic features reactivated during the subsequent extensional step. The so called 'La Cria' anticline also exposes the rocks involved in the range-related deformation. The anticline trends in an NE direction (Figure 3.5). One of the particularities of the La Cria anticline is its box-shaped architecture (i.e. near vertical series forming the anticline flanks and sub-horizontal series located at the summit, Figures 3.8a, 3.9a and 3.9e). Box-shaped folds generally forms along zones where a decollement (or a detachment) horizon or ramp exists. A similar deformation-type has been observed along the Cañar area along the tectonic unit that bounds the basin depocenter of the Cañar basin (Figure 3.4c).

It has been suggested that the La Cria anticline and major N-S verging thrust sheets along the Arcayama sierra and San Sebastian de Yulug areas formed during the same compressional step (Hungerbühler et al., 2002; Dunkley and Gaibor, in prep), which thrust the Saraguro Gp. above the Gray Mb. In fact, the Arcayama sierra summit is formed by rocks of the Saraguro Gp. overlying the Gray Mb. However, we found no evidence of thrusting in this area. The Gray Mb. is not deformed all over the most of its sedimentary sequence along the Arcayama sierra (Figure 3.7c). Furthermore, it unconformably overlies the deformed series of the Jacapa Fm. The Gray Mb. deformation zone (related with highly disturbed and vertical strata) is only concentrated in the proximity of the summit of the sierra along the uppermost series of the member. This suggests that the block located at the summit of the Arcayama sierra corresponds to a sedimentary klippe, which slided into the upper series of the Gray Mb. Because the tectonic deformation associated with the tectonic deformations is associated with the sedimentary klippe emplacement, a scenario in which a regional compressive tectonic step promotes the northward directed thrusting of the Saraguro Fm. over the undeformed Gray Mb. is excluded. To the west of the Arcayama sierra, the contact between the Saraguro Gp. and the Jacapa Fm. shows evidences of extension rather than compression (see below, section 3.4.3.3). Furthermore, we found no evidences of thrusting since the hill break slope is completely covered by

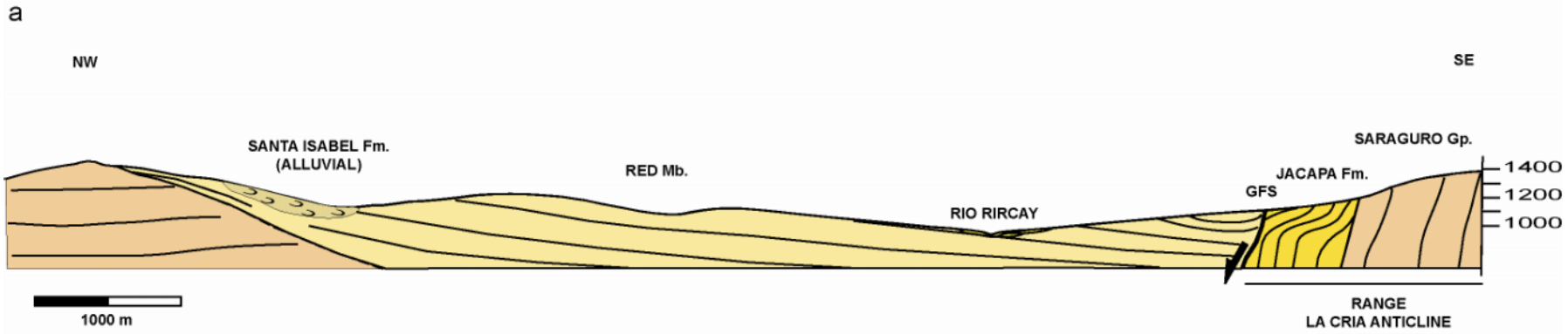

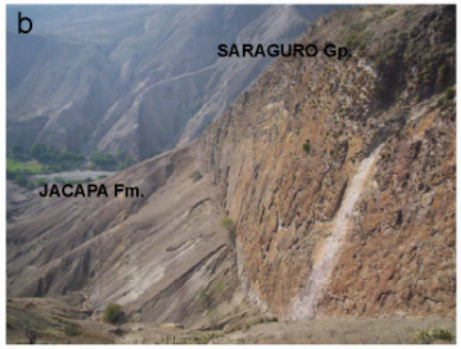

Fotos c, e; from J. Bourgois

Figure 4.9. a) S-E directed cross-section of the SIB along the central segment of the GFS. (No vertical exageration). **b)** Vertical contact between the Jacapa Fm. and the Saraguro Gp. **c)** Strongly deformed layers of the Jacapa Fm. **d)** Auto-breccia deposits along the base of the Jacapa Fm. Violet boulders correspond to material derived from the Jacapa Fm. itself **e)** Syncline structure along the limit between the Red Mb. and the Jacapa Fm. **f)** Normal fault scarp at the limit between the Jacapa Fm. and the Red Mb. See tex for further explanations.

an alluvial fan derived from the high hills of the Saraguro Gp. We consider that at the SIB the compressive deformation is exclusively concentrated along the range.

3.4.3.2 The extensional activity along the GFS

Studies of normal faults in zones of continental extension indicate that faults are all segmented along strike (i.e. Jackson, 1987; Gawthorpe and Leeder, 2000). Along individual segments the slip is stronger in the central parts of the segments and decreases gradually to the ending tips (Cowie and Scholz, 1992; Dawers et al., 1993; Gupta et al., 1998). The longest segments, highest slip rates and highest footwall topography (proxy for displacement) are located in the centre of the fault zone, the magnitude of these parameters decreasing towards its ends. Fault segment boundaries are often marked by local highs and lows in hangingwall and footwall elevations, respectively, and are often marked by an increased density of small displacement faults (Gawthorpe and Leeder, 2000). In a general sense, for a given amount of regional extension, topographic elevation depends upon fault spacing, so areas of small-scale distributed faulting at fault segment offsets and crossovers stand at higher elevations than the hangingwalls adjacent to large-displacement border faults. However, the nature of the foot-wall rocks also appears as a major feature in controlling the morphology of a normal fault (Goldsworthy and Jackson, 2000). At the Santa Isabel area, the GFS shows a strong segmentation (Figure 3.5; segments 1 to 3 in Figure 3.11) suggesting that probably each segment evolved differently through time. It includes: the north, central and south segments.

The north segment shows the most recent active tectonic features along the entire GFS. The extensional activity is clearly observed along a 300-400 m fault scarp placed to the southeast of Santa Isabel (Figures 3.8 and 3.11). Old exposure zones can be easily observed all over the height of the scarp, they extend 150-200 m high. Along the lower segments this scarp shows an elongated 2-5 m high fault exposure zone related to the younger tectonic activity. Cinematic markers obtained along this exposure zone have yielded a ~NW directed extension regime (Winter and Lavenue, 1989; Mediavilla, 1991). Further down, a typical normal fault-related scree cone forms originates from footwall-derived deposits. A thick alluvial deposit placed between the scree cone and the Rircay river complete downwards the normal-fault related sequence. The GFS north segment is highly concordant with the zone of greatest recent alluvial deposition and mass collapse along the north flank of the Rircay river (i.e. Santa Isabel locality, Figures 3.5 and 3.8a). This is a typical feature of normal fault systems where hanging wall alluvial is greater than the footwall derived one (Gawthorpe and Leeder, 2000). We consider that mass collapse and great alluvial deposition are related to recent fault-induced tilting of the half-graben floor. Winter and Lavenu (1989a) proposes a 0.5 mm/yr displacement rate based on the whole scarp height and a Quaternary age for the beginning of the extensional process.

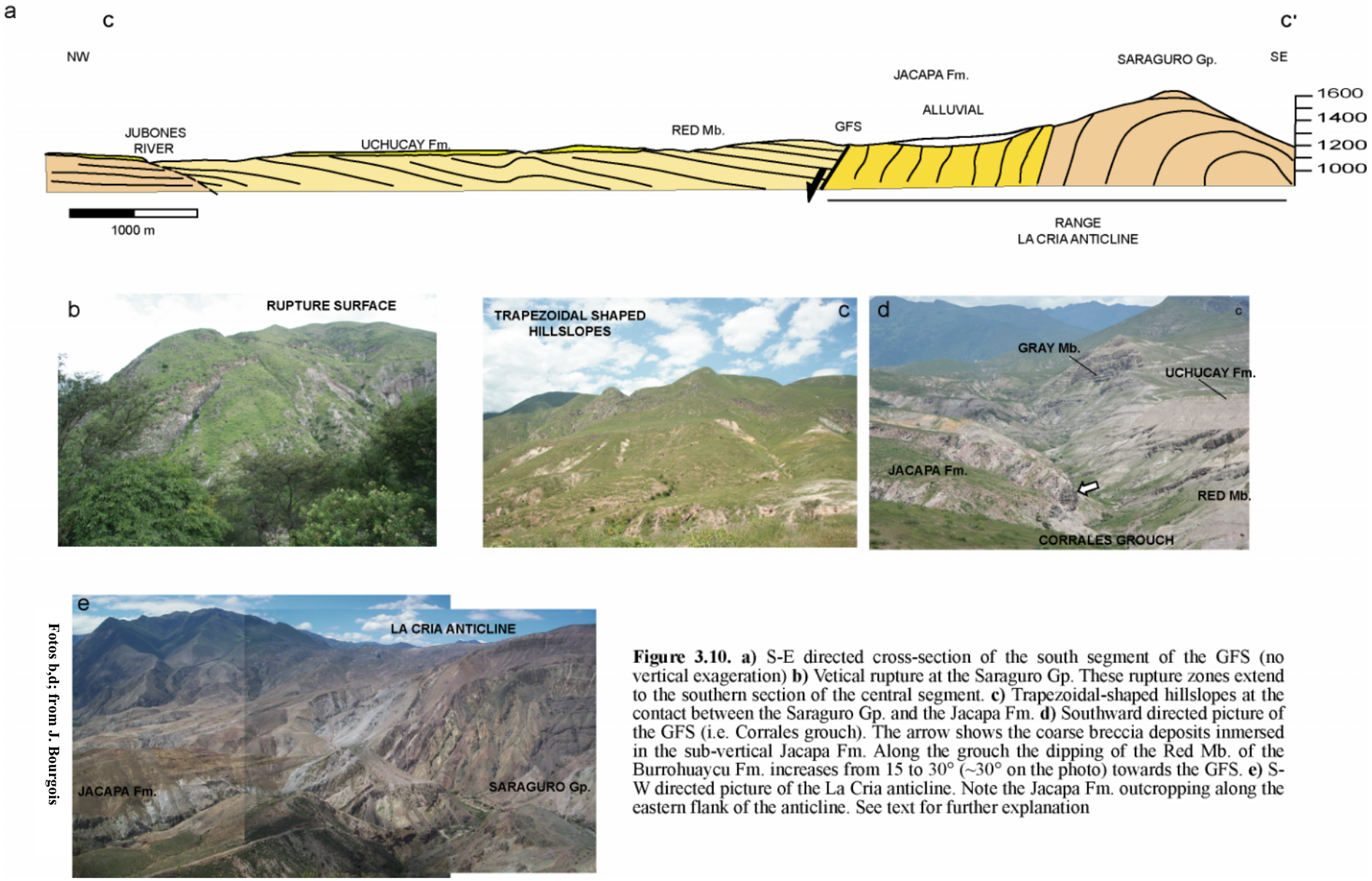

Fotos b,d; from J. Bourgois

Figure 3.10. a) S-E directed cross-section of the south segment of the GFS (no vertical exageration) **b)** Vetical rupture at the Saraguro Gp. These rupture zones extend to the southern section of the central segment. **c)** Trapezoidal-shaped hillslopes at the contact between the Saraguro Gp. and the Jacapa Fm. **d)** Southward directed picture of the GFS (i.e. Corrales grouch). The arrow shows the coarse breccia deposits inmersed in the sub-vertical Jacapa Fm. Along the grouch the dipping of the Red Mb. of the Burrohuaycu Fm. increases from 15 to 30° (~30° on the photo) towards the GFS. **e)** S-W directed picture of the La Cria anticline. Note the Jacapa Fm. outcropping along the eastern flank of the anticline. See text for further explanation

They propose a switch from compression to extension at the Plio-Quaternary limit (i.e. 2 Ma), this age being used for fault cinematics and chronology description. However, the attribution of a Quaternary age for scarp formation is quite arbitrary. No morphological marker was dated and the compression periods are best defined for the Miocene period and not for the Pliocene one (Lavenu et al., 1995a).

The limit between the central and north segments is defined by the abrupt disappearance of the major scarp. The north and central segments are separated by a NW trending linear zone coincident with the Cullo river. The persistent linearity of the river is assumed to be controlled by a transfer zone. This transfer zone is defined by a large (larger than average) catchment basin along the footwall block, which is a typical feature on ending segment transfer zones (Gawthorpe and Leeder, 2000). Not far from this transfer zone, wine-glass-shaped morphology (UTM 690500 9632500) has been considered as an evidence of fault prolongation from the active scarp of the north segment (Winter and Lavenu, 1989a). However, the proposed wine-glass-shaped deposit is formed by two different lithologies (i.e. coluvial deposits and fluvial deposits of the Burrohuaycu Fm. for the northern and southern lobes, respectively). It is most likely that this morphology is not derived from fault activity. In general, the central and northern parts of the central segment are characterized by the absence of fault-derived morphology. Tectonic activity concentrates along the southern parts of the segment. To the north of the range front a well-developed syncline (Figure 3.9e) develops next to the deformed series of the Jacapa Fm. This syncline formed by sediments of the Burrohuaycu Fm. is interpreted as a hangingwall feature related with normal fault activity. The existence of a normal fault at the contact between the syncline and the deformed Jacapa Fm. is constrained by the existence of pervasive shearing at the base of the syncline and the clear morphological evidence at the intersection of this contact with the surface. Here an ~30° northward dipping surface show clear features of a normal fault scarp (Figure 4.9f). Some of these features include: an eroded small scree cone and differential erosion between the plane and the hanging wall floor. Furthermore, cinematic markers such as striations and mylonitic joints characterizes a normal movement sense with a slightly-dextral component. The highly developed geometry of this second scarp and its relatively low-angle suggests that extensional deformation could not be only related to simple post-compressional gravity accommodation.

The Leon river separates the central and south segments. We consider that this zone corresponds to a transfer zone. The transition between the central and south segments is less abrupt than between the north and central ones. The southern segment is characterized by coherent steeped graded trapezoidal-shaped facets along the contact zone between the both vertical-bedding Saraguro Gp. and Jacapa Fm. The graded trapezoidal character is largely controlled by stratigraphy. However, down-trough sliding is very active along these polygonal-shaped facets especially along the range break-slope. Indeed, the most developed polygonal zones clearly interrupt the typical recent alluvial

piedmont fan morphology. Downwards, several morphological and structural aspects lead to think that the contact between the Burrohuaycu and Jacapa Fms. is controlled by the GFS.

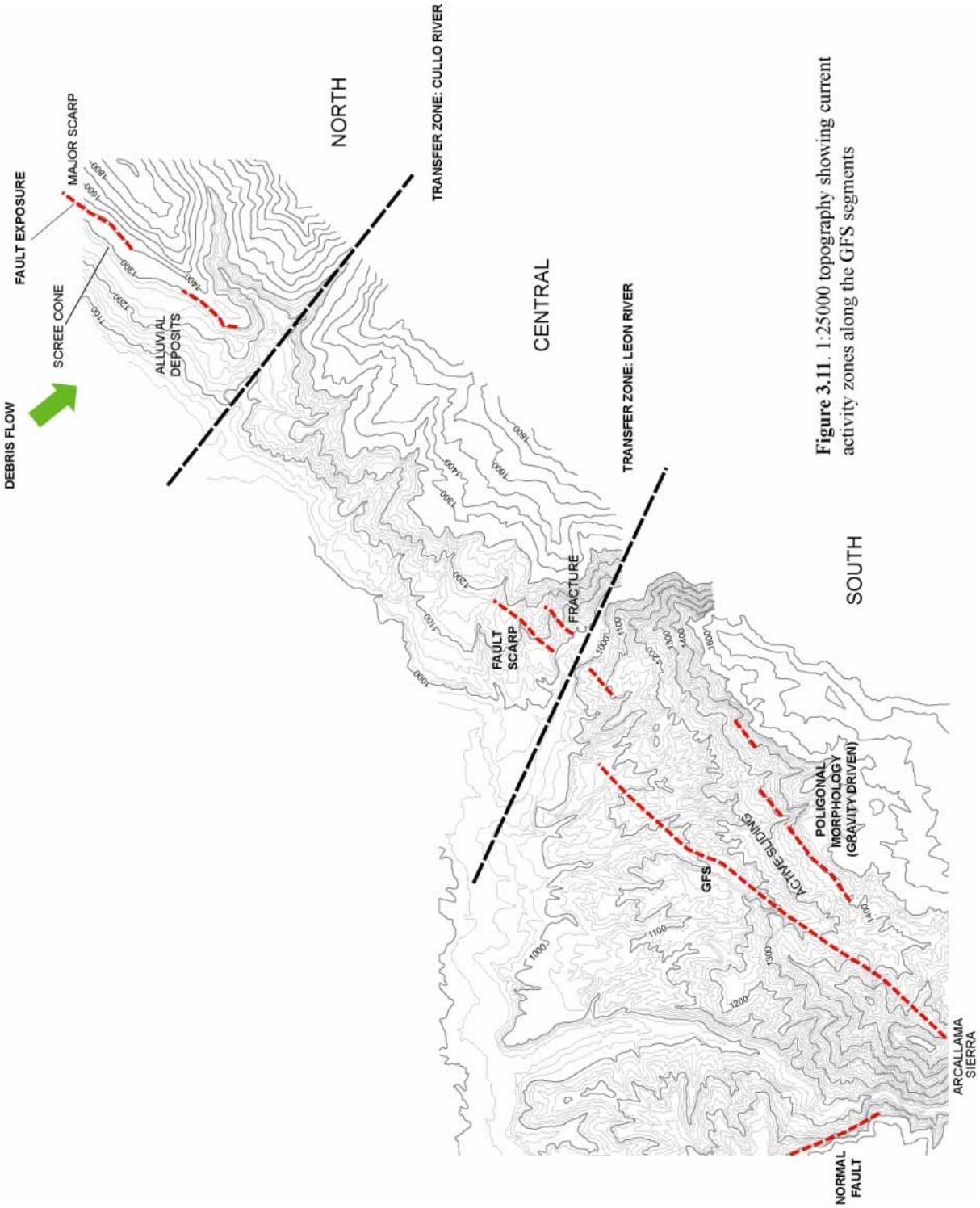

Figure 3.11. 1:25000 topography showing current activity zones along the GFS segments

Some of these aspects include: 1) the pervasive linearity of the contact, 2) the location of the Burrohuaycu Fm. exclusively northwards from the unconformity, and 3) the SE dipping of the Burrohuaycu Fm. strata and the increase of dipping as it approaches the fault plane. However, there is no clear fault-related morphology (Figure 3.10d). The GFS limits the Gray Mb. to the east which suggests long term activity of the GFS (i.e. all over the deposition of the Red and Gray Mbs.). However, it seems that this fault is more active during deposition of the Red Mb. Indeed, upwards the Gray Mb. lies sub-horizontally to N-W gently dipping. Moreover, if related to GFS tectonic activity, the Gray Mb. corresponds to a hangingwall block which summit is placed higher than the footwall summit. During deposition of the Gray Mb. the GFS was relatively less active or simply its slip rate could not keep pace with the deposition rate.

3.4.3.3 Other faulting zones

The Jacapa Fm. outcrops, south of the Uchucay locality, follow a highly linear contact with the Saraguro Gp. (UTM 681000 9626000). Here, no major deformation is observed along the Jacapa Fm. in high contrast with the eastward outcrops located next to the range. Geometrical disposition of the stratigraphic series suggests that faulting is normal. The contact between the two formations is vertical. The outer wall of the Saraguro Gp. extends downward to ~1100 m. Contrary, the top of the Jacapa Fm. is placed at ~1400 m and series dip towards the fault. The linear trend result therefore from the fact that the slip surface intercepts the surface at a high angle. Also, mapping contours of the fault indicate that it dips to the NW instead of SE as previously proposed. These structural aspects suggest that a reverse faulting contact is hard to envisage as it was proposed before (Pratt et al., 1997; Hammer, 1998). Other faulting zones extend along the limits of the Jacapa Fm.

3.5 DISCUSSION

3.5.1 Tectonic evolution of the SIB area

The Jacapa Fm. deposition took place during the first steps of basin formation (ancient basin), which probably develops along isolated basins controlled by extensional structures as exemplified by the normal fault bounding the Jacapa Fm. at the southernmost section of the SIB. However, no evidences of any structure acting at the period of Jacapa Fm. deposition exist along the main deposition area (i.e. the range). The ancient tectonic step is coeval with the Jacapa Fm. deposition is difficult to constraint accurately since the depositional area of the Jacapa Fm. has been highly modified by younger tectonic events. The current architecture (recent basin) of the SIB is formed by

two major steps of tectonic deformation, a compressive step, leading to strong deformation of the ancient basin depocenters (formation of the range) and a subsequent extensional step, which controls the younger basin evolution.

The range has been described as a NW verging compressive structure, which front thrust is located along the GFS. Dunkley and Gaibor (in prep.) define it as a single N-W verging structure between the Saraguro Gp. and the Jacapa Fm., while Hungerbühler et al. (2002) define it as a two faults verging structure system, one located between the Saraguro Gp and the Jacapa Fm. and the northern one located between the Jacapa and Burrohuaycu Fms. However, we found no evidences of disruption of the sedimentary sequence between the Saraguro Gp. and the Jacapa Fm. The deformed series of the Jacapa Fm. parallels the deformed section of the Saraguro Gp. at both sides of the range (i.e. at the La Cria anticline, Figure 3.10e). This suggests a most likely conformable limit between them prior to compressive deformation. No structure exists between both, sedimentary and volcanic sequences (Figure 3.10a). Whether a major fault controls a tectonic inversion of the Jacapa Fm. depocenters this fault is not located at the SIB area. The proposed tectonic inversion of a proto basin including the Jacapa Fm. can be envisaged only if all the rocks outcropping at the La Cria anticline were located along the same fault footwall-block. This last aspect is coherent with the box-shaped structure of the La Cria anticline, which suggests the existence of a decollement zone.

Hungerbühler et al. (2002) and Dunkley and Gaibor (in prep.) suggest that the compressive step leading to the formation of the range (as well as the north verging thrusting along the Cerro Arcayama and San Sebastian de Yulug areas) is well dated because the non deformed Uchucay Fm. lies discordantly on the Burrohuaycu Fm., which is assumed to be affected by the compressional event. In this way they dated the compressional event at ~10 Ma (i.e. the 9.4 Ma age of the undeformed Uchucay Fm. combined with the 10.5 Ma younger age obtained of the Burrohuaycu Fm.). We consider that there are two major inconsistencies with this model: 1) there are no evidences of tephra layer deposition in the ~100 m thick Uchucay Fm. The sample dated by Hungerbühler et al., (2002, UTM: 682810-9629759) corresponds rather to a pedogenic alteration and not to a tephra layer (Figure 3.7f). We consider that the age of the Uchucay Fm. is not well constrained and, 2) the Burrohuaycu Fm. is not affected by the compressive event and probably was not deposited during compression. Furthermore, there is no evidence of thrusting structures at the Arcayama sierra and the San Sebastian de Yulug areas. The deformed sediments are restricted to the range (i.e. Saraguro Gp. and Jacapa Fm). The Burrohuaycu Fm. shows a pervasive gently dipping to the S-E which resulted from the extensional tectonic activity of the GFS. This dipping increases as they approach the fault. Minor folding (such as that observed to the north of Sumaypamba) or changes in dip develop in response to local causes. Therefore, the unconformity between the Uchucay and Burrohuaycu Fms. does not correspond to the major regional unconformity dated as ~8.5-9 Ma observed along the whole

area between Cañar to the north and Loja to the south (Steinmann et al., 1999; Hungerbühler et al., 2002). The time span between compression to extension is related to the unconformity between the Jacapa and Burrohuaycu Fms. Furthermore, taking into account that the Jacapa Fm. age is not well constrained, it is difficult to propose an age for the compressive step. It is probably coeval with deposition of the Jacapa Fm. Nevertheless, it must be younger than the extensional step that leads to accumulation of the Burrohuaycu Fm (i.e. older than 14.7 Ma).

Our observations show that the Burrohuaycu Fm. accumulates during an extensional tectonic step fulltime. The GFS acts as a N-E directed N-W dipping normal fault as evidenced by major scarps developing along the north and central segments (Figures 4.8b and 4.9f). The SIB corresponds to a half-graben basin with sedimentary filling on-lapping the Saraguro Gp. and the Santa Isabel Fm. to the NW and dipping to the SE due to basin-floor tilting. It is difficult to explain the often complex and changing temporal and spatial patterns of fault activity in terms of sedimentation and subsidence. However, this can be a useful aspect to characterize long term fault activity. We assume that an extensional regime is active since deposition of the Burrohuaycu Fm. (i.e. before 14.7 Ma since the older ages as proposed by Hungerbühler et al. (2002) were obtained from the central section of the formation). The Red Mb. defines the period of GFS major extensional activity. This period is coeval with major basin-floor stepping that probably leads to S-E directed mass collapse of the Santa Isabel Fm. Indeed, in the central zone of the mapped area, at least two blocks of the Santa Isabel Fm. slipped on the Burrohuaycu Fm. The eastern block showing several pervasive shear zones that separate highly locally deformed rocks of the Burrohuaycu Fm. from the overlying slipped rocks of the Santa Isabel Fm. However, the south segment of the GFS does not show evidences of major current activity (at least not as big enough as conserving morphology face to erosional processes). Although the slip rate controls the variability in the appearance of normal faults, other factors such as the nature of the footwall rocks can be also important (Goldsworthy and Jackson, 2000). Because the footwall rocks of the southern part of the central segment (where fault scarp is well developed) does not differ from the footwalls rocks on the south segment. It seems that an important difference in current activity takes place along these two segments. The southern segment of the GFS shows almost no evidence of recent tectonic activity. However, we consider that the extensional strain that characterizes the area is (at least in part) responsible of the relaxation processes that take place mainly along the contact of the Saraguro Gp. and Jacapa Fm. series along the range slope-break. At Present the major extensional tectonic activity is concentrated along the north and central segments. The strong concentration of recent alluvial deposits and mass-collapse along the northern most active segments of the GFS show that tilting, and consequently fault slipping (as evidenced by well-developed fault-exposure zones), is active at Present.

We consider that the GFS forms after the compressional step. The model proposed here is different to that proposed by Dunkley and Gaibor (in prep), which suggest that the GFS could act as a normal fault in periods as olds as the time span of deposition of the Saraguro Gp. They reach this conclusion based on a proposed SE thickening of the Saraguro Gp. series. Considering that the Saraguro Gp. corresponds to the basin basement this thickening is very hard to check. Furthermore, as pointed out before, there is no structure bonding the Saraguro Gp. prior to the formation of the recent basin. Hungerbühler et al. (2002) proposed a model based on a NW dipping normal fault (Burrohuaycu Fm. depocenter) rotated and inverted during subsequent compression (Figure 3.11). An horizontal-axis rotation of at least 90°, from a NW dipping normal fault to a S-E dipping thrust fault (if possible, during inversion tectonics along a pre-existent fault or weakness zone), may have strong consequences in the sedimentary series that lie next to the structure. This is not the case of the Burrohuaycu series that lies next to the GFS, which are relatively undeformed once compared to the Jacapa Fm. series. The Burrohuaycu Fm. evolves fulltime in a weakly-disturbed extensional tectonic setting.

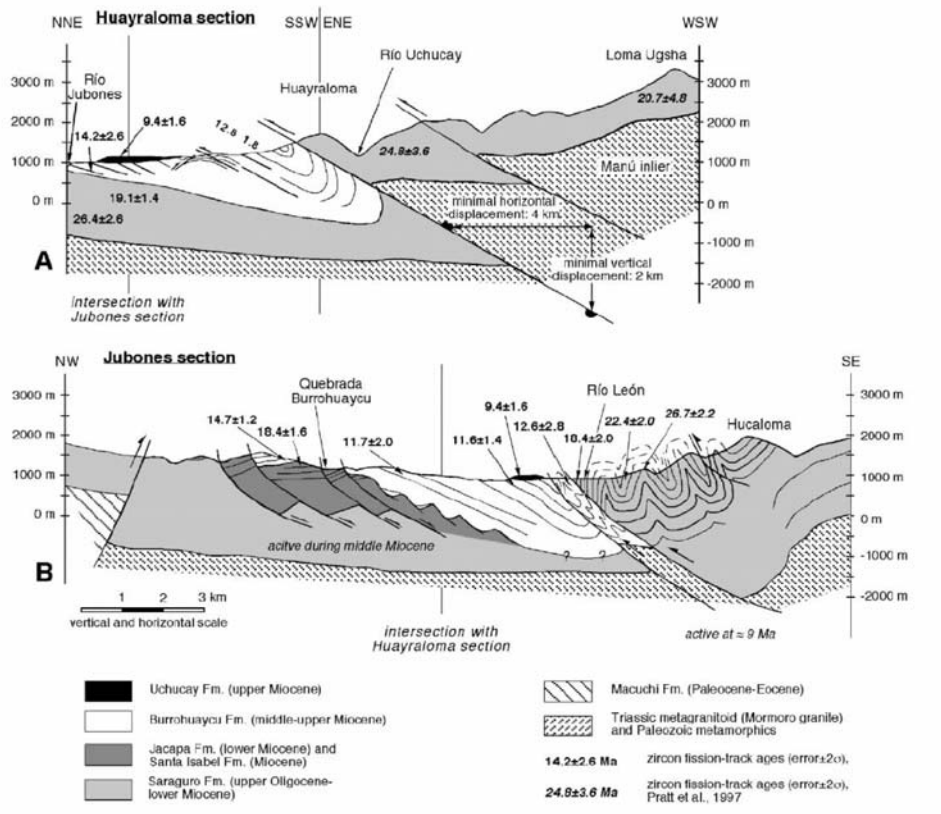

Figure 3.12. Cross-sections for the Santa Isabel basin proposed by Hungerbuhler et al. (2002). It is proposed that large scale thrusting of the late Oligocene–early Miocene Saraguro Gp. over the middle Miocene Burrohuaycu Fm. during basin inversion, which occurred at ~9 Ma. Deformation in the Burrohuaycu Fm. is considered to be sealed by the horizontally lying Uchucay Fm. Location of cross sections in Figure 3.5.

3.5.2 Regional tectonic implications

Further work is needed to establish a coherent geodynamic scenario that involves all the field observations obtained along the Cañar, Azogues and Santa Isabel intermontane basins. A model may however be in agreement with some aspects that we consider as first-order constraints on local basin and regional Andean evolution. These aspects include:

- All the intermountane basins exhibit two major sections: an eastward highly deformed section and a westward undeformed section. At the Santa Isabel basin, the Saraguro Gp. is highly deformed along the eastern limit of the basin. However, to the west, the Miocene series of the Saraguro Gp. shows no major deformation. No major structure exists along the Andean segment between the zone bounded by the PEF, the NF and the PNF to the west and the IDF and the GFS to the east (Figure 3.12). The upper Miocene-Pliocene volcaniclastic Tarqui Gp., which shows no major deformation along the block described above (Figure 3.1 and 3.12). The whole structure mostly looks like an undeformed crustal block. Deformation is concentred along the eastern limit of this block.

- It is most likely that the compressional step occurs at different periods, it is older than 14.7 Ma along the SIB, while along the Cañar area it is dated at ~8.5 Ma. It seems that compressional periods are not synchronous along the faults that delimit the intermontane basins. The whole structure seems to be coherent with an undeformed block migrating northwards resulting in dyachronous tectonic inversion along its eastern limits and ongoing subsidence along its southernmost limit, i.e. the SIB, which acts as a free border zone during the Miocene.

- At ~8-9 Ma an important exhumation took place along the Ecuadorian Andes (Steinmann et al., 1997; Spikings et al., 2001; Hugerbuhler et al., 2002) as well as along the Andes of Colombia and Peru (Gomez et al., 2005; Garver et al., 2005). This period is coeval with basin closing at the Cañar and Azogues areas (Lavenu et al., 1995; Steinmann et al., 1997; Hungerbühler et al., 2002; Lahuathe, 2005; Verdezoto, 2006). However, the SIB is unaffected by this step and furthermore, extensional tectonics are active along the SIB after 8-9 Ma.

Several aspects remain dubious. The NAB block drifting is proposed to have taken place along a crustal restraining bend to the north of 2°S that switch southwards to the Gulf of Guayaquil area (Ego et al., 1996; Winkler et al., 2005). Along this restraining bend, basin formation began at ~6.5 Ma (i.e. approximately the age of the last depositional pulses along the Cañar and Azogues areas). Does this age represent a major tectonic and sedimentary reorganization of the continental setting of the NAB?

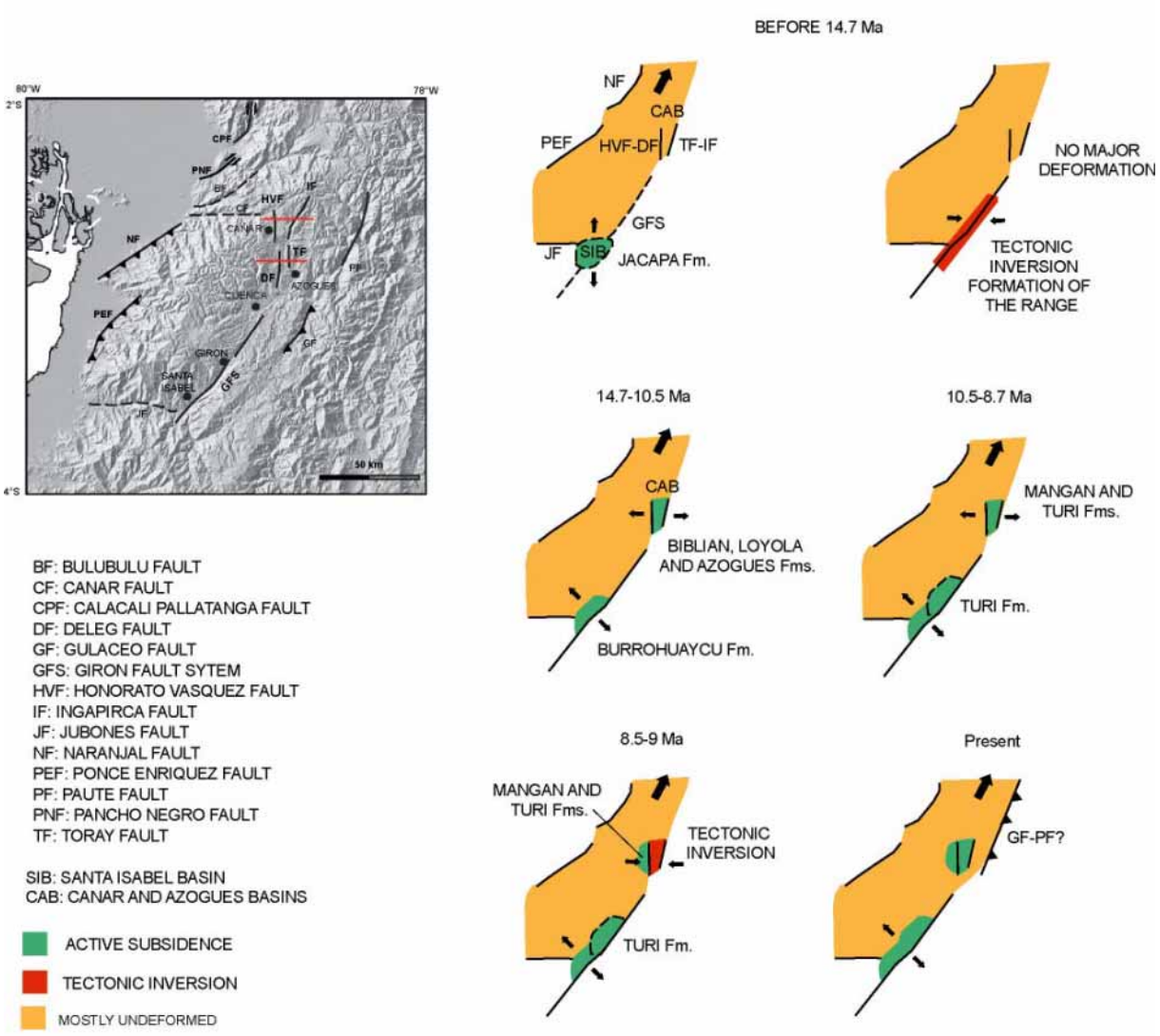

Figure 3.13. Cartoon showing the regional evolution of the Santa Isabel, Canar and Azogues basins. See text for further discussion

Extensional tectonic activity along the Ecuadorian Andean chain is scarce. Local normal faulting located along the northern Ecuadorian Andes seems mostly related to post-glacial elastic rebound rather than tectonism (Ego et al., 1996b). The GFS shows a strong activity in Present times, the most active north segment extending at least 20 km. This fault corresponds to the major normal active fault of the central and southern Ecuadorian Andes (if not the only one) and more important, it is located at the Gulf of Guayaquil-Tumbes basin (GGTB) latitude. Winter and Lavenu (1989b) suggested that the GFS could represent the landward limit of a continental zone governed by the GGTB tectonics. Furthermore, they proposed fault formation at the beginning of the Quaternary (which is in good agreement with the main opening age of the GGTB, i.e. 1.8-1.6 Ma). However, evidence presented by Winter and Lavenu (1989b) was weak and chronological periods were not well constrained. Did the major reorganization of the NAB southernmost limit that took place at ~1.8-1.6

Ma (Witt et al., 2006) influence the SIB area?; was the GFS reactivated during Quaternary times?. It is likely that the closing of the Cañar and Azogues basins produced a strong variation in the sediment input along the SIB. At this time, the GFS probably ceased to produce nearly sediment accumulation and/or the GFS passes from a depositional sytem to a non-depositional one, which difficults the analysis of its more recent evolution.

The master fault of GGTB evolution (i.e. the Tumbes detachment system) prolongs to the continent. It probably connects with the structures participating in NAB drifting accommodation. A connection between the GFS northern segments and the TDS could eventually takes place along the Jubones fault, which is considered to be the main limit between continental basement to the south, and oceanic basement to the north. Nevertheless, there is no direct evidence to argue that the SIB and the GGTB resulted from the activity of the same fault system. However, the pervasive extensional tectonics at the SIB results from the northward motion of an undeformed detached block (i.e. a phenomenon identical to that controlling the GGTB tectonics).

CHAPTER IV

GENERAL CONCLUSIONS

The displacement of an upper-plate sliver has been invoked as a major factor locally controlling subsidence along the Andean forearc and arc systems since at least the major reorganization of the subduction system at 25 Ma. The Gulf of Guayaquil-Tumbes basin defines the most subsiding zone (in terms of rate and width) resulting from the North Andean block drifting during the Neogene. However, intermontane basin formation has been also generally related to North Andean block drifting along Andean strike-slip settings. Some of the major constraints obtained in this work include:

The GGTB tectonics and evolution. A ~N-S tensional stress regime characterized the GGTB shelf area during Miocene to Quaternary times (Figure 4.1). The GGTB evolved along the shelf area along two main tectonic steps. The first one, during the Mio-Pliocene is characterized by low subsidence and low sedimentation rates. A relatively thick Mio-Pliocene accumulation of sediments took place along the shelf and its surrounding continental areas, including beneath the main early Pleistocene depocenters of the GGTB. Nevertheless, no major pre-Quaternary structure exists at the GGTB. Probably an on-shore detachment structure located between the Zorritos basin and the Amotapes massif controlled the subsidence during this period (Figure 4.1). The Pleistocene of the GGTB is marked by an abrupt increase in subsidence leading to maximum deposition of ~3500 m of sediments. Three major detachment faults, the Posorja, Jambelí and Tumbes detachment systems (PDS, JDS and TDS) controlled the subsidence of the GGTB depocenters including the Esperanza, Jambelí and Tumbes basins, respectively.

The PDS and the TDS extend only to the inner DFS and the complex zone of the junction between Banco Peru fault (BPF) and the Talara detachment, respectively. This system acts as a transfer system accommodating the detachment activity along the seaward edge of the GGTB. The subsidence related to the NAB northward drifting, which resulted in the GGTB, is mainly confined to the shelf zone (Figure 4.1). No connection exists between the NAB limits and the trench. The GGTB experienced a southward migration of activity during Quaternary. The northern edge of the GGTB migrated from the PDS to the northern major fault bounding the Esperanza graben. Similarly, tectonic activity migrated southward along the TDS. This is probably a consequence of progressive slip blocking northwards along the Santa Elena rise and the subsequent creation of a southward free border along the TDS.

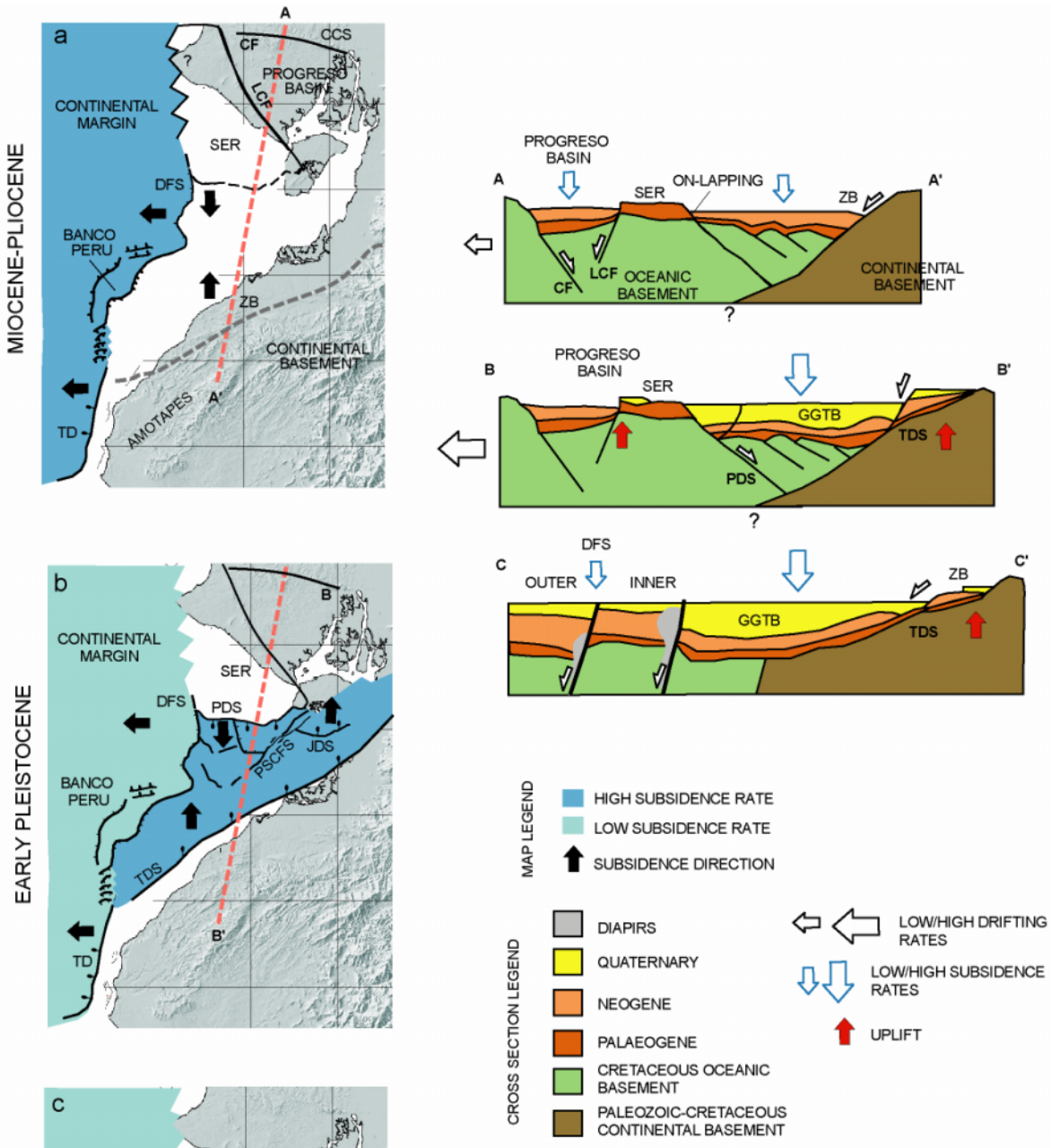

Figure 4.1. Schematic map views and cross sections of the tectonic reconstruction of the GGTB since Miocene times. The coastline is considered only as a geographic reference frame. **a)** During Mio-Pliocene times subsidence and related sedimentation rates are low. The dashed gray line corresponds to the northern limit of continental-type basement outcrops. **b)** Main periode of basin formation and depocenter individualisation. **c)** Present times. Abbreviations are as follows: CF, Carrizal fault; CCS, Chongon-Colonche sierra; CCS, Chongón-Colonche sierra; DFS, Domito fault system; GGTB, Gulf of Guayaquil-Tumbes basin; JDS, Jambeli detachment system; PDS, Posorja detachment system; SER, Santa Elena raise; TD, Talara detachment; TDS, Tumbes detachment system; ZB, Zorritos basin. See text for further explanation.

The TDS corresponds to the southernmost structure participating in accommodation of NAB drifting-related subsidence. It extends to the continent and probably connects with the transcurrent system assumed to represent the NAB eastern frontier. We consider that the TDS acts as the master fault in basin evolution. Gravity anomalies suggest that it probably corresponds to the shallow expression of one of the suture zones, which originated from the accretion of oceanic terranes along the South American continent. The PSCFS commonly associated to the southernmost tip of the NAB frontier acts as a transfer zone since early Pleistocene time. It accommodated the opposite verging directions between the southward dipping PDS and the northward dipping JDS. The PSCFS shows no landward prolongation to the north and no seaward prolongation to the south toward the trench, it ends at sites where no transfer motion is required. The PSCFS does not correspond to the main NAB frontier at the GGTB area as commonly accepted.

The transcurrent faulting along the basin limits and depocenters developed in response to extension. We consider, however that the architecture of the GGTB does not fit the classic pull-apart basin model in which subsidence develops in response to slip difference along one or two offset transcurrent faults.

Interplate coupling constraints. Two regimes characterize the continental margin and shelf at the GGTB latitude. The continental margin is related to subduction-erosion working at depth resulting in N-S trending seaward dipping normal faults. In contrast, the shelf is related to E-W to N-E detachment structures resulting from trench-parallel extension (i.e. N-S directed) related to NAB northward drifting. The trench-parallel extension is expressed by subsidence along the shelf area, while the continental margin is relatively unaffected by this process. Seismic evidence shows that the limit between the continental margin and the shelf is marked by an important contrast on interplate mechanical coupling. Indeed, the expulsion of fluids from the interplate limit has been related with increase of mechanical interplate coupling landward from the DFS (i.e. the GGTB shelf zone, Calahorrano, 2005). Our data show that the zone of fluid expulsion is coincident with a major diapiric zone located seaward from the inner DFS. It is probable that diapirs raise is activated by extensional tectonics originated from NAB northward drifting combined with raising fluids released from the interplate zone. The N-S directed strain resulting from NAB drifting is not resolved along the continental margin because of the important difference in interplate coupling. We suggest that the continental margin does not react to the subduction motion because it is buoyant. However, the landward increase of interplate mechanical coupling is not expressed by an increase of earthquake recurrence beneath the GGTB. The GGTB defines a seismic gap, which is bounded northward and southward by zones of high subduction-related earthquake recurrence. Low earthquake recurrence along the GGTB seems controlled by weak upper plate strength caused by NAB drifting-related lengthening of the crust and subduction erosion along its underside. Low seismic release seems to be a

typical characteristic of tectonic escape related trailing edges (i.e. the Sunda strait at the Sumatra subduction system, the Golfo de Penas at the Chile subduction system and the Bussol strait at the Japon subduction zone, Annex 1).

We suggest that tectonic escape systems are highly sensitive to local interplate coupling variations and that these variations are important to define the zones where subsidence results from escape tectonics. The modeling of convergence partitioning in terms of convergence obliquity, constant interplate coupling and constant overriding plate strength at the scale of the whole system seems to be insufficient when analyzing the trailing edge of the tectonic escape system. At the latitude of the GGTB obliquity of convergence is zero or negligible. The Pallatanga fault, proposed as the southernmost strike-slip continental limit of the NAB, is also located in front of a zone where obliquity is very small. An important consequence of the existence of this transcurrent deformation is that partitioning is currently taking place in zones where obliquity is negligible.

Evolution of the central Ecuadorian Andes intermontane basins. The central and southern Andes underwent major extensional periods leading to intermontane basin formation during at least the last 15 Ma. Transtensional and pure extensional regimes result in discrete intermontane basin formation along major pre-existing Andean trending structures, from north to south these basins include the Cañar, Azogues and Santa Isabel basins. Along the Cañar and Azogues basins active subsidence during ~15-9 Ma finishes with a compressive step at 8.5-9 Ma (Bourgois et al., in prep), which is probably related to an important Andean exhumation period (Steinmann et al., 1999; Hungerbühler et al., 2002). In contrast, in the Santa Isabel basin, the compressive step is older than ~15 Ma and extensional processes seems to be active from 15-9 Ma and during Present times. Our first approximation to a regional model on Andean intermontane evolution point out that the Santa Isabel basin represents the southern 'extensional free face' of an undeformed detached block that moves to the north promoting persistent subsidence to the south and diacrhonous compressive deformation along its eastern edge.

Regional geodynamic implications. The GGTB resulted from the N-S directed extensional strain linked to NAB drifting and recorded the most important subsidence of the southern Ecuadorian and northern Peruvian forearcs for at least the last 10 Ma. We consider that the high subsidence and related sedimentation rates of Quaternary age document an acceleration period of NAB drifting. This result is in agreement with tectonic observations along the NAB eastern edge where major tectonic deformation steps have been dated at ~2-3 Ma (i.e. Winkler et al., 2005). Considering that the rate and obliquity of the convergence between the Nazca and South America plates remain constant at least during the last 5 Ma, the subduction of the Carnegie ridge at the Pliocene-early Pleistocene limit is

proposed to be the main source of interplate coupling increase along the Ecuadorian margin. We assume that the subduction of the leading edge (or the subduction of a high) of the Carnegie ridge is at the origin of the interplate-coupling increase, which in turn produced the acceleration of the NAB northward drifting and the major periods of subsidence in its southernmost limits.

The total lengthening of a complete N-S transect between the PDS (to the north) and the TDS (to the South) ranges between 13.5 and 20 km (5-10% net lengthening). This lengthening is coherent with the documented NAB migration rates combined with an early Pleistocene age for GG area main opening pulse. This value suggests that the ~100 km displaced Andean zone located to the N-E of the GGTB is not entirely related with GGTB evolution, as it was proposed (Steinmann et al., 1999). It seems most likely that major Andean piedmont displacement ocurred prior to GGTB formation.

The subduction-erosion regime of the continental margin at the latitude of the GGTB extends to the south, down to the northern Peru continental margin (Bourgois et al., submitted), and to the north, up to the southern edge of the Carnegie ridge (Sage et al., 2006). At the GGTB latitude, subsidence along the continental margin began (at least) during middle Miocene, which is in agreement with ages proposed for the Peruvian continental margin (i.e. von Huene et al., 1988). On the other hand, subsidence along the GGTB favours sediment trapping on the shelf instead of reaching the continental margin and trench. This is a major aspect in controlling the subduction regime. The emersion of the GGTB during Pleistocene low-stands resulted in an increase in sediment input to the upper continental margin and trench. However, Banco Peru acted as a persistent barrier (even during low-stands) between the shelf and the upper continental margin.

.

The above evidence suggests that the NAB trailing tail was characterized by discrete basin formation during the Neogene, which was probably related to migration of the NAB limits. However, the GGTB high subsidence marked a major reorganisation of the NAB southern limits at 1.8-1.6 Ma.

References

References paper 2 not included

Aalto, K.R., and W. Miller (1999), Sedimentology of the Pliocene Upper Onzole Formation, an inner-trench slope succession in northwestern Ecuador, J. S. Am. Earth Sci., 12, 69-85.

Acosta, J., L. Lonergana, and M.P. Coward (2004), Oblique transpression in the western thrust front of the Colombian Eastern Cordillera, J. S. Am. Earth Sci., 17, 181-194.
Angelier, J., and B. Coletta (1983), Tension fractures and extensional tectonics, Nature, 301, 49-51.

Alvarado, A. (1998), Variation du champ de contrainte et de déformation, et quantification des déformations actives du Bloc cotier de l'Equateur, DEA, Géodynamique et Physique de la Terre, Université Paris XI-Ecole Normale supérieur de Paris

Aspden J., and M. Litherland (1992), The geology and Mesozoic collisional history of the Cordillera Real, Ecuador, Tectonophysics, 205, 187-204.

Aubouin, J., R. von Huene, M. Baltuck, R. Arnott, J. Bourgois, M. Filewicz, M. Helm, K. Kvenvolden, B. Lienert, T. McDonald, K. McDougall, Y. Ogawa, E. Taylor, and B. Winsborough (1982), Leg 84 of the Deep Sea Drilling Project: Subduction without accretion: Middle America Trench off Guatemala, Nature, 297, 458-460.

Aubouin, J., J. Bourgois, and J. Azéma (1984), A new type of active margin: The convergent-extensional margin, as exemplified by the Middle America Trench off Guatemala, Earth Planet. Sci. Lett., 67, 211-218.

Audemard, F. (1997), Holocene and historical earthquakes on the Boconó fault system, southern Venezuelan andes: trench confirmation, J. Geodyn., 24, 155-167.

Audemard, F. (2003), Geomorphic and geologic evidence of ongoing uplift and deformation in the Mérida Andes, Venezuela, Quat. Int., 101-102, 43-65.

Bangs, N., S. Gulick, and T. Shipley (2006), Seamount subduction in the Nankai trough and its potential impact on the seismogenic zone, Geology, 34, 701-704.

Barberi, F., M. Coltelli, G. Ferrara, F. Innocenti, J. Navarro, and R. Santacroce (1988), Plio-Quaternary volcanism in Ecuador, Geol. Mag., 125, 1-14.

Benitez, S., E. Jaillard, M. Ordoñez, and N. Jimenez (1993), Late Cretaceous to Eocene Tectonic Sedimentary Evolution of southern Coastal Ecuador, Geodynamic implications, paper presented at 2th International Symposium of Andean Geodynamics (ISAG), Oxford-UK, 21-23 September.

Benitez, S. (1995), Évolution géodynamique de la province côtière sud-équatorienne au Crétacé supérieur Tertiaire, Ph.d. thesis, 221 pp, Université Grenoble 1, Grenoble, 11 July.

Berggreen, W.A., D.V. Kent, and J.J. Flynn (1985), Paleogene geochronology and chronostratigraphy, the chronology of the geological record, Mem. Geol.. Soc. Am. 10, 141-195.

Boinet, T., J. Bourgois, H. Mendoza, and R. Vargas (1985), Le poinçon de Pamplona (Colombie): Un jalon de la frontière méridionale de la plaque Caraïbe, Bull. Soc. Géol. Fr., 8 (1), 403-413.

Bourdon, E., J.P. Eissen, M.A. Gutscher, M. Monzier, M.L. Hall and J. Cotten (2003), Magmatic response to early aseismic ridge subduction: the Ecuadorian margin case (South America), Earth Planet. Sci. Lett., 205, 123-138.

Bourgois, J., B. Calle, J. Tournon, and J.F. Toussaint (1982), The Andean ophiolitic megastructures on the Buga-Buenaventura transverse (Western Cordillera–Valle, Colombia), Tectonophysics, 82, 207-229.

Bourgois, J., J. Azéma, P.O. Baumgartner, J. Tournon, A. Desmet, and J. Aubouin (1984), The geologic history of the Caribbean-Cocos plate boundary with special reference to the Nicoya ophiolite complex (Costa Rica) and D.S.D.P. (legs 67 and 84 off Guatemala): A synthesis, Tectonophysics, 108, 1-32.

Bourgois, J., J.F. Toussaint, H. Gonzalez, J. Azéma, B. Calle, A. Desmet, L.A. Murcia, A.P Acevedo, E. Parra, and J. Tournon (1987), Geological history of the Cretaceous ophiolitic complexes of northwestern South America (Western and Central Cordilleras of the Colombia Andes), Tectonophysics, 143, 307-327.

Bourgois, J., G. Pautot, W. Bandy, T. Boinet, P. Chotin, P. Huchon, B. Mercier de Lepinay, F. Monge, J. Monlaü, B. Pelletier, M. Sosson, and R. von Huene (1988), Seabeam and seismic reflexion imaging of the tectonic regime of the Andean continental margin off Peru (4°S to 10°S), Earth Planet. Sci. Lett., 87, 111-126.

Bourgois, J., A. Eguez, J. Butterlin, and P. De Wever (1990), Evolution géodynamique de la Cordillère Occidentale des Andes d'Equateur: La découverte de la Formation éocène d'Apagua, C. R. Acad. Sci., Paris, 311(2), 173-180.

Bourgois, J., C. Guivel, Y. Lagabrielle, T. Calmus, J. Boulègue, and V. Daux (2000). Glacial-interglacial trench supply variation, spreading-ridge subduction, and feedback controls on the Andean margin development at the Chile triple junction area (45-48°S), J. Geophys. Res., 105, 8355-8386.

Bourgois, J., Lahuathe, J-C., Vaca, W., Verdezoto, P., Cornejo, R., 2006, Mapâ Geologico del Ecuador, Hoja de Cañar, escala 1:50000; Quito, Instituto Geografico Militar (IGM), Ministerio de Recursos Naturales y Energeticos (MRNE), Direccion Nacional de Geologia (DINAGE).

Bristow, C. (1973), Guide to the Geology of the Cuenca basin, southern Ecuador, Ecuadorian Geological and Geophysical Society, Quito, 54 pp.

Bosch, D., P. Gabriele, H. Lapierre, L. Malfere, and E. Jaillard (2002), Geodynamic significance of the Raspas Metamorphic Complex (SW Ecuador): geochemical and isotopic constraints: Tectonophysics, 345, 83-102.

Buck, W.R. (1988), Flexural rotation of normal faults, Tectonics, 7, 959-973.

Burke, K.; Sengor, C., 1886, Tectonic escape in the evolution of the continental crust, IN: Reflection seismology: The continental crust. Washington, DC, American Geophysical Union (Geodynamics Series. Volume 14), 1986, p. 41-53.

Calahorrano, A. (2005), Structure de la marge du Golfe de Guayaquil (Equateur) et propriété physique du chenal de subduction, à partir de données de sismique marine réflexion et réfraction, Ph.d. thesis, 227 pp, Université Paris VI, Paris.

Campbell, C.J. (1974), Ecuadorian Andes, in Mesozoic–Cenozoic orogenic belts, data for orogenic studies, Geol. Soc. London. Spec. Pub., 725-732.

Cande, S.C., and D.V. Kent (1995), Revised calibration of the geomagnetic polarity time scale for the Late Cretaceous and Cenozoic, J. Geophys. Res., 100, 6093-6095.

Cantalamessa, G., and C. Di Celma (2004), Origin and chronology of Pleistocene marine terraces of Isla de la Plata and of flat, gently dipping surfaces of the southern coast of Cabo San Lorenzo (Manabí, Ecuador). J. S. Am. Earth Sci., 16, 633-648.

Case, J.E., L. Duran, A. Lopez, and R. Moore (1971), Tectonic investigations in western
Colombia and Eastern Panama, Geol. Soc. Am. Bull., 82, 2685-2712.

Cloos, M. (1992), Thrust-type subduction-zone earthquakes and seamount asperities: A physical model for seismic rupture, Geology, 20, 601-604.

Collot J.Y., P. Charvis, M. Gutscher and E. Operto (2002), Exploring the Ecuador-Colombia active margin and inter-plate seismogenic zone, Eos Trans. AGU, 83 (17), 189-190.

Corredor, F. (2003), Seismic strain rates and distributed continental deformation in the northern Andes and three-dimensional seismotectonics of the north-western South America, Tectonophysics, 372, 147-166.

Cortés, M., J. Angelier, and B. Colletta (2005), Paleostress evolution of the northern Andes (Eastern Cordillera of Colombia): Implications on plate kinematics of the South Caribbean region, Tectonics, 24, TC1008, doi:1029/2003TC001551;

CowieP., and C. Scholz (1992), Physical explanation for the displacement-length relationship of faults using a post-yield fracture mechanics model, J. Struc. Geol, 14, 1113-1148.

Daly, M.C. (1989), Correlations between Nazca-Farallon plate kynematics and forearc basin evolution in Ecuador, Tectonics, 8, 769-790.

Dawers, H., M., Anders, and H. Scholz (1993), Growth of normal faults: displacemen-length scaling, Geology, 21, 1107-1110.

DeMets, C., R. Gordon, D. Argus, and S. Stein, S. (1990), Current plate motions: Geoph. J. Int.l, 101, 425-478.

Deniaud, Y., P. Baby, C. Basile, M. Ordoñez, G. Montentegro, and G. Mascle (1999), Ouverture et évolution tectono-sedimentaire du Golfe de Guayaquil: basin d'avant arc néogène et quaternaire du Sud des Andes équatoriennes, C.R. Acad. Sci. Paris, 328 (3), 181-187.

Deniaud, Y. (2000), Enregistrements sédimentaire et structurale de l'évolution géodynamique des Andes équatoriennes au cours du Néogène : étude des bassins d'avant-arc et bilans de masse. Ph.d. thesis, 157 pp, Université Grenoble 1, Grenoble.

Dhont, D., G. Backé and Y. Hervoüet (2005), Plio-Quaternary extension in the Venezuelan Andes: Mapping from SAR JERS imagery, Tectonophysics, 399, 293-312.

Dimate, C., L. Rivera, A. Taboada, B. Delouis, A. Osorio, E. Jimenez, A. Fuenzalida, A. Cisternas and I. Gomez (2003), The 19 January 1995 Tauramena (Colombia) earthquake: geometry and stress regime, Tectonophysics, 363, 159-180.

Dumont, J., E. Santana and W. Vilema (2005), Morphologic evidence of active motion of the Zambapala Fault, Gulf of Guayaquil (Ecuador), Geomorphology, 65, 223-239.

Dunkley, P and A. Gaibor (1997), Geology of the Cordillera Occidental of Ecuador between 2-3°S, Proyecto de Desarrollo minero y control ambiental, Programa de información cartográfica y geológica, CODIGEM-BGS, Quito.

Dunkley, P., and Gaibor, A., in prep, Mapa Geológico de la zona Girón. DNGM, Quito.

Eberhart-Philips, D., Haeussler, P., Freymueller, J., et al, (2002), The 2002 Denali fault earthquake, Alaska: a large magnitude, slip-partitioned event, Science, 300, 1113-1118.

Ego, F., M. Sébrier, A. Lavenu, H. Yepes, and A. Eguez (1996), Quaternary state of stress in the Northern Andes and the restraining bend model for the Ecuadorian Andes, Tectonophysics, 259, 101-116.

Ego, F., M. Sebrier, E. Carey-Gailhardis, and B. Beate (1996), Do the Billecocha normal faults reveal extension due to lithosperic body forces in the northern Andes?, Tectonophysics, 265, 255-273.

Eguez, A., A. Alvarado, H. Yepes, M. Machette, C. Costa, and R. Dart (2003), Database and Map of Quaternary faults and folds of Ecuador and its offshore regions, Open-File report 03-289. Sp. pub. USGS- Inter. Lithos. Pr.

Farrell, J., J. Clements, and L. Gromet (1995), Improved chronostratigraphic reference curve of late Neogene seawater 87/86Sr, Geology, 23, 403-406.

Feininger, T., and C.R. Bristow (1980), Cretaceous and Palaeogene geologic History of Coastal Ecuador, Geologische Rundschau, 69, 849-674.

Fierro, J. (1991) Estudio geodinámico de la Cuenca intramontañosa cenozoica de Malacatos (Sur del Ecuador), Unpublished thesis, EPN, Quito, Ecuador.

Freymueller, J.T., J. Kellog, and V. Vega (1993), Plate motions in the North Andean region, J. Geophys. Res., 98, 21853-21863.

Gailler, A., 2005, Structure de la marge d'Equateur - Colombie par modélisation des données de sismique grand angle marines - influence sur le fonctionnement de la subduction et la sismicité, PhD thesis, Université Nice-Sophia Antipolis, France.

Garcia M. and W. Vilema (1986). Sintesis Geologica de la Isla Puná. IV Cong.Ecuat. D.G.M. Quito-Ecuador.

Gardner, T., J. Marshall, D., Merritts, et al. (2001), Holocene forearc block rotation in response to seamount subduction, southeastern Peninsula Nicoya, Costa Rica, Geology, 29, 151-154.

Garrison, J., and J. Davidson (2003), Dubious case of slab melting in the northern volcanic zone of the Andes, Geology, 31, 565-568.

Garver, J.I., P.W. Reiners, L.Walker, J. Ramage and S.E. Perry (2005), Implications for timing of Andean uplift from thermal resetting of radiation-damaged Zircon in the Cordillera Huayhuash, Northern Peru, J. Geol., 113, 117-138.

Gawthorpe, R., and R. Leeder (2000), Tectono-sedimentary evolution of active extensional basins, Basin. Res., 12, 195-218.

Goldsworthy, M., and J. Jackson (2000), Active normal fault evolution in Greece revealed by geomorphology and drainage patterns, , J. Geol. Soc. London, 157, 967-981.

Gomez, E., T.E. Jordan, R.W. Allmendinger, K. Hegarty, S. Kelleey and M. Heizler (2003), Controls on architecture of the Late Cretaceous to Cenozoic southern Middle Magdalena Valley Basin, Colombia, Geol. Soc. Am. Bull.,115,131-147.

Gomez, E., T.E. Jordan, R.W. Allmendinger, K. Hegarty and S. Kelleey (2005), Syntectonic Cenozoic sedimentation in the northern middle Magdalena Valley Basin of Colombia and implications for exhumation of the northern Andes, Geol. Soc. Am. Bull., 117, 547-569.

Graindorge, D., A. Calahorrano, P. Charvis, J.Y Collot, and N. Bethoux (2004), Deep structures of the Ecuador convergent margin and the Carnegie Ridge, possible consequence on great earthquakes recurrence interval, Geophys. Res. Lett., 31, L04603, doi:10.1029/2003GL018803.

Gregory-Wodzicki, K. (2000), Uplift history of the Central and Northern Andes: A review, Geol. Soc. Am. Bull., 112, 1091-1105.

Guillier, B., J.L. Chatelain, E. Jaillard, H. Yepes, G. Poupinet, and J.F. Fels (2001), Seismological evidence on the geometry of the orogenic system in central-northern Ecuador (South America), Geophys. Res. Lett., 28 (19), 3749-3752.

Gupta, S., P. Cowie, H. Dawers, and J. Underhill (1998), A mechanism to explain rift-basin subsidence and stratigraphic patterns through fault-array evolution, Geology, 26, 595-598.

Gutscher, M.A., J. Malavieille, S. Lallemand and J.Y. Collot (1999), Tectonic segmentation of the North Andean margin : impact of the Carnegie ridge collision, Earth Planet. Sci. Lett., 168, 255-270.

Hammer, C. (1998), Geologie des intermontanen Beckens von Sta. Isabel (Miozan, Sudecuador): Sudteil Master's Thesis, Institute of Geology ETH-Zurich, 99 p.

Hampel, A. (2002), The migration history of the Nazca Ridge along the Peruvian active margin: a re-evaluation, Earth Planet. Sci. Lett., 203, 665-679.

Hampel, A., N., Kukowski, J. Bialas, C. Huebscher, and R., Heinbockel (2004), Ridge subduction at an erosive margin: The collision zone of the Nazca Ridge in southern Peru, J. Geophys. Res., 109, Issue B2, CiteID B02101.

Handschumacher, D.W. (1976), Post-Eocene plate tectonics of Eastern Pacific: in: The Geophysics of the Pacific basin and its margin: American Geophys. Union Geophys. Mon., p. 799-804.

Haq, B.U., J. Hardenbold, and P.R. Vail (1988), Mesozoic and Cenozoic chronostratigraphy and cycles of sea-level change, Spec. Publ. Soc. Econ. Paleontol. Min., 42, 71-108.

Helg, U. (1997), Geologie des intermontanen Beckens von Sta. Isabel (Miozan, Sudecuador): Beckennordteil Master's Thesis, Institute of Geology ETH-Zurich, 128 p.

Hey R. (1977), Tectonic evolution of the Cocos-Nazca spreading center, Geol. Soc. Am. Bull., 88, 1404-1420.

Hughes R. and L Pilatasig (2002), Cretaceous and Tertiary terrane accretion in the Cordillera Occidental of the Andes of Ecuador, Tectonophysics, 345, 29-48.

Hungerbühler, D., M. Steinmann, W. Winkler, D. Seward, A. Eguez, D.E. Peterson, U. Helg and C. Hammer (2002), Neogene stratigraphy and Andean geodynamics of southern Ecuador, Earth. Sci. Rev., 57, 75-124.

Izquierdo, O. (1991), Estudio geodinámico de la Cuenca intramontañosa cenozoica de Loja (Sur del Ecuador), Unpublished thesis, EPN, Quito, Ecuador.

Jackson, J.A. (1987), Active normal faulting and crust extension, In : Continental Extensional Tectonics, Geol. Soc. London. Spec. Pub., 28, 1-17.

Jaillard, E., S. Benítez, and G. Mascle (1997), Les déformations paléogènes de la zone d'avant-arc sud-équatorienne en relation avec l'évolution géodynamique, Bull. Soc. Géol. Fr., 168 (4), 403-412.

Jaillard, E., M., Ordoñez, J., Suárez, J. Toro, D. Iza and W., Lugo (2004), Stratigraphy of the late Cretaceous–Paleogene deposits of the Cordillera Cccidental of Central Ecuador: geodynamic implications, , J. South Am. Earth Sci., 17, 49-58.

Kay, S.M. (2005), Andean adakites from slab melting, forearc subduction erosion and crustal thickening, paper presented at 12th Congreso Latinoamericano de Geologia, Quito-Ecuador.

Kellogg, J.N., and V. Vega (1995), Tectonic development of Panama, Costa Rica and the Colombian Andes: Constraints from Global Positioning System (GPS) geodetic studies and gravity, Geologic and tectonic development of the Caribbean plate boundary in southern Central America, edited by P. Mann, Spec. Pub. Geol. Soc. Am., 295, 75-90.

Kenerley, J., L., Almeida, and J. Calle (1973), Mapa geológico del Ecuador, Hoja Saraguro, Instituto Geográfico Militar, Dirección General de Geología y Minas (DGGM), Institute of Geological Sciences London (IGS).

Kerr, A., J. Aspden, J. Tarney and L. Pilatasig (2002), The nature and provenance of accreted oceanic terranes in western Ecuador: geochemical and tectonic constraints, J. Geol. Soc. London, 159, 577-594.

Kodaira, S., A., Nakanishi, J. Park, A.I.,, Tetsuro Tsuru, and Y., Kaneda (2003), Cyclic ridge subduction at an inter-plate locked zone off central Japan, Geophys. Res. Lett., 30, 72-1 72-4.

Lahuathe, J. (2005), Levantamiento geológico y análisis de la deformación tectónica entre las latitudes : 2°28' S y 2°37'S. Provincia de Cañar, Unpublished thesis, EPN, Quito, Ecuador.

Lambeck, K., Y. Yokoyama, and T. Purcell (2002), Into and out of the Last Glacial Maximum: sea level change during oxygen isotope stage 3 and 2, Quat. Sci. Rev., 21, 343-360.

Lapierre, H., D. Bosch, V. Dupuis, M. Polvé, R.C. Maury, J. Hernandez, P. Monté, D. Yeghicheyan, E. Jaillard, M. Tardy, B. Mércier de Lépinay, M. Mamberti, A. Desmet, F. Keller, and F. Sébrier (1999), Multiple plume

events in the genesis of the peri-Caribbean Cretaceous oceanic plateau province, J. Geophys. Res., 105, 8403-8421.

Lavenu, A., C. Noblet., M., Bonhomme, A. Eguez, F. Dugas, and G. Vivier (1992), New K/Ar age dates of Neogene and Quaternary volcanic rocks from the Ecuadorian Andes: implications for the relationship between sedimentation, volcanism, and tectonics, J. S. Am. Earth Sci., 5, 309-320.

Lavenu, A., C. Noblet., and T. Winter (1995a) Neogene ongoing tectonics in the southern Ecuadorian Andes: analysis of the evolution on the stress field, J. Struct. Geol., 17, 47-58.

Lavenu, A., T. Winter and F. Dávila (1995b), A Pliocene-Quaternary compressional basin in the Interandean depression, Central Ecuador, Geophys. J. Int., 121, 279-300.

Lelgemann, H., M.-A. Gutscher, J. Bialas, E. R. Flueh, W. Weinrebe, and C. Reichert (2000), Transtensional basins in the Western Sunda Strait, Geophys. Res. Lett., 27, 3545-3548.

Lions R. (1995), Evolution géodynamique d'un bassin d'avant arc Néogène en contexte décrochant: l'ouverture du Golfe de Guayaquil. D.E.A., Université Joseph Fourier-Grenoble I, 30 p.

Litherland, M., and J., Aspden (1992), Terrane-boundary reactivation: a control on the evolution of the Northern Andes, J.South Am. Earth Sci., 5, 71-76.

Litherland, M., J., Aspden, and R. Jemielita (1994), The metamorphic belts of Ecuador, British Geological survey, Overseas Memoir 11, 147 pp.

Lonsdale, P. (1978), The Ecuadorian subduction system, AAPG. Bull., 62, 2454-2477.

Lonsdale, P. and K. Klitgord (1978), Structure and tectonic history of the eastern Panama Basin, Geol. Soc. Am. Bull., 89, 981-999.

Luzieux, L., F. Heller, R. Spikings, C. Vallejo, and W. Winkler (2006), Origin and Cretaceous tectonic history of the coastal Ecuadorian forearc between 1°N and 3°S: paleomagnetic, radiometric and fossil evidence, Earth Planet. Sci. Lett., in press.

Malfait, B.T., and M.G. Dinkleman (1972), Circum-Caribbean tectonic and igneous activity and the evolution of the Caribean plate, Geol. Soc. Am. Bull., 83, 251-272.

Mamberti, M., H. Lapierre, D. Bosch, E. Jaillard, R. Ethien, J. Hernandez, and M. Polvé (2003), Accreted fragments of the Late Cretaceous Caribbean–Colombian Plateau in Ecuador, Lithos, 66, 173-199.

Mediavilla, J. (1991), Evolución geodinámica de la cuenca Terciaria de Girón-Santa Isabel, Sur del Ecuaador, Unpublished thesis, EPN, Quito, Ecuador.

Megard, F. (1984), The Andean orogenic period and its major structures in central and northern Peru, J. Geol. Soc. London, 141, 893-900.

Meschede, M., and U. Barckhausen (2000), Plate tectonic evolution of the Cocos-Nazca spreading center. In Silver, E.A., Kimura, G., and Shipley, T.H. (Eds.), Proc. ODP, Sci. Results, 170, 1-10.

Michaud, F., C. Witt ; and J.Y. Royer, Influence of the subduction of the Carnegie ridge on Ecuadorian geology : reality and fiction, to be submitted.

Noblet, C., A. Lavenu, and F. Schneider (1988), Etude géodynamique d'un basin intramontagneux tertiaire sur décrochements dans les Andes du sud de l'Equateur : l'exemple du bassin de Cuenca, Geodynam, 3, 117-138.

Noblet, C., and R. Marocco (1989), Lacustrine megaturbidites in an intermontane strike-slip basin: the Miocene Cuenca basin of South Ecuador, International Symposium of Intermontane basins, Geology and Resources, 282-293, Chiang Mai-Thailand.

Olade, R. (1980), Informe geo-volcanológico: Proyecto de investigación geotérmica de la República del Ecaudor. Organización Latinoamericana de Energía, Quito.

Paris, G., N. Michael, R. Machette, R.L. Dart, and K. Haller (2000), Map and Database of Quaternary Faults and Folds in Colombia and its Offshore Regions, Geological Survey, Open-File Report 00-0284.

Pardo-Casas F., and P. Molnar (1987), Relative motion of the Nazca (Farallon) and South America plate since late Cretaceous times, Tectonics, 6, 233-248.

Pedoja, K. (2003), Les terrasses marines de la marge Nord Andine (Equateur et Nord Pérou): relations avec le contexte géodynamique, Ph.d. thesis, 413 pp, Université Paris VI, Paris.

Pedoja, K., L. Ortlieb, J.F. Dumont, M. Lamothe, B. Ghaleb, M. Auclair and B. Labrousse (2006), Quaternary coastal uplift along the Talara Arc (Ecuador, Northern Peru) from new marine terrace data, Marin. Geol., 228, 73-91.

Pecora, L., E. Jaillard and H. Lapierre (1999), Accrétion paléogene et décrochement dextre d'un terrain océanique dans le Nord du Perou, C. R. Acad. Sci. Paris, 329(6), 389-396.

Pennington, W.D. (1981), Subduction of the eastern Panama Basin and seismotectonics of northwestern South America, J. Geophys. Res., 86, 10753-10770.

Pilger, R.H. (1984), Cenozoic plate kinematics, subduction and magmatism: South American Andes, J. Geol. Soc. London, 141, 793-802.

Porter, S.C. (1989), Some geological implications of average Quaternary glacial conditions, Quat. Res., 32, 245-261.

Pratt W., J. Figueroa, and B. Flores (1997), Mapa Geológico de la Cordillera Occidental del Ecuador entre 3-4°S, Codigem-Min Energía-BGS Publs, Quito.

Rea, D.K. and B.T. Malfait (1974), Geologic evolution of the Northern Nazca Plate, Geology, 2, 317-320.

Reynaud, C., E. Jaillard, H. Lapierre, G. Mascle, and V. Dupuis (1999), Oceanic plateau and island arcs of southwestern Ecuador: their place in the geodynamic evolution of the northwestern America, Tectonophysics, 307, 235-254.

Sage, F., J. Collot, and C. Ranero (2006), Interplate patchiness and subduction-erosion mechanisms: Evidence from depth-migrated seismic images at the central Ecuador convergent margin, Geology, 34, 997-1000.

Sallarès, V. and P. Charvis (2003), Crustal thickness constraints on the geodynamic evolution of the Galapagos Volcanic Province, Earth Planet. Sci. Lett., 214, 545-559.

Samaniego, P., H. Martin, C. Robin, and M. Monzier (2002), Transition from calc-alkalic to adakitic magmatism at Cayambe volcano, Ecuador: Insight into slab melts and mantle wedge interactions, Geology, 30, 967-970.

Samaniego, P., H. Martin, M. Monzier, C. Robin, M. Fornari, J.P. Eissen and J. Cotten (2005), Temporal evolution of magmatism in the northern volcanic zone of the Andes: the geology and petrology of Cayambe Volcanic Complex (Ecuador), J. Petrol., doi: 10.1093/petrology/egi053.

Scholl, D., R. von Huene, T. Vallier, and D. Howell (1980), Sedimentary masses and concepts about tectonic processes at underthrust ocean margins, Geology, 8, 564-568.

Scholz, C., and C. Small (1997), The effect of seamount subduction on seismic coupling, Geology, 25, 487-490.

Shackleton, N.J. (1997), The deep sea sediment record at the Pliocene-Pleistocene boundary, Quat.Int., 40, 33-35.

Sheperd, G.L. and R. Moberly (1981), Coastal structure of the continental margin northwest Peru and southwest Ecuador, In: L.D. Kulm et al. (Ed.), Nazca Plate: crustal formation and Andean convergence, Mem. Geol. Soc. Am. 154, 351-391.

Smalley, P., A. Higgins, R. Howarth, H., et al., (1994), Seawater Sr isotope variations through time: a procedure for constructing a reference curve to date and correlate marine sediments rocks, Geology, 22, 431-434.

Soulas, J.P., A. Eguez, H. Yepes, and V. Perez (1991), Tectónica activa y riesgo sismico en los Andes ecuatorianos y el extremo sur de Colombia, Bol. Geol. Ecuat., 2(1), 3-11.

Somoza, R. (1998), Updated Nazca (Farallon)-South America relative motions during the last 40 My: implications for mountain building in the central Andean region, J. South Am. Earth Sci., 3, 211-215.

Spencer, J.E. (1984), Role of tectonic denudation in warping and uplift of low angle normal faults, Geology, 12, 95-98.

Spikings, R.A., A.Winkler, D. Seward and R. Handler (2001), Along-strike variations in the thermal and tectonic response of the continental Ecuadorian Andes to the collision with heterogeneous oceanic crust, Earth Planet. Sci. Lett., 186, 57-73.

Spikings, R.A. and P.V. Crowhurst (2004), (U-Th)/He termochronometric constraints on the Late Miocene-Pliocene tectonic development of the northern Cordillera Real and the Interandean depression, Ecuador, J. South Am. Earth Sci., 17, 239-251.

Steinmann, M., D. Hungerbühler, D. Seward and W. Winkler (1999), Neogene tectonic evolution and exhumation of the southern Ecuadorian Andes: a combined stratigraphy and fission track approach, Tectonophysics, 307, 255-276.

Stern, C.R. (2004), Active Andean volcanism: its geologic and tectonic setting, Revista Geologica de Chile, 31, 161-206.

Subarya, C., M. Chlieh, L. Prawirodirdjo, et al. (2006), Plate-boundary deformation associated with the great Sumatra-Andaman earthquake, Nature, 440, 46-51.

Taboada, A., L. Rivera, A. Fuenzalida, A. Cisternas, H. Philip, H. Bjwaard, J. Olaya, and C. Rivera (2000), Geodynamics of the northern Andes: subductions and intracontinental deformation (Colombia), Tectonics, 19, 787-873.

Tibaldi, A., and L. Ferrari (1992), Latest Pleistocene-Holocene tectonics on the Ecuadorian Andes, Tectonophysics, 205, 109-125.

Toro, J., and E. Jaillard (2005), Provenance of the Upper Cretaceous to upper Eocene clastic sediments of the Western Cordillera of Ecuador: Geodynamic implications, Tectonophysics, 399, 279-292.

Trenkamp, R., J.N. Kellogg, T. Freymuller, and P.H Mora (2002), Wide plate margin deformation, southern Central America and northwestern South America, CASA GPS observations, J. South Am. Earth Sci., 15, 157-171.

Tzedakis, P.C., V. Andrieu, J.L. De Beaulieu, S. Crowhurst, M. Follieri, H. Hooghiemstra, D. Magri, M. Reille, L. Sadori, N.J. Shackleton, and T.A. Wijmstra (1997), Comparison of terrestrial and marine records of changing climate of the last 500,000 years, Earth Planet. Sci. Lett., 150, 171-176.

Vallejo,C., R. Spikings, L. Luzieux, W.Winkler, D. Chew, and L. Page (2006), The early interaction between the Caribbean Plateau and the NW South American Plate, Terr. Nov. 18, 264–269.

Van Andel, T.H., G. Heath, B. Malfait, D. Heinrichs, and J. Ewing, (1971), Tectonics of the Panama Basin, astern quatorial Pacific: Geol. Soc. Am. Bull, 82.

Vega, M., Baby, P., Brusset, S., Vega, N., Monges, C., Bolanos, R., and Marocco, R., 2005, Structural and stratigraphic architecture of the Tumbes forearc basin (northern Peru): 6th International Symposium on Andean Geodynamics (ISAG), Barcelone, p. 776-778.

Velandia F., J. Acosta, R. Terraza and H. Villegas (2005), The current tectonic motion of the Northern Andes along the Algeciras Fault System in SW Colombia, Tectonophysics, 399, 313-329.

Vera R. (1982). Geología de la Isla Santa Clara. Unpublished thesis. ESPOL. Guayaquil-Ecuador.

Verdezoto, P. (2006), Levantamiento geológico del sector comprendido entre las latitudes 2°37'S y 2°50'S, Provincias de Cañar y Azuay, con especial enfoque sobre las secuencias Miocénicas, Unpublished thesis, EPN, Quito, Ecuador.

Veizer, J. (1989), Strontium isotopes in seawater through time, Ann. Rev. Eart. Sci., 17, 141-167.

Villagomez, D., A. Eguez, W. Winkler, and R. Spikings (2002), Plio-Quaternary sedimentary and tectonic evolution of the Central Inter-andean Valley in Ecuador, paper presented at 4th International Symposium on Andean Geodynamics (ISAG), IRD, Toulouse, France, September 16-18.

Von Huene, R., E. Suess, and the Leg 112 Shipboard Scientist, 1988, Ocean Drilling Program Leg 112, Peru continental margin: Part 1, Tectonic History, Geology, 16, 934-938.

von Huene, R., J. Bourgois, J. Miller, and G. Pautot, (1989), A large Tsunamogenic landslide and debris along the Peru Trench, J. Geophys. Res., 94, 1703-1714.

von Huene, R., and D. Scholl (1991), Observations at convergent margins concerning sediment subduction, subduction erosion, and the growth of continental crust, Rev. Geophys., 29(3), 279-316.

Wernicke, B. (1981), Low-angle faults in the Basin and Range province: Nape tectonics in an extending orogen, Nature, 291, 645-648.

White, S., R. Trenkamp, and J. Kellog, 2003, Recent crustal deformation and the earthquake cycle along the Ecuador-Colombia subduction zone, Earth Planet. Sci. Lett., 216, 231-242.

Wilson, D.S., and R. Hey (1995), History of rift propagation and magnetization intensity for the Cocos-Nazca spreading center, J. Geophys. Res., 100, 10041-10056.

Winkler, W., D. Villagomez, R. Spikings, P. Abegglen, St. Tobler and A. Eguez (2005), The Chota basin and its significance for the inception and tectonic setting of the inter-Andean depression in Ecuador, J. South Am. Earth Sci., 19, 5–19.

Winograd, I.J., J.M. Landwehr, K.R. Ludwig, T.B. Tyler, and A.C. Riggs (1997), Duration and structure of the past four interglaciations, Quat. Res., 48, 141-154.

Winter, T., and A. Lavenu (1989), Morphological and microtectonic evidence for a major active right-lateral strike-slip fault across central Ecuador (South America), Ann. Tect., 3(2), 123-139.

Winter, T., and A. Lavenu (1989b), Tectonique active en Equateur : ébauche d'une nouvelle interprétation géodynamique, Bull. Ins. Fr. Et. And, 1, 95-115.

Winter, T., J. Avouac, and A. Lavenu (1993), Late Quaternary kinematics of the Pallatanga strike slip fault (Central Ecuador) from topographic measurements of displaced morphological features, Geophys. J. Int., 115, 905-920.

Witt C., J. Bourgois., F. Michaud, M. Ordoñez, N. Jimenez, and M. Sosson (2005), Development of the Golfo de Gu ayaquil (Ecuador) as an effect of the North Andean Block tectonic escape since the Lower Pleistocene, Paper presented at the VI International Symposium on Andean Geodynamics, IRD-Universitat de Catalunya, Barcelona , 12-14 Sept.

Witt C., J. Bourgois., and F. Michaud (2006), Quaternary tectonic history of the Gulf of Guayaquil-Tumbes basin as the signature of the North Andean block tectonic escape, paper presented at the Back-bone of the Americas, Geol. Soc. Of Am., Mendoza, Argentina, 3-7 Abril.

Witt C., J. Bourgois., F. Michaud, M. Ordoñez, N. Jimenez, and M. Sosson (2006), Development of the Golfo de Guayaquil (Ecuador) as an effect of the North Andean Block tectonic escape since the Lower Pleistocene, Tectonics, v. 25, TC3017, doi:10.1029/2004TC001723.

Witt, C., and Bourgois, J., in prep, The Gulf of Guayaquil-Tumbes basin at the North Andean block trailing edge: a forearc basin originating from trench-parallel extension.

ECUADOR

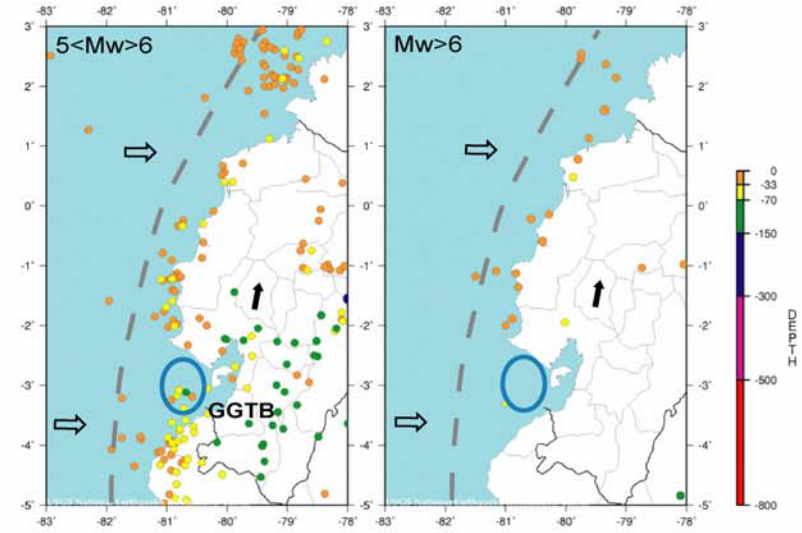

INDONESIA

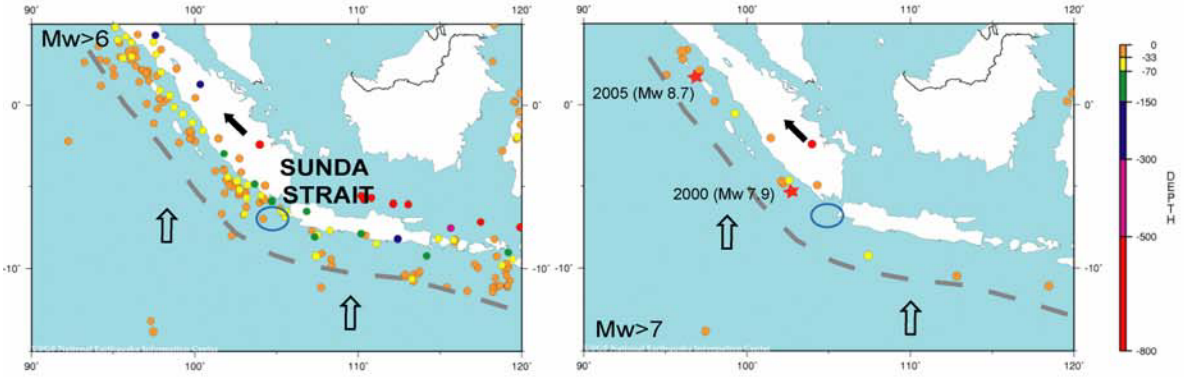

KURIL ARC

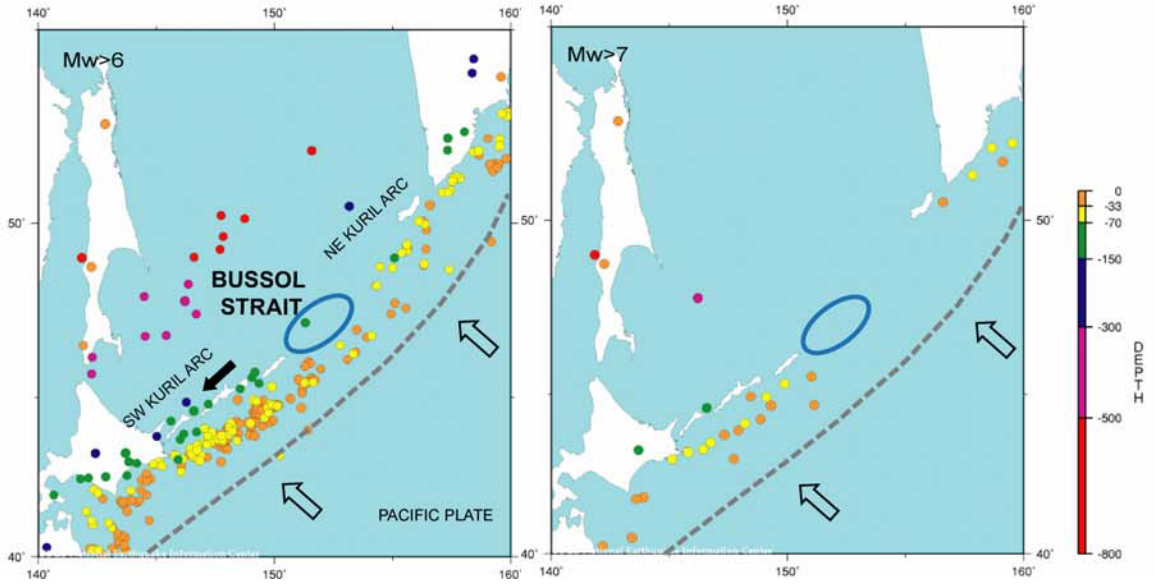

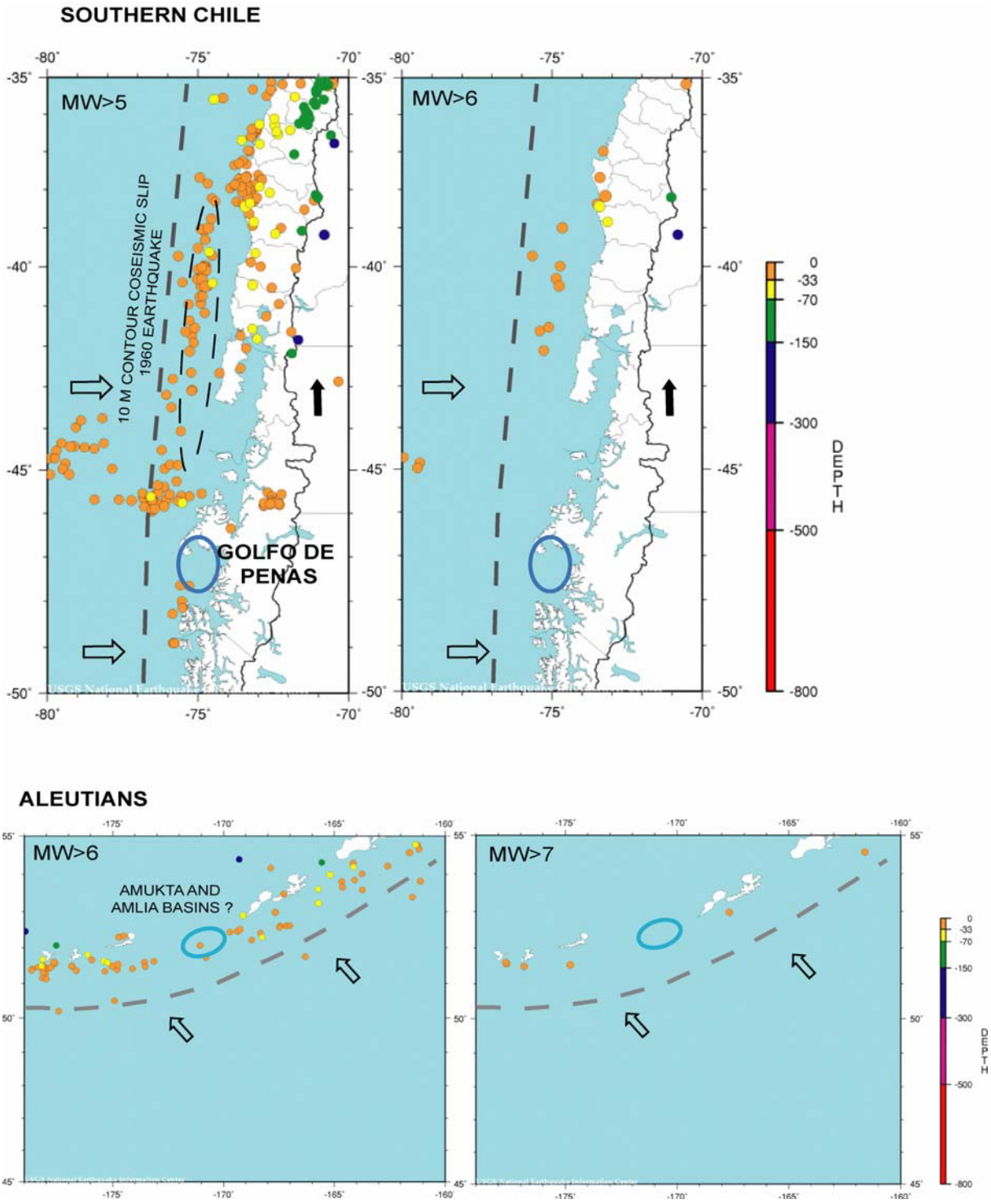
SOUTHERN CHILE
MW>5
MW>6
10 M CONTOUR COSEISMIC SLIP
1960 EARTHQUAKE
GOLFO DE
PENAS
DEPTH
0
-33
-70
-150
-300
-500
-800
ALEUTIANS
MW>6
MW>7
AMUKTA AND
AMLIA BASINS ?